Development of the models to accurately assess the environmental impacts of shipping emissions

by

Sanaz Jahangiri

BEng (Hons) in Naval Architecture, Tehran Polytechnic, 2009

MEng in Offshore Engineering, Tehran Polytechnic, 2011

A thesis submitted in fulfilment of the requirement for the degree of

Doctor of Philosophy

in

Maritime Engineering

National Centre for Maritime Engineering and Hydrodynamics,

Australian Maritime College (AMC), University of Tasmania.

May 2019

Abstract

Maritime transportation is amongst the most popular modes of transport due to its cost effectiveness & efficiency, overall safety and relatively environmentally friendly operations. This trend is expected to increase with the number of global fleet of vessels forecasted to continue increasing. However, exhaust emissions from ships are one of the major sources of air pollutants. Unlike land-based transportation, which is strictly governed by stringent environmental rules and regulations, the shipping environmental regulators are still continuously amending their legislation with regards to emissions.

While it is evident that shipping emissions are of concern globally, the global effects tend to be more dispersed and it is difficult to be attributed to the original sources. Continued implementation of the amendments to the MARPOL Convention Annex VI regulations is an attempt to reduce emissions on a global scale. In-port emissions account for a relatively small proportion of the total emissions due to shipping, yet they have some of the most significant health impacts on the surrounding population. It is commonly known that these emissions are linked to cardiopulmonary and cancer related health problems, with an estimated number of deaths due to sulphur oxides (SO_x) emissions from shipping alone during 2012 of approximately 87,000 worldwide. Regulated pollutants including SO_x, nitrogen oxides (NO_x), particulate matter (PM) and the hundreds of other constituents of exhaust emissions generated by the combustion of fuels depend on the quality of the fuel and the characteristics of combustion.

To examine these risk and the potential benefits of control measures, ship exhaust emissions need to be quantified. However, precise measurement and collection of emission data is challenging due to factors such as diversity of engine types and configurations, various operation modes, ship mobility, etc. Several approaches to estimate shipping emissions have been developed. One such solution is online computer-based monitoring of shipping pollution, which utilizes measurement system as part of the fixed ship equipment. Online monitoring mechanisms provide data over an extended period, but it is costly in time, assets, and well-trained human resources. On top, the measurement results are with low precision and sometimes unreliable. Therefore, there is a need to consider more on-board measurements that will enhance the accuracy of emission prediction models.

Following the above, the objective of this thesis is to contribute to green and sustainable shipping operations by developing empirical-based models to better predict and assess the environmental impacts of shipping emissions. Although the methodologies developed in this PhD research have general applicability, the focus of experimental work was in Australian Ports due to their accessibility.

For the experimental work we collaborated with fellow researchers from Queensland University of Technology - Australia (QUT) and Maine Maritime Academy - USA (MMA) to develop in-vessel emission measurement systems. The measurements were taken in October and November of 2015 on two large cargo ships at the Ports of Brisbane, Gladstone, and Newcastle. The first on-board measurement was performed on CSL vessel I (to ensure confidentially the identity of ship is suppressed) from 26th to 31st of October 2015 when the vessel was en route from Port of Brisbane to Port of Gladstone. The second measurement was conducted on CSL vessel II from 3rd to 6th of November 2015 on a voyage from Gladstone to Sydney. All measurements were carried out on both the main and auxiliary engines of both ships for three ship operating conditions: at berth, while manoeuvring, and while cruising. Data from on-board measurements and laboratory analysis was used to develop a model for emission factor estimation for ships operating in different conditions.

Because the utilization of inbuilt measurements proves to be difficult, time-consuming and resource-demanding as well as restricted by limitations, it is difficult to convince ship-owners to purchase and install recommended measurement devices. Therefore, emission inventories are utilized, which are mathematical models to estimate emissions discharged into the atmosphere. This research presents a comprehensive study to identify vessel-specific inventory families predicting the primary emissions from ocean-going vessels when at berth, while maneuvering and while cruising.

The effectiveness of emission factors applied in current inventories, however, needs to be evaluated, because of their general over- or under-estimations. There is also a need to develop the models to predict the emissions considering different environmental and operational factors more preciously. Therefore, the on-board measurement data acquired in this study were utilized to develop new sets of emission factor equations for emission inventory considering different main engine types for at-sea and in-port operations. To this end, non-linear regression analysis was used to develop the new models and the results were statistically

compared with the conventional models applied for emission inventories in shipping operations. Our results showed a better prediction of the developed emission quantity than current inventories for different engine types during in-port and at-sea activities, with the sum of primary emissions coming closest to the actual sea emission calculations and to the smallest standard values. This study also created a generalized rational algorithm to rank inventory families based on the precision of their predictions for a given operational mode of a specific vessel. The implications of this study, together with the developed algorithm to rank inventory families, were applied to offer a novel future policy for cost-effective and reliable emission estimation caused by shipping operations.

The emissions from vessels utilizing heavy fuel oil include large amounts of NOx, SOx and PM, presenting significant health risk to people living near ports. Atmospheric dispersion modelling can be used to predict the ground level concentrations of gaseous pollutants and similarly the deposition of PM. While several dispersion models such as AERMOD, AUSPLUME and ISCST3 exist, selecting an appropriate model is important to match the size and complexity of the domain. Some simple ones like Gaussian-plume models require less computational time and resources to run, requiring only simplified meteorological and geographic datasets where they approximate plume behavior mathematically incorporating a simple description of the dispersion process. This may result in inaccurate results in obtaining the final concentrations. To overcome the shortcomings of steady-state Gaussian-plume models, we applied a more advanced atmospheric dispersion model (CALPUFF) to assess ground-level concentrations. To the best of our knowledge, this is the first comprehensive report describing the concentration, distribution and sources of shipping emissions within Australian ports. Another point to add is that the health of residents living near ports is most likely affected by different shipping activities. Therefore, our study also helped provide guidance on the minimum distances between emission sources and urbanized areas (homes, schools, and businesses) needed to safeguard human health, through health impact risk assessment.

Lastly, to develop a baseline measurement of the current state of risk from shipping emissions, we developed a complete methodology, based on the Australian Environmental Health Risk Assessment Framework to assess the human health risk from shipping emissions, applying Downwash algorithm and Near-field modelling as well as the Air-shed areas from CALPUFF dispersion modelling results. We discussed carcinogenic and ecological impact

assessments in depth. The final risk results are validated against National and European guidelines. The results showed no stack tip downwash happening as of the high stack outlet velocity and at a low reference wind speed. The results suggested that the dispersion models commonly used for regulatory applications generally underestimate the lower ranges of pollutant concentrations and overestimate high concentrations in the near field. This study also offered a significant contribution to developing a baseline measurement of the current state of risk from emissions of the ocean-going vessels visiting the port, and suggested that, given the expected development of many Australian ports in the near future, the need for continual monitoring of shipping emissions is an essential and necessary area of research.

Declarations

Declaration of originality and authority of access

This thesis contains no material which has been accepted for a degree or diploma by the university or any other institution, except by way of background information and duly acknowledged in the thesis, and to the best of my knowledge and belief no material previously published or written by another person except where due acknowledgement is made in the text of the thesis, nor does the thesis contain any material that infringes copyright.

This thesis may be made available for loan and limited copying and communication in accordance with the Copyright Act 1968.

……..

Sanaz Jahangiri

Statement of Co-Authorship

The following people and institutions contributed to the publication of work undertaken as part of this thesis:

Sanaz Jahangiri, National Centre for Maritime Engineering & Hydrodynamics, Australian Maritime College, University of Tasmania

Professor Kiril Tenekedjiev, National Centre for Maritime Engineering & Hydrodynamics, Australian Maritime College, University of Tasmania

Professor Natalia Nikolova, National Centre for Ports & Shipping, Australian Maritime College, University of Tasmania

Ushen Kam, Australian Maritime College, University of Tasmania

Dr. Vikram Garaniya, Australian Maritime College, University of Tasmania

Dr. Rouzbeh Abbassi, School of Engineering, Macquarie University

Dr. Hossein Enshaei, Australian Maritime College, University of Tasmania

Professor Richard J. Brown, Biofuel Engine Research Facility, Queensland University of Technology

Thuy C. Van, Biofuel Engine Research Facility, Queensland University of Technology

Dr. Ali M. Pourkhesalian, Biofuel Engine Research Facility, Queensland University of Technology

Professor Zoran Ristovski, Biofuel Engine Research Facility, Queensland University of Technology

Author details and their roles:

Paper 1, < Emission Inventories for Ship Operations: Methodological Comparison with On-board Measurements >:

Located in chapter 2

Candidate was the primary author and she conducted the design of the technique and analysis. Co-authors assisted with refinements and presentation. Candidate was involved in the model development and data analysis.

[Candidate: 70%, KT: 15%, NN: 15 %]

Paper 2, < Empirical Testing of Inventories applying on-board measurements of engine exhaust emissions at port and at sea >:

Located in chapter 2, chapter 3 and chapter 4

Candidate was the primary author and she conducted the design of the technique and analysis. Co-authors assisted with refinements and presentation. Candidate was involved in the model development and data analysis.

[Candidate: 55%, KT: 30%, NN: 15 %]

Paper 3, < An improved emission inventory method for estimating engine exhaust emissions from ships >:

Located in chapter 3

Candidate was the primary author who conducted the design and analysis of the work while all co-authors assisted with refinements and presentation. Candidate was involved in the model development and data analysis.

[Candidate: 75%, KT: 10%, NN: 15 %]

Paper 4, < Emission Inventories for Ship Operations: Methodological Comparison with On-board Measurements >

Located in chapter 3

Candidate was the primary author and conducted the design of the technique and analysis. Co-authors assisted with refinements and presentation. Candidate was involved in the model development and data analysis.

[Candidate: 59%, UK: 20%, VG: 3%, RA: 3%, HE: 3%, RB: 3%, TV: 3%, AP: 3%, ZR: 3%]

Paper 5, < Application of a Developed Dispersion Model to Port of Brisbane>:

Located in chapter 5

Candidate was the primary author and he conducted the design of the technique and analysis. Co-authors assisted with refinements and presentation. Candidate was involved in the model development and data analysis.

[Candidate: 80%, KT: 10%, NN: 10 %]

Paper 6, < Health Risk Assessment of engine exhaust emissions within Australian Ports - A case study of Port of Brisbane>:

Located in chapter 6

Candidate was the primary author and he conducted the design of the technique and analysis. Co-authors assisted with refinements and presentation. Candidate was involved in the model development and data analysis.

[Candidate: 70%, KT: 10%, NN: 20%]

We the undersigned agree with the above stated "proportion of work undertaken" for each of the above published peer-reviewed manuscripts contributing to this thesis:

Signed:

Prof. Kiril Tenekedjiev

(Primary Supervisor)

Australian Maritime College

University of Tasmania

Date: 15/05/2019

Signed:

Mr. Michael van Balen

(Principal)

Australian Maritime College

University of Tasmania

Date: 15/05/2019

3

9

9

Statement of published work contained in the thesis

The publishers of the research articles comprising the Chapters 2-6 hold the copyright for that content, and access to the material should be sought from the respective journals and conference proceedings. The papers are published at the time of writing and may be made available for loan and limited copying and communication in accordance with the Copyright Act 1968.

The following researchers contributed to the publication of work undertaken as part of this thesis:

- Sanaz Jahangiri, (**Candidate**) – Australian Maritime College, University of Tasmania, Launceston, Australia.
- Prof. Kiril Tenekedjiev, (**KT**) – Australian Maritime College, University of Tasmania, Launceston, Australia.
- Prof. Natalia Nikolova, (**NN**) – Australian Maritime College, University of Tasmania, Launceston, Australia.
- Dr. Rouzbeh Abbassi, (**RA**) – School of Engineering, Macquarie University, Sydney, Australia and Australian Maritime College, University of Tasmania, Launceston, Australia.
- Mr. Ushen Kam, (**UK**) – Australian Maritime College, University of Tasmania, Launceston, Australia.
- Dr. Vikram Garaniya, (**VG**) – Australian Maritime College, University of Tasmania, Launceston, Australia.
- Dr. Hossein Enshaei, (**HE**) – Australian Maritime College, University of Tasmania, Launceston, Australia.
- Prof. Richard J. Brown, (**RB**) – Biofuel Engine Research Facility, Queensland University of Technology, Brisbane, Australia.
- Mr. Thuy C. Van, (**TV**) - Biofuel Engine Research Facility, Queensland University of Technology, Brisbane, Australia.
- Dr. Ali M. Pourkhesalian, (**AP**) - Biofuel Engine Research Facility, Queensland University of Technology, Brisbane, Australia.
- Prof. Zoran Ristovski, (**ZR**) - Biofuel Engine Research Facility, Queensland University of Technology, Brisbane, Australia.

Chapter 2 – (part of Paper 1 – published in the IAMU 2018 Conference and part of Paper 2 – published in the Journal of Sustainable Development of Transport and Logistics)

Paper 1: Emission Inventories for Ship Operations: Methodological Comparison with On-board Measurements

Candidate was the primary author and she conducted the design of the technique and analysis. Co-authors assisted with refinements and presentation. Candidate was involved in the model development and data analysis.

[Candidate: 70%, KT: 15%, NN: 15 %]

Paper 2: Empirical Testing of Inventories applying on-board measurements of engine exhaust emissions at port and at sea

Candidate was the primary author and she conducted the design of the technique and analysis. Co-authors assisted with refinements and presentation. Candidate was involved in the model development and data analysis.

[Candidate: 55%, KT: 30%, NN: 15 %]

Chapter 3 – (part of Paper 2 – published in the Journal of Sustainable Development of Transport and Logistics & Paper 3 – published in the Journal of Sustainable Environment Research & Paper 4 – published in the Coasts & Ports 2017 Conference)

Paper 2: Empirical Testing of Inventories applying on-board measurements of engine exhaust emissions at port and at sea

Candidate was the primary author and she conducted the design of the technique and analysis. Co-authors assisted with refinements and presentation. Candidate was involved in the model development and data analysis.

[Candidate: 55%, KT: 30%, NN: 15 %]

Paper 3: An improved emission inventory method for estimating engine exhaust emissions from ships

Candidate was the primary author who conducted the design and analysis of the work while all co-authors assisted with refinements and presentation. Candidate was involved in the model development and data analysis.

[Candidate: 75%, KT: 10%, NN: 15 %]

Paper 4: Development of Emission Factors for Ships' Emissions at Berth

Candidate was the primary author and she conducted the design of the technique and analysis. Co-authors assisted with refinements and presentation. Candidate was involved in the model development and data analysis.

[Candidate: 59%, UK: 20%, VG: 3%, RA: 3%, HE: 3%, RB: 3%, TV: 3%, AP: 3%, ZR:3%]

Chapter 4 – (part of Paper 2 – published in the Journal of Sustainable Development of Transport and Logistics)

Paper 2: Empirical Testing of Inventories applying on-board measurements of engine exhaust emissions at port and at sea

Candidate was the primary author and she conducted the design of the technique and analysis. Co-authors assisted with refinements and presentation. Candidate was involved in the model development and data analysis.

[Candidate: 55%, KT: 30%, NN: 15 %]

Chapter 5 – (Paper 5 – published in the Journal of American Environmental Sciences)

Paper 5: Application of a Developed Dispersion Model to Port of Brisbane

Candidate was the primary author and he conducted the design of the technique and analysis. Co-authors assisted with refinements and presentation. Candidate was involved in the model development and data analysis.

[Candidate: 80%, KT: 10%, NN: 10 %]

Chapter 6 – (Paper 6 – published in the Journal of Environmental Practice)

Paper 6: Health Risk Assessment of engine exhaust emissions within Australian Ports - A case study of Port of Brisbane

Candidate was the primary author and he conducted the design of the technique and analysis. Co-authors assisted with refinements and presentation. Candidate was involved in the model development and data analysis.

[Candidate: 70%, KT: 10%, NN: 20%]

Acknowledgements

I am grateful to my mother and father, brother and sister-in-law, who have provided me moral and emotional support in my life. My gratitude also goes to other extended family members and friends who have supported me along the way.

A very special gratitude goes out to all colleagues at the Australian Maritime College (University of Tasmania) for helping and providing the academic guidance, support and helping me secure the funding for my PhD studies.

My special note and thanks goes to my current supervisory team - Prof. Kiril Tenekedjiev, Prof. Natalia Nikolova and Dr. Rouzbeh Abbassi. It was fantastic to have the opportunity to work my research under your supervision. What an unfolding experience to go through!

And finally, last but by no means least, also to everyone in the research hub. It was great sharing the hub with all of you during last three years.

Thanks for all your encouragement!

To my life-coach, my grandmother, Taj Arvani

Table of Contents

List of Figures

List of Tables

Abbreviations

AB	at berth
AC	air consumption
AE	auxiliary engine
AGA	Annual General Assembly
AIS	automatic identification system
AMC	Australian Maritime College
AS	actual speed
BC	black carbon
BC	British Columbia
BOM	Bureau of Meteorology
BSFC	brake-specific fuel consumption
CARB	California Air Resources Board
CH_4	methane
CO	carbon monoxide
CO_2	carbon dioxides
CRF	concentration-response function
DM	decision maker
DR	dilution ratio
E	Emission
ECA	emission control area
EF	emission factor
EMFR	exhaust mass flow rate

EMS	emission registration and monitoring shipping
EPA	Environmental Protection Agency
ER	emission rate
GHG	greenhouse gas
GRT	gross registered tonnage
HAP	hazardous air pollutant
HC	hydro carbon
HFO	heavy fuel oil
HSD	high speed diesel
IAMU	International Association of Maritime Universities
IARC	International agency for research on cancer
ILCR	incremental lifetime cancer risk
IMI	international maritime industry
IMO	International Maritime Organization
ISO	International Standards Organization
IVC	intake valve closing
LF	load factor
LNG	liquified natural gas
LPM	Lagrangian particle model
MAD	mean absolute deviation
MCC	mixing controlled combustion
MCR	maximum continuous rate
MDO	marine diesel oil
ME	main engine

MEET methodology for emissions and energy consumption for transport

MOPSEA monitoring programme on air pollution from sea-going vessels

MMA Maine Maritime Academy

MSD medium speed diesel

NEPM National environment protection measure

NERI National Environmental Research Institute

NNE north-northeast

NO nitrogen monoxide

NOAA National Oceanic and Atmospheric Administration

NO_2 nitrogen dioxides

NO_x nitrogen oxides

N_2O nitrous oxide

OC organic carbon

OGV ocean-going vessel

P installed power

PM particulate matter

$PM_{2.5}$ particulate matter that have a diameter of less than 2.5 micrometres

$PM_{10.0}$ particulate matter that have a diameter of less than 10.0 micrometres

P_{act} actual engine power

PMC premixed combustion

PRM plume rise module

QUT Queensland University of Technology

RPM revolutions per minute

RSZ reduces speed zone

S sulphur

SFOC specific fuel oil consumption

SLPM standard litre per minute

SMED Swedish methodology for environmental data

SO_x sulphur oxides

SOC specific oil consumption

SS shaft speed

SSD slow speed diesel

SSW south-southwest

STEAM ship traffic emission assessment model

UK United Kingdom

USEPA United States Environmental Protection Agency

V vanadium

VOC volatile organic compounds

UTM universal transverse Mercator

UTC universal time coordinated

WHO World Health Organization

Chapter 1: Introduction to the research project

1.1.Background and rationale

Transportation of cargo and crude oil by ships dates back many years and has played a vital role especially in transferring oil from the Middle East all over the world (Ducruet and Wang 2018). Today, maritime transport is still recognized as the most preferred mode of global transport for goods transfer (Siddiqui, Verma et al. 2018). Several reasons have contributed to its long lasting popularity, including transportation via ship, recognised to be a cost effective option in comparison to other modes of transport due to the large payload it can carry (Kruse, DeSANTIS et al. 2018). In addition, shipping is also a relatively safe transport option (Chen, Zhang et al. 2018) and is regarded as one of the most environmentally friendly modes of transportation producing less emissions in comparison to road and rail transport (Chen, Zhang et al. 2018). With its current popularity, the number of sea-going vessels are forecasted to grow continuously over the years (Unctad 2014).

With the increase in vessel operations arises the significance of pollution due to shipping operations spawned by the tendency to consume low quality fuel oil (Deniz and Kilic 2010). Hence, it is vital to track the emissions and understand their potential effect on the surrounding environment. However, unlike land-based emissions which are monitored by stringent rules and regulations, the shipping sector still lacks reliable approaches to monitor and estimate shipping emissions a factor crucial in improving environmental performance (California Air Resources Board 2005, Corbett, Winebrake et al. 2007). Shipping operations are known to release large amounts of primary pollutants in atmosphere including Carbon Dioxide (CO_2), Carbon Monoxide (CO), Nitrogen Oxides (NO_x), Sulphur Oxides (SO_x), Particulate Matters (PM) and Volatile Organic Compounds (VOC) (Eyring, Kohler et al. 2005). Concerns have been sparked over these shipping emissions that are associated with adverse effects on human health and the surrounding environment. For example, NO_2 and CO emissions result in flu like symptoms, while SO_x-emissions cause breathing issues and premature births. Many statistics have also revealed asthma cases, heart related diseases and premature deaths (Lu, Brook et al. 2006, Kim, Hwang et al. 2010). In addition, researchers (Corbett, Winebrake et al. 2007) reported lung cancer deaths and heart attacks that have been recorded worldwide due to PM

emissions in the port areas of Europe, East Asia and South Asia. Many studies (Kilic and Deniz 2010, Merk 2014, Moreno-Gutierrez, Calderay et al. 2015) reviewed shipping emissions and their impacts based on several methodologies on different scales, namely in different ports and countries. Researchers (Corbett and Koehler 2003, Rakopoulos and Giakoumis 2009) reported that ocean-going vessels account for 14-31 % global emissions of NO_x, 4-9% SO_x and 3% CO_2 worldwide. A previous study (Merk 2014) also reported that CO_2 from shipping emissions are responsible for approximately 2-3% of global emissions which is higher than the amount of non-GHG emissions; while SO_x and NO_x are responsible for 5-10 % and 17-31% respectively. A detailed study carried out on shipping emissions (Blasco, Duran-Grados et al. 2014) also reported similar results. With the increase in the global fleet of vessels in operation, these emissions are forecast to largely increase over the coming years. It is predicted that primary emissions will increase about four times with ship numbers tripling by 2050 (Corbett and Koehler 2003). Recently, it has also anticipated that CO_2 could increase by 50% and 250% of the current emissions by the year 2050 (Ristovski, Miljevic et al. 2012). Considering their alarming health risks to both the ecological entities and humans residing in the surrounding port areas, it is highly important to address the situation and implement solutions that are able to consider and measure shipping emissions precisely. Hence, estimating and evaluating the shipping emissions has become an increasing concern.

Currently, several methods for estimating the emissions from ocean going ships exist. Online monitoring of ship emissions is one of these methods. It may provide on-board data on a continuous real time basis; however, this method suffers from the lack of appropriate instrumentation and reliability (Radischat, Sippula et al. 2015). The other approach is ship plumes-based measurements, which is an on-board measurement carried out on a specific vessel. It provides real time emissions data of the vessel. However, this approach is costly in time and human resources, and it is also challenging trying to engage the vessel owners to install the necessary measurement instrumentation (Chen, Huey et al. 2005, Cappa, Williams et al. 2014). Many previous studies reviewed on-board measurement (LIyods 1990, LIyods 1995, Cooper, Peterson et al. 1996, Wright 1997, Cooper and Andreasson 1999, Lyyranen, Jokiniemi et al. 1999, Skjølsvik, Andersen et al. 2000, Cooper 2001, Endresen, Sorgard et al. 2003, Sinha, Hobbs et al. 2003, Petzold, Feldpausch et al. 2004, Chen, Huey et al. 2005, Kasper, Aufdenblatten et al. 2007, Petzold, Hasselbach et al. 2008). Petzold et al. (Petzold, Hasselbach et al. 2008) worked on a 4-stroke engine type, while Kasper et al. (Kasper, Aufdenblatten et al. 2007) put the focus on PM emissions of a 2-stroke marine engine type.

Lloyds (LIyods 1990, LIyods 1995), and Corbett et al. (Corbett and Koehler 2003) considered different emissions in various engine types. Researchers (Cooper, Peterson et al. 1996, Cooper 2001, Cooper 2003) studied the emissions from the MEs and AEs of ferries. Some studies (LIyods 1990, LIyods 1993, Wright 1997, Lyyranen, Jokiniemi et al. 1999, Petzold, Feldpausch et al. 2004, Kasper, Aufdenblatten et al. 2007, Petzold, Hasselbach et al. 2008) reported their findings on SSD and MSD engines on test rigs. Many factors affect ship emissions such as; type of ship, type of engine, operations etc. Most on-board measurement datasets from international shipping statistics and global standards tend to ignore shipping emission measurements in port, and accordingly inconsistent emission predictions are faced near shore (LIyods 1990, LIyods 1993, LIyods 1995, Corbett and Koehler 2003). Hence, more updated and detailed on-board measurement emission factors (EF) s in terms of fuel type, fuel parameters, regions of study, vessel characteristics, engine specifications, and in-port activities need to be considered. Although the methodology is precise due to real-time emission measurement, using on-board measurement is not always possible due to time and human resource restrictions. It is also challenging to engage vessel owners to install the necessary measurement instrumentation (Chen, Huey et al. 2005, Cappa, Williams et al. 2014).

Therefore, the emission inventories are the most commonly applied method to estimate ship emissions (Skjølsvik, Andersen et al. 2000, Endresen, Sorgard et al. 2007, Dalsoren, Eide et al. 2009). Numerous considerations are considered in creating these emission inventories, such as the region of study, the vessel characteristics, engine specifications, ship modes, etc.

To advocate for accurate estimation of total emissions due to shipping activities, several available methodologies are developed by different researchers. In this study, a total of 13 inventory methodologies are reviewed which includes; the Tier I-III (named after IMO NO_x Technical Code) (Trozzi and DeLauretis 2013), the methodology applied by Corbett et al., ENTEC (one of the UK's largest environmental and engineering consultancies) (Entec 2007), Methodology for calculating Transport Emissions and Energy consumption (MEET) (Auth, Tuv et al. 1999), Ship Traffic Emission Assessment Model (STEAM) (Jalkanen, Brink et al. 2009), Monitoring Programme on Air Pollution from Sea-going Vessels (MOPSEA) (Gommers, Verbeeck et al. 2007), International Maritime Organisation (IMO) (IMO 2014), Swedish Methodology for Environmental Data (SMED) (Cooper, Gustafsson et al. 2004), Emission Registration and Monitoring Shipping (EMS) (Van der Gon, Tno. et al. 2010), US Environmental Protection Agency (USEPA) (USEPA 2008), and National Environmental

Research Institute (NERI) (Olesen, Winther et al. 2009). These methodologies can be summarised and categorised into three groups, namely a full bottom-up approach, a full top-down approach, or a combination of both, as suggested by Miola et al. (Miola and Ciuffo 2011). These approaches are characterised based on the emissions evaluation and the geographical characterisation. A full bottom-up approach evaluates the emissions by a single ship, considering vessel characteristics (i.e. ship type, building date, engine load and power, specific fuel oil consumption) at a specific position (Moreno-Gutierrez, Calderay et al. 2015). This approach allows the primary contributors of the emissions to be detected and assessed, thus providing a clear understanding of the effects on the primary emissions. Corbett et al., ENTEC, STEAM, MOPSEA, NERI, EMS, US EPA, and SMED also fall into this category. On the other hand, a fully top-down approach considers the emissions from a more global scale, employing generalized factors such as fuel usage statistics of different fuel types and engine types installed on specific vessels as indicators of emissions (Miola and Ciuffo 2011). While none of the discussed methodologies in this thesis considered a full top-down approach, Tier I-III are top-down in terms of emission inventory, and bottom-up in terms of geographical distribution. Meanwhile MEET and IMO estimate emissions based on a bottom-up emission inventory and top-down based on the geographical distribution. Ultimately, each of these methodologies have reported a set of emission factors that are used as the key element in the calculation of the pollutants emitted for the comparative analysis. Most of these methodologies comprised inconsistent factors and assumptions including fuel consumption, navigation areas, ship modes, engine and vessel specifications which cause different variability in emission. Hence, it is necessary to find the most appropriate emission inventory methodology in terms of considered factors and assumptions.

Whichever approach is adopted, each inventory method predicts a set of emission factors (EF) s that will deviate from the experimental measurement values. The main reason for the observed discrepancies between the observed and predicted EFs is that most of the inventories are developed under specific assumptions that include fuel type, consumption units of fuel, ship navigation locations, types of ships, the nature of engines, type of the vessels, etc., which in any particular case will be different from the actual one. It is therefore important to develop a good-enough emission inventory mechanism that is premised on the factors and assumptions which are as close as possible to the actual factors and assumptions for the vessel whose EFs are to be predicted.

Moreover, utilising the quantified emissions within the area of interest, an atmospheric dispersion modelling based on the local meteorological and geographical conditions needs to be considered to simulate the dispersion of the engine exhaust emissions within Australian Ports. An atmospheric dispersion model mathematically simulates the physics and chemistry governing the fate, and transport of pollutants in the atmospheric environment. Dispersion models can take many forms from graphs to numerical formulae. These models most normally appear in the form of computer algorithms, easy to use interfaces and online help facilities.

The process of air pollution modelling contains four stages (data input, data processing, data output, and data analysis). The accuracy and uncertainty of each stage must be determined and evaluated to ensure a reliable assessment of the significance of any potential adverse effects. In the data input stage, the effective parameters are background concentration of the pollutant, the source data including site description and emission rate, the model options including receptor grid, and dispersion parameters, and local topographical features. The data processing stage is the type of the selected atmospheric dispersion model, based on the input data and the modelling itself. The data output stage is then the prediction of ground level concentrations of pollutants. Finally, the data analysis stage deals with the assessment of potential environmental and health effects.

Several dispersion models exist, depending on the size and complexity of the domain and the type of pollutant source. The Gaussian-plume models require less computational time and resources. These models require only simplified meteorological and geographic datasets. Different Gaussian models such as AERMOD, AUSPLUME and ISCST3 were developed and validated by different researchers (Cohan, Wu et al. 2011, Zadakbar, Abbassi et al. 2011, Abrutyte, Zukauskaite et al. 2014). These approximate plume behaviour mathematically in a most straightforward way. The models incorporate a simplistic description of the dispersion process; though fundamental assumptions made result in non-accurate reflection of the reality. Limitations in Gaussian-plume models may produce not accurate dispersion results for many types of sources:

- Ignoring the real transport time (that may be several hours) by assuming the pollutant material is transported instantly to receptors. They do not consider that wind may only be blowing at a constant speed.

- Inverse dependency of the steady-state plume equation to the wind speed, the models fail during low wind speed or calm conditions.
- Overwriting or ignoring input data below a minimum wind speed set of 0.5 or 1.0 m/s.
- Overestimating terrain impingement effects during stable conditions in moderate terrain areas by not considering turning or rising wind caused by the terrain itself.
- Considering transport and dispersion conditions uniform long enough across the entire modelling domain limits the practical conditions which is rarely truly uniform for the material to reach the receptor.

- Being memory-less when calculating ground-level concentration in each hour limits an accurate simulation of inversion break-up in the mornings, fumigation and also diurnal recycling of pollutants over cities.

Most researchers (Bluett, Gimson et al. 2004, NSWEPA 2005, Holmes and Morawska 2006) agree that atmospheric modelling of coastal regions provides a challenge due to the complex meteorological conditions present at different sites. The ability of simpler Gaussian-plume models in these conditions is questionable and suggests the need to use more advanced puff or Lagrangian based models.

Most advanced air pollution models calculate the pollutant concentration downwind of a source using the following parameters:

- Contaminant emission rate;
- Emission source characteristics;
- Local topography;
- Area meteorology;
- Ambient or background concentrations of pollutant.

A number of more advanced dispersion models have been developed to overcome the short comings of steady-state Gaussian-plume models (Scire, Strimaitis et al. 2000). Lonati et al. (Lonati, Cernuschi et al. 2010) demonstrated the adaptability of the CALPUFF model in evaluating the impact of the development of a new port in the Mediterranean Sea. Different primary pollutants such as NO_x, SO_x, PM, CO and heavier volatile organic compounds (VOCs) were modelled based upon predicted vessel traffic to the port. The vessel traffic was estimated based on the forecast total cargo throughput of the port calculated from local industry. The

predicted concentrations within the region of interest can be considered as both annual averages and daily averages. The data averaged annually is also considered with more weighting considering uncertainties in the input data. Moreover, the nature of puff modelling in CALPUFF means it is time-dependent and capable of predicting emissions over long ranges (> 50km). This also means the model can deal with both complex terrains and meteorological conditions, making it suitable for coastal regions and areas of widely varying wind conditions. The downside of this is increased input data required.

Also, regarding the mentioned significant health risk from emissions of OGVs to populations surrounding ports as well as damaging the environment, a risk-based framework will be needed to be developed to assess the impact of the shipping emissions on human health and ecological entities in surrounding environment. This could also assist upgrading decision-making policies regarding air pollution monitoring and management.

Health risk assessment is the process of estimating the potential impact of a chemical, physical, microbiological or psychosocial hazard on a given human population or ecological system, under a specific set of conditions and within a particular time frame (EnHealth 2012). The assessment follows strict common sense and can be applied to a whole series of rules or procedures (WHO 2000).

The current risk assessment methods, however, do not allow actual estimates of low levels of exposure to environmental hazards, which means that emissions from international ships increasingly focus on proposed regulations in local, national, and international contexts (Bailey and Solomon 2004, California Air Resources Board 2006). However, regulatory deliberations have not been adequately informed since the extent of the health effects of shipping emissions has been unknown. Previous evaluations of regional shipping health impacts focused on European or Western United States regions and ignored short- and long-range Southern hemispheric pollutant transport (California Air Resources Board 2006), which undermined the global impact of shipping in local and regional jurisdictions and does not inform international policy-making correctly. Therefore, during the presentation of numerical calculations of risks, caution should be taken while assigning strict meaning to the numbers. The accuracy of differential risks estimates can be influenced by exposed population and variability in the environmental agents, inherent limitations in toxicological data, and the complexity of the

exposure conditions. During quantification of some components such as exposure assessment and collection of data all uncertainties should be reflected in the risk assessment outcomes.

There are two types of risk assessment: qualitative and quantitative. Qualitative assessment relies on professional judgement; it is simple, rapid and can be very useful. The risk level can subsequently be explained either quantitatively or qualitatively (by categorising risks into low, medium, and high). The approach utilised in AS/NZS ISO 31000:2009 is the practical guidance on risk management (Standards Australia 2009). This study, however, adopts a quantitative assessment to calculate risks, which does not rely heavily on judgment. This type of approach is more reliable as it takes into account the complexity of the process a lot more than it is possible with a qualitative approach (Department of the Environment 2016). The quantitative study approach used in the research involves computation of final risk value from the far and the near fields' concentrations i.e. low levels of environmental hazards exposure for the case study of the Port of Brisbane. The perspective includes the Gaussian plumes and outcomes from CALPUFF dispersion modelling regarding the results from the health impact evaluation, short-term and long-term guideline validation assessment, ecological effects, and estimation of carcinogenic risks from the diesel particulate. CALPUFF is an advanced dispersion modelling used in estimating emissions of long-range transports from an area, point, lines, and volume sources. The source-receptor distances range from 50 km to several hundred kilometres. CALPUFF can produce hourly files on ambient concentrations for every species in the model including extinction coefficient and both dry and wet deposition fluxes. The extinction coefficient is associated with visible applications.

There are three tiers to quantitative risk assessment. The tiered approach provides means for assessing an issue under consideration with an appropriate complexity level. Each tier supplies an equal degree of health protection. The level of uncertainty decreases with a growth in the number of assessment details, and the conceptual comprehension of the site condition is refined. As a result, the degree of caution that should be substituted for knowledge in the process of risk assessment is reduced.

- **Tier I** – it considers a particular amount of data and several guideline values. The assessment notes if the risk falls above or below the guideline. In some cases, circumstance requires an approach to be formed based on a specific issue or site due to the complexity and costs of contemporary environmental health risk. Tier 1,

which is the most straightforward perspective, is supposed to be the first screening-type evaluation of vulnerability utilising the conservative default exposure parameter estimate and comparing it to the published health guidelines. A prudent or conservative approach means assessing and managing the uncertainties inherent in a risk assessment that reduce the likelihood of harm.

- **Tier II** – it involves more modelling, extra data, and a deeper understanding of the situation and evaluates the risks involved. The approach works in terms of calculations and considers parameters and data sets.
- **Tier III** – it is significantly more complicated. Studies at this level may take years and can involve personal monitors when people observe their exposure to a hazard under investigation (EnHealth 2012). Tier III can include a much greater amount of detail and be probabilistic such as in Monte Carlo simulations. Tier III evaluations are rare, partly due to the tendency of any risk assessment to move gradually from tier I but also because if tier I indicates that risk is acceptable, then there is no point in moving to tier II.

Tier II and III procedures require the collection of extra data on exposure and a detailed analysis and evaluation of data on dose response. These tiers involve computation of dosage on target tissues or translating dosages for animals to humans. Most jurisdictions uphold the tier approach of assessment for risks, but the correct usage and number of tiers varies.

A tier II assessment is applied in this study, if concentrations and ship stacks are port-wide, and their final calculations are validated with available guidelines.

Exposure pathways are the processes that take a chemical or another agent into the environment from its release point to a situation in which a person becomes exposed. The routes of exposure are often reasonably obvious, but there may be some less obvious cases, such as the movement of contaminated groundwater or volatile chemicals from contaminated groundwater. The development of this process can be beneficial in identifying and quantifying the pathways of exposure. The identification of concentrations and their risk to the population around Port of Brisbane were carried out regarding existing sensitive receptors. In formulating the scope of the problem, the chemicals to focus on and their sources, the pathway that connects the sources

and receptors in a risk scenario for engine exhaust shipping emissions (air emissions) is inhalation.

1.2. Problem definition and objectives

Ship emissions, which include gaseous particles and particulate matter (PM), have negative effects on both environmental and public health (Corbett, Winebrake et al. 2007, Blasco, Duran-Grados et al. 2014, Mueller, Jakobi et al. 2015, Reda, Schnelle-Kreis et al. 2015). Viana et al (Viana, Hammingh et al. 2014) investigated and found that shipping related emissions are one of major contributors to global air pollution, especially in coastal areas. They cause an increase in the levels and composition of both particulate and gaseous pollutants and the formation of new particles in densely-populated regions (Gonzalez, Rodriguez et al. 2011, Viana, Hammingh et al. 2014). This is obvious as over 70% of ship emissions may spread 400 km inland and significantly contribute to air pollution in the vicinity of coastal areas and harbors (Eyring, Isaksen et al. 2010). As a result, Corbett et al (Corbett, Winebrake et al. 2007) estimated that annually shipping-related $PM_{2.5}$ emissions are the causes of approximately 60,000 deaths associated with cardiopulmonary and lung problems around the world. Most deaths occur in highly populated and PM concentration areas such as Asia and Europe, and the number of annual mortalities were predicted to increase 40% by 2012 (Corbett, Winebrake et al. 2007). Moreover, shipping activities significantly contribute to ocean acidification (Hassellov, Turner et al. 2013). Therefore, quantitative and qualitative estimation of pollutant emissions from ships and their distribution are becoming more significant (Blasco, Duran-Grados et al. 2014). Another concern relating to shipping transportation is the fuel used. Heavy fuel oil (HFO), which contains many impure compositions such as sulphur and metals, are used by almost all ships owing to the economic benefit (Mueller, Jakobi et al. 2015). Corbett (Corbett and Koehler 2003) has estimated that approximately 80% of fuel consumed by the world ship fleet is HFO. This calls for the need of research into ship emission related issues.

Emissions from ships are regulated by the International Maritime Organisation (IMO) through Annex VI of the International Convention for the Prevention of Pollution from Ships – the Marine Pollution Convention (MARPOL) (IMO 1997). Continued implementation of the amendments to the MARPOL Annex VI is an attempt to reduce ship emissions on a global scale (IMO 2008a, IMO 2008b, IMO 2011). Main regulations to limit sulphur content of any fuel oil used on board and NO_x emissions are being implemented. In European areas,

regulations for ship emissions are more stringent than in other places. In particular, from January 1st 2010, European directive requires all ships at berth or anchorage in European harbours to use fuel oil with sulphur content of less than 0.1% by weight (European Parliament 2005). However, further regulation should be implemented because the fuel shift to low sulphur was insufficient to reduce small-sized PM emissions (Winnes and Fridell 2009).

This research aims to achieve five main objectives:

- Demonstrate real time in-vessel continuous emissions measurements of Particulate Matter (PM), NO_x, SO_x, CO_2, HC and CO measurements using portable gas instrumentation including PM size distributions.
- Identify the best vessel-specific inventory family to predict primary emissions from ocean-going vessels when at berth, while maneuvering and while cruising and create generalized rational algorithm to rank inventory families based on the precision of their predictions for a given operational mode of a specific vessel
- Develop more accurate models for emission inventories in shipping operations by considering different environmental and operational factors and offer a novel future policy for cost-effective and reliable emission estimation caused by shipping.
- Apply a validated and complex atmospheric dispersion modelling to the quantified data to predict the ground-level concentrations of gaseous pollutants and the deposition of particulate matter, based on local meteorological and geographical conditions.
- Develop a risk-based framework to assess the impact of the shipping emission on human health considering the local metrological and geographical conditions.

1.3.Methodology

The methodology utilised to solve the research objectives of this project could be broken down into six main phases.

PHASE 1

The Measurements of emissions were taken on-board following the procedures elaborated in ISO 8178-2:2008 and ISO 8178-1:2006. The on-board emission measurement campaign was divided into 4 separate experiments. The first one was to measure the NO_x, SO_x, CO_2, and CO emissions from the auxiliary engines when the vessels were at berth. The second, third, and fourth experiment were to measure the NO_x, SO_x, CO_2, CO, HC, and PM emissions from the ME when the vessels was at berth, maneuvering, and cruising respectively. For the main engine experiments the probes of the exhaust gas were sampled between the turbocharger and the economizer of the ME. To cool the probe for PM measurement, the sample was diluted with air. The rates of the samples' dilution were estimated by comparing the CO_2 emission rate in the initial sample with, the CO_2 emission rate of the diluted sample measured with Sable CA-10 CO_2 monitor. Simultaneously the shaft speed and the actual engine power were measured every 5 sec. The specific oil consumption was determined as a quadratic function of the engine load factor (the actual engine power measured in % of the maximum continues rating of the engine). The average air consumption was assessed as a linear function of the load factor. The instantaneous exhaust mass flow rate was assessed as the sum of the air consumption with the product of specific oil consumption and engine power. For the auxiliary engine experiments, the probes of the exhaust gas were sampled after the turbocharger. The measurement equipment was Testo 350 XL only. In this experiment HC, and PM were not measured. The shaft sped, engine power, specific oil consumption, air consumption and exhaust mass flow rate were obtained as in the main engine experiments.

PHASE 2

The minimal mean absolute deviation criterion was applied to rank the inventory families under operational mode of the vessel. The preferences of any decision maker over a specific inventory family for a selected operational mode of a given vessel will depend only on the deviations of the inventory prediction emissions from the six emissions measured in the on-board experiment. The parameters in the terminology of decision analysis are called attributes. We then needed to rank those vectors for each of the

operational modes of a vessel. We implicitly substituted the missing values with the mean of the known absolute deviations (that is with mean absolute deviation).

We then used the mean absolute deviation criterion to marginalize the stated six-dimensional preference problem into a one-dimensional ranking problem. Completely rational decisions can be obtained if a value function is built, which accurately reflects the preferences of the decision making. The function will be additive because the decision making holds the mutual preferential independence over the 6 attributes: from two inventories, the decision making will prefer the one which has more favorable deviation for any attribute, if the rest of the attributes are pair-wise equal. The inventories must be then ranked in descending order of the value function. The value function is normalized in the closed interval [0; 1] in a sense that it should be 1 if all deviations are 0% (the best-case scenario) and it should be 0, if all deviations are -100% (the worst-case scenario).

Alternatively, the decision making may use one and the same function over each attribute for each mode, since they all measure the opinion of the decision making regarding the precision of predictions. The form of the attribute value functions depends solely on the preferences of the decision making. There is not much discussion in literature regarding the rational construction of value functions. However, as far as value functions are a special case of utility functions under risk, then the techniques for construction of such functions may be adopted for the case of value functions.

The weight coefficients in the value function then measure the importance of each pollutant in the overall assessment of preferences over emission inventories. It is only natural to expect that pollution levels have different significance depending on the regime – pollution close or in ports are causing more direct harm than emissions while at sea, while still the pollution is of global importance. There are elaborate methods to elicit the weight coefficients, which are nothing else but scaling constants in the utility theory. Scaling constants are elicited subjectively, where the decision making must identify the probability, which makes him/her indifferent when comparing.

PHASE 3

Constructing the value functions, we will then be able to choose which inventory method is the best (most preferred) for each operational mode. The following algorithm can be utilized to select the best inventory method for a given type of ship operation:

1. Define the vector of deviations $\vec{\Delta} = (\Delta NO_x, \Delta SO_x, \Delta CO_2, \Delta CO, \Delta HC, \Delta PM)$ for each inventory method (with at least five emission deviations calculated).
2. Impute missing values in the vector of deviations by replacing them with the mean of the known deviations' absolute values.
3. Construct the attribute value functions $v_i(.)$ for the selected type of operation.
4. Elicit the scaling constants a_i for i=1, 2, …, 6 for the selected type of operation.
5. Construct the value function v as function of six attributes and their scaling constants.
6. Calculate $v(\vec{\Delta})$ for each of the deviation vectors from step 1).
7. Choose the inventory family that has the highest value, calculated in step 6).

While our algorithm assumes we need at least five calculated deviations (in step 1), this requirement may be modified and is prescriptive, not mandatory. If all six deviations are calculated, then step 2 of the above algorithms will be obsolete.

PHASE 4

Establishing a methodology to determine an improved new sets of emission factor equations through non-linear regression analysis, to help improve emission models and inventory calculations for different main and auxiliary engine types for at-sea and in-port operations.

PHASE 5

Applying a complex atmospheric dispersion modelling - CALPUFF based on local meteorological and geographical conditions to assess ground-level concentrations at receptors surrounding the sources as well as quantifying the dispersion and deposition of these emissions, considering their distribution across the local population mass.

PHASE 6

Assessing the risk of these emissions, a methodology has been developed based on modifying the Australian Environmental Health Risk Assessment Framework. The methodology includes a detailed inventory of in-port and at-sea emissions using an activity-based approach applying Downwash and Near-field as well as the Air-shed areas from CALPUFF dispersion modelling results for Port of Brisbane in the calendar year 2013. The final risk values are compared against National and European guidelines. Various Health impact assessments as well as carcinogenic and ecological effects are discussed in depth.

1.4.Research novelty

Particulate, gaseous emissions and volatile organic compounds from ships have attracted increasing attention for their potential impacts on air quality (Gaston, Quinn et al. 2013, Aksoyoglu, Baltensperger et al. 2016, Marelle, Thomas et al. 2016), climate change (Olivié, Cariolle et al. 2012, Liu, Fu et al. 2016), and human health (Brandt, Silver et al. 2013, Broome, Cope et al. 2016). Ocean-going cargo vessels contribute significantly to global air pollutant emissions from ships, accounting for 84, 88, and 87% of global marine NO_x, SO_x, and $PM_{2.5}$ emissions, respectively (Johansson, Jalkanen et al. 2017). Measurements of ship emission rates for particulate, gaseous components and volatile organic compounds are essential for compiling emission inventories and quantifying the impacts of emissions on air quality, climate change, and human health. In the last decade, numerous measurement campaigns have been conducted to determine emission rates for ocean-going vessels. The emission rates measured for regulated pollutants such as SO_2 and NO_x (Agrawal, Malloy et al. 2008, Agrawal, Welch et al. 2008, Agrawal, Welch et al. 2010, Khan, Ranganathan et al. 2013) are comparable to Lloyds service data (ENTEC UK Limited 2002) and emission estimates from the USEPA (USEPA 2009) and CARB (California Air Resources Board 2008). Recent studies have also focused on emissions of unregulated chemical compounds (Agrawal, Malloy et al. 2008, Agrawal, Welch et al. 2008, Moldanova, Fridell et al. 2013); correlations between such compounds and various fuel types (Jayaram, Agrawal et al. 2011, Lack, Cappa et al. 2011, Celo, Dabek-Zlotorzynska et al. 2015), engine loads (Agrawal, Welch et al. 2010, Sippula, Stengel et al. 2014). However, in comparison to on-road vehicles, emissions of particulate and gaseous species from HFO-fueled vessels remain poorly understood, especially under real-

world operating conditions. The measurements of these increasing emissions are relatively few with the absence of the data in Australian waters. On-board measurement studies only focused on part of a whole ship voyage such as at-berth, manoeuvring, or ocean-going, and to our knowledge none of them investigated the whole ship journey. Further on-board measurement studies need to be carried out to improve the quality of the data on ship emission factors and contribute to the limited ship emission databases, especially for a whole ship voyage.

Measurements were taken in October and November 2015 on two large cargo ships at the Ports of Brisbane, Gladstone, and Newcastle. The first on-board measurement was performed on CSL vessel I (to ensure confidentially the identity of ship is suppressed) from 26th to 31st of October, 2015 when she was running from Port of Brisbane to Port of Gladstone. The second measurement was conducted on CSL vessel II from 3rd to 6th of November, 2015 on her voyage from Gladstone to Sydney. All measurements were carried out on both the main and auxiliary engines of two ships for three ship operating conditions, which are at berth, manoeuvring, and at sea.

Because the utilization of inbuilt measurements proves to be difficult, time-consuming and resource-demanding, it is difficult to convince ship-owners to purchase and install recommended measurement devices (Chen, Huey et al. 2005, Cappa, Williams et al. 2014). Therefore, emission inventories are utilized, which are mathematical models to estimate emissions discharged into the atmosphere (Skjølsvik, Andersen et al. 2000, Endresen, Sorgard et al. 2007, Dalsoren, Eide et al. 2009). Currently, limited guidance regarding the development of port emission inventories exist and therefore any current emission inventories suffer from poor quantification of port activity and use of outdated emission factors for assessing the impact of ports on regional and global air quality (Browning and Bailey 2006, USEPA 2009) . The measurements reported here, therefore, provide a baseline allowing for assessment of how well different emission inventory techniques agree in terms of the derived emission factors and estimated emissions.

Several emission inventories exist, which include emissions originating from ship traffic in different sea areas (Agrawal, Welch et al. 2008, Jalkanen, Johansson et al. 2016, Johansson, Jalkanen et al. 2017). However, few comparisons of these inventories, focusing on specific emission sectors like shipping, exist in literature (Jalkanen, Johansson et al. 2014, Li, Borken-Kleefeld et al. 2018, Ring, Canty et al. 2018, Zhong, Zheng et al. 2018). These studies have

applied basic comparisons between these inventories applying the available datasets from International shipping routes, reported emissions by Member States, Proxy data on worldwide international shipping, AIS data and vessel characteristics but rarely compared with or from the real-time shipping engine exhaust emission measurements (Winnes, Styhre et al. 2015, Jalkanen, Johansson et al. 2016, Russo, Leitao et al. 2018, Zhong, Zheng et al. 2018). Presenting a comprehensive case study to review and compare commonly used emission inventories and to identify the best vessel-specific inventory family predicting the primary emissions from ocean-going vessels when at berth, while manoeuvring and while cruising, the primary emission rates of NO_x, SO_x, CO_2, CO, HC, and PM were measured during on-board experimental measurement campaign, for the three modes of the vessel's operation. The emissions were predicted with 13 families of emission inventories and prediction deviations have been also calculated. Therefore, one following novel aspect in this study is:

1. Creation of a generalized rational algorithm to rank inventory families based on the precision of their predictions for given operational modes of a specific vessel comparing to real-time emission measurement. Moreover, the implications of the case study together with the developed algorithm to rank inventory families was applied to offer a novel future policy for cost-effective and reliable emission estimation caused by shipping.

Accurate and up-to-date ship emission inventories are key inputs for air quality modelling, and are essential for a better understanding, and cost-effective control, of the impacts of air emissions from shipping activities on the environment and human health. One of the challenges in improving the accuracy of ship emission inventories is due to their mobility, poorly integrated models, and limited data (Matthias, Bewersdorff et al. 2010). Information on these types of emissions is limited due to a lack of dynamical features, such as the geographical or temporal variations of emissions. This information can be critically important for all transportation emissions, which present a substantial spatial and temporal variation (Jalkanen, Johansson et al. 2016). For the maritime transport sector, characterization of shipping activity is a challenging task, and has large uncertainties in emission assessments (USEPA 2004, Wang, Corbett et al. 2008). Therefore, studies concerning ship emissions are mainly based on statistical analysis of cargo volumes (Schrooten, De Vlieger et al. 2009), vessel arrivals and departures (Whall, Cooper et al. 2002), voluntary weather reports from ships (Corbett,

Winebrake et al. 2007) or search and rescue services (Endresen, Sorgard et al. 2003, Wang, Corbett et al. 2008). Tools such as the Automatic Identification System (AIS) can significantly reduce the uncertainty concerning ship activities and their geographical distribution. However, most accurate inventories are dependent on real-time information and therefor there is a need for a state-of-art of the most up-to date and available emission inventories regarding ship exhaust emissions. There is also a need to consider different mathematical approaches by emission inventories, to find better ways to manage the many changeable parameters of fuel consumption and engine specifications used to estimate emissions (Frey, Bharvirkar et al. 1999, Streets, Bond et al. 2003, Zheng, Zhang et al. 2009). Therefore, another novel aspect in this study is:

2. Development of new sets of emission factor equations to account for real-time emission measurements through non-linear regression analysis, to help improve emission models and inventory calculations for different engine types for at-sea and in-port operations.

To assess the impact of ship emissions on nearby urban areas, two different kinds of approaches exist: experimental observations and numerical modelling of atmospheric dispersion. Some authors carried out monitoring campaigns on selected pollutants and applied data analysis techniques (e.g. source apportionment) to evaluate the contribution of each source (Pérez and Pey 2011, Cesari, Genga et al. 2014) . However, the collection of monitoring observation followed by data analysis is a quite long and expensive procedure and does not always produce clear indications, due to the presence of other sources of pollutants such as: urban traffic, domestic and commercial heating, industry. Therefore, the use of dispersion models is more frequent. Many different dispersion models have been adopted (Saxe and Larsen 2004, Fan, Zhang et al. 2016, Chen, Wang et al. 2017, Merico, Gambaro et al. 2017, Chen, Zhao et al. 2018). Gariazzo et al. (Gariazzo, Papaleo et al. 2007) used a Lagrangian particle model to assess the impact of harbour, industrial and urban activities on air quality in the Taranto area (Italy). Merico et al. (Merico, Gambaro et al. 2017) have studied air quality shipping impact in the Adriatic/Ionian area focusing on four port-cities. Poplawski et al. (Poplawski, Setton et al. 2011) have used CALPUFF model to investigate the impact of cruise ship emissions on level concentrations of fine particulate matter ($PM_{2.5}$), Nitrogen dioxide (NO_2) and Sulphur dioxide (SO_2) in James Bay, Victoria, British Columbia (BC), Canada. The same model CALPUFF was used in order to assess the impact on local air quality due to atmospheric emissions of a

new port in project in the Mediterranean Sea (Lonati, Cernuschi et al. 2010). There have also been some dispersion modeling studies within Australia (Davis 2014, NSWEPA 2017, Pacific Environment 2017). Issues have identified by these studies including a lack of regulatory emission limits on ship in Australia; a lack of validated emissions data from ships to use in such assessments; and potential adverse effects on air quality that may occur at sensitive receptor locations close to port facilities. These, along with the imminent development of many Australian ports, highlights the continual need for monitoring of emissions and simulation of the emission concentrations.

The Port of Brisbane, Queensland's largest general cargo port, has been considered as a case study. The aim is the development of a methodology to assess the impact of pollutant emissions from marine engines in different shipping mode and from heavy Sulphur residual fuel oil. Simulations are performed with CALPUFF dispersion modelling which is a complex validated software applied for the meteorological studies and is preferred to a Lagrangian model. Therefore, another novel aspect in this study is:

3. Simulate the complex atmospheric dispersion of the shipping emissions within the Port of Brisbane

The marine transport sector contributes significantly to air pollution, particularly in coastal areas (ENTEC UK Limited 2002, Cofala, Amann et al. 2007, Wang, Corbett et al. 2007). Given nearly 70% of ship emissions occur within 400 km of land (Endresen, Sorgard et al. 2003, Eyring, Kohler et al. 2005), ships have the potential to contribute significant pollution in coastal communities (Viana, Hammingh et al. 2014).

Numerous studies in recent years have consistently linked air pollution to negative health effects for exposed populations (Kaiser 2005, Nel 2005). Ambient concentrations of primary emissions have been associated with a wide range of health impacts including asthma, heart attacks, and hospital admissions. These also include premature mortality closely associated with increases in cardiopulmonary and lung cancer mortalities in exposed populations (Pope, Burnett et al. 2002).

Emissions from international ships are increasingly a focus for proposed regulation in local, national, and international arenas (Bailey and Solomon 2004, California Air Resources Board 2006). Yet, in many ways regulatory deliberations have not been fully informed, as the extent of shipping emissions health impacts has been unknown. Previous assessments of regional

shipping-related health impacts focused on European or Western United States regions, and ignore long-range and hemispheric pollutant transport (Cofala, Amann et al. 2007). This undercounts international shipping impacts within local and regional jurisdictions and does not properly inform international policy decision making.

Shipping is a growing industry in Australia and this makes an important contribution to the Australian economy. Currently, ships are subject to limited state and national emissions control regulations and different state governments are considering options to reduce ship-related emissions. To consider this information, therefore, one other following novel aspect in this study is:

4. Development of a new framework for environmental risk assessment of shipping emissions. This involves exposure assessment determining the actual concentrations received by the human receptors in the adjacent areas. From the known ground level concentrations, the amount of contaminant consumed through inhalation can be approximated.

This study clearly demonstrates the suitability of the Australian risk-based framework for assessing shipping emissions within Australian ports. The complete application of such a methodology to shipping emissions is unique and holds great potential for future development.

1.5.Structure of the thesis

This thesis follows a "thesis by publication" structure, where Chapters 2 to 6 are comprised of research papers published during the HDR studies of the candidate. The outline of the thesis structure is given below.

Chapter 1: Introduction to the research project

This is the preface of this research that details the motives for the project, providing necessary background information and relevance. Subsequently, the project objectives, methodology and the novel outcomes are defined. It also outlines the structure of the thesis, linking together the succeeding chapters that are comprised with academic papers.

Chapter 2: On-board measurement campaign

This chapter discusses the details of the on-board measurement campaign performed and contains the methodology and work carried out pertaining to the campaign, and description of the pilot and main measurement campaign (test vessel, instrumentation setup and on-board measurements). It also describes detailed on-board measurement results for ships at berth, manoeuvring and cruising.

The content is based on a conference paper to the 19th Annual General Assembly – AGA 2018 of the International Association of Maritime Universities (IAMU), student session:

Jahangiri S, Nikolova N and Tenekedjiev K. Emission Inventories for Ship Operations; Methodological Comparison with On-board Measurements. AGA 2018 / IAMU Student - International Association of Maritime Universities (IAMU). ISBN 978-84-947311-7-4. Pages 33-40. October 2018.

The chapter also uses parts of the published journal article in the Journal of Sustainable Development of Transport and Logistics:

Jahangiri S, Nikolova N and Tenekedjiev K. Empirical Testing of Inventories Applying On-board Measurements of Exhaust Emissions at Port and at Sea. Journal of Sustainable Development of Transport and Logistics. Volume 3, Issue 2. Pages 6-33. Doi: https://dx.doi.org/10.14254/jsdtl.2018.3-2.1. December 2018.

Chapter 3: Development of Emission Inventories and comparison analysis between measured and predicted emission factors

Chapter 3 compares the on-board experimental measurements with the predictions of the inventory methods introduced in section 1.1. It demonstrates that most methods systemically over-predict or under-predict the on-board measured total emission amounts and therefore follows (here and in Chapter 4) with suggested solutions by this research study.

Chapter 3 is also motivated by the requirement of a mathematical model that can improve the prediction of emissions. Considering real-time emission measurements during 11-d emission measurements on-board of two ocean going vessels at berth and during sailing, new sets of emission factor equations are developed. Vessel I and Vessel II had their engine exhaust emissions measured to develop models for the emissions produced during different shipping

operations. Equations were developed applying 70% of measured emission rates randomly for at berth, manoeuvring and cruising modes for each primary emission.

The regression models were based on the independent variables, which in this study were data on maximum continuous rate (MCR) (as x_1), shaft speed (SS) (as x_2), and emissions (Y). Applying dependant variables affects the accuracy of the results. In the case of this study, fuel consumption was dependent on engine load, and the base Specific Fuel Oil Consumption (SFOC) value was influenced by engine stroke type and power. Primarily, engine-model specific base values of SFOC provided by the engine manufacturers were used.

The data on engine power, engine revolution, and other parameters including intercooled air temperature, scavenging air pressure and cooling fresh water were recorded every five seconds for the main engine. The equations developed from non-linear regression analysis and at a 95% confidence interval.

The content uses material from a published journal article in the Journal of Sustainable Development of Transport and Logistics:

Jahangiri S, Nikolova N and Tenekedjiev K. Empirical Testing of Inventories Applying On-board Measurements of Exhaust Emissions at Port and at Sea. Journal of Sustainable Development of Transport and Logistics. Volume 3, Issue 2. Pages 6-33. Doi: https://dx.doi.org/10.14254/jsdtl.2018.3-2.1. December 2018.

This chapter is also based on the published journal paper in the Journal of Sustainable Environment Research:

Jahangiri S, Nikolova N and Tenekedjiev K. An improved emission inventory method for estimating engine exhaust emissions from ships. Journal of Sustainable Environment Research. Volume 28, Issue 6. Pages 374-381. Doi: https://doi.org/10.1016/j.serj.2018.08.005. October 2018.

This chapter is also based on the published conference paper in the Proceedings of Coasts & Ports 2017 Conference:

Jahangiri S, Kam US, Garaniya V, Abbassi V, Enshaei H, Brown RJ, Van TC, Pourkhesalian AM and Ristovski Z. Development of Emission Factors for Ships' Emissions at Berth. Coasts & Ports 2017 Conference – Cairns. ISBN: 9781922107916. Pages 646-652. June 2017.

Chapter 4: Development of vessel-specific inventory families at port and and at sea

Chapter 4 presents a comprehensive case study to identify the best vessel-specific inventory family predicting the primary emissions from ocean-going vessels when at berth, while manoeuvring and while cruising. In the case study, the primary emission rates were measured during on-board experimental measurement campaign for the three modes of the vessel's operation. The emissions were predicted with 13 families of emission inventories and prediction deviations have been calculated. The chapter also creates generalized rational algorithm to rank inventory families based on the precision of their predictions for a given operational mode of a specific vessel. Applying the implications of the case study together with the developed algorithm to rank inventory families, the chapter also offers a novel future policy for cost-effective and reliable emission estimation caused by shipping.

Following the need highlighted in section 1.1. to quantify the concentrations of the engine exhaust emissions and assessing their risks on the human and environment, Chapters 5 and 6 discuss the dispersion modelling and the risk assessment of these emissions.

This chapter is based on the published journal paper in the Journal of Sustainable Development of Transport and Logistics (see Chapter 3).

Chapter 5: Dispersion modelling

Chapter 5 introduces the complex CALPUFF dispersion modelling to presents emissions concentrations within Australian ports in general, and in a case study of Port of Brisbane in particular. It is based on a comprehensive inventory of vessel emissions in Port of Brisbane over a year, using actual vessel movements, and applies atmospheric dispersion modelling to this quantified data to predict the ground-level concentrations of gaseous pollutants and the deposition of particulate matter, based on local meteorological and geographical conditions.

This chapter is based on the published journal paper in the American Journal of Environmental Sciences:

Jahangiri S, Nikolova N and Tenekedjiev K. Application of a Developed Dispersion Model to Port of Brisbane. American Journal of Environmental Sciences. Volume 14, Issue 4. Pages 156-169. Doi: 10.3844/ajessp.2018.156.169. October 2018.

Chapter 6: Revision of a health risk-assessment framework for the application of shipping emissions

Chapter 6 furthers the dispersion modelling outcomes by assessing the risk of these emissions through a complete methodology has been developed, based on the Australian Environmental Health Risk Assessment Framework. The methodology includes a detailed inventory of in-port and at-sea emissions using an activity-based approach applying Downwash and Near-field as well as the Air-shed areas from CALPUFF dispersion modelling results for Port of Brisbane in the calendar year 2013. The final risk values are validated against National and European guidelines. Various Health impact assessments as well as carcinogenic and ecological effects are discussed in depth. This study offers a significant contribution to developing a baseline measurement of the current state of risk from emissions of the ocean-going vessels visiting the port, and suggests that, given the expected development of many Australian ports in the near future, the need for continual monitoring of shipping emissions is an important and necessary area of research.

This chapter is based on the published journal paper in the Journal of Environmental Practice:

Jahangiri S, Nikolova N and Tenekedjiev K. Health Risk Assessment of engine exhaust emissions within Australian Ports: A case study of Port of Brisbane. Journal of Environmental Practice. Volume 21, Issue 1. Pages 20-35.
Doi:https://doi.org/10.1080/14660466.2019.1564427. March 2019.

Chapter 7: Conclusions and future work

The closing chapter provides an overall summary of the project, bringing together the outcomes of the individual chapters. It also provides conclusions on the key findings and outcomes. Recommendations for future work is also detailed in this section.

Appendix A: Supplementary Data

This Appendix accompanies all the above mentioned Chapters to present the comprehensive dataset measured and parameters calculated during the on-board measurement campaign; the required Security Clearances and Approvals; all the developed emission factor equations and the detailed results and figures produced accordingly; setting up and running the CALPUFF model; and the presentations of present the comprehensive ground and higher-level

concentrations of the primary emissions as well as the short- and long-term health endpoints and concentration-response functions.

Appendix B: Full Papers Published

This Appendix presents the published version of all the publications the candidate was the main author to during her PhD studies.

Appendix C: Other Publications

This Appendix the list of all other publications the candidate was the co-author during her PhD studies.

Chapter 2: On-board measurement campaign

The measurements for this study were taken in October and November 2015 on two large cargo ships at the Ports of Brisbane, Gladstone, and Newcastle. The first on-board measurement was performed on CSL vessel I (to ensure confidentially the identity of ship is suppressed) from 26th to 31st of October, 2015 when she was running from Port of Brisbane to Port of Gladstone. The second measurement was conducted on CSL vessel II from 3rd to 6th of November, 2015 on her voyage from Gladstone to Sydney.

2.1. Test vessels

All measurements have been carried out on both the main and auxiliary engines of two ships for three ship operating conditions, which are at berth, manoeuvring, and at sea. Main information of ships and engines can be seen in Table 2.1.

Table 2.1 *General information about two ships*

.	CSL Vessel I	CSL Vessel II
Ship's Owner	CSL Australia	CSL Australia
Ship's Type	General cargo	Bulk carrier
Classification Society	Lloyd's Register	Lloyd's Register
Flag	Australia	Barbados
Port of Registry	Sydney	Bridgetown
IMO Number	Confidential	Confidential
Build Year	1981, converted 2008	2002
Builder	Mitsui Engineering & Ship Building Co., Japan	Cosco Nantong Shipyard Nantong, China
Net Tonnage	11250 tonnes	16160 tonnes
Gross Tonnage	30909 tonnes	27198 tonnes
Deadweight	40876 metric tonnes	49502 metric tonnes
Length Overall	184.5m	187.5m

Breadth	32.2m	31.0m
Depth	15.32m	16.75m
Main Engine	Mitsui B&W 6L80GFCA 12080 kW x 102 RPM	Man B&W 6S50MC 6880 kW x 102 RPM
Auxiliary Engine	Daihatsu 6DK-20 960 kW @ 900 RPM	Wartsila 425 kW x 900 RPM

2.2. General description of on-board measurements campaign

Measurements of emissions were taken on-board following the procedures elaborated in ISO 8178-2:2008 (Jalkanen, Johansson et al. 2012) and ISO 8178-1:2006 (Auth, Tuv et al. 1999). The on-board emission measurement campaign was divided into 4 separate experiments. The first one was to measure the NO_x, SO_x, CO_2, and CO emissions from the AE when the vessel was at berth. The second, third, and fourth experiment were to measure the NO_x, SO_x, CO_2, CO, HC, and PM emissions from the ME when the vessel was at berth, maneuvering, and cruising respectively.

For the main engine experiments the probes of the exhaust gas were sampled between the turbocharger and the economizer of the ME. The emission rates of SO_x, CO_2, CO, and HC were measured with main gas analyzer Testo 350 XL. The emission rates HC were measured with Horiba MEXA 584L 5-gas analyzer. The mass concentration of PM was measured with Dust Trak Aerosol Monitor 8530 (TSI) separately for $PM_{2.5-10}$ (with aerodynamic diameters between 2.5 and 10 μm), $PM_{1.0-2.5}$ (with aerodynamic diameters between 1.0 and 2.5 μm), and $PM_{1.0}$ (with aerodynamic diameters less than 1.0 μm). To cool the probe for PM measurement, the sample was diluted with air. The rates of the samples' dilution were estimated by comparing the CO_2 emission rate in the initial sample with the CO_2 emission rate of the diluted sample measured with Sable CA-10 CO_2 monitor. Simultaneously the shaft speed (SS) and the actual engine power (P_{act}) were measured every 5 sec. The specific oil consumption (SOC) was determined as a quadratic function of the engine load factor LF (the actual engine power measured in % of the maximum continues rating of the engine). The average air consumption (AC) was assessed as a linear function of the load factor. The instantaneous exhaust mass flow rate (EMFR) was assessed as the sum of AC with the product of SOC and P_{act}.

For the auxiliary engine experiments, the probes of the exhaust gas were sampled after the turbocharger. The measurement equipment was Testo 350 XL only. In this experiment, HC and PM were not measured. The SS, P_{act}, SOC, AC and EMFR were obtained as in the ME experiments.

For each of the experiments the probes were taken at equal inter-sample interval Δt. If the duration of the experiment is T, then the count of the probes sampled for measurement is $N=T/\Delta t$. The time when the i-th probe was sampled is $t_i=(i\text{-}0.5)\Delta t$ for $i=1,2,\ldots,N$. The parameters of the measurement process for each of the experiments are given in Table 2.2.

Table 2.2 *Measurement process parameters*

Experiment	Inter-sample Interval (h)	Count of Samples	Duration (h)	Duration (h, min, s)
ME at berth for NO_x	1/3600	1569	0.4358	26 min, 9 s
ME at berth for SO_x, CO	1/3600	1577	0.4381	26 min, 17 s
ME at berth for CO_2	1/3600	1521	0.4225	25 min, 22 s
ME at berth for HC	300/3600	4	0.3333	20 min
ME at berth for PM	300/3600	5	0.4167	25 min
AE at berth for NO_x, SO_x, CO_2, CO	1/3600	9476	2.632	2 h, 37 min, 56 s
ME maneuvering for NO_x	1/3600	6553	1.820	1 h, 49 min, 13 s
ME maneuvering for SO_x	1/3600	6558	1.822	1 h, 49 min, 18 s
ME maneuvering for CO_2	1/3600	6522	1.812	1 h, 48 min, 42 s
ME maneuvering for CO	1/3600	6542	1.817	1 h, 49 min, 2 s
ME maneuvering for HC	300/3600	5	0.4167	25 min
ME maneuvering for PM	300/3600	27	2.250	2 h, 15 min
ME cruising for NO_x, SO_x, CO_2, CO	1/3600	15305	4.251	4 h, 15 min, 5 s
ME cruising for HC, PM	300/3600	64	5.333	5 h, 20 min

2.3. On-board measurements

For the five gases (NO_x, SO_x, CO_2, CO, and HC) the measured instantaneous emission rates at time t_i were converted into instantaneous emission factors (EFs) using the atmospheric pressure, the exhaust gas temperature, the exhaust flow rate (which is the total fuel and air consumption divided by the mass density of the exhaust gas), the molar mass of the gas, the air density, and the engine power. The later was linearly interpolated for each t_i from the measured engine power data. For each of the three types of PM ($PM_{2.5-10}$, $PM_{1.0-2.5}$, and $PM_{1.0}$) the mass concentrations were converted into instantaneous emission factors (EFs) using the exhaust flow rate, the dilution rate (calculated from the difference of the CO_2 measured before and after the dilution of the hot probe with cold air), the air density, and the actual engine power (P_{act}). The EF of the PM is calculated as the sum of the EFs for $PM_{2.5-10}$, $PM_{1.0-2.5}$, and $PM_{1.0}$. When not measured, the EF for $PM_{2.5-10}$ is assessed as 20% of the EF of PM (Hockstad and Hanel 2018). In the same way when not measured, the EFs for $PM_{1.0-2.5}$, and $PM_{1.0}$ are substituted with the mean of the respective measured EFs. The micro emission in the interval Δt centered around time t_i was calculated as the instantaneous emission factor multiplied by P_{act} and by Δt. The total emission during any experiment was estimated as sum of the micro emissions measured. The measured average emission factors given in Table 2.3 were calculated as the total emissions divided by the product of the average engine power with the experimental time T. The average shaft speed, the average actual power of the engine, the average load factor, the average air consumption, and the average exhaust mass flow rate for each of the experiments are also given in Table 2.3

While at berth, the AEs run to generate the required auxiliary power (Auth, Tuv et al. 1999) and can be said to be the key emission producer (Du, Chen et al. 2011). Major activities include, but are not limited to, light supply to the ship, refrigeration, heating, ventilation, and electric equipment electric loads (Auth, Tuv et al. 1999). The AEs operate with greater load factor (LF) than ME and therefore produce higher EFs (Table 2.3).

The main engine runs on heavy fuel oil (HFO) with 3.13% Sulphur mass content that was adopted for the fuel type in this study. HFO is a fuel type preferred for most ship's boilers and engines (Goldsworthy and Galbally 2011), with a Sulphur content ranging from 2% to 3.5% with a 2.6% average globally (IMO 2010). The properties of the HFO used in our study are given in Table 2.4. For most ships sailing to Australia, the average fuel Sulphur content of the

HFO may be higher than this average (Goldsworthy and Goldsworthy 2015). Also, HFO combustion is very complex and may emit primary gases (Goldsworthy and Galbally 2011).

.

Table 2.3 *Experimental condition and measured EFs*

Experiment	Ave. SS (rpm)	Ave. P_{act} (kW)	Ave. LF (%)	Ave. AC (kg/h)	Ave. EMFR (kg/h)	Ave. SOC (g/kWh)	Average Measured Emission Factors in (g/kWh)					
							NO_x	SO_x	CO_2	CO	HC	PM
ME at berth for NO_x	38.11	509.0	7.399	5860	5990	256.6	10.1					
ME at berth for SO_x, CO	38.15	510.5	7.421	5877	6008	256.5		9.10		1.48		
ME at berth for CO_2	38.25	507.5	7.376	5842	5972	256.6			476			
ME at berth for HC	36.62	451.5	6.563	5197	5313	257.7					0.400	
ME at berth for PM	39.8	578.2	8.404	6656	6804	255.2						2.23
AE at berth for NO_x, SO_x, CO_2, CO	900.0	265.0	57.61	2862	2930	256.0	11.2	26.2	1140	1.74		
ME maneuvering for NO_x	65.31	2444	35.53	28140	28690	226.4	11.5					
ME maneuvering for SO_x	65.30	2442	35.51	28120	28670	226.4		13.8				
ME maneuvering for CO_2	65.45	2453	35.65	28240	28790	226.3			687			
ME maneuvering for CO	65.29	2443	35.50	28120	28670	226.4				2.43		
ME maneuvering for HC	80.94	3785	55.01	43570	44380	214.3					0.239	
ME maneuvering for PM	67.84	2653	38.56	30540	31130	224.0						1.70
ME cruising for NO_x, SO_x, CO_2, CO	89.50	5595	81.33	64410	65560	205.5	19.0	18.1	764	1.12		
ME cruising for HC, PM	89.26	5663	82.31	65190	66340	203.1					0.146	0.391

Table 2.4 *Properties of the heavy fuel oil used*

Density at 15º C	**986 kg/m^3**
Viscosity at 50º C	377 mm^2/s
Micro - carbon residue	14.6% mass
Sulphur (S)	3.13% mass
Ash	0.0640% mass
Vanadium (V)	141 mg/kg

Since NO_x and CO emissions are combustion dependent, service history and individual maintenance are a concern (Cooper 2003). Higher amounts of nitrogen in fuels can produce NO_x emissions (Cooper 2003). For this study, nitrogen content was 0.68% of the total mass. Thermally, greater nitrogen fixation during combustion is required if temperature periods are long and the engine is slow. The level of PM in marine diesel emissions may vary with fuel type or combustion conditions and more will be generated by higher amounts of fuel Sulphur plus ash content. Dependency on PM fuel emissions becomes less conspicuous compared to CO_2 and SO_2 emissions due to induced PM combustion emissions (Cooper 2003). According to Agrawal et al. (Agrawal, Malloy et al. 2008), the higher the quantity of ash content, the higher the PM EFs, although, in a general sense, there is insufficient data on the measurement of PM and differences in engine models, fuel used, instrumentations and working conditions (Hallquist, Fridell et al. 2013).

Variations in engine power and speed may result in poor combustion, which can lead to increased HC and PM emission rates. PM concentration is largely dependent on the conditions of engine load, which is higher at low LFs and vice-versa (Winnes and Fridell 2009): if the average power is considered with LFs remaining at their lowest in berth, the EF results for PM produce greater amounts. However, EF averages for NO_x, CO_2 and SO_x in cruising mode are higher than when maneuvering at berth. All NO_x emissions are temperature dependent, increasing with a rise in temperature. Hence, the rate of emission of NO_x is dependent on a ship's engine power and engine LF (Sinha, Hobbs et al. 2003). If the engine is steady, with a speed higher than its power, while in operation it may run for longer and at higher temperatures, producing higher NO_x emissions. Pollution rates, then, increase with increased engine power. The demand of engine power, air consumption and mass flow of exhaust emissions increase

during cruising. Moreover, an elevated engine load increases the average engine power, which in turn additionally increases the influence of the fuel's carbon and Sulphur content (Table 2.3) on the EFs of SO_x and CO_2 for cruising modes compared with other operating modes (Table 2.3). Generally, the CO emissions recorded were low, a result of high oxygen surplus concentrations and an adequate combustion process, but if engines are poorly maintained at small power ranges, CO proportions may increase expectedly due to considerable relative concentration (Kristensen 2010). In this study, generally the EFs for CO are low but they increase at the maneuvering phase. Variable engine speed and power may lead to poor combustion during the maneuvering phase leading to increased CO emission rates (Fu, Ding et al. 2013).

Figure 2.1 shows the amount of measured O_2 [%], CO_2 [%], NO_x [ppm], CO [ppm], and SO_x [ppm] for the auxiliary engine while at berth. Apart from the initial peak, the amount of emissions remains stable. The initial peak is due to the cold start of the engine. Further details regarding the cold start, incomplete combustion, and its effect can be found in the literature (Jun, Gillenwater et al. 2001, Standards Australia 2009, Winnes and Fridell 2009, Khair and Jääskeläinen 2011, Lee and Jeong 2012, Roberts, Brooks et al. 2014). After the cold start, the engine operates on stable condition.

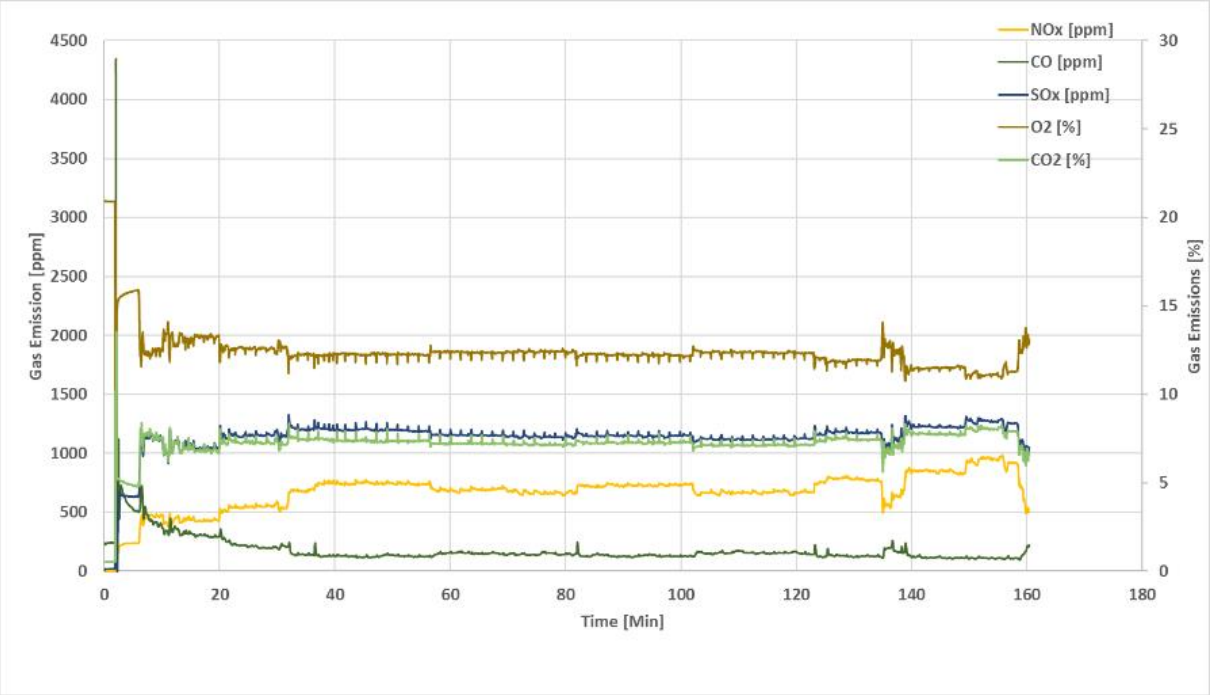

Figure 2.1 *Measured O_2 [%], CO_2 [%], NO_x [ppm], CO [ppm], and SO_x [ppm] for the auxiliary engine at berth*

Measurements on the main engine were also conducted when the ship arrived at its destination port (Figure 2.2). Both the shaft power and the shaft speed change continuously at berth (Figure 2.3). This influences the amount of emissions. In other words, when the engine speed and power experience sudden changes, the amount of emissions change accordingly. Apart from cruising, the ship navigates at a constant speed (rpm). During maneuvering and at berth, the speed varies at different timings. The sudden changes are due to different factors such as wind and wave currents. At other time lapses, rather than the sudden changes, a stable trend can be seen for the shaft speed and the shaft power, which indicates a normal working condition of the ME while at berth.

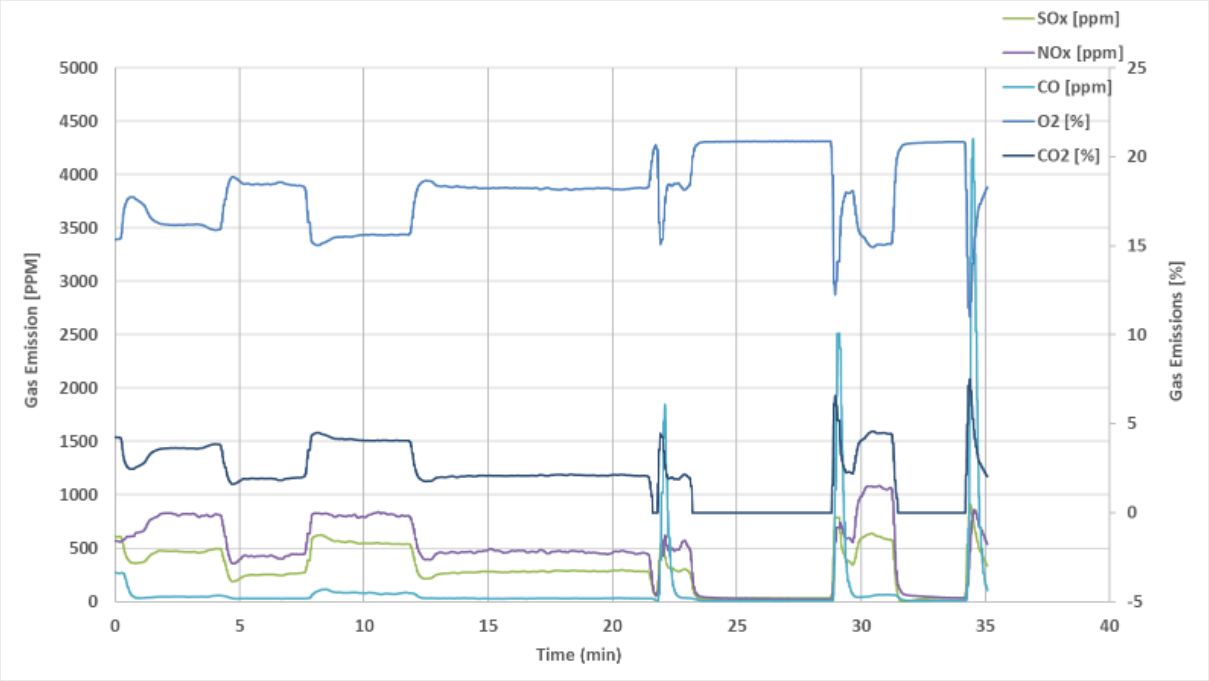

Figure 2.2 *Measured O2 [%], CO_2 [%] NO_x [ppm], CO [ppm], and SO_x [ppm] for the ME at berth*

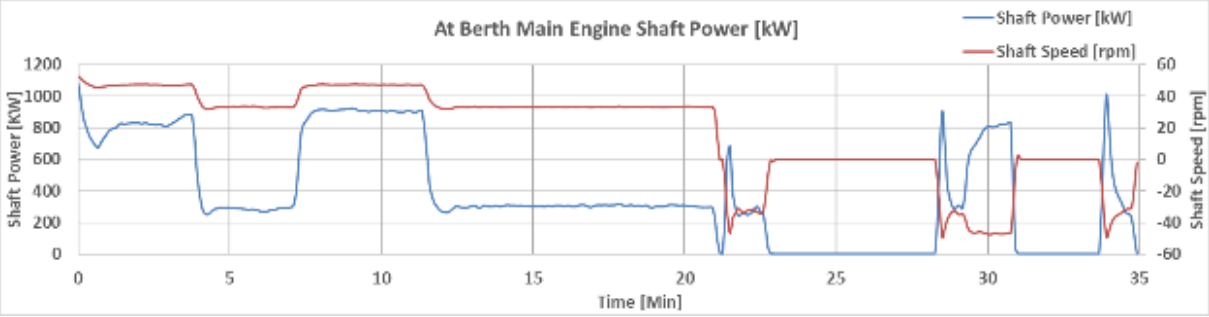

Figure 2.3 *Shaft speed and shaft power for the ME at berth*

Emissions during maneuvering differ significantly from the emissions while at berth and cruising. Figure 2.4 shows the amount of measured O_2 [%], CO_2 [%], NO_x [ppm], CO [ppm], and SO_x [ppm]. Like at berth conditions, the emission amounts change abruptly when the shaft speed and shaft power have a sudden change (Figure 2.5). These changes are due to the underwater hull geometry, the pivot point, the lateral motion, the rudder, propeller and the thrusters function. The land shape and insufficient under keel distance when entering shallow water for maneuvering, should be also taken into consideration. Navigation is always directly affected by shallow water, and at the same time, elements derived from propeller action and the combined effects of the surrounding environment on the hull, affect the navigation in maneuvering (House 2007).

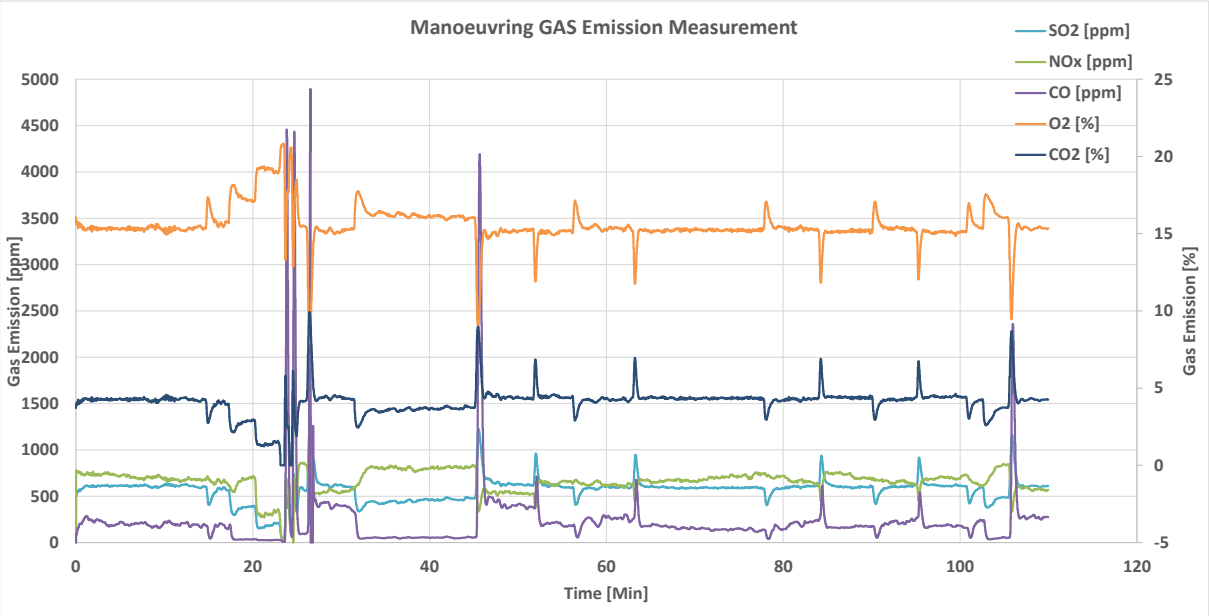

Figure 2.4 *Measured O2 [%], CO_2 [%], NO_x [ppm], CO [ppm], and SO_x [ppm] for the ME during manoeuvring*

When the ship departed and was at normal cruising speed, the measurement for emissions was carried out on three different occasions and one is presented here (Figure 2.6). While cruising, the ship moves at a constant speed (rpm) and hence only the shaft power changes in different timings (Figure 2.7). Except the initial cold-start of the main engine at cruising which may need a higher shaft power to run the ship initially, a stable trend can be seen for the emissions as the engine experiences a normal working condition at cruising.

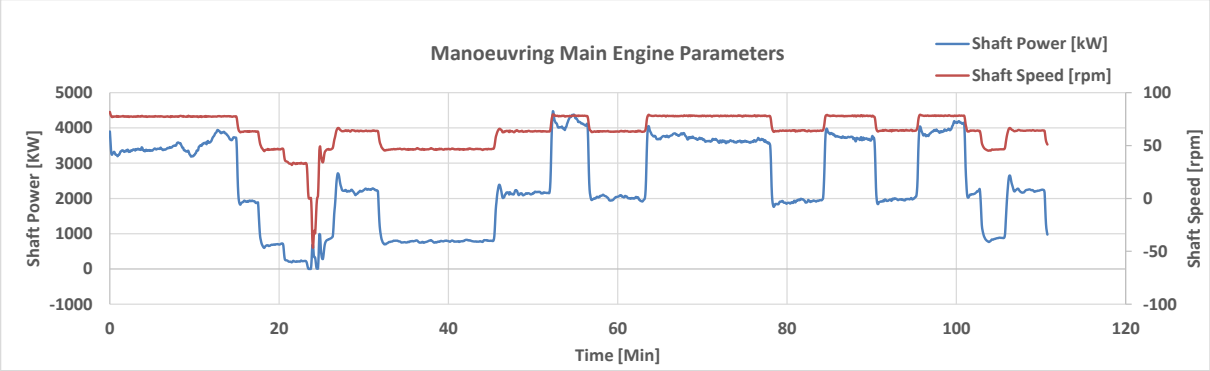

Figure 2.5 *Shaft speed and shaft power for the ME during manoeuvring*

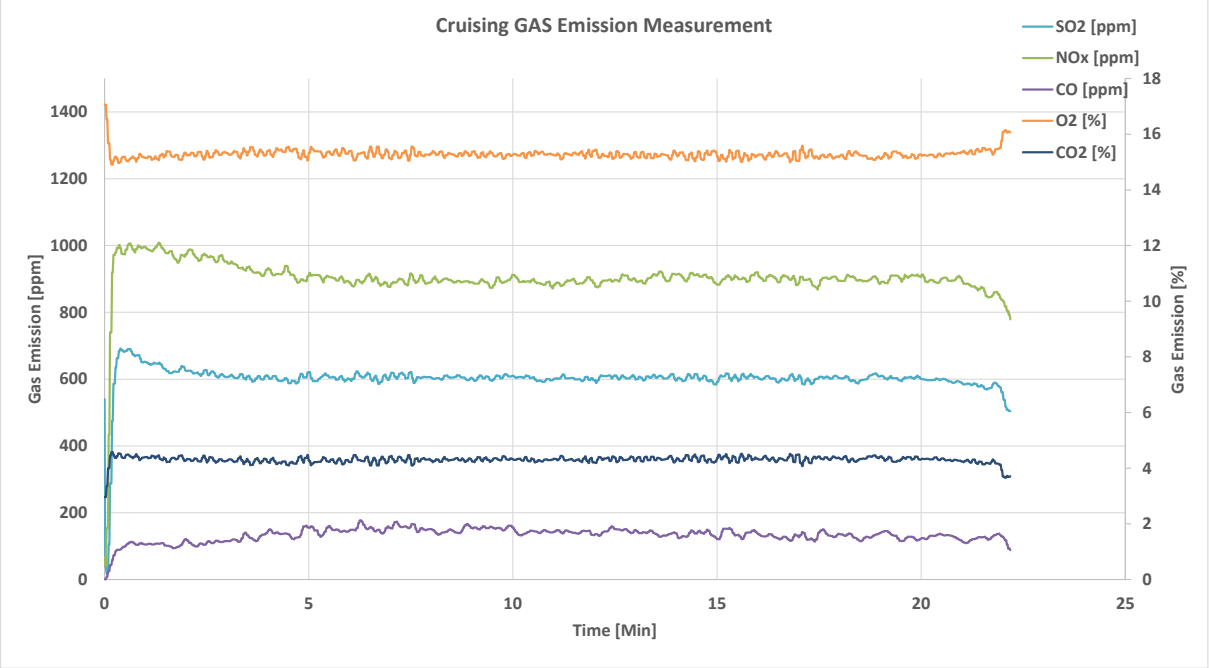

Figure 2.6 *Measured O2 [%], CO_2 [%], NO_x [ppm], CO [ppm], and SO_x [ppm] for the ME during cruising*

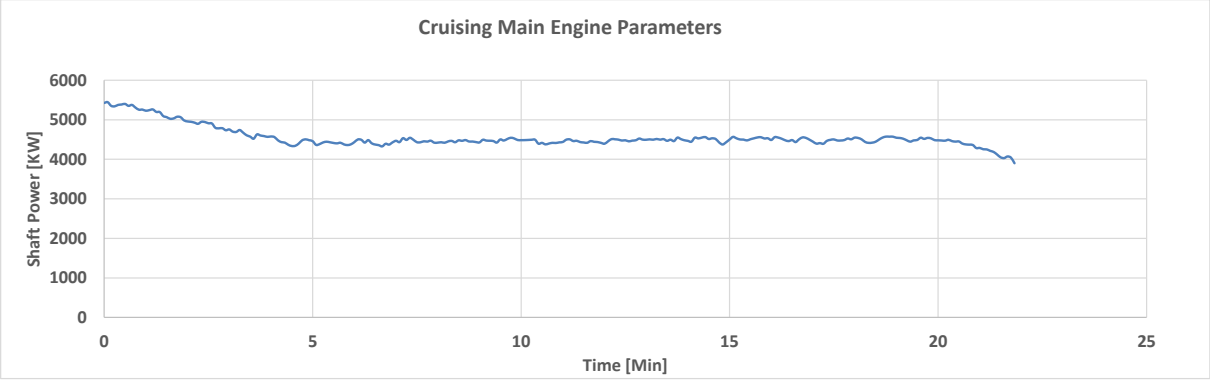

Figure 2.7 *Shaft power for the ME during cruising*

Chapter 3: Development of Emission Inventories and comparison analysis between measured and predicted emission factors

In this chapter, the on-board experimental measurements are compared with the predictions of the inventory methods introduced in section 1.1. As specified in Chapter 1, the objective of this chapter is also to develop new sets of EF equations to take into consideration real-time emission measurements during 11-d emission measurements on-board of two ocean-going vessels at berth and during sailing. They were tested on two ocean-going vessels, running on slow speed diesel main engines at berth while manoeuvring and cruising. Both vessels ran on heavy diesel fuel. Regression analysis, along with a consideration of fuel consumption and engine parameters, was used to develop the equations. The results show a better prediction of emission quantity than current inventories for different engine types, in in-port and at-sea activities, with the sum of primary emissions coming closest to the actual sea emission calculations and also to the smallest standard values. This should be helpful when upgrading environmental policies.

3.1. Comparison analysis between measured and predicted EFs

As highlighted in section 2.2, the primary emission rates (or the mass concentration for PM) of the main engine were measured at berth, while maneuvering, and while cruising. For the auxiliary engines the only rates measured were NO_x, SO_x, CO_2 and CO emissions at berth. In section 2.3, the measured emission rates were converted to EFs and the results were shown in Table 2.3. The total emission amount of given type released in the atmosphere during one experiment (e.g. CO emission of the ME during the maneuvering experiment) can be calculated by integrating the time curve of the instantaneous emissions for the time span of the experiment (e.g. 1 h, 49 min, 2 sec for CO emission of the ME during the maneuvering). The instantaneous emission in g/h at time *t* is the EF at time *t*, multiplied by the actual engine power at time *t*. The total emission amount measured for each "pollutant" (inclusive of CO_2, which technically is not a pollutant) from the four experiment types are given in kg on the first row of Table 3.1, Table 3.2 , Table 3.4 and Table 3.5. For each total emission amount measured, we have tried to predict the results with as many inventories as possible from the list of inventories given in

section 1.2. Each of the inventories is predicting the EF generally as a function of the load factor, the type of the fuel, the Sulphur content of the fuel, the type of the engine, the operation mode, the built date of the engine, the shaft rotational speed, specific fuel consumption, etc. The inventory-predicted emission factor for any emission has been converted into inventory-predicted total emission amount by multiplying with the average engine power and the experiment time *T*. We opted to calculate the total predicted emissions in that simplified way instead of integrating the instantaneous emission curves to mimic more closely the real utilization of the inventory prediction. The inventory deviations of the predicted total emission amount in % from the experimentally measured total emission amounts can be calculated for all "pollutants" (note that CO_2 is not a pollutant), and for any inventory method that can predict that pollutant. Those inventory deviations from the four experiment types are given in Table 3.1, Table 3.2 , Table 3.4 and Table 3.5 (from the second row onward).

Example 1.

MEET inventory prediction for CO emission of the auxiliary engine is

$$EF_{CO}^{MEET} = \left[20.7 - 0.218(LF) - 0.0231P_{act} + 0.000345P_{act}(LF)\right]SOC/1000$$

For the auxiliary engine at berth the average load factor LF is 57.6%, the average engine power P_{act} is 265 kW, the average specific oil consumption SOC is 256 g/kWh (see Table 2.3). So,

$$EF_{CO}^{MEET} = \left[20.7 - 0.218(57.6) - 0.0231(265) + 0.000345(265)(57.6)\right](256.0)/1000 \approx 1.87 \text{ g/kWh}$$

For CO emission from the auxiliary engine at berth the experimental time is 2.632 h (see Table 2.2). The MEET predicted total CO emission amount is

$$CO^{MEET} = EF_{CO}^{MEET} P_{act} T = 1.87(265)(2.632)/1000 \approx 1.304 \text{ kg}$$

The MEET inventory deviation in % from 1.214 kg, which is the experimentally measured total CO emission amount for the auxiliary engine at berth (see Table 3.2) is

$$\Delta CO^{MEET} = 100\left(CO^{MEET} - CO^{mes}\right)/CO^{mes} = 100(1.304 - 1.214)/1.214 \approx 7.43\%$$

That result is shown in Table 3.2.

Example 2.

The ENTEC prediction for the NO_x emission factor from the main engine when the vessel is maneuvering was $EF_{NO_x}^{ENTEC} = 12.0$ g/kWh. The latter value considers that the vessel is at maneuvering, that the main engine is post-2000 SSD, and that the fuel is HFO. For NO_x emission from the main engine when maneuvering the experimental time is 1.820 h (see Table 2.2), and the average engine power P_{act} is 2444 kW (see Table 2.3). The ENTEC predicted total NO_x emission amount is

$$NO_x^{ENTEC} = EF_{NO_x}^{ENTEC} P_{act} T = 12.0(2444)(1.820)/1000 \approx 53.4 \text{ kg}$$

The ENTEC inventory deviation in % from 51.17 kg, which is the experimentally measured total NO_x emission amount for the main engine at maneuvering (see Table 3.4) is

$$\Delta NO_x^{ENTEC} = 100\left(NO_x^{ENTEC} - NO_x^{mes}\right)/NO_x^{mes} = 100(53.4 - 51.17)/51.17 \approx 4.33\%$$

That result is shown in Table 3.4.

Example 3.

US EPA inventory prediction for SO_x emission of the main engine is

$$EF_{SO_x}^{US\ EPA} = 2.3735(SOC)(FSF) - 0.4792$$

For SO_x emission of the main engine at berth the specific oil consumption SOC=256.5 g/kWh (see Table 2.3), and the fuel Sulphur fraction in the HFO is FSF=0.0313 (see Table 2.4). So,

$$EF_{SO_x}^{US\ EPA} = 2.3735(256.5)(0.0313) - 0.4792 \approx 18.54 \text{ g/kWh}$$

For SO_x emission of the main engine the experimental time T is 0.4381 h (see Table 2.2), and the average engine power P_{act} is 510.5 kW (see Table 2.3). The US EPA predicted total SO_x emission amount is

$$SO_x^{US\ EPA} = EF_{SO_x}^{US\ EPA} P_{act} T = 18.54(510.5)(0.4381)/1000 \approx 4.147 \text{ kg}$$

The US EPA inventory deviation in % from 2.035 kg, which is the experimentally measured SO_x emission amount for the main engine at berth (see Table 3.1) is

$$\Delta SO_x^{US\ EPA} = 100\left(SO_x^{US\ EPA} - SO_x^{mes}\right)/SO_x^{mes} = 100(4.147 - 2.035)/2.035 \approx 104\%$$

That result is shown in Table 3.1.

3.1.1. Inventories performance when the vessel is at berth

The experimentally measured total emission amounts and the inventory predictions for the main engine at berth are shown in Figure 3.1. The experimentally measured total emission

amounts and the inventory deviations in % from the experimental values for the main engine at berth are given in Table 3.1.

Most methods systemically over-predict the on-board measured total emission amounts of NO_x, CO_2, CO, and HC from the main engine at berth. The SO_x inventories' predictions are well scattered around the measured total emission amounts. The PM inventories' predictions are somewhat scattered around the measured total emission amount, although some under-prediction is obvious. The inventory predictions for NO_x, CO_2, and PM are somewhat satisfactory because the absolute deviations do not exceed 68.8%, 72.6%, and 86.3% respectively. However, the inventory predictions for SO_x, CO, and HC are completely unreliable with maximal absolute deviations reaching 104%, 1610%, and 1390% respectively.

Table 3.1 *Inventory deviations from the experimentally measured total emission amounts in % for the main engine at berth. The experimental measurements are given in the second row in kg per time equal to the experiment duration according to the third column of Table 2.2*

Inventory	**NO_x**	**SO_x**	**CO_2**	**CO**	**HC**	**PM**
Experiment	2.248	2.035	102.0	0.3319	0.06022	0.5373
Tier III	38.1	37.4	NaN	-0.276	350	7.62
ENTEC	18.4	27.5	43.4	NaN	350	7.62
MEET	-11.4	76.9	72.6	1610	1390	-86.3
STEAM	114	-34.2	31.0	NaN	NaN	NaN
MOPSEA	68.8	-34.1	30.8	6.46	-41.0	-47.5
NERI	18.4	-56.0	34.1	7.81	25.0	-83.9
EMS	77.7	18.7	33.5	79.2	45.0	-41.7
US EPA	64.8	104	162	668	987	-77.7
IMO	64.8	-49.1	21.1	-65.5	42.5	-39.5

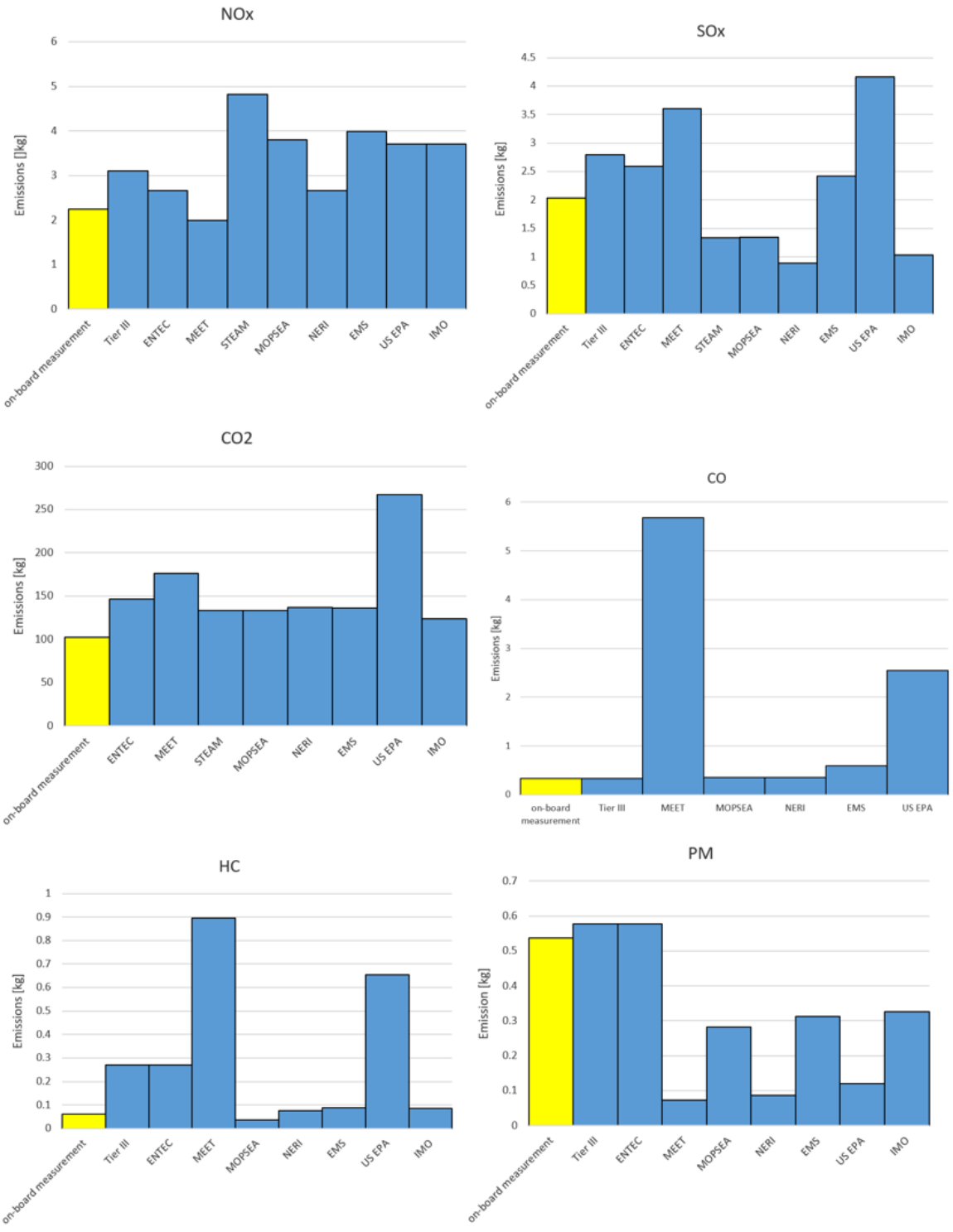

Figure 3.1 *Total emission amounts' measurement and inventory prediction at berth for the main engine*

The inventories, which produce least absolute deviations for the main engine at berth are MEET for NO_x with -11.4% deviation, EMS for SO_x with 18.7% deviation, IMO for CO_2 with 21.1%

deviation, MOPSEA for CO with 6.46% deviation, NERI for HC with 25.0% deviation, and jointly TIER III & ENTEC for PM with 7.62% deviation.

The experimentally measured total emission amounts and the inventory predictions for the auxiliary engines at berth are shown in Figure 3.2. The experimentally measured total emission amounts and the inventory deviations in % from the experimental values for the auxiliary engines at berth are given in Table 3.2.

Most methods systemically over-predict the on-board measured total emission amounts of NO_x, whereas at the same time systemically under-predict the on-board measured total emission amounts of SO_x and CO_2 from the auxiliary engines at berth. The CO inventories' predictions are somewhat scattered around the measured CO total emission amount, although some under-prediction can be detected. The CO_2 is more or less well predicted by every inventory method, with absolute deviations less than 45.4%. The inventory predictions for NO_x, SO_x, and CO also are somewhat satisfactory because their respective absolute deviations do not exceed 81.8%, 98.5%, and 54.0%.

The inventories, which produce least absolute deviations for the auxiliary engines at berth, are MEET for SO_x, and CO_2 with -38.8%, and -28.2% deviations respectively, NERI for NO_x with -1.50% deviation, and MOPSEA for CO with -5.79% deviation.

The experimentally measured total emission amounts for the main engine and the auxiliary engines at berth were converted to hourly emission amounts, by dividing the former with the respective experimental time in hours. The combined hourly emission amount from all engines at berth has been calculated as the sum of the hourly emission amounts from main engine and from auxiliary engines. The experimentally measured combined hourly emission amounts are given in on the first row of Table 3.3, except for the HC and PM column where the hourly emission amount are from the main engine only (see section 2.2). The inventory deviation in % for any hourly emission amount prediction is the same as that of the total emission amount prediction. The combined hourly emission amount prediction can be calculated as the sum of two independent hourly amount predictions: one for the main engine and one for the auxiliary engines. It is trivial to prove that the inventory deviation from the experimentally measured combined hourly emission amount in % is a weighted average of the two inventory deviations from total emission amounts in % (one for the main engine and one for the auxiliary engines). The weight coefficients are the experimentally measured hourly emission amounts from the main engine and auxiliary engines respectively.

Table 3.2 *Inventory deviations from the experimentally measured total emission amounts in % for the auxiliary engines at berth. The experimental measurements are given in the second row in kg per time equal to the experiment duration according to the third column of Table* ***2.2***

Inventory	NO_x	SO_x	CO_2	CO
Experiment	7.790	18.26	795.5	1.214
Tier III	27.1	-47.3	NaN	-6.36
ENTEC	9.24	-53.0	-36.7	NaN
MEET	94.3	-38.9	-28.2	7.43
STEAM	2.97	-77.1	-45.4	NaN
MOPSEA	-21.2	-74.8	-40.0	-5.79
NERI	-1.50	-98.5	-38.4	-8.08
EMS	34.3	-54.5	-38.8	54.0
US EPA	31.6	-54.2	-36.6	-36.8
SMED	25.4	-60.3	-36.7	-48.3
IMO	81.8	-78.5	-38.5	-64.2

Example 4.

Let us concentrate on NO_x emission at berth. The measured total emission amount for NO_x from the main engine at berth is 2.248 kg for T=0.4358 h (see Table 3.1). It follows that the measured hourly emission amount for NO_x from the main engine at berth is 2.248/0.4358=5.158 kg/h. The measured total emission amount for NO_x from the auxiliary engines at berth is 7.790 kg for T=2.632 (see Table 3.2). It follows that the measured hourly emission amount for NO_x from the auxiliary engines at berth is 7.790/2.632=2.960 kg/h. So, the measured combined hourly emission amount for NO_x from all engines at berth will be 5.158+2.960=8.117 kg/h (see Table 3.3).

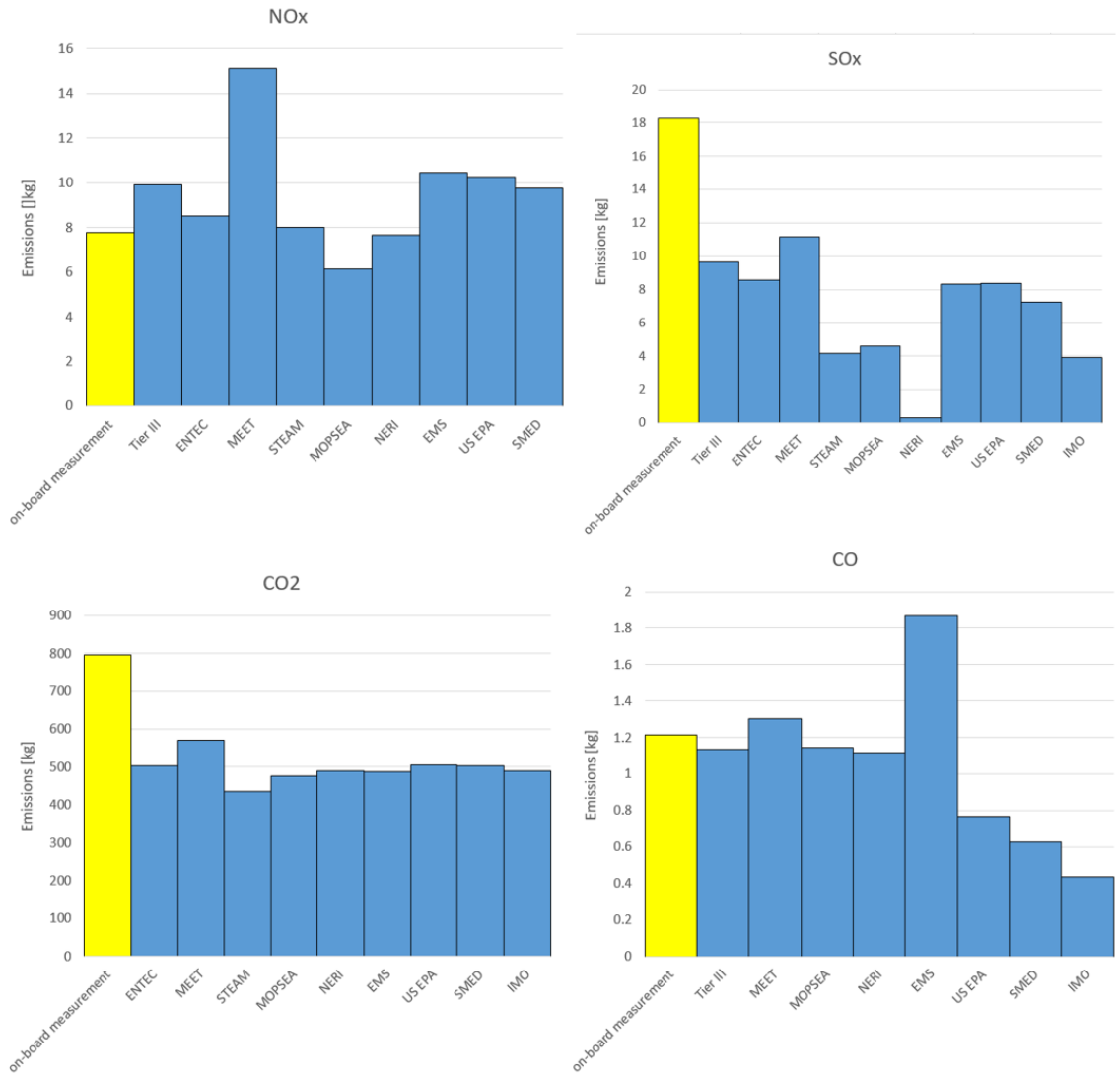

Figure 3.2 *Total Emission amounts' measurement and inventory prediction at berth for auxiliary engines*

Let us use the NERI inventory for NO_x at berth. The NERI inventory deviation from the experimentally measured 2.248 kg total NO_x emission amount from main engine at berth is 18.4% (see Table 3.1). It follows that NERI inventory deviation from the experimentally measured 5.158 kg/h hourly NO_x emission amount from ME at berth will be also 18.4%. The NERI inventory deviation from the experimentally measured 7.790 kg total NO_x emission amount from the auxiliary engines at berth is -1.50% (see Table 3.2). It follows that NERI inventory deviation from the experimentally measured 2.960 kg/h hourly NO_x emission amount from the auxiliary engines at berth will be also -1.50%. So, the NERI inventories deviation

from the experimentally measured 8.117 kg/h combined hourly NO_x emission amount from all engines at berth will be,

[18.4(5.158) -1.50 (2.960)]/8.117 ≈11.2%

That result is shown in Table 3.3.

Table 3.3 *Inventory deviations from the experimentally measured combined hourly emission amounts in % for the main engine plus the auxiliary engines at berth. The experimentally measured combined hourly emission amounts are given in the first row in kg/h.*

Inventory	NO_x	SO_x	CO_2	CO	HC	PM
Experiment	8.117	11.58	543.6	1.219	0.1806	1.289
Tier III	34.2	-13.3	NaN	-2.58	350	7.62
ENTEC	15.1	-20.7	-1.13	NaN	350	7.62
MEET	27.2	7.56	16.6	1000	1390	-86.3
STEAM	73.6	-59.9	-11.5	NaN	NaN	NaN
MOPSEA	36.0	-58.5	-8.58	1.83	-41.0	-47.5
NERI	11.2	-81.5	-6.21	1.80	25.0	-83.9
EMS	61.9	-25.2	-6.69	69.7	45.0	-41.7
US EPA	52.7	9.43	51.6	401	987	-77.7
IMO	71.0	-66.7	-12.0	-65.0	42.5	-39.5

The experimentally measured combined hourly emission amounts and the inventory predictions for all engines at berth are shown in Figure 3.3. The experimentally measured combined hourly emission amounts and the inventory deviations in % from the experimental values for all engines at berth are given in Table 3.3. The deviations in the last two columns of Table 3.3 are the same as the deviations in last two columns of Table 3.1 because there were no measurements of the HC and PM emissions from the auxiliary engines berth (see Table 2.2).

Most methods systemically over-predict the on-board measured combined hourly emission amounts of NO_x and HC, whereas systemically under-predict the on-board measured combined hourly emission amounts of SO_x and CO_2 when the vessel is at berth. The CO and PM inventories' predictions are somewhat scattered around the measured combined hourly emission amounts, although some under-prediction is present. The inventory predictions for NO_x, SO_x, CO_2 and PM are somewhat satisfactory because the absolute deviations do not exceed 73.6%, 81.5%, 51.6%, and 86.3% respectively. However, the inventory predictions for

CO and HC are completely unreliable with maximal absolute deviations reaching 1000% and 1390% respectively.

The inventories, which produce least absolute deviations from the experimentally measured combined hourly emission amounts at berth, are NERI for NO_x, CO, and HC with 11.2%, 1.80%, and 25.0% deviations respectively, MEET for SO_x with 7.56% deviation, and ENTEC for CO_2, and PM with -1.13%, and 7.62%. Tier III for PM has the same result as ENTEC.

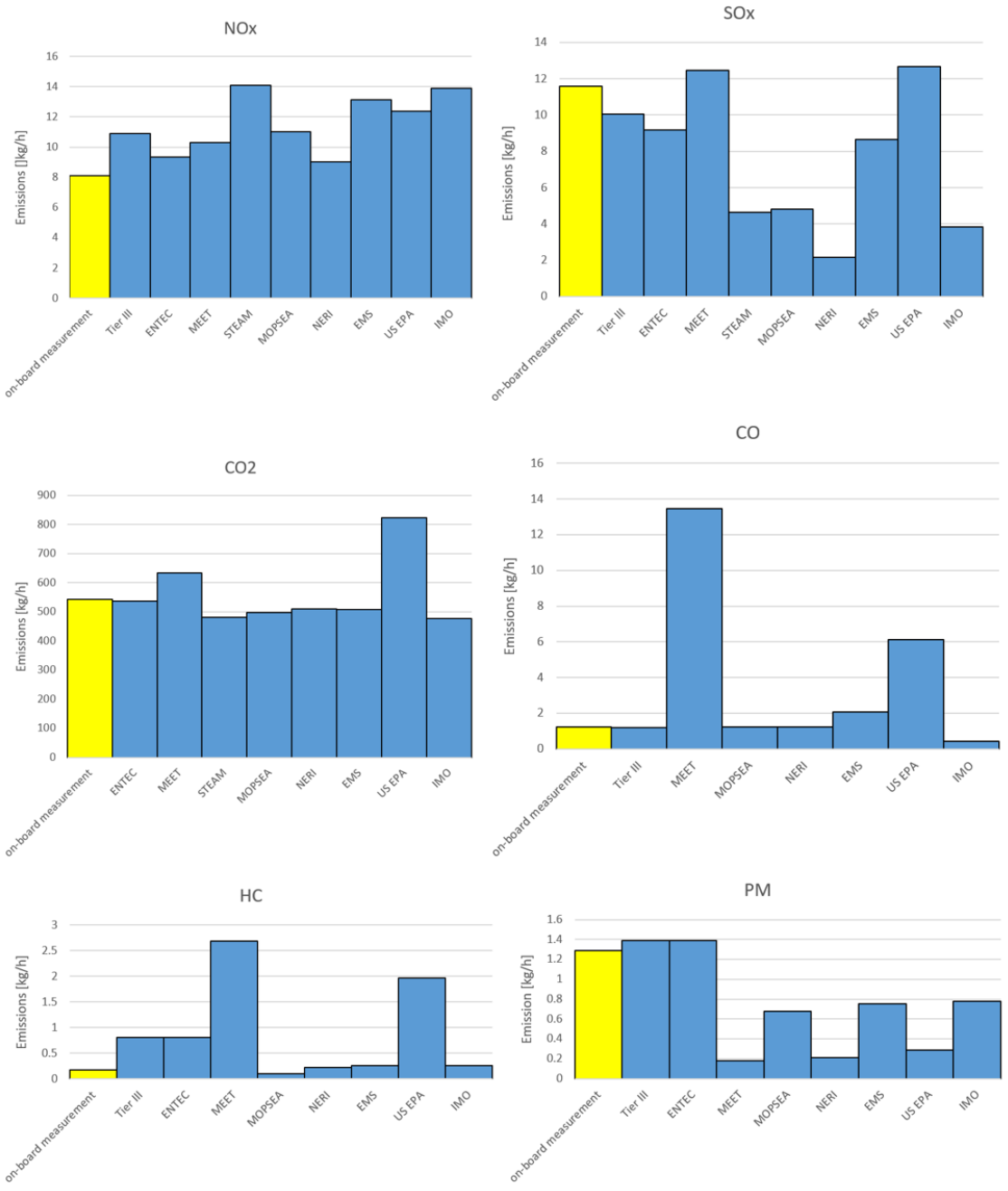

Figure 3.3 *Combined hourly emission amounts' measurement and inventory prediction at berth for the main engine plus the auxiliary engines*

3.1.2. Inventories performance when the vessel is maneuvering

The experimentally measured total emission amounts and the inventory predictions for the main engine when the vessel is maneuvering are shown in Figure 3.4. The experimentally measured total emission amounts and the inventory deviations in % from the experimental values for the main engine when maneuvering are given in Table 3.4.

Table 3.4 *Inventory deviations from the experimentally measured total emission amounts in % for the main engine at maneuvering. The experimental measurements are given in the second row in kg per time equal to the experiment duration according to the third column of Table* ***2.2***.

Inventory	NO_x	SO_x	CO_2	CO	HC	PM
Experiment	51.17	61.28	3051	10.79	0.3772	10.18
Tier III	21.7	-9.26	NaN	-39.1	653	40.8
ENTEC	4.33	-15.8	-0.607	NaN	653	40.8
MEET	53.9	3.09	5.45	161	222	-84.2
STEAM	69.5	-56.5	-9.26	NaN	NaN	NaN
MOPSEA	75.6	-56.4	-9.41	29.1	59.3	-7.90
NERI	69.5	1.63	-7.08	-34.2	109	36.1
US EPA	57.4	0.907	4.86	-42.4	151	-67.9
SMED	18.2	-28.1	-0.670	-59.2	149	52.5
IMO	45.2	-66.4	-16.1	-78.9	138	-20.8

Most methods systemically over-predict the on-board measured total emission amounts of NO_x, and HC, whereas under-predict the CO_2 emission amounts. The SO_x, CO, and PM inventories' predictions are somewhat scattered around the measured total emission amounts for the main engine when the vessel is maneuvering. The CO_2 is well predicted by every inventory method, with absolute deviations less than 16.1%. The inventory predictions for NO_x, SO_x, and PM are somewhat satisfactory because the absolute deviations do not exceed

69.55%, 66.4%, and 84.2% respectively. However, the inventory predictions for CO and HC are very unreliable with maximal absolute deviations reaching 161% and 653% respectively.
The inventories, which produced least absolute deviations for the main engine when maneuvering, are MOPSEA for CO, HC, and PM with 29.1%, 59.3%, and -7.9% deviations respectively, ENTEC for NO_x, and CO_2 with 4.33%, and -0.607% deviations respectively, and NERI for SO_x with 1.63% deviation.

3.1.3. Inventories performance when the vessel is cruising

In comparison to the other two operational modes (at berth and during maneuvering), more inventories are available for prediction of total emission amounts while the vessel is on cruising mode. The experimentally measured total emission amounts and the inventory predictions for the main engine when the vessel is cruising are shown in Figure 3.5. The experimentally measured total emission amounts and the inventory deviations in % from the experimental values for the main engine when cruising are given in Table 3.5.
Most methods systemically under-predict the on-board measured total emission amounts of NO_x, SO_x, and CO_2, whereas at the same time systemically over-predict the on-board measured total emission amounts of CO, HC, and PM from the main engine when the vessel is cruising. The NO_x and CO_2 are well predicted by every inventory method, with absolute deviations less than 21.0% and 24.6% respectively. The inventory predictions for SO_x and CO also are somewhat satisfactory because the absolute deviations do not exceed 74.4% and 55.9% respectively. However, the inventory predictions for HC and PM are completely unreliable with maximal absolute deviations reaching 312% and 335% respectively.
The inventories, which produce least absolute deviations for main engine at cruising, are MEET for SO_x, CO_2, and PM with -28.7%, -13.9%, and -37.6% deviations respectively, STEAM for NO_x with -3.67% deviation, SMED for HC with 104% deviation, and jointly NERI & US EPA for CO with 24.5% deviation.

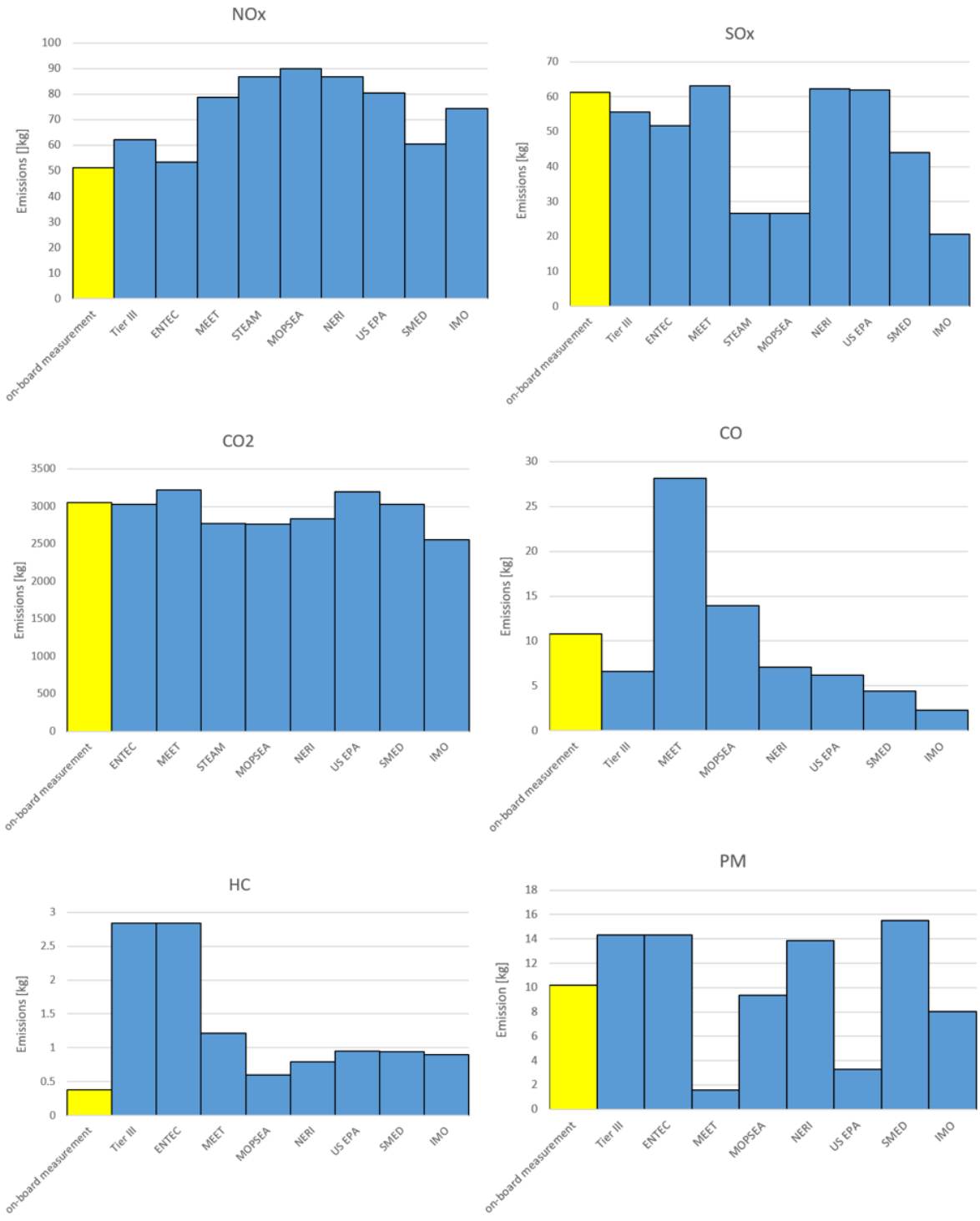

Figure 3.4 *Total emission amounts' measurement and inventory prediction when maneuvering for the main engine*

Table 3.5 *Inventory deviations from the experimentally measured total emission amounts in % for the main engine at cruising. The experimental measurements are given in the first row in kg per time equal to the experiment duration according to the third column of Table* ***2.2***.

Inventory	NO_x	SO_x	CO_2	CO	HC	PM
Experiment	451.9	430.3	18180	26.76	4.401	11.80
Tier I	-16.8	-30.9	NaN	31.6	271	187
Tier II	-5.78	-30.9	NaN	31.6	312	299
Tier III	-7.89	-30.9	NaN	31.6	312	335
Corbett	-10.5	-44.7	-14.3	NaN	312	220
ENTEC	-21.0	-42.0	-18.9	NaN	312	335
MEET	-5.78	-28.7	-13.9	35.1	234	-37.6
STEAM	-3.67	-66.9	-18.5	NaN	NaN	NaN
MOPSEA	-6.31	-66.8	-18.6	36.0	79.1	276
NERI	-4.73	-30.3	-14.4	24.5	312	268
US EPA	-4.73	-30.3	-14.4	24.5	312	268
SMED	-10.5	-50.2	-18.9	-55.9	104	233
IMO	-12.1	-74.4	-24.6	-54.5	291	245

3.2.Development of emission equations for the Main Engines

Equations were developed applying 70% of measured ERs randomly for at berth, manoeuvring and cruising modes for each primary emission.

The regression models were based on the independent variables, which in this study were data on maximum continuous rate (MCR) (as x_1), shaft speed (SS) (as x_2), and emissions (Y). Applying dependant variables affects the accuracy of the results. In the case of this study, fuel consumption was dependent on engine load, and the base SFOC value was influenced by engine stroke type and power. Primarily, engine-model specific base values of SFOC provided by the engine manufacturers were used.

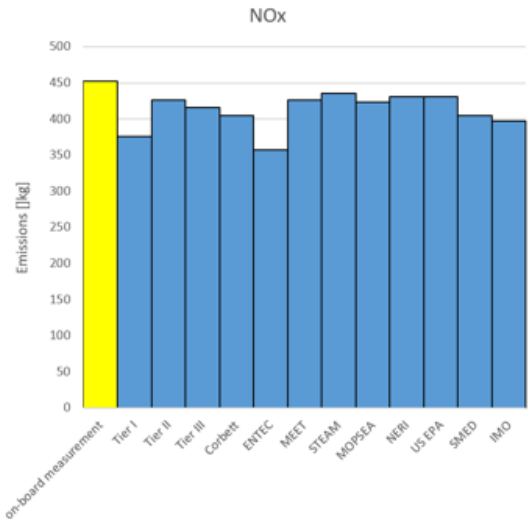
NOx
Emissions [kg]
500
450
400
350
300
250
200
150
100
50
0
on-board measurement
Tier I
Tier II
Tier III
Corbett
ENTEC
MEET
STEAM
MOPSEA
NERI
US EPA
SMED
IMO

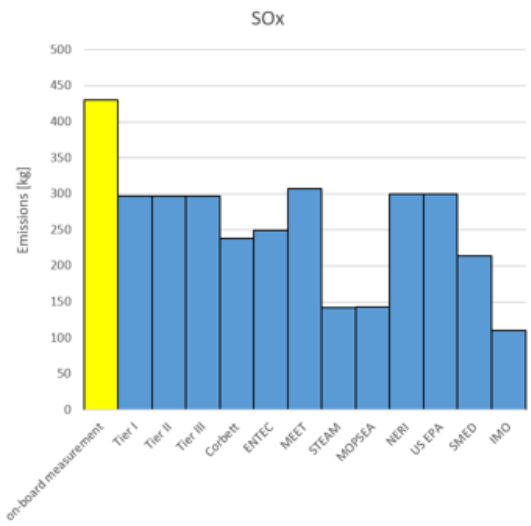
SOx
Emissions [kg]
500
450
400
350
300
250
200
150
100
50
0
on-board measurement
Tier I
Tier II
Tier III
Corbett
ENTEC
MEET
STEAM
MOPSEA
NERI
US EPA
SMED
IMO

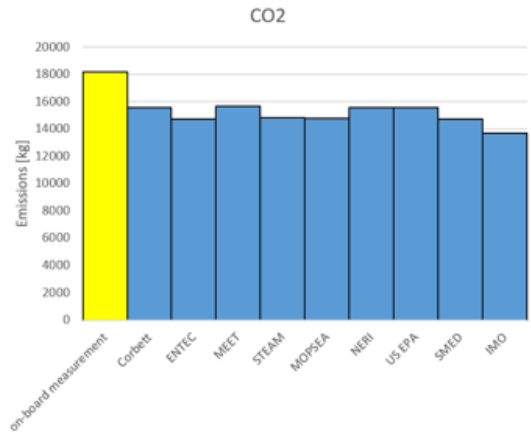
CO2
Emissions [kg]
20000
18000
16000
14000
12000
10000
8000
6000
4000
2000
0
on-board measurement
Corbett
ENTEC
MEET
STEAM
MOPSEA
NERI
US EPA
SMED
IMO

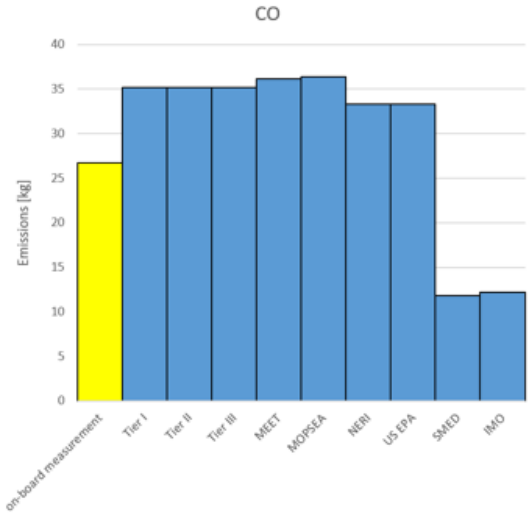
CO
Emissions [kg]
40
35
30
25
20
15
10
5
0
on-board measurement
Tier I
Tier II
Tier III
MEET
MOPSEA
NERI
US EPA
SMED
IMO

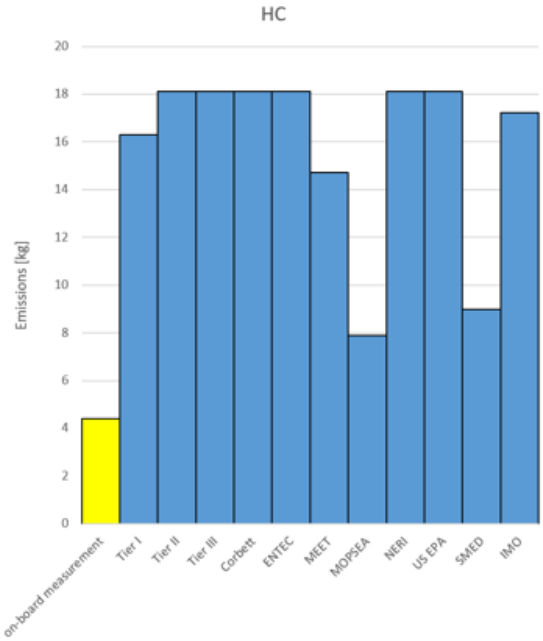
HC
Emissions [kg]
20
18
16
14
12
10
8
6
4
2
0
on-board measurement
Tier I
Tier II
Tier III
Corbett
ENTEC
MEET
MOPSEA
NERI
US EPA
SMED
IMO

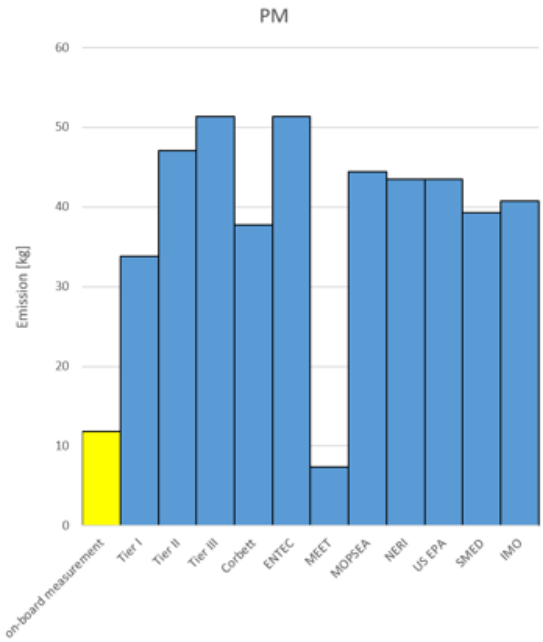
PM
Emission [kg]
60
50
40
30
20
10
0
on-board measurement
Tier I
Tier II
Tier III
Corbett
ENTEC
MEET
MOPSEA
NERI
US EPA
SMED
IMO

Figure 3.5 *Total emission amounts' measurement and inventory prediction when cruising for the main engine*

Instantaneous total fuel consumption is influenced by many independent factors. The fuel consumption of main engines used in propulsion is commonly estimated as a product of the constant SFOC and instantaneous engine power, which gives a linear relationship between fuel consumption and engine power. Ideally, all power systems that require fuel to operate should be modelled separately: the main engines for propulsion, auxiliary engines for power generation, and boilers for heat generation; however, in practice separate modelling is currently not feasible. In any case the methodologies for evaluating power and fuel consumption are fairly simple, and different assumptions were observed to provide biased estimates, especially for auxiliary engines. The SFOC effect, dependent on MCR quantities, was hidden in the developed equations; but as the objective was to analyse the variation effect of independent variables over time on final emissions, the chemical contents of the fuel (carbon, sulphur and nitrogen) were not considered as these are not time-dependant.

Table 3.6 shows the range of on-board measurement datasets used to develop the equations. The data on engine power, engine revolution, and other parameters including intercooled air temperature, scavenging air pressure and cooling fresh water were recorded every five seconds for the main engine. The only restrictions on the use of the developed EF equations would have been any datasets outside the ranges noted in Table 3.6 for Emissions, MCR and SS, but the applied dataset roughly covered a good range for all the variables mentioned in practical shipping operations.

Datafit 9 software, using different model groups including three-parameter power, three- to eleven-parameter polynomial, six and ten Taylor series polynomials, was employed to define the models. The actual emission rates (measured instantaneously in variable timings (h) and variable engine powers (kW)) recorded every five seconds as the base for EFs in units of either ppm or %. They were then normalised to standard conditions: a temperature of 273.1 K and pressure of 101.3 kPa. Final emissions in grams were then calculated.

Table 3.6 *Applied dataset range (the minimum and maximum points)*

Mode		Emissions (g)	MCR[a] (%)	SS[b] (RPM)
At berth	SO_2	8.7–18.8	2.5–12.8	31.5–47.4
	NO_x[c]	6.0–20.0	1.0–12.6	-46.1–49.4[d]
	CO_2	337.6–951.5	1.8–12.6	31–47.2
	CO	0.3–0.9	3.3–12.0	30.3–47.2
Manoeuvring	SO_2	60.1–108.5	37.4–60.0	73.8–89.0
	NO_x	31.1–68.4	29.4–63.7	69.8–80.9
	CO_2	2949–4303	29.4–63.7	69.8–80.9
	CO	7.7–15.3	31.3–63.5	71.1–80.9
Cruising	SO_2	108.7–145.0	59.6–91.6	85.9–90.8
	NO_x	81.2–108.8	59.6–91.6	85.9–90.8
	CO_2	4949.0–5888.0	59.6–90.8	85.9–90.8
	CO	8.9–15.7	59.6–91.6	85.9–90.8

Having applied Datafit 9 software, the maximum quantity of six parameters was used in this study. The equations, developed from non-linear regression analysis, are at a 95% confidence interval. The regression model's curve's alignment with the data points can be predicted by the R_a^2 value (the below equation), where n is the number of points in the data sample and k is the number of independent regressors (the number of variables in the models excluding dependant variables and constants) (Harel 2009). The adjusted R^2 is necessary because the value of the percentage of variation can only be explained by those independent variables that affect the dependent variables. Simply put, the adjusted R^2 will increase if a more useful variable is added and decrease if an un-useful (dependant) variable is added. The methodology framework is shown in Figure 3.6.

$$R_a^2 = 1 - [((1 - R^2)(n-1)) / (n-k-1)]$$

[a] Maximum Continuous Rate
[b] Shaft Speed
[c] NO + NO_2
[d] Negative amounts occur when the shaft churns backward to completely stop the ship at berth.

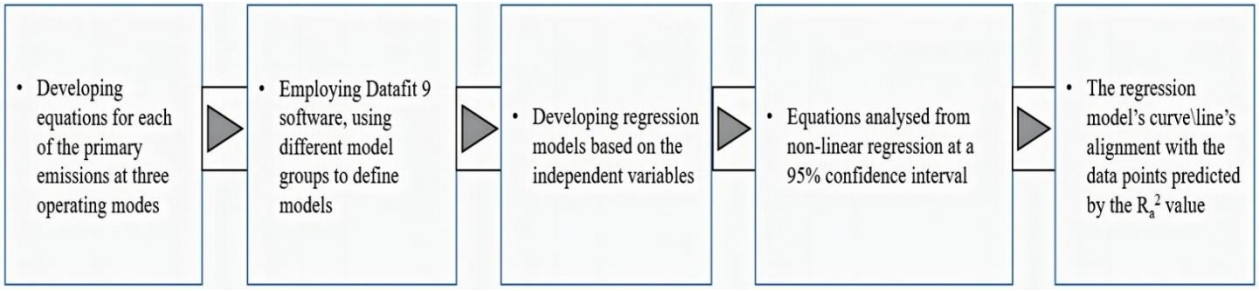

Figure 3.6 *The methodology framework for developing the equations*

3.2.1. On-board measurement campaign

Measurements of main engine at berth were conducted when Vessel I arrived at its destination port but before the main engine were turned off. Both shaft power and SS keep changing while berthing to stop the ship making headway (Figure 3.7); and both strongly affect the quantity of emissions, as depicted in Figure 3.7: that is, when engine speed and power suddenly undergo either positive or negative change, emissions fluctuate accordingly. Sudden change may be caused by external factors such as wind, waves or currents, or by tugs or anchors. Figure 3.7 shows the primary emissions, measured while the vessel was manoeuvring at the destination port. As with at-berth conditions, the levels of emissions change abruptly when SS and shaft power undergo a sudden change, often required to ensure smooth and safe berthing (Fu, Ding et al. 2013), but changes may also be caused by the geometry of the hull, the pivot point, lateral motion, the rudder, the propeller or the thrusters. The geological features of the port and under-keel clearance also affect emissions levels. Normal cruising speed was also visible for emissions (Figure 3.7).

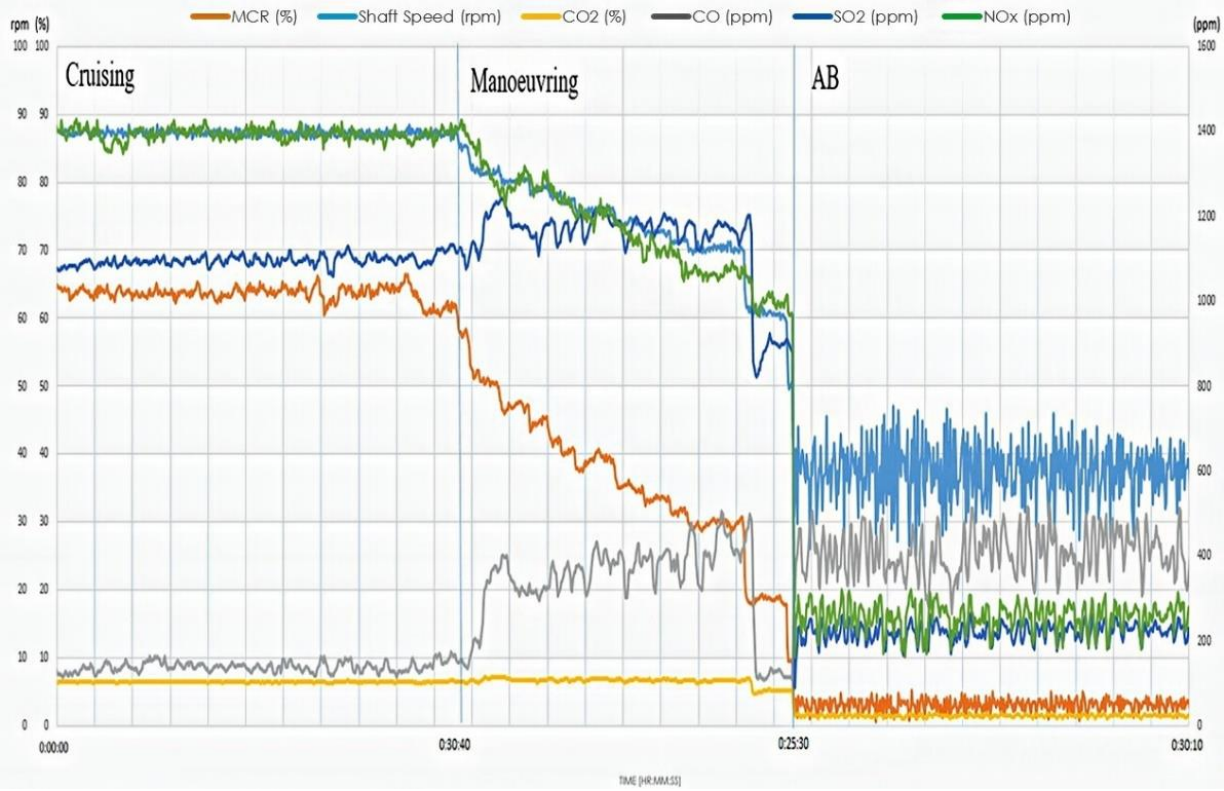

Figure 3.7 *Main engine emission changes at berth, manoeuvring, and cruising*

3.2.2. Validation of emission equations

Applying the percent-predicted method, the remaining random 30% of the emission datasets of Vessels I and II were predicted using the equations presented in Appendix A. By comparing existing inventories with the actual emissions calculated, it is possible to estimate primary emissions for various engine types. Our predicted inventories are closest to actual on-board estimations, at berth or while manoeuvring or cruising (Appendix A).

The standard error of the regression or estimate value (S) (the below equation) demonstrates the mathematical superiority of our predicted emission inventory over other inventories in use. The value is calculated with y' as the instantaneous calculated emission in our and other inventories and N as the total number of datasets for each primary emission of different engine types in different shipping operations. Having the smallest values, our inventories show superiority over other inventories (Appendix A).

$$S = \sqrt{\frac{\sum (y - y')^2}{N}}$$

Figure 3.8 presents some samples of the trends of instantaneous emissions at different MCRs, and again our predicted inventories show the greatest affinity with on-board measurements. Full samples of the primary emissions in different shipping operations are presented in Appendix A.

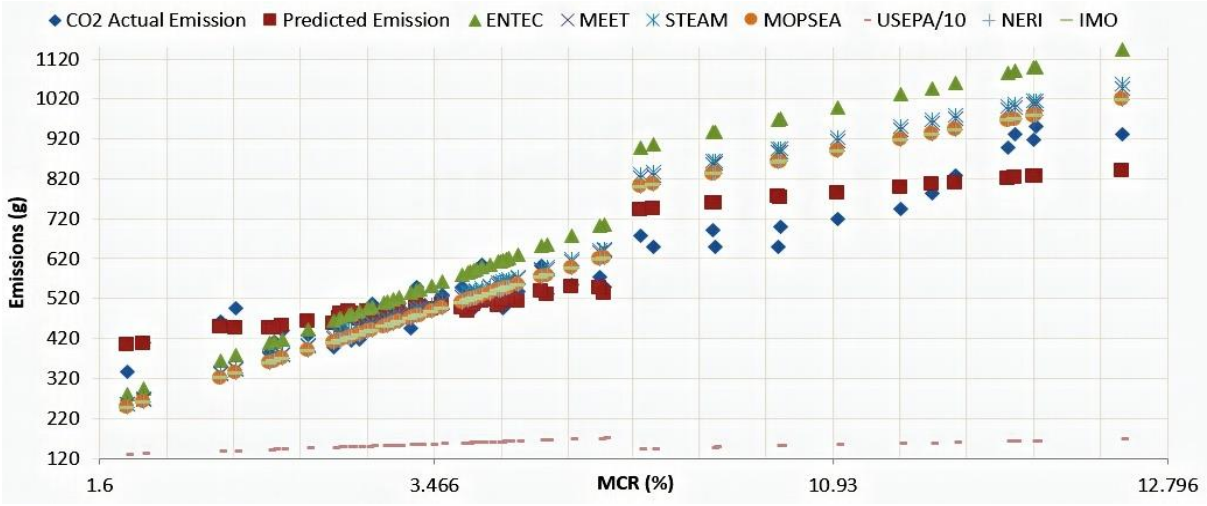

(a) CO_2 emissions at berth

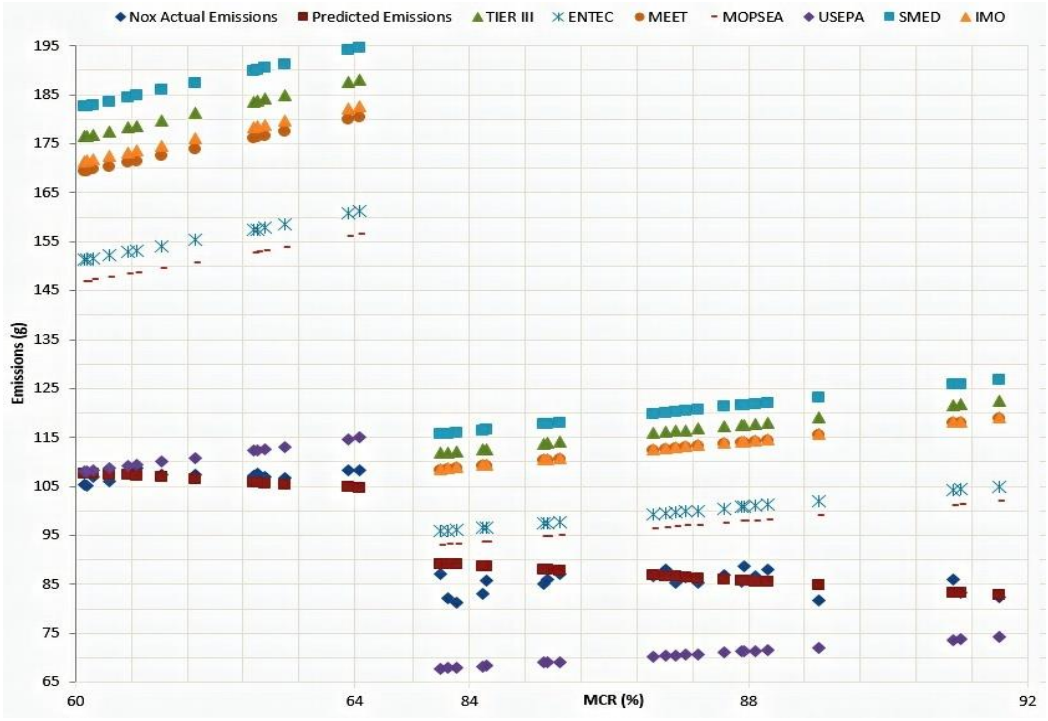

(b) NO_x emissions at cruising

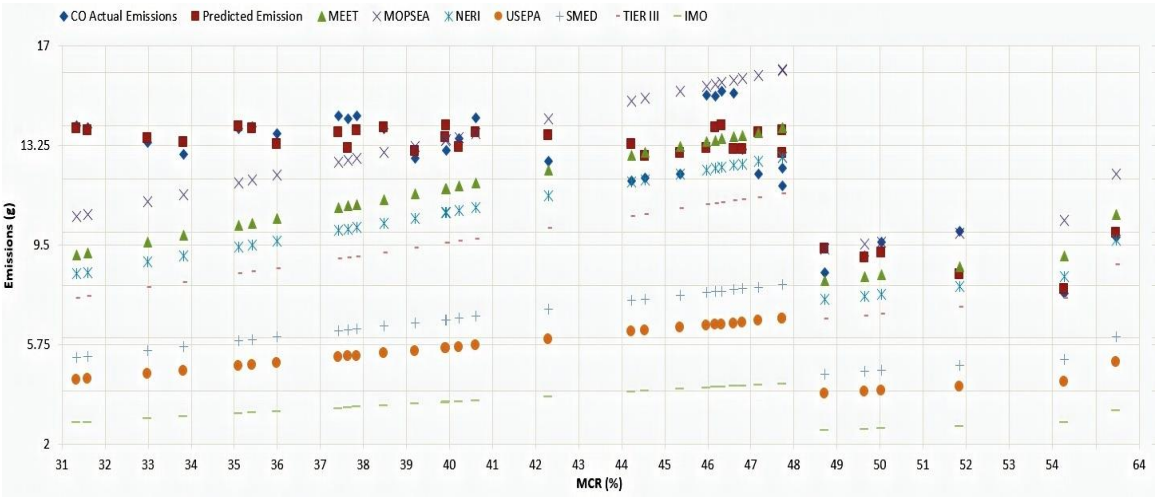

(c) CO emissions at manoeuvring

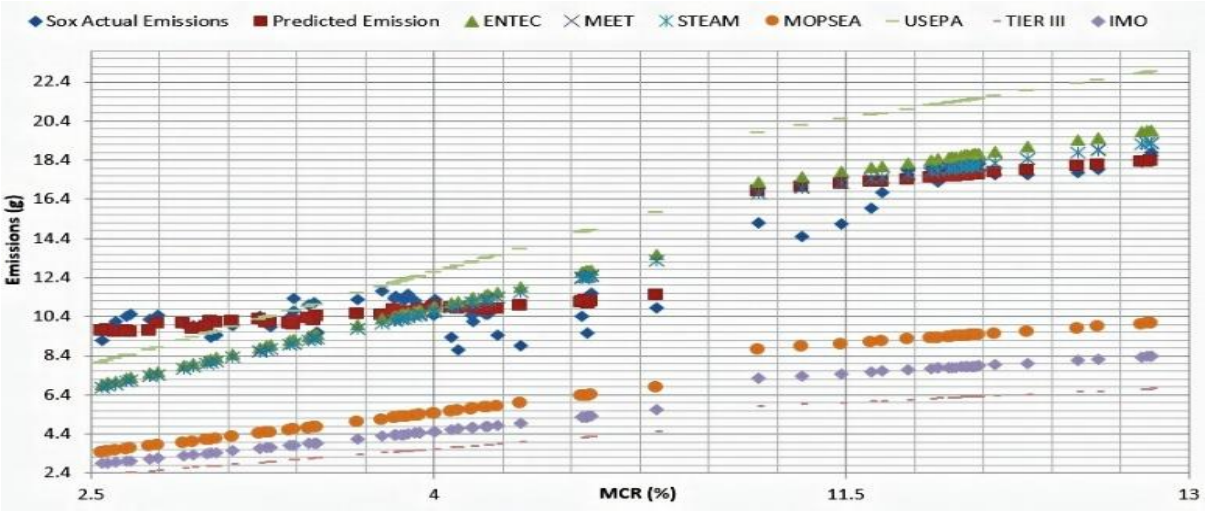

(d) SO_x emissions at berth

Figure 3.8 *Sample of some trends of predicted and available inventory ME emissions (g) in different shipping operation*

Current inventories lack detailed EF datasets for different engine types, shipping modes and emissions. As they also widely ignore national air quality programs, there is a growing need to evaluate their impact on air quality and health.

The engine ER changes (Figure 3.7) are non-linear, indicating a need to simulate emissions more practically in the mathematical model. In our study the effects of changes in engine parameters on emissions are considered for the first time.

Reasons for some non-precise estimations by each of the inventories are provided below:

- TIER III (Trozzi and DeLauretis 2013) datasets do not include CO_2 emissions for main engines; the effects of engine type and shipping activity not considered; and only limited averages of the fuel sulphur content and SFOC are considered. The data on fuel consumption are based on national data on sold fuels, not on engine fuel consumption.

- Entec (Whall, Scarbrough et al. 2010) assumes the engine EF values in different shipping activities and engine loads; and there is considerable uncertainty in some of the assumptions about engine load use in port. The quantities of fuel sulphur and carbon contents and SFOC are averaged, and when applying the inventory to smaller fleets, the error between the assigned EFs and the fleet value increases. Other factors that may be relevant, such as how cold-started engines or various engine loads affect performance in the course of manoeuvring, are ignored.
- Methodology for Emissions and Energy consumption for Transport (MEET) (Auth, Tuv et al. 1999) calculates averaged fuel consumption and engine loads for engines rather than addressing specific situations that may affect performance: for instance, the same EF is used for CO engines at berth and manoeuvring; and for the CO engines of slow- and medium-speed diesel engines. It does not consider the effect of using different marine fuels in engine NO_x EFs in different shipping operations.
- Ship Traffic Emission Assessment Model (Jalkanen, Brink et al. 2009) datasets do not include CO emissions. As a requirement of the SO_x Emission Control Area regulations of the International Maritime Organisation (IMO), only a sulphur mass-percentage of 1.5 is assumed and modelled for main engines. Different engine specifications or shipping operations are not considered when assigning engine NO_x EFs. Engine loads can often influence EFs: for instance, engines operating under a low load may have higher emissions, particularly during harbour manoeuvring; such variations in EFs as a function of engine load are not considered.
- Monitoring programme on air pollution from sea-going vessels (MOPSEA)'s (Gommers, Verbeeck et al. 2007) activity data are gathered from information systems not designed for inventory emissions, so it takes time and experience to repurpose the data to suit them to the emission model, and the work needs to be simplified and tailored to be fit for inventory purposes. This model too makes various assumptions about fuel use and the percentage of MCR which do not reflect these parameters in practice: for example, averaged engine EFs per ship type are used instead of specific figures. There is inadequate focus on engine loads during different shipping activities, and no coverage of engine load variations over 85% or under 10% in NO_x and CO EFs. Nor is there adequate direction for dealing with missing data, or for implementing and using Automatic Identification System (AIS) data.
- National Environmental Research Institute (NERI) (Olesen, Winther et al. 2009) uses the same CO EFs without consideration of engine type or shipping activity; nor are

consistent emission data available as a function of the engine age. In addition, country-specific EFs for CO_2 do not consider engine types or shipping activities.

- United States Environmental Protection Agency (USEPA)'s (USEPA 2000) basis for its operating data seems to have various assumptions that are not validated by the Energy and Environmental Analysis as their contractor. It categorises engines by individual cylinder displacement, which may not indicate a true relationship with high, medium, and slow speeds. Large inconsistencies appear between the output given at full load and the actual ratings of the engine, pointed out in Lloyd's analysis. The data analysis is mostly carried out on engines with a rating of less than 8000 kW, and the applicability of the EFs obtained to engines of all sizes is debatable. There is no consistency between engines' rated power and testing conditions, so EPA categories cannot be determined. There is no agreement on the actual numbers or types of engine, and no reporting of engine markers or displacements. In some instances, the reported maximum power and engine ratings show discrepancies. The Environment Canada report defines the three modes and engine load factor variations under which its engines were tested and does not consider the extent of variation that may exist between engines in the same category; 'normal cruise' and 'docking operation' conditions are undefined in the procedures of the BC Ferry Test Program. Engine NO_x and CO have the same EFs, regardless of fuel or engine used or consideration of shipping activity.
- Swedish Methodology for Environmental Data (Cooper, Gustafsson et al. 2004) inventory likewise Entec (Whall, Scarbrough et al. 2010), mentioned in above paragraphs, suffers from non-precise EFs. Also, there is a great deal of uncertainty about 'manoeuvring' (the assumption is that engines operate at 20% MCR), as well as the need for manoeuvring emissions to take into consideration that emissions from cold state engines, especially CO emissions, which would be significantly different than those from warmer engines. Variability of emissions can also be caused by rapid changes to load during manoeuvring: this study takes none of these into account. Engine EFs (derived from steady state loads of 70–100%) are multiplied 'at sea' by 0.8 for NO_x and by 2.0 for CO for all engines running on diesel. This means that there is significant uncertainty regarding the results. Emission estimations for engines at berth are not considered. The estimates of the fuel sulphur in various fuels over the years are unspecified, and it is assumed that between 1990 and 2003, fuel-dependent EFs of CO_2 were constant. Considering that EFs are different and there is anticipated uncertainty,

specifying exactly how biased emission estimations can be, especially when only at-sea EFs are at play, is difficult.

- IMO (IMO 2014) bases its SO_x base line EFs on a 2.7% sulphur content HMO, although the world average of fuel sulphur is in constant change. The effect of using different fuel types is not considered in applying base SFOC values to engines; the parabolic SFOC dependency on engine load is not considered in HFO; and transient engine load changes are not considered in CO EFs. There are uncertainties about how many active ships exist, and which are allocated to domestic or international voyages. Currently discrepancies occur between the number of active ships described by the IHSF and those observed on AIS, although this will reduce slightly as the availability of AIS data improves. The bottom-up method is used when location information is available, but AIS coverage is not so consistently high for the voyage-by-voyage details to be identified either. Some uncertainties may also arise if the ship is not visible on AIS and its speed is estimated.

3.3.Development of emission equations for the Auxiliary Engines

For each primary emission (NO_x, SO_x, CO_2 and CO), an equation is developed to estimate the emissions. Non-linear regression analysis are performed on 70% of data randomly selected from two on-board measurements of AEs of Vessels I and II at berth.

Determining the independent variable to be included in the regression model requires selecting the sets of data as Y (emissions) and X (maximum continuous rate (MCR)). SFOC amounts are dependent on MCR amounts, so the effect is hidden in MCR quantities. Also, shaft speed during AE emission measurements at berth is constant and is not considered as a variable in developing EF equations. The ranges of applied on-board measurement datasets to develop the equations are shown in Table 3.7.

The equations developed from non-linear regression analysis shown in Table 3.8 are at a 95% confidence interval. The R^2 value indicates how well the data points fit the curve or line of the regression model.

The equations developed and tabulated in Table 3.8 allow prediction of the emissions of the remaining random 30% of the datasets of Vessels I and II. The results of the calculation are presented here, named the predicted emission inventory. This inventory and the actual calculated emissions are benchmarked against existing inventories for estimating primary emissions for different engine types in port (Table 3.9).

Table 3.7 *Applied dataset range (the minimum and maximum points)*

Mode		Emissions (g)	MCR (%)
At berth –AE	SO_x	119.0 – 721.6	29.6 – 96.5
	NO_x	14.2 – 323.4	26.6 – 96.5
	CO_2	2269.9 – 4692.5	23.6 – 96.4
	CO	13.3 – 47.0	27.1 – 96.5

Table 3.8 *Developed EF equations with the adjusted Ra^2 factor*

Mode	EF equations (g)	R^2
At berth – AE	$SO_x = -0.3\,x^2 + 50.7\,x - 1139.7$	0.9401
	$NO_x = -0.1\,x^2 + 12.6\,x - 280.7$	0.9302
	$CO_2 = 9.7 - \frac{9.2}{x} + \frac{4.3}{x^2} - \frac{0.6}{x^3}$	0.9916
	$CO = -0.02\,x^2 + 2.1\,x - 37.0$	0.7672

Table 3.9 *Results of actual on-board estimation, predicted emission inventory and available inventories (g)*

At berth–AE	SO_x	NO_x	CO_2	CO
Actual On-board Estimation	12183.3	4627.4	129800.8	630.7
Predicted Emission Inventory	12319.4	4703.3	130375.7	646.8
MEET(Auth, Tuv et al. 1999)	9646.9	5555.2	127345.8	998.0
NERI (Olesen, Winther et al. 2009)	Same as MEET	Same as IMO	126955.8	977.1
US EPA (USEPA 2000)	11448.5	7265.6	120352.8	511.7
TIER III (Trozzi and DeLauretis 2013)	3338.7	9585.0	Not Specified	1152.1
ENTEC (Entec 2007)	8075.6	8235.0	114966.4667	Not Specified
STEAM (Jalkanen, Brink et al. 2009)	9636.9	Same as IMO	128458.2	Not Specified
MOPSEA (Gommers, Verbeeck et al. 2007)	5008.1	6856.8	123764.2	1159.8
SMED (Cooper, Gustafsson et al. 2004)	6828.1	9787.5	Same as ENTEC	549.6
IMO (IMO 2014)	4173.4	7792.3	123923.4	431.3

As shown, in all cases, the predicted inventories offer the closest match to the actual on-board estimations, compared with other available inventories.

To validate the mathematical superiority of the predicted emission inventory compared with other inventories, the standard error of the regression or estimate value (S) is used. It represents the average distance that the predicted values, and the values from available inventories, fall from the actual estimation emission, which is used to describe the average accuracy. Smaller values indicate whether the predicted emission inventory or available emission inventories are closer to the fitted line of actual data points.

Table 3.10 *Comparison of S value for the predicted inventories and existing inventories*

At berth – AE	SO_x	NO_x	CO_2	CO
Predicted Emission Inventory	55.09	22.6	0.1	3.9
TIER III	232.5	170.7	-	26.5
ENTEC	127.1	124.8	0.9	-
MEET	94.8	115.1	0.6	21.0
STEAM	95.01	-	0.6	-
MOPSEA	194.6	79.8	0.6	26.8
NERI	-	-	0.6	19.4
US EPA	64.1	89.8	0.6	8.3
SMED	154.2	177.6	-	8.1
IMO	213.5	109.8	0.6	-

The standard error endorses the superiority of all predicted inventories as they have the smallest value compared with the actual emissions for different engine types in port in the remaining 30 % of emissions from both Vessel I and Vessel II (Table 3.10).

Trends of instantaneous emissions versus different MCRs are provided in Figure 3.9, which also reveal that the predicted inventories provide results closer to the actual on-board measurements than existing inventories.

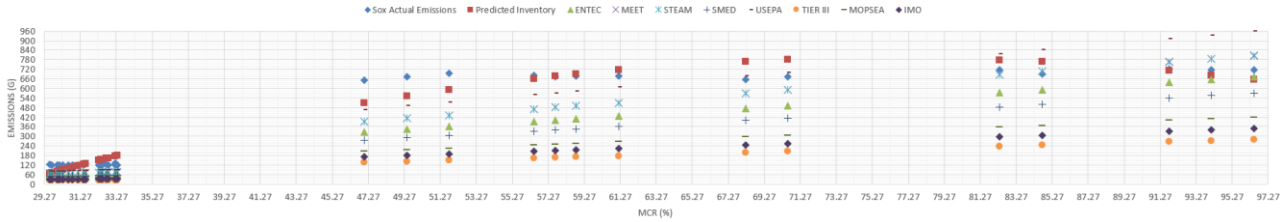

(a) SO_x emissions at berth

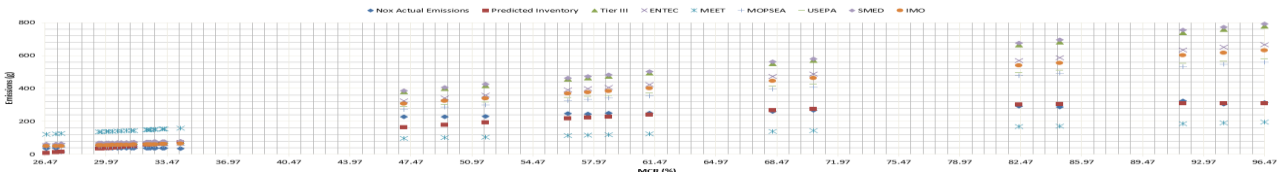

(b) NO_x emissions at berth

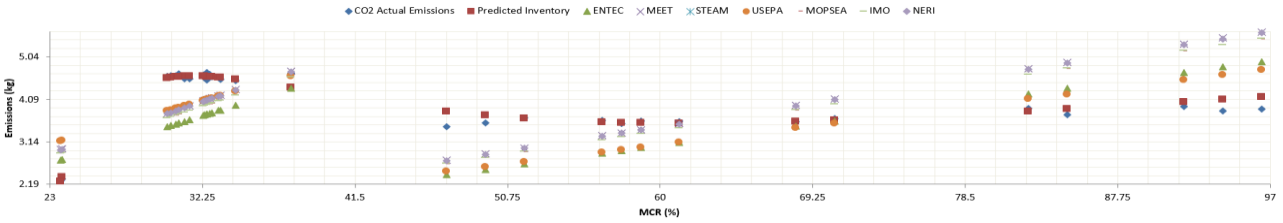

(c) CO_2 emissions at berth

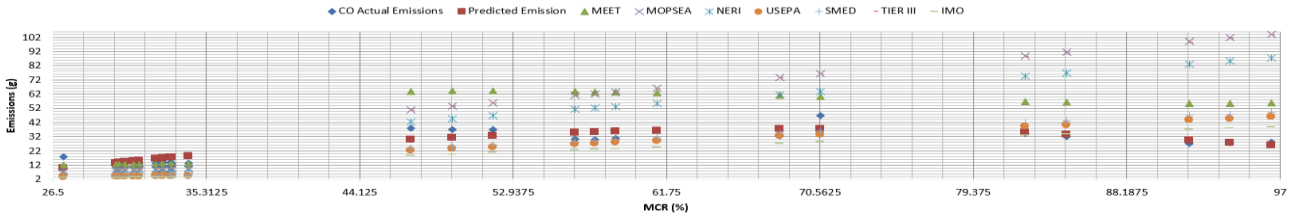

(d) CO emissions at berth

Figure 3.9 *Trends of predicted and available inventory emissions (g) for AE at berth*

The scarce definitive information on the energy use and fuel consumption of sea-going ships at berth means that estimation of their emissions are still considerably inaccurate. This lack needs to be addressed by more regular monitoring (Van der Gon, Tno. et al. 2010). There is a need to simulate emissions more realistically in mathematical approaches. This study is the first to consider the effect of changes in MCR in non-linear regression analysis, on emissions. Below is a list of weaknesses in each of the nine inventories that resulted in non-precise emission estimation:

MEET:

- The methodology has applied simplified approach for NO_x EFs in AEs ignoring harbour activities and engine type.
- Averaged amounts of fuel consumption and engine loads have been used.
- Although they are dependant, the methodology considers the simultaneous effect of engine power and load factor as independent parameters for AE CO.

NERI:

- See the comments under MEET and IMO.
- The same EF for CO is used regardless of engine type and shipping activity, because of the lack of consistent emission data as a function of engine-built year.
- The methodology applies country-specific EF for CO_2.

USEPA:

- The engine categories are based on individual cylinder displacement, which may not hold true correspondence to engines in the high speed, medium speed, and slow speed categories, used by IMO and Lloyd's in preceding analyses.
- Lloyd's data also indicates large inconsistencies at full load versus actual engine ratings in the measured output.
- The engine rated power related to test conditions are very inconsistent across engines.
- The same EFs are given for NO_x and CO regardless of the fuel type or engine type, with limited shipping activity consideration.

TIER III:

- CO_2 emissions is not included in the datasets.
- There is no consideration of the effect of engine type and shipping activity on CO.
- EFs are based on nationally collected data on sold fuel, not real fuel consumption.
- Limited averaged amounts of SFOC and fuel sulphur content are considered.

ENTEC:

- CO emissions is not included in the datasets.
- Assumptions are made in assigning EFs in different shipping activities, engine loads along with limited averaged fuel sulphur and carbon content, and SFOC.
- The use of a combined EF for high-speed diesel (HSD) and MSD AEs will increase the uncertainty for NO_x emissions at berth.

- Engine types for the AE have not been specified and an approximated 50:50 range between HSD and MSD has been applied.

STEAM:

- CO emissions is not included in the datasets.
- Like IMO, it considers only crankshaft rpm as a parameter to assign the NO_x EFs regardless of other engine specifications or of shipping operations.
- A default sulphur mass-percentage of 1.5 for the AE has been assumed in the model.

MOPSEA:

- There is no coverage of engine loads in NO_x and CO EFs for AE.
- The model foresees only the energy used for air conditioning, ventilation, hotel requirements, and preheating of heavy fuel by auxiliaries.

SMED:

- The same comments as listed under ENTEC are applicable.
- Fuel-dependent emission factors of CO_2 have been assumed not to vary over the period 1990–2003, and has been calculated from a carbon content of 86.7% for all fuels.
- Only a very rough estimate of the fuel sulphur in different fuels and years could be made for the purposes of this study.

IMO:

- SO_x base line EFs are based on HFO with 2.7% sulphur content. Further regional variations of fuel sulphur content are not taken into account and this percentage is assumed to be the average that is representative for the global fleet in each year.
- Only a constant value for SFOC in the AE is used.
- All CO EFs represent steady-state operation; emissions and transient engine loads and their changes are not considered.
- Assumptions have been considered regarding AE loads. EFs and SFOC remain areas of uncertainty for the AEs.

Chapter 4: Development of vessel-specific inventory families at port and at sea

The objective of this chapter is to present a comprehensive case study to identify the best vessel-specific inventory family that predicts the primary emissions from an ocean-going vessel when at berth, while maneuvering and while cruising. The other main purpose of the chapter is to generalize the implication of the case study by advising a novel policy, which will allow different authorities to estimate the shipping emissions in a cost-effective and reliable way. The emissions rates of nitrogen oxides, Sulphur oxides, carbon dioxide, carbon monoxide, hydrocarbon, and particulate matter from the main engine and from the auxiliary engines are measured for different modes of ship operations in an on-board experiment campaign. The measured total emission amounts were predicted with 13 families of emission inventories and prediction deviations have been calculated. A procedure was advised for estimating the prediction inventory deviations of the combined hourly emission amounts from the main engine plus the auxiliary engines. Each inventory family has been formalized as a six-dimensional vector of prediction deviations for any mode of operation. The best vessel-specific inventory families were identified using the minimal mean absolute deviation criteria. A more rational procedure to rank inventories is considered, which treats the missing value problem and constructs a six-attribute value function. The use of preferential analysis and value functions further clarifies the recommended choice of inventory method. In this case study we demonstrated that the most suitable inventory families will provide reliable predictions with acceptable deviations from the measured emissions. At berth and for maneuvering, the best inventory family turned out to be MOPSEA (with 32.2% and 39.6% mean absolute deviations respectively). For cruising, the most precise inventory family is MEET (with 59.2% mean absolute deviation), whereas MOPSEA being the third best. However, some of the other inventories produce unacceptably high deviation, well above 100%. The practical implication is that while inventory methods can produce precise and cost-effective predictions, they should never be used without experimental verification. That is why, we provide an algorithm to use on-board experimental measurements to identify the best vessel-specific inventory family, which predicts the primary emission of a ship at a given mode of operation. The proposed algorithm and the implications of the case study are utilized to motivate a proposal for a novel future policy for a cost-effective and reliable emission estimation from shipping.

4.1.Best family inventory when the vessel is at berth

For each inventory family the mean value of its absolute deviations from the experimentally measured combined hourly emission amounts is shown in the last column of Table 4.1. With all its imperfections these values can serve as a "quick and dirty" marginalization of the 6-dimensional preference problem into a 1-dimensional ranking problem in ascending order of the Mean Absolute Deviation (MAD). The average absolute deviation of a data set is the average of the absolute deviations from a central point. It is a summary statistic of statistical dispersion or variability. In this general form, the central point can be the mean, median, mode, or the result of another measure of central tendency. All inventory families, which do not predict at least five of the six combined hourly emission amounts, are disqualified and their MADs are shown bolded in Table 4.1. According to the minimal MAD criterion the best inventory family at berth is MOPSEA with the 32.2% MAD. That family predicts all six of the emissions. The other inventory families, which predict all six of the combined hourly emission amounts, are MEET, NERI, EMS, US EPA, and IMO.

Table 4.1 *Inventory deviations from the experimentally measured combined hourly emission amounts in % for the main engine plus the auxiliary engines at berth. The experimentally measured combined hourly emission amounts are given in the first row in kg/h. The mean absolute deviations in % are shown in the last column*

Inventory	NO_x	SO_x	CO_2	CO	HC	PM	MAD
Experiment	8.117	11.58	543.6	1.219	0.1806	1.289	0.000
Tier III	34.2	-13.3	NaN	-2.58	350	7.62	81.5
ENTEC	15.1	-20.7	-1.13	NaN	350	7.62	78.9
MEET	27.2	7.56	16.6	1000	1390	-86.3	422
STEAM	73.6	-59.9	-11.5	NaN	NaN	NaN	**48.3**
MOPSEA	36.0	-58.5	-8.58	1.83	-41.0	-47.5	32.2
NERI	11.2	-81.5	-6.21	1.80	25.0	-83.9	34.9
EMS	61.9	-25.2	-6.69	69.7	45.0	-41.7	41.7
US EPA	52.7	9.43	51.6	401	987	-77.7	263
IMO	71.0	-66.7	-12.0	-65.0	42.5	-39.5	49.5

4.2.Best family inventory when the vessel is maneuvering

For each inventory family the MAD criterion is shown in the last column of Table 4.2. All inventories, which do not predict at least five of the six total emission amounts, are disqualified and their mean values are shown bolded in Table 4.2.

According to the minimal MAD criterion, the best inventory family for the main engine, when the vessel is maneuvering, is MOPSEA with the 39.6% MAD. That family predicts all six of the emissions. The other inventory families which predict all six of the total emission amounts are MEET, NERI, US EPA, SMED, and IMO.

Table 4.2 *Inventory deviations from the experimentally measured total emission amounts in % for the main engine at maneuvering. The experimental measurements are given in the second row in kg per time equal to the experiment duration according to the third column of Table* ***2.2****. The mean absolute deviations in % are shown in the last column*

Inventory	NO_x	SO_x	CO_2	CO	HC	PM	MAD
Experiment	51.17	61.28	3051	10.79	0.3772	10.18	0.000
Tier III	21.7	-9.26	NaN	-39.1	653	40.8	153
ENTEC	4.33	-15.8	-0.607	NaN	653	40.8	143
MEET	53.9	3.09	5.45	161	222	-84.2	88.3
STEAM	69.5	-56.5	-9.26	NaN	NaN	NaN	**45.1**
MOPSEA	75.6	-56.4	-9.41	29.1	59.3	-7.90	39.6
NERI	69.5	1.63	-7.08	-34.2	109	36.1	42.9
US EPA	57.4	0.907	4.86	-42.4	151	-67.9	54.1
SMED	18.2	-28.1	-0.670	-59.2	149	52.5	51.3
IMO	45.2	-66.4	-16.1	-78.9	138	-20.8	61.0

4.3.Best family inventory when the vessel is cruising

For each inventory family the MAD criterion is shown in the last column of Table 4.3. All inventories, which do not predict at least five of the six total emission amounts, are disqualified and their mean values are shown bolded in Table 4.3.

According to the minimal MAD criterion, the best inventory family for the main engine, when the vessel is cruising is MEET with the 59.2% MAD. That family predicts all six of the

emissions. The other inventory families which predict all six of the total emission amounts, are MOPSEA, NERI, US EPA, SMED, and IMO.

Table 4.3 *Inventory deviations from the experimentally measured total emission amounts in % for the main engine at cruising. The experimental measurements are given in the first row in kg per time equal to the experiment duration according to the third column of Table* ***2.2****. The mean absolute deviations in % are shown in the last column*

Inventory	NO_x	SO_x	CO_2	CO	HC	PM	MAD
Experiment	451.9	430.3	18180	26.76	4.401	11.80	0.000
Tier I	-16.8	-30.9	NaN	31.6	271	187	107
Tier II	-5.78	-30.9	NaN	31.6	312	299	136
Tier III	-7.89	-30.9	NaN	31.6	312	335	143
Corbett	-10.5	-44.7	-14.3	NaN	312	220	120
ENTEC	-21.0	-42.0	-18.9	NaN	312	335	146
MEET	-5.78	-28.7	-13.9	35.1	234	-37.6	59.2
STEAM	-3.67	-66.9	-18.5	NaN	NaN	NaN	**29.7**
MOPSEA	-6.31	-66.8	-18.6	36.0	79.1	276	80.5
NERI	-4.73	-30.3	-14.4	24.5	312	268	109
US EPA	-4.73	-30.3	-14.4	24.5	312	268	109
SMED	-10.5	-50.2	-18.9	-55.9	104	233	78.7
IMO	-12.1	-74.4	-24.6	-54.5	291	245	117

4.4.Improvement of the Minimal Mean Absolute Deviation criterion

A problem related to the case study described in sections 4.1 to 4.3 is the application of the minimal mean absolute deviation criterion to rank the inventory families under specific operational mode of the vessel. That criterion is not entirely rational, as it was pointed in the text. In this section we will discuss a more elaborate and rational method for ranking.

In sections 4.1 to 4.3, we arranged the possible inventory methods according to preference three times (for each mode of operation). The preferences of any decision maker (DM) over a specific inventory family for a selected operational mode of a given vessel will depend only on the deviations of the inventory prediction emissions from the six emissions measured in the on-board experiment. Let us denote those deviations (in %) as follows: $\Delta_1 = \Delta NO_x$, $\Delta_2 = \Delta SO_x$,

$\Delta_3 = \Delta\mathrm{CO}_2$, $\Delta_4 = \Delta\mathrm{CO}$, $\Delta_5 = \Delta\mathrm{HC}$ and $\Delta_6 = \Delta\mathrm{PM}$. The six values can be organized in a 6-dimensional vector of deviations $\vec{\Delta}$ as follows:

$$\vec{\Delta} = \left(\Delta_1, \Delta_2, \ldots, \Delta_6\right) = \left(\Delta\mathrm{NO_x}, \Delta\mathrm{SO_x}, \Delta\mathrm{CO_2}, \Delta\mathrm{CO}, \Delta\mathrm{HC}, \Delta\mathrm{PM}\right)$$

The parameters $\Delta_1, \Delta_2, \ldots, \Delta_6$ in the terminology of decision analysis are called attributes. Some of the vectors can have one attribute missing (because some inventory families do not predict all six of the emissions). We need to rank those vectors for each of the operational modes of a vessel.

Example 5.

In our case study during maneuvering, according to Table 3.4, we have six vectors (for MEET, MOPSEA, NERI, US EPA, SMED and IMO) with all 6 deviations:

$\vec{\Delta}^{MEET}_{maneuvering}$ =(53.9,3.09,5.45,161,222, -84.2)

$\vec{\Delta}^{MOPSEA}_{maneuvering}$ =(75.6,-56.4,-9.41,29.1,59.3,-7.90)

$\vec{\Delta}^{NERI}_{maneuvering}$ =(69.5,1.63,-7.08,-34.2,109,36.1)

$\vec{\Delta}^{US\ EPA}_{maneuvering}$ =(57.4,0.907,4.86,-42.4,151,-67.9)

$\vec{\Delta}^{SMED}_{maneuvering}$ =(18.2,-28.1,-0.670,-59.2,149,52.5)

$\vec{\Delta}^{IMO}_{maneuvering}$ =(45.1,-66.4,-16.1,-78.9,138,-20.8)

During maneuvering we also have two other vectors with missing values, but with at least four emission deviations calculated (for Tier III, and ENTEC):

$\vec{\Delta}^{Tier\ III}_{maneuvering}$ =(21.7,-9.26,NaN,-39.1,653,40.8)

$\vec{\Delta}^{ENTEC}_{maneuvering}$ =(4.33,-15.8,-0.607,NaN,653,40.8)

In sections 4.1 to 4.3, we implicitly substituted the missing values with the mean of the known absolute deviations (that is with MAD). There are other more elaborate methods to impute

missing values (Cohen, Cohen et al. 2003, Acock 2005), but this problem goes beyond the scope of the thesis (see (Nikolova, Toneva-Zheynova et al. 2012) for further discussion).

In sections 4.1 to 4.3, we used the mean absolute deviation criterion to marginalize the stated six-dimensional preference problem into a one-dimensional ranking problem. However, it has been stated in this thesis that the criterion in question is "quick and dirty". Completely rational decisions can be obtained if a value function is built, which accurately reflects the preferences of the DM. The function will be additive because the DM holds the mutual preferential independence over the 6 attributes: from two inventories, the DM will prefer the one that has more favorable deviation for any attribute, if the rest of the attributes are pair-wise equal, and the decision will never depend on the equal deviations (French and Insua 2010). That is why, it is possible to construct a value function over the vector of deviations in the form:

$$v\left(\vec{\Delta}\right) = v\left(\Delta\mathrm{NO_x}, \Delta\mathrm{SO_x}, \Delta\mathrm{CO_2}, \Delta\mathrm{CO}, \Delta\mathrm{HC}, \Delta\mathrm{PM}\right) =$$
$$= a_1 v_1\left(\Delta\mathrm{NO_x}\right) + a_2 v_2\left(\Delta\mathrm{SO_x}\right) + a_3 v_3\left(\Delta\mathrm{CO_2}\right) + a_4 v_4\left(\Delta\mathrm{CO}\right) + a_5 v_5\left(\Delta\mathrm{HC}\right) + a_6 v_6\left(\Delta\mathrm{PM}\right)$$

The inventories have to be ranked in descending order of the value function. The value function is normalized in the closed interval [0; 1] in a sense that it should be 1 if all deviations are 0% (the best-case scenario) and it should be 0 if all deviations are -100% (the worst-case scenario). In the above equation, the constants a_i, for i=1, 2, …, 6 are the weight coefficients, which reflect the importance of each attribute into the overall preference of the DM over the six-dimensional vectors $\vec{\Delta}$. Each of the six constants should be non-negative and they should sum to one. The one-dimensional functions $v_i(.)$, for i=1, 2, …, 6 are the attribute value functions over each of the emission deviations (which are value-difference functions (French & Insua, 2010)). Each of $v_i(.)$ is normalized so that v_i(-100%)=0, v_i(0%)=1, and $\lim_{\Delta_i \to \infty} v_i\left(\Delta_i\right) = 0$. The function should increase from -100% to 0% and decrease from 0% to "plus infinity" %. An example of such a function is given on Figure 4.1.

It is perfectly rational that the attribute value functions are different for each of the attributes and for each of the vessel modes of operation. Alternatively, the DM may use one and the same function over each attribute for each mode, since they all measure the opinion of the DM regarding the precision of predictions. The form of the attribute value functions depends solely on the preferences of the DM. There is not much discussion in literature regarding the rational construction of value functions. However, as far as value functions are a special case of utility

functions under risk, then the techniques for construction of such functions may be adopted for the case of value functions. The single attribute utility function is constructed usually by eliciting several nodes of their function and then applying either an analytical non-linear function to approximate the utility on the elicited nodes, or linear function to interpolate over the elicited nodes. We will demonstrate how to elicit several nodes of the one-dimensional function $v_i(.)$. It is already known that $v_i(-100\%)=0$, $v_i(0\%)=1$, and $\lim_{\Delta_i \to \infty} v_i\left(\Delta_i\right) = 0$. The DM can select a set of M additional deviation values $\left\{\Delta_{i,1}, \Delta_{i,2}, \ldots, \Delta_{i,M}\right\}$ for the i^{th} emission. To find the value of the one-dimensional function $v_i\left(\Delta_{i,j}\right)$ at the deviation $\Delta_{i,j}$ the DM has to identify the probability p_j where he/she is indifferent between:

A) the option of getting $\Delta_{i,best} = 0\%$ with probability p_j or getting $\Delta_{i,worst} = -100\%$ with probability $(1-p_j)$. This option is denoted as $<\Delta_{i,best}\left(p_j\right)\Delta_{i,worst}>$.

B) the option of getting a deviation $\Delta_{i,j}$ for sure.

If p_j is identified by the DM so that the latter is indifferent between the two stated options, then $v_i\left(\Delta_{i,j}\right) = p_j$. In fact, the DM has to solve M preferential equations of the type $<\Delta_{i,best}\left(p_j\right)\Delta_{i,worst}> \sim \Delta_{i,j}$ where the symbol ~ stands for indifference. The recommended method to elicit such nodes is called probability equivalence method, but there are other more complicated methods (see (French and Insua 2010) as well as (Nikolova, Hirota et al. 2006) for discussion on methods to elicit nodes of one-dimensional value functions).

The weight coefficients in the value function measure the importance of each pollutant in the overall assessment of preferences over emission inventories. It is only natural to expect that pollution levels have different significance depending on the regime – pollution close or in ports are causing more direct harm than emissions while at sea, while still the pollution is of global importance. There are elaborate methods to elicit the weight coefficients, which are nothing else but scaling constants in the utility theory. Scaling constants are elicited subjectively, where the DM must identify the probability p_i, which makes him/her indifferent when comparing:

A) the option of getting $\vec{\Delta}_{best} = (0,0,0,0,0,0)$ with probability p_i or getting $\vec{\Delta}_{worst} = (-100,-100,-100,-100,-100,-100)$ with probability (1–p_i). This option is denoted as $< \vec{\Delta}_{best}\ (p_i)\ \vec{\Delta}_{worst} >$.

B) the option of getting for sure a deviation vector, where only the *i*-th deviation is set to its best level 0%, and the others are at their worst level of -100%: $\vec{\Delta}_{corner,i} = (\Delta_1 = -100,\ldots,\Delta_{i-1} = -100,\Delta_i = 0,\Delta_{i+1} = -100,\ldots,\Delta_n = -100)$. Such vector is a.k.a. corner vector.

If p_i is identified by the DM so that the latter is indifferent between the two stated options, then a_i=p_i. In fact, the DM has to solve six preferential equations of the type $< \vec{\Delta}_{best}\ (p_i)\ \vec{\Delta}_{worst} > \sim \vec{\Delta}_{corner,i}$ (see (Keeney and Raiffa 1993) for detailed discussion on multi-dimensional utility functions and identification of scaling constants).

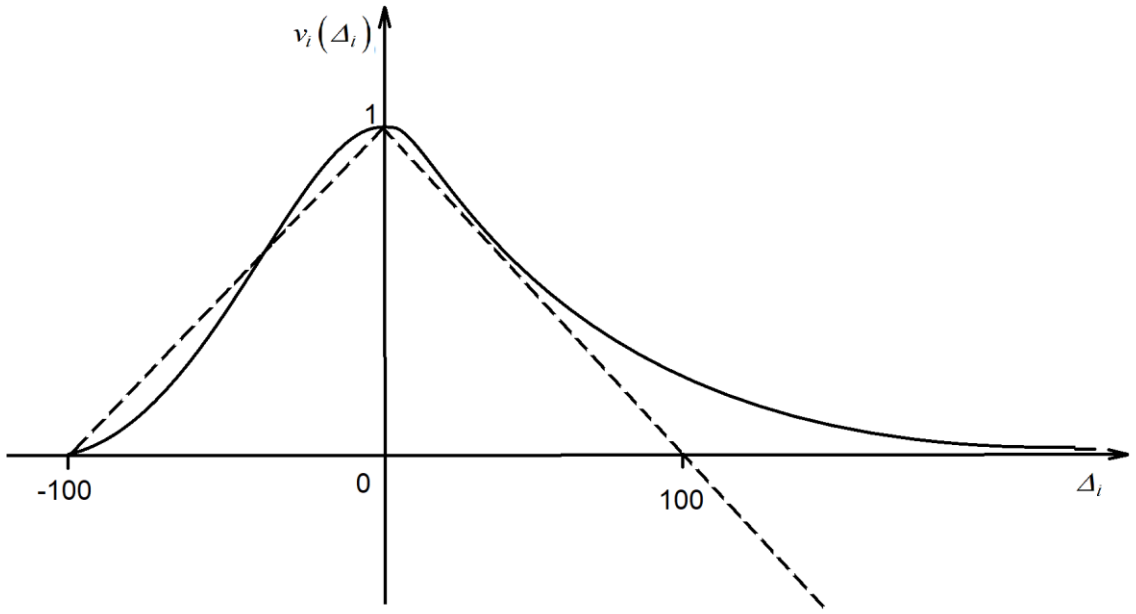

Figure 4.1 *Example of the value functions* $v_i(.)$ *over an emission deviation (solid line). The function* $v_{quick}(\Delta_i) = 1-|\Delta_i|/100$ *is shown for reference (dashed line)*

4.5. Choosing the best inventory family for a given type of operation

Constructing the value functions, we will be able to choose which inventory method is the best (most preferred) for each operational mode. The following algorithm can be utilized to select the best inventory method for a given type of ship operation:

Algorithm to select the best inventory method for a selected type of operation:

1. Define the vector of deviations $\vec{\Delta} = (\Delta NO_x, \Delta SO_x, \Delta CO_2, \Delta CO, \Delta HC, \Delta PM)$ for each inventory method (with at least five emission deviations calculated).

2. Impute missing values in the vector of deviations by replacing them with the mean of the known deviations' absolute values.

3. Construct the attribute value functions $v_i(.)$ for the selected type of operation.

4. Elicit the scaling constants a_i for i=1, 2, …, 6 for the selected type of operation.

5. Construct the value function v as function of six attributes and their scaling constants.

6. Calculate $v(\vec{\Delta})$ for each of the deviation vectors from step 1).

7. Choose the inventory family that has the highest value, calculated in step 6).

While our algorithm assumes we need at least five calculated deviations (in step 1), this requirement may be modified and is prescriptive, not mandatory. If all six deviations are calculated, then step 2 of the above algorithms will be obsolete. We will demonstrate the application of this algorithm in an example.

Example 6.

Let us select the best inventory method for operation during maneuvering. There are eight vectors that satisfy step 1 of the Algorithm (that at least five pollution deviations are calculated) and they were given in Example 5.

Following step 2 of the Algorithm, we identify the following imputed values for the two vectors containing missing values. For the inventory Tier III, the deviation in CO_2 will be:

$$\Delta_3 = \left(|\Delta_1| + |\Delta_2| + |\Delta_4| + |\Delta_5| + |\Delta_6|\right) / 5 = (21.7 + 9.26 + 39.1 + 653 + 40.8) / 5 \approx 153 = \mathrm{MAD}^{TIER\ III}$$

Then $\vec{\Delta}^{Tier\ III}_{maneuvering}$ =(21.7,-9.26,153,-39.1,653,40.8).

For the inventory family ENTEC, the deviation in CO will be:

$$\Delta_4 = \left(|\Delta_1| + |\Delta_2| + |\Delta_3| + |\Delta_5| + |\Delta_6|\right) / 5 = (4.33 + 15.8 + 0.607 + 653 + 40.8) / 5 \approx 143 = \mathrm{MAD}^{ENTEC}$$

Then $\vec{\Delta}^{ENTEC}_{maneuvering}$ =(4.33,-15.8,-0.607,143,653,40.8).

Following step 3 of the Algorithm, let the DM believe that all attribute value functions are the same and are equal to $v_{sa}(.)$:

$v_1(.) \equiv v_2(.) \equiv \ldots \equiv v_6(.) \equiv v_{sa}(.)$.

The following preferential equations were solved in order to elicit additional nodes from $v_{sa}(.)$:

<0% (0.17) -100%> ~ –75% => $v_{sa}(-75\%) = 0.17$

<0% (0.40) -100%> ~ –50% => $v_{sa}(-50\%) = 0.40$

<0% (0.75) -100%> ~ –25% => $v_{sa}(-25\%) = 0.75$,

<0% (0.75) -100%> ~ 25% => $v_{sa}(25\%) = 0.75$

<0% (0.60) -100%> ~ 50% => $v_{sa}(50\%) = 0.60$

<0% (0.50) -100%> ~ 75% => $v_{sa}(75\%) = 0.50$

<0% (0.429) -100%> ~ 100% => $v_{sa}(100\%) = 0.429 \approx 0.43$

<0% (0.273) -100%> ~ 200% => $v_{sa}(200\%) = 0.273 \approx 0.27$

<0% (0.20) -100%> ~ 300% => $v_{sa}(300\%) = 0.20$

The function $v_{sa}(.)$ is then approximated with the following analytical form:

$$v_{sa}(x)=\begin{cases}\dfrac{100+x}{75-x} & \text{for } -100\le x\le -25\\ \dfrac{2500-x^2}{2500} & \text{for } -25<x<25\\ \dfrac{75}{x+75} & \text{for } x\ge 25\end{cases}$$

Figure 4.2 presents the approximated function $v_{sa}(x)$, for $x\in[-100;\infty)$ (we can see the similarities of this function to the example one presented on Figure 4.1).

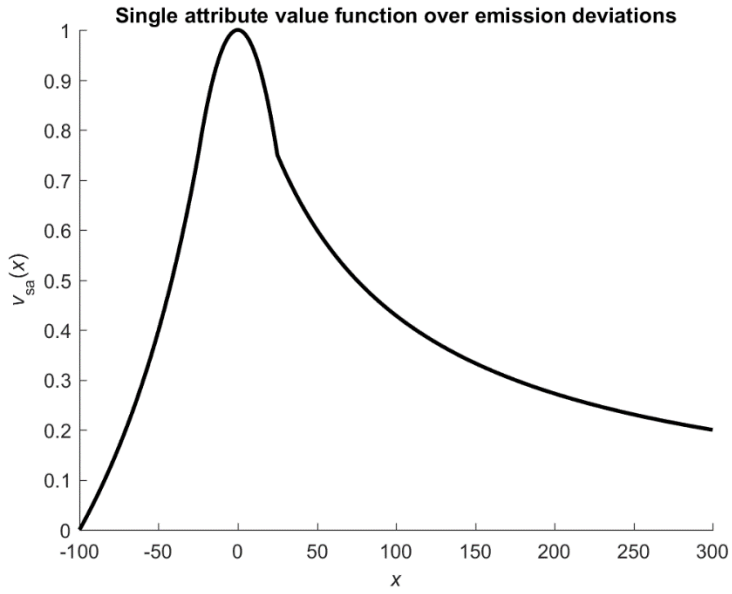

Figure 4.2 *Graphics of the single attribute function* $v_{sa}(x)$

The DM has also elicited the following scaling constants:

$< \vec{\Delta}_{best}\ (0.10)\ \vec{\Delta}_{worst} > \sim \vec{\Delta} = (-100,0,0,0,0,0)$ => a_1=0.10

$< \vec{\Delta}_{best}\ (0.25)\ \vec{\Delta}_{worst} > \sim \vec{\Delta} = (0,-100,0,0,0,0)$ => a_2=0.25

$< \vec{\Delta}_{best}\ (0.05)\ \vec{\Delta}_{worst} > \sim \vec{\Delta} = (0,0,-100,0,0,0)$ => a_3=0.05

$< \vec{\Delta}_{best}\ (0.30)\ \vec{\Delta}_{worst} > \sim \vec{\Delta} = (0,0,0,-100,0,0)$ => a_4=0.30

$< \vec{\Delta}_{best}\ (0.10)\ \vec{\Delta}_{worst} > \sim \vec{\Delta} = (0,0,0,0,-100,0)$ => a_5=0.10

$< \vec{\Delta}_{best}\ (0.20)\ \vec{\Delta}_{worst} > \sim\ \vec{\Delta} = (0,0,0,0,0,-100)$ => a_6=0.20

Following step 4 of the Algorithm, the six-attribute value function is constructed:

$$v(\vec{\Delta}) = v(\Delta\mathrm{NO_x}, \Delta\mathrm{SO_x}, \Delta\mathrm{CO_2}, \Delta\mathrm{CO}, \Delta\mathrm{HC}, \Delta\mathrm{PM}) =$$
$$= 0.10 v_{sa}(\Delta\mathrm{NO_x}) + 0.25 v_{sa}(\Delta\mathrm{SO_x}) + 0.05 v_{sa}(\Delta\mathrm{CO_2}) + 0.30 v_{sa}(\Delta\mathrm{CO}) + 0.10 v_{sa}(\Delta\mathrm{HC}) + 0.20 v_{sa}\Delta\mathrm{PM}$$

Following step 5 of the Algorithm, we can calculate the value function over each of the inventories. For example, for MEET we have:

$$v(\vec{\Delta}^{MEET}_{maneuvering}) = v(53.9,3.09,5.45,161,222,-84.2)$$
$$= 0.10 v_{sa}(53.9) + 0.25 v_{sa}(3.09) + 0.05 v_{sa}(5.45) + 0.30 v_{sa}(161) + 0.10 v_{sa}(222) + 0.20 v_{sa}(-84.2)$$
$$= 0.10 \times 0.5818 + 0.25 \times 0.9962 + 0.05 \times 0.9881 + 0.30 \times 0.3178 + 0.10 \times 0.2525 + 0.20 \times 0.0992$$
$$= 0.4971$$

In the same way we can calculate the value function over the other seven inventory families:

$v(\vec{\Delta}^{MOPSEA}_{maneuvering})$ =v(75.6,-56.4,-9.41,29.1,59.3,-7.90)=…=0.6480

$v(\vec{\Delta}^{NERI}_{maneuvering})$ =v(69.5,1.63,-7.08,-34.2,109,36.1)=…=0.7072

$v(\vec{\Delta}^{US\ EPA}_{maneuvering})$ =v(57.4,0.907,4.86,-42.4,151,-67.9)=…=0.5814

$v(\vec{\Delta}^{SMED}_{maneuvering})$ =v(18.2,-28.1,-0.670,-59.2,149,52.5)=…=0.5534

$v(\vec{\Delta}^{IMO}_{maneuvering})$ =v(45.2,-66.4,-16.1,-78.9,138,-20.8)=…=0.4083

$v(\vec{\Delta}^{Tier\ III}_{maneuvering})$ =v(21.7,-9.26,153,-39.1,653,40.8)=…=0.6390

$v(\vec{\Delta}^{ENTEC}_{maneuvering})$ = v(4.33,-15.8,-0.607,143,653,40.8)=…=0.6173

Following step 6 of the Algorithm the recommended inventory family when maneuvering would be NERI, because it has the highest value of the value function (0.7072). The second-best inventory family would be MOPSEA with value function of 0.6468. The overall ranking is: 1) NERI (0.7072); 2) MOPSEA (0.6480); 3) TIER III (0.6390); 4) ENTEC (0.6173); 5) US EPA (0.5814); 6) SMED (0.5534); 7) MEET (0.4971); 8) IMO (0.4083). The selection of the NERI inventory family is a slight improvement compared to the one achieved with the minimal MAD criterion in section 4.1, where the MOPSEA was selected, but NERI was ranked second.

It is interesting to compare the ranking of the two methods. According to the MAD criterion, the ranking was: 1) MOPSEA (39.6); 2) NERI (42.9); 3) SMED (51.3); 4) US EPA (54.1); 5) IMO (61.0); 6) MEET (88.3); 7) ENTEC (143); 8) TIER III (153). In general, the two rankings are very similar except for ENTEC and TIER III. The six remaining inventory families have almost the same ranking by the two methods. This concludes Example 6.

Let us assume that the DM wants to use the same attribute value function for all six attributes in the form $v_{quick}(\Delta_i) = 1-|\Delta_i|/100$. This function is shown with dashed line on Figure 4.1, where it can be seen it somehow resembles the "precise and rational" $v_i(\Delta_i)$ given with solid line. Let the same DM be happy to use six equal scaling constants and therefore $a_i=1/6$ for $i=1,2,\ldots,6$. The main advantage of using the $v_{quick}(.)$ with equal weight coefficients is that the six-attribute value function can be built quickly by skipping the elaborate procedure in section 4.4.1 and demonstrated in Example 6. The function $v_{quick}(\Delta_i)$ is not normalized because it takes negative values for deviations greater than 100%. However, the only place where this normalization matters is the skipped procedure for elicitation of the scaling constants using corner vectors. So, the six-attribute value function, which models the preference of the discussed DM, will take the form:

$$v\left(\vec{\Delta}\right) = v\left(\Delta\mathrm{NO_x}, \Delta\mathrm{SO_x}, \Delta\mathrm{CO_2}, \Delta\mathrm{CO}, \Delta\mathrm{HC}, \Delta\mathrm{PM}\right) =$$
$$= \tfrac{1}{6} v_{quick}\left(\Delta\mathrm{NO_x}\right) + \tfrac{1}{6} v_{quick}\left(\Delta\mathrm{SO_x}\right) + \tfrac{1}{6} v_{quick}\left(\Delta\mathrm{CO_2}\right) + \tfrac{1}{6} v_{quick}\left(\Delta\mathrm{CO}\right) + \tfrac{1}{6} v_{quick}\left(\Delta\mathrm{HC}\right) + \tfrac{1}{6} v_{quick}\left(\Delta\mathrm{PM}\right) =$$
$$= \frac{1-\left|\Delta\mathrm{NO_X}\right|/100}{6} + \frac{1-\left|\Delta\mathrm{SO_X}\right|/100}{6} + \frac{1-\left|\Delta\mathrm{CO_2}\right|/100}{6} + \frac{1-\left|\Delta\mathrm{CO}\right|/100}{6} + \frac{1-\left|\Delta\mathrm{NC}\right|/100}{6} + \frac{1-\left|\Delta\mathrm{PM}\right|/100}{6} =$$
$$= 1 - \tfrac{1}{100} \frac{\left|\Delta\mathrm{NO_x}\right| + \left|\Delta\mathrm{SO_x}\right| + \left|\Delta\mathrm{CO_2}\right| + \left|\Delta\mathrm{CO}\right| + \left|\Delta\mathrm{HC}\right| + \left|\Delta\mathrm{PM}\right|}{6} = 1 - \tfrac{1}{100} w\left(\vec{\Delta}\right)$$

It is obvious that under the discussed circumstances the value function $v(.)$ is a negative affine transformation of the MAD criterion $w(.)$. So according to the value function uniqueness theorem (French 1993) the maximization of the six-attribute value function $v(.)$ will produce the same result as the application of the minimal MAD criterion. The later happens to be a special case of the six-attribute value function $v(.)$, where the scaling constants are equal, and the six attribute functions are in the form $v_{quick}(\Delta_i) = 1-|\Delta_i|/100$. That is why the ranking of inventory families with the minimal MAD criterion is "quick and dirty" approach, which often produce satisfactory results as in Example 6. However, using the more elaborate 6-atrribute value function approach will guarantee that the selected inventory family will fully correspond

to the DM preferences as is the case presented in Example 6. The benefits of using this approach are evident when the inventory families generate results that may be considered outliers for a given emission type. Such was the case in Example 6, where ENTEC and TIER III have an absolute deviation of 653% on HC, which is an obvious outlier compared to the other emission types (see Table 4.2). While those outlier measurements distort completely the ranking of ENTEC and TIER III using the minimal MAD criterion, the value function approach (see Figure 4.2) strongly reduces the influence of the outliers as it reaches saturation as values increase. This allowed ENTEC and TIER III to improve their ranking (from positions 7 and 8 to positions 4 and 3 respectively). This is closer to the real DM preferences.

4.6.Policy implications of the study

We can formulate some implications from the case study given in chapter 3 and improved in chapter 4. It is very likely that for any standard ship in a specific mode of operation there is an inventory method that will produce emission predictions with high precision. If on-board measurement experiments are available, we have a chance of identifying which is the most suitable method and from what we demonstrated in this thesis, this is a comparatively easy task. The best inventory method will most likely give small deviations from the measured emissions. However, if we try to choose blindly one inventory family for some mode of operation (without backing this up by any real time measurements) there is a high chance that we will choose a method that produces unacceptably high errors. The case study demonstrated that some methods deviate substantially in their predictions (by well over 100%). In that sense, one of the important contributions of this thesis is to demonstrate the importance of experimental data to identify suitable inventory family for each of vessel's modes of operation.

This case study demonstrated an efficient way forward for emission estimation of a ship during technical exploitation in a quick and precise manner. It is possible that on-board measurements of the ship emission can be conducted at the time the ship is put in exploitation as well as at times of regular ship repairs. Using those measurements, the inventory method, which predicts the emissions with minimal error can be identified for each mode of operation of the vessel. The identified inventory methods can be used by various regulatory authorities during exploitation of the ship to calculate emissions during regular exploitation. The discussed inventory methods are beneficial first for the policy makers, who need to assess the pollution

caused by shipping in order to implement reasonable boundaries to that pollution. Ship owners, on the other hand, can use the identified inventories to get precise prediction on the actual pollution their vessels cause to the environment during various modes of operation so that they can take adequate measures to minimize the penalties imposed by regulatory bodies.

There are four obvious alternatives to the above-formulated policy:

- To use inventory methods selected by the policy makers without the benefit of verifying them with real measurement for each ship. As it was demonstrated by our case study, this method will almost surely produce shipping emission estimate with low precision. Therefore, the policy changes will most likely be inadequate. In fact, that is the situation now.
- To regulate that every vessel should acquire and maintain its own measurement devices. They may even design their own family of inventories and justify their applicability for the ships they operate. That alternative would be unreasonably expensive for the ship owners, and very impractical because of the many problems that may arise when the machine crew starts interacting with the emission measurement system. As a result, even if the latter works in a given moment of time, the measurement results will be highly unreliable. Furthermore, the maritime and environmental authorities will use their own measurement systems rather than utilizing those on the ship (due to their necessity to comply with strict international regulations).
- To require that every vessel should develop ship-specific inventories based on an on-board measurement campaign. This problem is almost impossible mathematically, because the data to create the inventory models will never be enough. On top, the policy makers would have a hard time dealing with so many different unknown models instead of using several known inventories. As a result, the assessed shipping emissions will be with even greater error than they are today.
- To use only empirical data from on-board measurements. The main disadvantage of this strategy is that the best inventories for a specific ship and type of operation contain prior knowledge, which will not be utilized. Additionally, the problems with the policy makers will be the same as in the previous alternative.

It seems that neither one of the discussed alternatives is satisfactory.

Based on the arguments given in the current section we propose the following policy for estimating the shipping emissions for future implementation:

> Creation of a generalized rational algorithm to rank inventory families based on the precision of their predictions for given operational modes of a specific vessel comparing to real-time emission measurement. Moreover, the implications of the case study together with the developed algorithm to rank inventory families was applied to offer a novel future policy for cost-effective and reliable emission estimation caused by shipping.

Using the available deviations, any authority can identify the best inventory family for each of the three modes of operations, depending on their preferences encoded in the six-attribute value function. Those vessel-specific inventory families will ensure cheap and relatively precise estimation of the primary emissions from shipping both locally and globally.

Chapter 5: Dispersion modelling

The emissions from vessels utilising heavy fuel oil include large amounts of nitrogen oxides, sulphur dioxide and particulate matter, presenting significant health risks to people living near ports. To determine the effect of these emissions on human health, complex atmospheric dispersion modelling using CALPUFF assesses ground-level concentrations at receptors surrounding the sources. This chapter demonstrates the application of the methodology by applying it to Port of Brisbane for the full 2013 calendar year. Results reveal that with the imminent development of many Australian ports, there is a need for continual monitoring of emissions caused by shipping.

5.1. Port Overview

Port of Brisbane is a multi-modal port on the Brisbane River on the east coast of Australia, currently managing 29 operational berths. There are also a number of privately managed berths: Fisherman Islands, at the mouth of the Brisbane River, hosts twelve container berths, a number of bulk product berths, and one general purpose berth; and more dry- and wet-bulk terminals are sited up-river towards Hamilton Reach, where a cruise terminal and naval base are located (Port of Brisbane 2015). The port is unique because of the long distance between the outer port limit and the berths on the river: a channel of 82.9 km to the entrance beacons is located approximately seven kilometres seaward of the outermost berth on Fisherman Islands. The port boundary extends from the pilot boarding ground at the north to the lowest reaches of the Brisbane River in the south and is defined by Moreton Island to the east and the Australian mainland to the west.

Pilots join the vessels at the pilot boarding ground at the outer port limit, near Caloundra Heads. Vessels then move to the entrance beacon under their own power, typically at a speed close to normal cruising. At the entrance beacons, most are assisted by tugs to their destination berth. During this final leg, vessels travel at a restricted speed dictated by their draft and under-keel clearance. Occasionally vessels may hold fast at the ship-to-ship transfer anchorages near the entrance beacons until a berth becomes available. Once at berth, they load and offload cargo and supplies as required. Some may reposition to another berth during their call at the port, depending on the types of cargo they are handling.

Upon departure, vessels are assisted by tugs to manoeuvre out of the berth and, depending on their length, to move some distance towards the entrance beacons. Some need to wait for

suitable tidal movements before proceeding down-river and through the channel. They go under their own power to the pilot boarding ground, where the pilot disembarks, and the vessel goes on its way. Departure transits usually take less time than arrivals.

5.2. Vessel emissions inventory

To measure the emission rates of the key pollutants, as well as the fuel consumption and greenhouse gas emissions of ocean-going vessels (OGVs) within the port, a detailed emissions inventory model was constructed. Being applied to Port of Brisbane for a five-year period, this methodology is then applicable to most ports or wider coastal regions. Harbour craft (including tugs and ferries) were not included in the inventory as studies have shown that compared to OGVs, their emissions are of minor importance (Lucialli, Ugolini et al. 2007, Jalkanen, Brink et al. 2009).

Vessel movement data was obtained from records collected by Port of Brisbane. The five-year dataset, from 2010 to 2014, included identification of individual vessels, their type, and the time at which they reached the pilot boarding ground, their destination berths and times of departure (Clarkson 2015). No information indicated the time at which a vessel passed a key transit mark such as the entrance beacons when entering or departing port. When a vessel was placed at anchor during some part of its call to the port, two separate entries were made: the first listed the anchorage as the destination port, and the second listed the actual destination port. Data for vessels repositioning during a call were recorded in the same manner. Many anomalies in the data relate to multiple berth visits or those involving anchorage, and arrival or departure times are often incomplete or highly erratic. For consistency, such records were discarded: a total of 1268 records (9%) over the five years.

During a visit to the port, vessels undertake several movements, and each is assigned a single operating mode. Vessels are ‘in transit’ for most of both the inbound and outbound passages, from the pilot boarding ground to berth, and vice-versa. The average speed of the vessel while in transit was calculated from the times recorded in the dataset and the known distance of each transit. While it is known that vessels slowed at the entrance beacons to be assisted by tugs, nothing in the data indicated the time spent in the restricted speed zone. To overcome these limitations, two approaches are taken: first, the restricted speed zone is disregarded, and the complete inward and outward voyages are treated as transiting; and second, an approximate time taken to travel from the entrance beacons to the berth is reached by looking at a limited

set of automatic identification system data. It was then concluded that in general the times were relatively similar regardless of the vessel type or size, and one hour for the inbound voyage and half an hour for the outbound voyage were typical.

A separate operating mode was assigned to a vessel at berth, and the time spent at berth was recorded in the original data set. Time taken to dock, and un-dock was included as transit time, with arrival and departure times recorded as the time that the first (or last) mooring line was secured (or released). Although the methodology provides for the inclusion both of vessels at anchor and those manoeuvring between berths, these are not included in the case study because most were unreliable entries and were thus excluded.

During the period of interest 2935 unique vessels visited the port, each categorised as one of 32 different types (Clarkson 2015). For the purpose of the emission inventory, many of these types were similar or the same in terms of operating and engine characteristics, and are re-categorised into eleven standard categories, shown in Table 5.1.

Table 5.1 *Classifications of vessels based upon the supplied vessel type*

Defined vessel types	Data supplied vessel types	Defined vessel types	Data supplied vessel types
Auto Carrier	miscellaneous class vehicle carrier	ro-ro	landing craft passenger/ro-ro cargo ship ro-ro cargo ship
Bulk Carrier	bulk/oil carrier bulk carrier cement carrier self-discharging bulk carrier woodchip carrier	tanker	chemical/oil products tanker chemical tanker crude oil tanker LPG tanker oil products tanker
Container Ship	container ship	navy vessel	naval ship
Cruise Ship	passenger/general cargo ship passenger cruise ship	reefer	refrigerated cargo ship
General Cargo Ship	general cargo ship livestock carrier	not applicable	barge barge carrier dredger tug yacht
Miscellaneous	fishing vessel heavy load carrier research ship trawler	not applicable	

Only one vessel was classed as ‘miscellaneous’ in the supplied data. This was an auto carrier, and it is denoted as such in the redefined categories. One vessel was described as a passenger/general cargo ship but was in fact a passenger cruise ship. In the data supplied, many self-discharging bulk carriers were incorrectly labelled as bulk/oil carriers. It has been suggested by Starcrest (Starcrest Consulting Group 2005) that self-discharging bulk carriers have higher berthed emissions, caused by their auxiliary unloading equipment; in this study, all bulk carriers are assigned to one category.

In addition to the OGVs, 30 yachts, 16 dredgers and several barges and tugs (fewer than 100) were captured in the dataset. These are deemed irrelevant as they are not OGVs and are consequently are omitted from the emissions inventory. The dredge and tug data were sporadic and did not represent the entire dredge and tug activities within the port and are also omitted.

For each vessel type, default engine powers (both main and auxiliary) are assigned as well as average service speeds, sourced from the USEPA (USEPA 2009) and based on surveys conducted in nine US ports. The problem with using such values is that they do not consider the size of individual vessels, so the average size of the vessels visiting the ports surveyed has the greatest bearing on the averaged main engine powers; the averaged service speeds and auxiliary engine powers are also affected (Clarkson 2015). The default vessel values are shown in Table 5.2. The power ratios between the auxiliary and main engines exhibit strong correlation with those suggested by other studies (Starcrest Consulting Group 2005, Goldsworthy and Renilson 2013).

The emissions for the main and auxiliary engines are calculated separately. The load factor for the main engine during each mode is based on the propeller law relationship, eq 1 from Browning et al (Browning and Bailey 2006). The correction of 0.83 is added to compensate for the fact that vessels do not operate at 100% MCR at service speed (USEPA 2009); USEPA suggests that its supplied cruise speeds are approximately 0.94 of the service or maximum speed.

Table 5.2 *Averaged vessel specifics based on vessel type*

Defined vessel types	Main engine type	Average service speed (knots)	Average main engine power (kW)	Average aux engine power (kW)	Average boiler power (kW)	
					RSZ	Hotel
Auto Carrier	SSD	18.8	11,155	2,967	371	371
Bulk Carrier	SSD	14.5	8,350	2,854	109	109
Container Ship	SSD	21.9	26,122	5,747	506	506
Cruise Ship	MSD	21.1	27,357	7,605	750	750
General Cargo Ship	SSD	15.3	6,709	1,738	106	106
Miscellaneous	MSD	12.7	9,564	2,573	0	0
Navy Vessel	MSD	21.1	27,357	7,605	750	750
Reefer	SSD	19.7	10,060	4,084	464	464
RO-RO	MSD	16.0	11,687	3,027	109	109
Tanker	SSD	14.7	9,667	2,040	371	371

As no information was available on the fuel used by individual vessels, it is assumed that HFO was being used in all cases; likewise, all auxiliary engines are assumed to be medium-speed diesel engines. No account was available of vessels operating on gas turbines or unconventional diesel–electric arrangements. For Port of Brisbane, which primarily handles containerised and bulk cargo, any such difference is assumed to be negligible (Clarkson 2015)—an assumption that might not hold true if this study were adapted for a predominantly cruise or naval port:

$$LF = 0.83 \times \left(\frac{AS}{SS} \right)^3$$

where *LF* is the load factor, *AS* is the actual speed of the vessel and *SS* is the service speed of the vessel.

The load factors for auxiliary engines (Clarkson 2015) are based upon default values obtained from previous studies (Starcrest Consulting Group 2005). These are summarised in Table 5.3.

Table 5.3 *Auxiliary load factors used in the emission inventory*

Defined vessel types	Transit aux LF	RSZ aux LF	Berth aux LF
Auto Carrier	0.15	0.45	0.26
Bulk Carrier	0.17	0.45	0.22
Container Ship	0.13	0.5	0.18
Cruise Ship	0.32	0.32	0.32
General Cargo Ship	0.17	0.45	0.22
Miscellaneous	0.17	0.45	0.22
Navy Vessel	0.32	0.32	0.32
Reefer	0.15	0.45	0.32
RO-RO	0.15	0.45	0.30
Tanker	0.24	0.33	0.26

To calculate emissions, individual emission factors are required for each pollutant being investigated. The values suggested by Goldsworthy and Renilson (Goldsworthy and Renilson 2013) and Clarkson (Clarkson 2015) are utilised in this study because they are most relevant to Australian conditions (Table 5.4).

Table 5.4 *Emission factors expressed in g/kWh*

Engine type	BSFC	NO_x	SO_x	CO	CO_2	$PM_{10.0}$	$PM_{2.5}$	VOC	HC	N_2O	CH_4
Main (SSD)	195	18.1	10.3	0.5	622	1.42	1.31	0.3	0.69	0.031	0.006
Main (MSD)	205	13.2	2.0	1.1	654	0.31	0.29	0.2	0.65	0.031	0.004
Aux (MSD)	217	13.9	2.12	1.1	692	0.32	0.29	0.4	0.52	0.031	0.004
Boiler	305	2.1	16.1	0.2	973	1.47	1.35	0.1	0.1	0.08	0.002

The emissions for both the main and auxiliary engines are calculated using the below equation proposed in (Corbett, Fischbeck et al. 1999):

$$E = \frac{P \times LF \times A \times EF}{1000}$$

where E is the emissions in kg, P is the installed power of the main or auxiliary engine, A is the time of operation in that mode and EF is the emission factor in $g/(kWh^{-1})$.

5.3. CALPUFF modelling: domain and time period

The modelling domain chosen for the model is a 100 km x 100 km grid with 1 km grid spacing. The domain is centred at the Bureau of Meteorology, Brisbane Aero monitoring station considering the coordinates for the domain corners. Note that CALPUFF requires all coordinates to be input in universal transverse Mercator format. The modelling period is the full 2013 calendar year from 1 January 2013 00:00 to 1 January 2014 00:00.

Applying a contour plot of land-use categories over the modelling domain, land-use data for Australia is from NOAA (NOAA 2017). This data set covers all of Australia and can be used for setting up models at other sites in Australia. Elevation data for the modelling domain is from the Shuttle Radar Topography Mission (USGS 2017). This also includes a contour plot of terrain elevation over the modelling domain. Coastline data for Australia is from the Global Self-consistent Hierarchical High-resolution Geography Database (NOAA 2017). Surface meteorological data, from the BoM monitoring stations, as well as Precipitation and Upper air data are listed in

Table 5.5 and shown in Figure 5.1.

The missing soundings have been repaired by manually substituting upper air data modelled using the fifth-generation Penn State/NCAR Mesoscale Model. For modelling sites in Australia, local upper air data must be purchased and repaired if necessary. If no suitable data are available, then 3D gridded prognostic data can be purchased instead. Overwater meteorological parameters have instead been modelled using CALMET with the Initial Guess overwater meteorology initialised based on the available upper air data. 3D gridded prognostic wind data is not included in the model because suitable observational upper air data (comprehensive data) is available from the Brisbane Aero meteorological monitoring station. For other locations in Australia, it may be necessary to include 3D gridded prognostic data if upper air data is unavailable. The complete setting up and running the CALPUFF model using CALApps GUI is presented in the Appendix A.

Table 5.5 *Surface meteorology stations used in the CALPUFF model*

Station name (full)	Station name	Station ID	UTM X (km)	UTM Y (km)	Time zone	Anemometer height (m)
AMBERLEY AMO	YAMB	40004	471.498	6943.783	UTC+1000	10
CAPE MORETON LIGHTHOUSE	CPMN	40043	546.232	7010.001	UTC+1000	10
ARCHERFIELD AIRPORT	YBAF	40211	500.770	6950.241	UTC+1000	10
BRISBANE AERO	YBBN	40842	512.774	6970.173	UTC+1000	10
BRISBANE	BRIS	40913	503.843	6960.309	UTC+1000	10
BANANA BANK NORTH BEACON	MBPS	40925	532.911	6954.517	UTC+1000	10
INNER RECIPROCAL MARKER	MBPC	40926	523.924	6984.334	UTC+1000	10
SPITFIRE CHANNEL BEACON	MBPN	40927	526.420	7008.209	UTC+1000	10
REDCLIFFE	REDC	40958	509.130	6989.537	UTC+1000	10

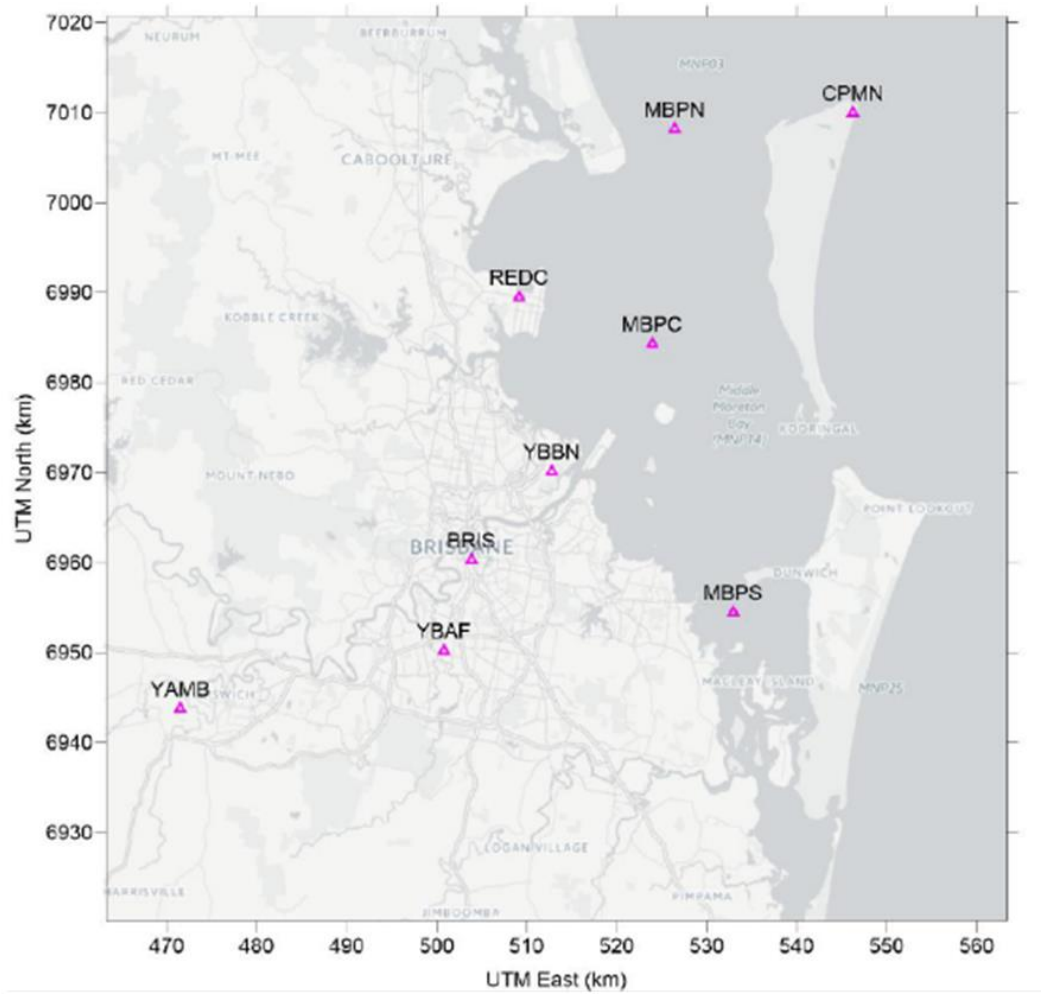

Figure 5.1 *Surface meteorology stations used in the CALPUFF model*

Ten sources were modelled in the CALPUFF model, as summarised in Table 5.6 and shown in Figure 5.2. Three-point sources were positioned at the centre of the berths at Luggage Point, QLC Wharf and Viva Energy Wharf, corresponding to emissions from vessels in port (at berth). A second set of four-point sources extended from the berths to Fisherman Islands, Caltex Tanker Wharf, Pinkenba Bulk Terminal and Hamilton Wharves, corresponding to emissions while entering the port, manoeuvring. The last three-point sources match the navigation of ships while in transit near the pilot boarding ground, in Moreton Bay, and near Dunwich. A stack height of 20m and diameter of 0.8m is assumed for all vessels; and an exit velocity of 25m/s at 539.6K is modelled.

Table 5.6 *Sources used in the CALPUFF model (Emission rates in g/s)*

Source numbers	Source Name	UTM X (km)	UTM Y (km)	SO_2	NO_2	CO	$PM_{10.0}$	$PM_{2.5}$
1	Pilot Boarding Ground	520.475	7001.062	33.43	53.8	4.3	4.7	4.57
2	Moreton Bay	525.721	6987.281	33.43	53.8	4.3	4.7	4.57
3	Dunwich	533.788	6954.203	33.43	53.8	4.3	4.7	4.57
4	Fisherman Islands	517.499	6972.094	32.44	40.63	3.21	3.78	3.67
5	Caltex Tanker Wharf	515.651	6967.705	32.44	40.63	3.21	3.78	3.67
6	Luggage Point	514.814	6969.871	31.46	27.46	2.12	2.85	2.76
7	QLC Wharf	513.449	6967.051	31.46	27.46	2.12	2.85	2.76
8	Viva Energy Wharf	508.618	6964.238	31.46	27.46	2.12	2.85	2.76
9	Pinkenba Bulk Terminal	507.133	6964.062	32.44	40.63	3.21	3.78	3.67
10	Hamilton Wharves	504.879	6964.804	32.44	40.63	3.21	3.78	3.67

A sample wind rose plot at 517.499 UTM X (km), 6972.094 UTM Y (km) where the Fisherman Islands source is located, is shown in Figure 5.3. During the one-year period analysed, winds typically blew along different axes, including SSW to NNE (%10) and S to N (%10) in total. The winds were stronger and more prevalent in the SSW direction. Wind speeds varied from 1.8 ms-1 to 10 ms-1.

Figure 5.4 also shows the variances in the flow around the entire model and in particular close to the chosen sources at some arbitrary chosen times. Over the year modelled, the effect of the coast on the meteorology is quite distinct. The diurnal temperature changes and corresponding shifts in wind direction, precipitation and mixing height can be seen to cause confused flow around source points. These flows confirm the need for the more advanced modelling capabilities of CALPUFF. In addition, they demonstrate representative domain conditions using observational data, while sufficient data on surface stations are also available.

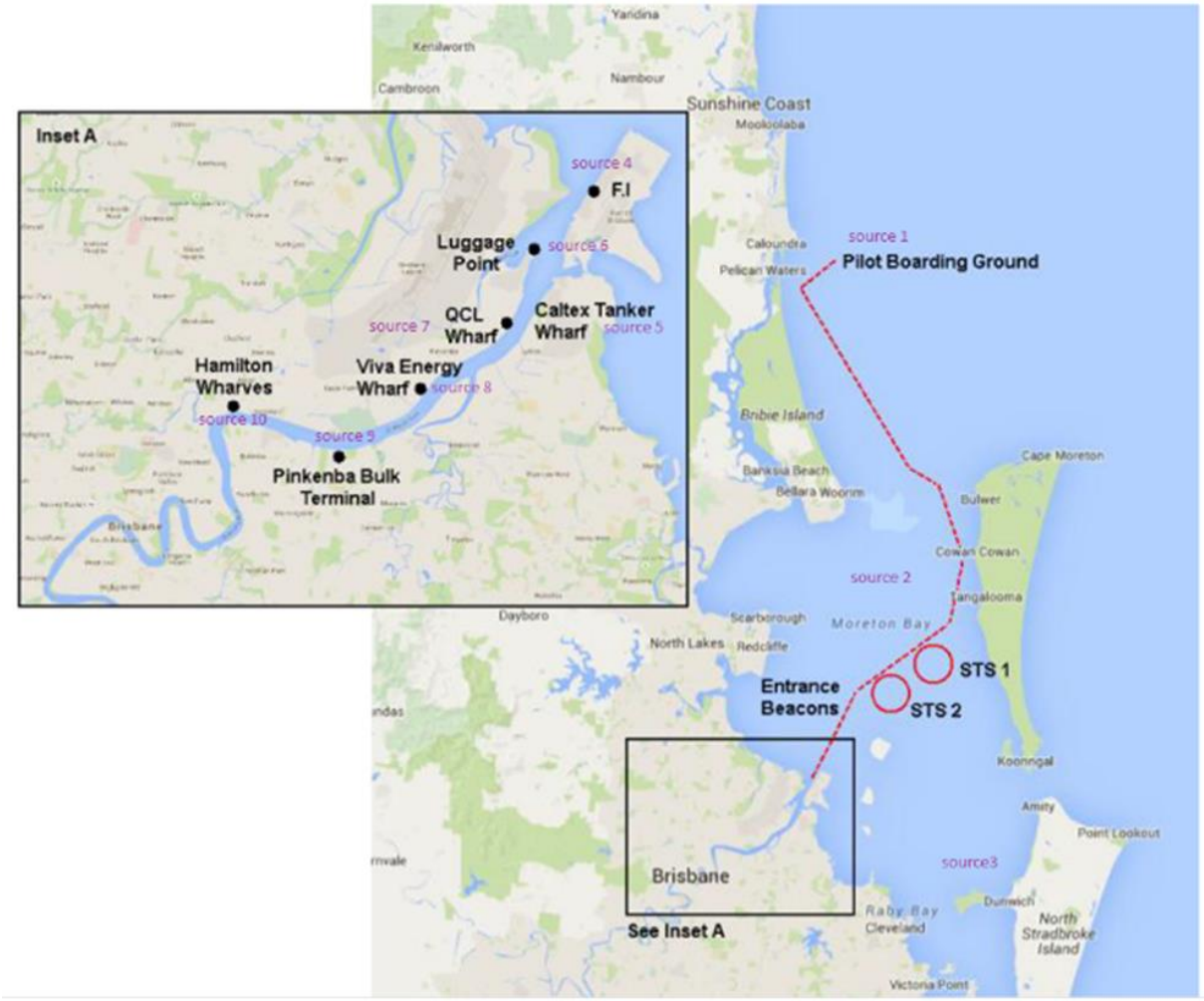

Figure 5.2 *Sources used in the CALPUFF model*

5.4. Analysis and results

The averaged ground level concentrations of SO_2, NO_x, CO and $PM_{2.5}$ over a year were calculated using CALPUFF. Concentrations across the whole domain were calculated at the 1km spaced gridded receptors. Some sample averaged concentration plots of dispersion contour plot are shown below in Figure 5.5.

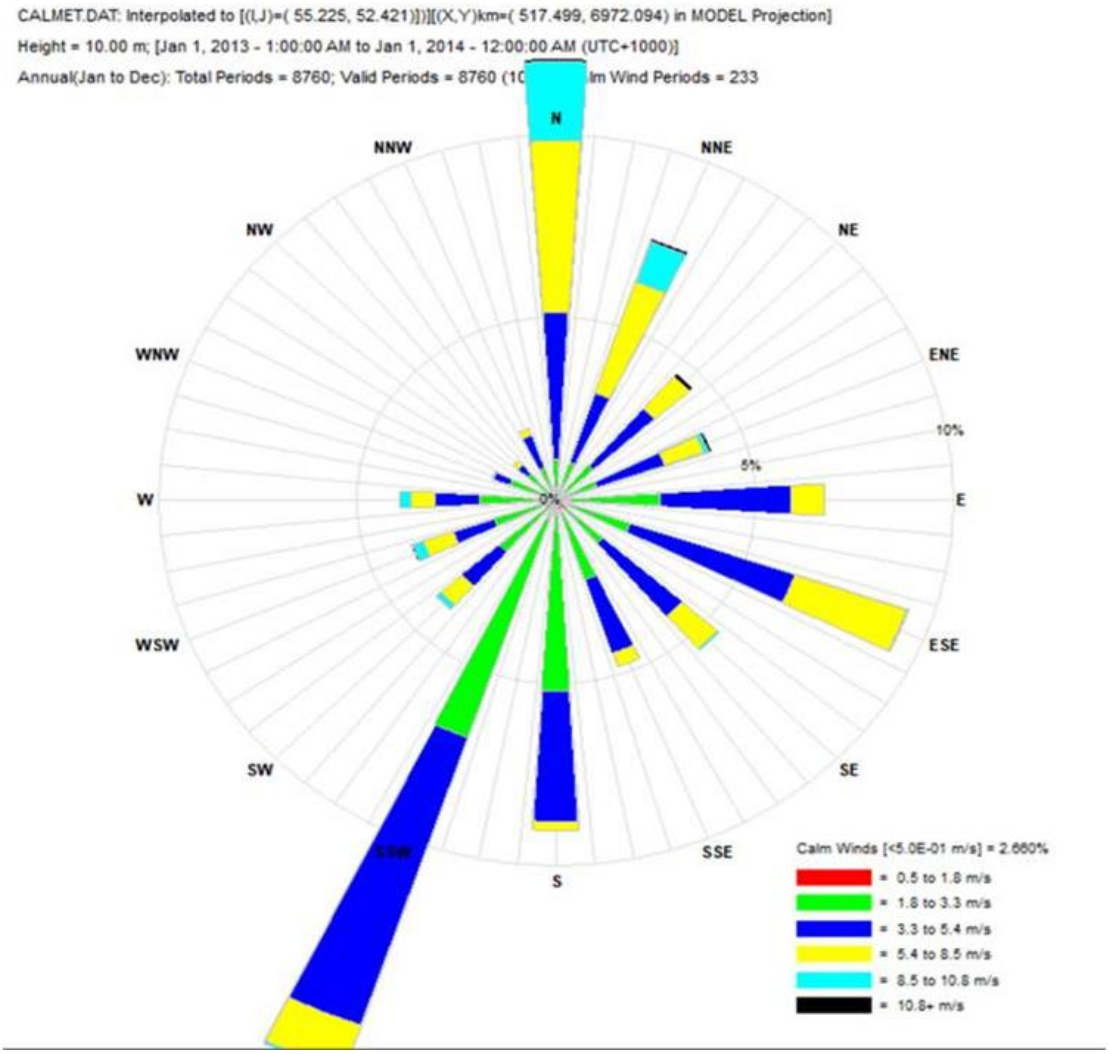

Figure 5.3 *Wind rose plots at Fisherman Islands location (517.499 UTM X (km), 6972.094 UTM Y (km)*

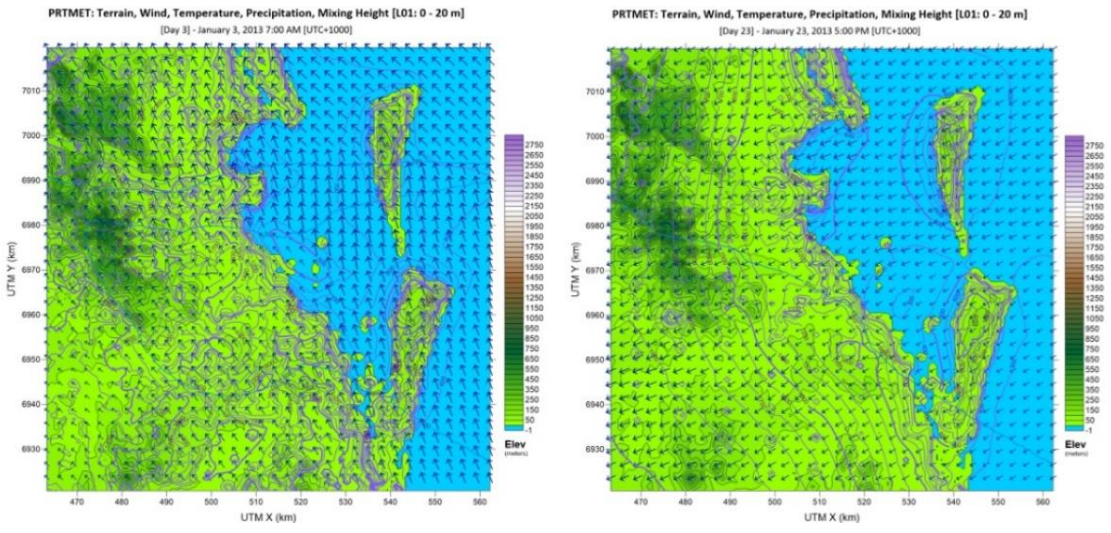

4a. Variances in Day 3 *4b. Variances in Day 23*

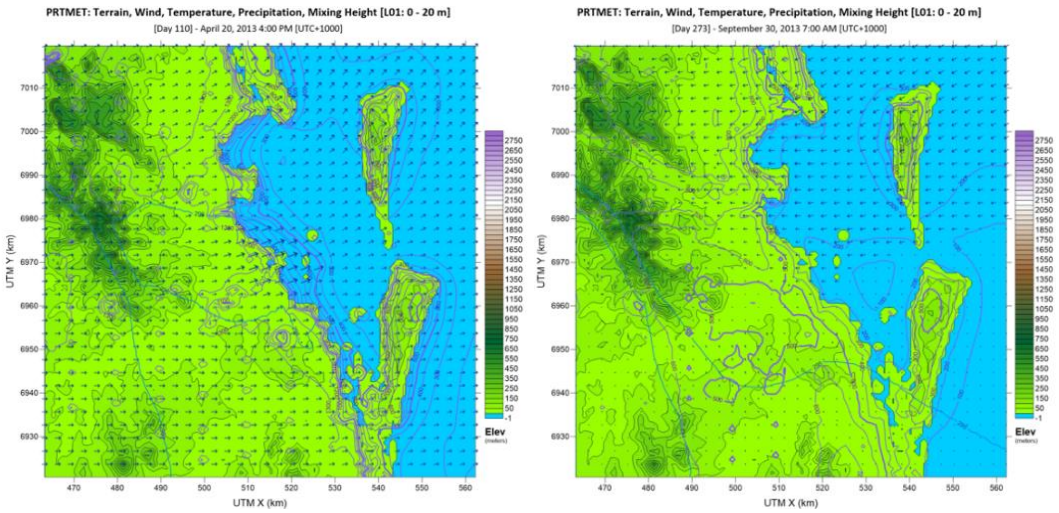

4c. Variances in Day 110 *4d. Variances in Day 273*

Figure 5.4 *Sample wind fields, precipitation and mixing heights across the domain from 0000 January 1 2013 to 0000 January 1 2014*

Due to the wide varying wind conditions across the modelling period, dispersion of all pollutants (and deposition of $PM_{2.5}$ and $PM_{10.0}$) showed different trends. The concentrations represented in the figure above are based on the emission rates adapted from the Port of Brisbane emissions inventory. The case study coverage, given the availability of full data, is rigorous enough to draw solid conclusions suggesting there is the potential for further investigation into actual risk estimations on Australian ports and the need to calculate hazard values.

Health Impact Assessment includes calculating average concentrations (Figure 5.5) across the air shed for the appropriate averaging times and applying the Concentration-response function (CRF) provided from a review of the literature (Erbas, Kelly et al. 2005, Jalaludin, Khalaj et al. 2008, Williams 2012). This study uses demographic data from the Australian Bureau of Statistics. The levels of contaminants were measured twice: once with and once without background concentrations. This was to reveal the contribution from ships, which it would be useful to compare with impacts from all sources. Addressing health points defined by the CRFs, like mortality due to respiratory failure, is a useful aim.

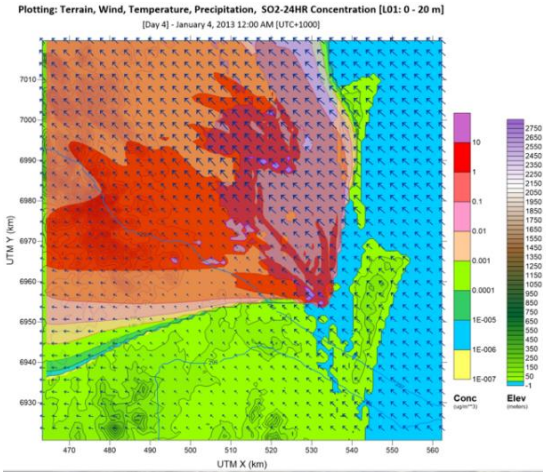

5a. Concentration plot of SO_2

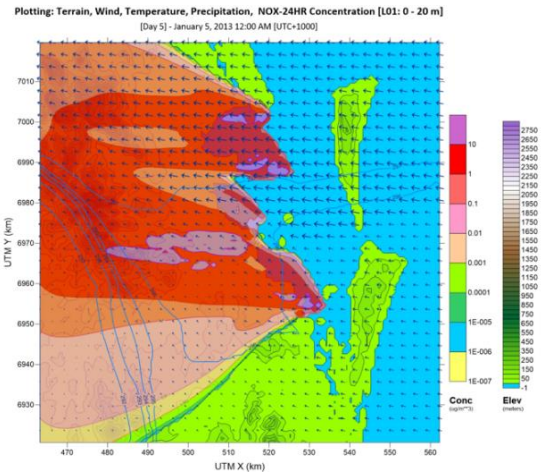

5b. Concentration plot of NO_x

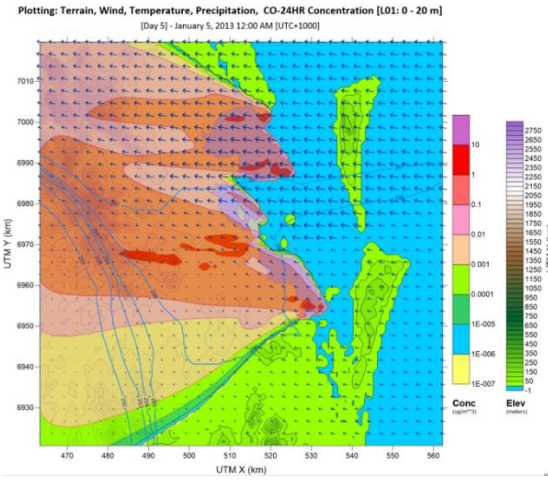

5c. Concentration plot of CO

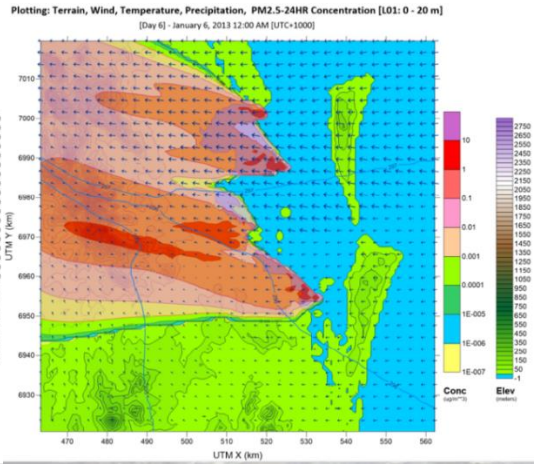

5d. Concentration plot of $PM_{2.5}$

Figure 5.5 *Sample averaged concentration plot of SO_2, NO_x, CO and $PM_{2.5}$*

The Health Impact Assessment is an international policy tool, increasingly used to assess complex hazards and risks of exposure in particular communities. A comparison of risks to residents living near different ports illustrates how this study's risk assessment supports the aims of a Health Impact Assessment, important components of which are to identify where and when public health is most likely to be affected, and to recommend ways to reduce or eliminate the threat (Department of the Environment 2016). This study indicates that the health of residents living near ports is most likely to be affected by well shipping activities. The obvious response is to minimise exposure for those living near ports when emissions from shipping operation activities are at their highest. This study is one small part of what needs to be a comprehensive overview that incorporates all relevant pathways and exposure scenarios,

including occupational exposure, to enable a better understanding of the impacts of primary emissions on public health. A full Health Impact Assessment can identify where and when public health is most likely to be affected and indicate strategies to reduce negative health impacts. Out preliminary results, indicating that people living near Port of Brisbane face significant health risks, warrant further study.

In TAPM, chemically inert emissions are transported by advection and diffusion, and are deposited on both land and sea. Sea breezes and air flows influenced by landforms, along with other elements relevant to local levels of air contamination, are predicted in our model, set against the 2013 meteorology. It is an advantage to have the local meteorology predicted by the model. The air quality modules used in the simulations, the Lagrangian Particle Model (LPM) and the Plume Rise Module (PRM), represent near-source dispersion with some accurately. Our worst-case approach assessed exposure, by inhalation, of the toxic compounds expected in primary emissions; although they did not exceed the thresholds established by this study, no conclusions about the degree of ‘safe’ exposure can yet be reached.

The value of any model depends on the quality of the data that it is to process, and this is true of advanced dispersion and integrated emission models. If the available data are inadequate, better results may be obtained using land use regression or geo statistical models.

Chapter 6: Revision of a health risk-assessment framework for the application of shipping emissions

Emissions from ocean-going vessels present a significant health risk to populations surrounding ports and damage the environment. Emissions from ships using heavy fuel oil include substantial amounts of sulphur dioxide, nitrogen oxides, and particulate matter. To assess the risk of these emissions, a complete methodology has been developed, based on the Australian Environmental Health Risk Assessment Framework. The method includes a detailed inventory of in-port and at-sea emissions using an activity-based approach applying downwash and near-field areas from first principles equations as well as the air-shed regions from CALPUFF dispersion modelling results for Port of Brisbane in the calendar year 2013. The final risk values are validated against national and European guidelines. Various health impact assessments, as well as carcinogenic and ecological effects, are discussed in depth. This chapter offers a significant contribution to developing a baseline measurement of the current state of risk from emissions of the ocean-going vessels visiting the port, and suggests that, given the expected development of many Australian ports in the near future, the need for continual monitoring of shipping emissions is an essential and necessary area of research.

6.1. Health risk assessment

Health risk assessment is the process of estimating the potential impact of a chemical, physical, microbiological or psychosocial hazard on a given human population or ecological system, under a specific set of conditions and within a particular time frame (EnHealth 2012). The assessment follows strict common sense and can be applied to a whole series of rules or procedures (WHO 2000). Figure 6.1 presents in detail the stages of risk assessment.

The current risk assessment methods, however, do not allow actual estimates of low levels of exposure to environmental hazards, which means that emissions from international ships increasingly focus on proposed regulations in local, national, and international contexts (Bailey and Solomon 2004, California Air Resources Board 2006, Cofala, Amann et al. 2007). However, regulatory deliberations have not been adequately informed since the extent of the health effects of shipping emissions has been unknown. Previous evaluations of regional shipping health impacts focused on European or Western United States regions and ignored short- and long-range Southern hemispheric pollutant transport (California Air Resources

Board 2006, Cofala, Amann et al. 2007), which undermined the global impact of shipping in local and regional jurisdictions and does not inform international policy-making correctly. Therefore, during the presentation of numerical calculations of risks, caution should be taken while assigning strict meaning to the numbers. The accuracy of differential risks estimates can be influenced by exposed population and variability in the environmental agents, inherent limitations in toxicological data, and the complexity of the exposure conditions. During quantification of some components such as exposure assessment and collection of data all uncertainties should be reflected in the risk assessment outcomes.

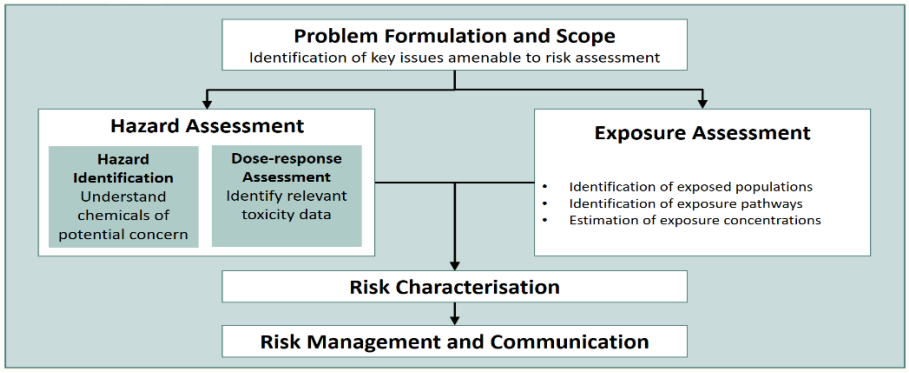

Figure 6.1 *Stages of risk assessment*

Following the above explained approach, there are two types of risk assessment: qualitative and quantitative. Qualitative assessment (Figure 6.2) relies on professional judgement; it is simple, rapid and can be very useful. The risk level can subsequently be explained either quantitatively or qualitatively (by categorising risks into low, medium, and high). The approach utilised in AS/NZS ISO 31000:2009 is the practical guidance on risk management (Standards Australia 2009).

Probability of Occurrence	Consequence of Occurrence				
	Very Low	Low	Moderate	High	Very High
Very Low					
Low					
Moderate					
High					
Very High					

Low Risk Medium Risk High Risk

Figure 6.2 *Example Risk Matrix*

This study, however, adopts a quantitative assessment to calculate risks, which does not rely heavily on judgment. This type of approach is more reliable as it takes into account the complexity of the process a lot more than it is possible with a qualitative approach (Department of the Environment 2016). The quantitative study approach used in the research involves computation of final risk value from the far and the near fields' concentrations i.e. low levels of environmental hazards exposure for the case study of the Port of Brisbane. The perspective includes the Gaussian plumes and outcomes from CALPUFF dispersion modelling regarding the results from the health impact evaluation, short-term and long-term guideline validation assessment, ecological effects, and estimation of carcinogenic risks from the diesel particulate. CALPUFF is an advanced dispersion modelling used in estimating emissions of long-range transports from an area, point, lines, and volume sources. The source-receptor distances range from 50 km to several hundred kilometres. CALPUFF can produce hourly files on ambient concentrations for every species in the model including extinction coefficient and both dry and wet deposition fluxes. The extinction coefficient is associated with visible applications.

There are three tiers to quantitative risk assessment. Figure 6.3 is a schematic description of the particular elements that might comprise tiers I, II, or III. The tiered approach provides means for assessing an issue under consideration with an appropriate complexity level. Each tier supplies an equal degree of health protection. The level of uncertainty decreases with a growth in the number of assessment details, and the conceptual comprehension of the site condition is refined. As a result, the degree of caution that should be substituted for knowledge in the process of risk assessment is reduced.

- **Tier I** – it considers a particular amount of data and several guideline values. The assessment notes if the risk falls above or below the guideline. In some cases, circumstance requires an approach to be formed based on a specific issue or site due to the complexity and costs of contemporary environmental health risk. Tier 1, which is the most straightforward perspective, is supposed to be the first screening-type evaluation of vulnerability utilising the conservative default exposure parameter estimate and comparing it to the published health guidelines. A prudent or conservative approach means assessing and managing the uncertainties inherent in a risk assessment that reduce the likelihood of harm.
- **Tier II** – it involves more modelling, extra data, and a deeper understanding of the situation and evaluates the risks involved. The approach works in terms of calculations and considers parameters and data sets.

- **Tier III** – it is significantly more complicated. Studies at this level may take years and can involve personal monitors when people observe their exposure to a hazard under investigation (EnHealth 2012). Tier III can include a much greater amount of detail and be probabilistic such as in Monte Carlo simulations. Tier III evaluations are rare, partly due to the tendency of any risk assessment to move gradually from tier I but also because if tier I indicates that risk is acceptable, then there is no point in moving to tier II.

Tier II and III procedures require the collection of extra data on exposure and a detailed analysis and evaluation of data on dose response. These tiers involve computation of dosage on target tissues or translating dosages for animals to humans. Most jurisdictions uphold the tier approach of assessment for risks, but the correct usage and number of tiers varies.

A tier II assessment is applied in this study, assuming that concentrations and ship stacks are port-wide and their final calculations are validated with available guidelines.

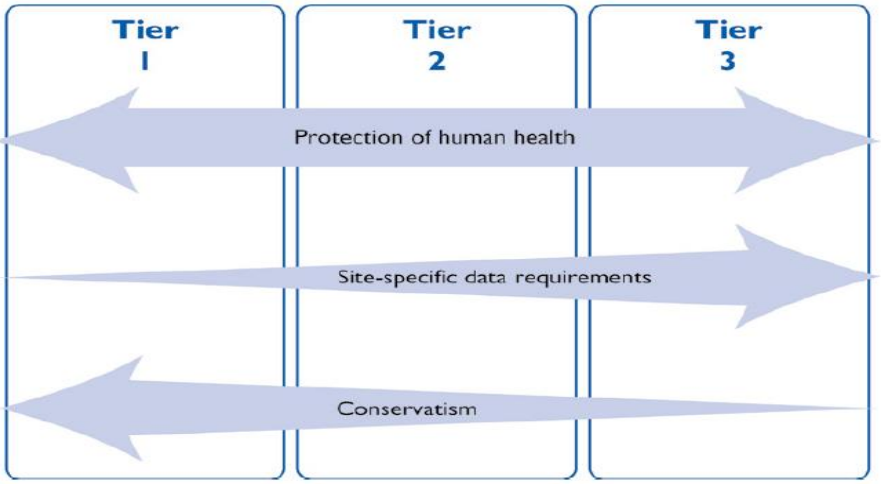

Figure 6.3 *Elements of a tiered approach to a health risk assessment*

Exposure pathways are the processes that take a chemical or another agent into the environment from its release point to a situation in which a person becomes exposed. The routes of exposure are often reasonably obvious, but there may be some less obvious cases, such as the movement of contaminated groundwater or volatile chemicals from contaminated groundwater. The development of this process can be beneficial in identifying and quantifying the pathways of exposure (Figure 6.4).

The identification of concentrations and their risk to the population around Port of Brisbane were carried out about existing sensitive receptors. In formulating the scope of the problem, the chemicals to focus on and their sources, the pathway that connects the sources and receptors in a risk scenario for engine exhaust shipping emissions (air emissions) is inhalation.

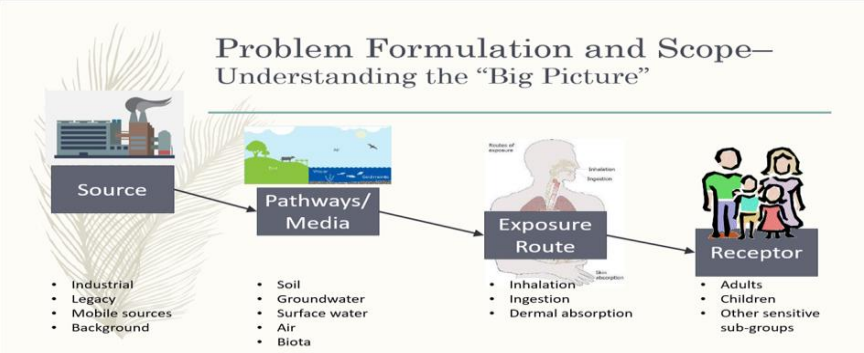

Figure 6.4 *The principle of source–pathway–receptor*

The ship and its environment are the main areas of focus for risk assessment. For a case study of Port of Brisbane, an impact assessment on local air quality due to at-berth, manoeuvring, and cruise ship emissions is presented. Air quality impact assessment has been carried out on different emission scenarios designed to produce long-term (i.e. annual average) and short-term (i.e. daily and hourly average) expected concentration levels to be compared to current air quality limits in the study area. Moreover, it is useful to divide the risk assessment component of the study into three sections, given that the CALPUFF model would not be the best model with time-changing emissions regarding the time pattern of near-and near-field vessel traffic:

- ***Downwash****: an area that may be affected on the ship itself (or on nearby ships). Calculations derived from first principle equations were applied to the average 1-hour and 24-hour levels of PM. Of interest in this case was the maximum concentration that someone on a ship could be exposed to.*
- ***Near-field****: potential impacts to receptors on the port area. Gaussian plume modelling from first principles equations, averaging times of 1 hour or 24 hours for PM, were applied to calculate these concentrations.*
- ***Airshed impacts****: The modelling domain chosen for the model is a 100 km x 100 km grid with 1 km grid spacing. The domain is centred at the Bureau of Meteorology, Brisbane Aero monitoring station. Potential impacts to the entire airshed, with*

pollutant concentrations assessed via CALPUFF dispersion modelling, using all averaging times as required. Receptors in this case were:

- *The single worst affected location anywhere in the airshed. For this location, a comparison against available guidelines, and an assessment of carcinogenic risk from diesel particulate, were completed. Other sensitive receptors of interest, such as schools, kindergartens, hospitals, retirement homes, were chosen, and data from CALPUFF dispersion modelling were extracted for those locations. Assessment of risks at these locations was as per the single worst-case location, as described above.*
- *The average location across the impacted airshed was detected and average concentrations across the airshed for the appropriate averaging times were calculated. Concentration-response functions (CRF)s derived from a study of the literature were used to calculate relevant health incidence rates*
- *Assessment of carcinogenic risks from diesel particulate as well as in-depth toxicology reviews and ecological effects of concentrations were also completed.*

6.2.Building downwash algorithm

The downwash computations are obtained from the first principle equation presented by Briggs (Briggs 1974). The primary objective of the section is to describe the state of the research on downwash phenomena of emissions as pollutants. The accounting for the downwash of pollutant dispersion is crucial since it can lead to curbing of dangerous circumstances by determining in advance the configurations of the stacks, buildings, and effluents. The concentration of effluents is a region that can lead to harmful effects on the environment. The most recent studies regarding stacks and structures are presented in this study. The models used are appropriately established and applied in the regulation of air pollution codes. This procedure of downwash correction is also still utilised in the regulation of plume rise models. It is recommended that 1-hour averages are used when possible (or 24 hours of PM) to assess the risk. In this case, our focus is in the maximum concentration of the emissions under consideration that might affect a person on a ship. Building a downwash algorithm requires a cross-sectional area to be chosen and its dimensions combined with the velocity assumption that the mass emission rate from the chimney equals the one from downwash carry, which

works on the principle of the conservation of mass. The final stage consists of choosing the downwash area and velocity to which to apply the algorithm.

The stack outlet area should be perpendicular to the direction of travel. If it is within a certain distance of the chimney, and if the ship is within the wake region, we assume that a certain percentage of concentrations is dragged into the wake. This assumption gives the rules for choosing the area and velocity. In theory, if there is a very high chimney (more than 2.5 times the height of surrounding buildings in the port area), concentrations will not decline. Similarly, if the plume rises very quickly, then nothing will be reduced. A plume may increase quickly if it has a higher velocity than a low wind, or if there is high momentum associated with temperature. A reasonable assumption is that there is an area equal to the cavity area and that the plume area equals the cavity area. This leads to assuming a 100% downwash option, which has been considered in this study. The dimension of the cavity is called the 'cross stream width' which it is roughly the width of the building and the height of the cavity which is taken around a factor of three: three × two or three × the building height. The specific empirical values depend on the shape of the building, which in this study is the area that the crew occupies on the ship.

The cavity and stack tip are the two types of downwash procedures to be considered while conducting risk assessment. Cavity modules calculate the portion of plume mass obtained by and recirculated in the closer wake. The above method has not been used in the study because no crew could have been noticed in this area. The downwash velocity takes place when the speeds of the stacks are divided by the average velocities of free streams (Briggs 1974), which has also been implemented in our study (Table 6.1).

Table 6.1 *Stack tip downwash calculations*

Parameters	Units	Description/Comments
V_o	25 m/s	Stack Outlet Velocity
H_s	20 m	Stack Outlet Height relative to Sea Level
D_o	0.8 m	Stack Outlet Diameter
U	2 m/s	Reference Wind Speed
V_o/U	12.5	If $V_o/U < 1.5$ Stack Tip Downwash Applies.
H'_s	20 m	If Stack Tip Downwash Applies: $H_s + 2 \times D_o \times ((V_o/U) - 1.5)$ If Not: H_s

No stack tip downwash occurred during the time of this study because of the high stack outlet velocity and low reference wind speed (Table 6.1), which means that people on the ship were not affected by either kind of downwash.

There is, however, another way that a crew may be affected. Depending on the rate of plume rise, the cavity may extend or intercept the plume. A portion of that plume will then be down washed into the cavity area and envelop the depth of the ship so that it covers the cavity of the vessel and not just the stack tip. This will be deflected around the ship, however, at some point, a separation occurs, and, instead of following the contour of the vessel, the flow separates, and an eddy develops that may affect people aboard. As ships are designed to have velocities high enough to counter this, the enhanced turbulence effect is ignored in this study, which assumes the stacks are above the wake region. The effect is part of the screening assessment level, but it is a conservative, high estimation, and its application to ships differs from buildings due to their different geometrical shapes. The nature of a vessel is that it is streamlined to flow through the water, and the average wind speed in the cavity is less in the downwash zone, resulting in a softer effect. The eddy, down washed cavity will result in a lower concentration effect that may be better investigated in the near-field and air-shed area scenarios (also discussed in sections 6.2.2 and 6.2.3). Such outcome occurs because in the case of the eddy it is not the concentrated plume that matters but a mixture of the plume and the entire wake. In our scenario, we can ignore the number as it is very small.

6.3. Gaussian Plume modelling

One of the most valuable tools in the estimation of atmospheric transport emissions in risk assessment is the Gaussian plume model (Zhang, Hodgson et al. 2000, Amoatey, Omidvarborna et al. 2017, Khaniabadi, Sicard et al. 2018). The wind makes the dispersion of airborne concentration extremely complicated due to its variability in velocity. Additionally, the terrain of the land on the earth surface complicates the issue even further. Thus, there is no complete general equation expressing the physical association between the causative meteorological factors and processes in ambient concentrations of air pollution. The Gaussian plume model is the most widely used model for air pollution dispersion. Therefore, the distribution of the near-field plume is assumed to conform to a Gaussian distribution. The expression is then a function of the height of the stack, buoyancy, and emission velocity, which describes the shape of the plume in the nearest port areas. This study is a screening-level assessment, which assists in finding concentrations and their risk values as well as assessing

them and analysing how different variables may influence outcomes. The evaluation is done by selecting particular locations and heights at which to intersect the pure plume, provide the calculations for the concentrations under study, which may dilute in a certain amount of air, and analyse their effect on people living in the port.

The four input variables for a Gaussian distribution are emission rate, velocity, and temperature as well as wind speed. Other inputs such as the surface roughness are ignored as this study does not consider emissions being spread over the countryside; it is looking at relative changes such as how variance affects the final risk values. For a Gaussian distribution, there is no highly turbulent atmosphere, and neutral and stable atmospheric conditions are assumed in a generalised model.

Under neutral conditions, the plume rise equations are a function of the buoyancy and the exit velocity (Briggs 1974) (Table 6.2). This includes both a stable plume that is pure and an unstable one that is meandering. The stable plume continues to be the same size and retains high concentration until it reaches instability and then mixes vertically. Meandering plumes mix horizontally. Where the spread in the vertical direction and the horizontal direction of the test plume smoke is neutral, there is no change in height or temperature. Different stability classifications explain variable particulate matters (PM). For example, classification D neutral means that it is adiabatic, which in atmospheric terms, implies there is no energy exchange between the various heights.

Table 6.2 *Gaussian dispersion and plume rise calculations and risk values*

Parameters	Units	Description/Comments
Q	1.27e-06 Kg/hour $PM_{2.5}$ – Cruising	Mass Emission Rate of Particulate Matter
	1.02e-06 Kg/hour $PM_{2.5}$ – Manoeuvring	
	7.67e-07 Kg/hour $PM_{2.5}$ – At Berth	
	5.29e-08 Kg/24-hour $PM_{2.5}$ – Cruising	

	4.25e-08 Kg/24-hour $PM_{2.5}$ – Manoeuvring	
	3.19e-08 Kg/24-hour $PM_{2.5}$ – At Berth	
	1.31e-06 Kg/hour $PM_{10.0}$ – Cruising	
	1.05e-05 Kg/hour $PM_{10.0}$- Manoeuvring	
	7.92e-07 Kg/hour $PM_{10.0}$ – At Berth	
	5.44e-08 Kg/24-hour $PM_{10.0}$ – Cruising	
	4.38e-08 Kg/24-hour $PM_{10.0}$- Manoeuvring	
	3.29e-08 Kg/24-hour $PM_{10.0}$ – At Berth	
G	9.81 g/ms^2	Gravity Acceleration
T_a	298 K	Ambient Temperature
U	2 m/s	Reference Wind Speed
T_o	539 K	Stack Outlet Temperature
R_o	0.4 m	Stack Outlet Radius
V_{oz}	25 m/s	Stack Outlet Velocity
X	100 m	Receptor Downwind Distance from the Stack
Y	0 m	Receptor Transverse Distance Relative to the Plume* * The plume goes straight to the receptor, so it is zero

H_s'	20 m	Adjusted Stack Outlet Height Relative to Sea Level
H_s	20 m	Stack Outlet Height Relative to Sea Level
A	0.50 $m^2 = \pi \times Ro^2$	Stack Cross-section Area
F_o	31.73 $m^4/s^3 = (G/Ta) \times (T_o - T_a) \times V_{oz} \times Ro^2)$	Buoyancy Flux
σ_y	26.43 m if Class A 18.89 m if Class B 11.62 m if Class D 8.15 m if Class F	Standard Deviation of the Plume Distribution (y direction)
σ_z	26.43 m if Class A 17.32 m if Class B 7.99 m if Class D 1.58 m if Class F	Standard Deviation of the Plume Distribution (z direction)
H	74.57 m = $H_s' + (1.6 \times ((Fo \times X)^2)^{1/3}) / U$	Plume Total Centreline Height Relative to Sea Level
Z'	54.57 m if PG: A, B and D 6.05 m if PG: F	Plume Rise Relative to Stack Outlet Height
Z	0-78 m	Receptor Vertical Distance above Sea Level
C (x,y,z)		Local Concentration of the Pollutant at the Receptor

Comparing the results with the final values in guidelines (Table 6.3), only ground level concentrations (*Z*=0) in the first row exceed the final risk values, indicating severe human exposure to ambient PM in the most developed and populated areas in Port of Brisbane. The guideline values account for the elevation of the source above the ground surface. The emission of pollutants and the atmospheric dynamics, which failed to distribute pollutants to the upper spheres of the atmospheric air and to other regions, explain why the ground level concentrations

in this study exceed the recommended safety limits. The uncontrolled level of urbanisation in terms of the emissions from urban sites together with emissions from automobiles, industries, and the combustion of solid wastes explains the level of pollutants in the atmosphere. The pollutants that are emitted remain concentrated and localised at ground level, because the stable atmosphere hinders their flow either vertically or horizontally. Low wind speeds, often below 5km/h during the time of this study, and high levels of humidity, limited the diffusion of pollutants from a source region to other areas, as well as from the ground level upwards. Near-field studies consider the potential effects of pollutants on people on-shore, and employs the methods used in Gaussian plume modelling. As explained, except for ground-level concentrations, the maximum predicted concentrations appear reasonable and their comparison with the proposed screening model predictions show excellent agreement with the recommended risk values. In these near-field assessments, emissions forecasts take into consideration the mass of emissions and the duration and period of their release. Applying onsite turbulent velocity and wind as input returns estimated enough measurements of concentrations. This study collected data on emission patterns created near the source, and the results indicate that traditional models of dispersion, primarily utilised for regulation purposes, occasionally overestimate concentrations in the near field but underestimate the lower ranges of pollutant concentrations. Studies also indicate that the PRIME algorithm, utilised to compute dispersions in the wake cavities, overestimates pollutant concentrations in the near field and neglects upwind meandering (Isakov, Sax et al. 2004). Some studies offer an algorithm available in CALPUFF, a new model for regulating dispersion, which might calculate concentrations with high precision by accounting for upwind meandering near a source (Barclay and Borissova 2013). However, CALPUFF cannot offer reliable near-field concentration measurements from sources responsible for modern emissions if plume spreads are measured using estimates of turbulent velocities near to sources (Carotenuto, Gualtieri et al. 2018). This study, designed to formulate a refined modelling perspective for near field application for regulation, used a case study approach, and the evaluation of its result showed a corresponding agreement with the literature.

Table 6.3 *Final risk guideline values*

Pollutant	Averaging time	NEPM (µg/m^3)	WHO (µg/m^3)
PM_{10}	24 hours	50	50
PM_{10}	1 hour	2.08	2.08
$PM_{2.5}$	24 hours	25	25
$PM_{2.5}$	1 hour	1.4	1.4

6.4.CALPUFF dispersion modelling

6.4.1. Health impact risk assessment

The Health Impact Assessment is an international tool used to assess complex hazards and risks of exposure in particular areas. A comparison of risks to residents living near different ports illustrates how this study's risk assessment supports the aims of the Assessment, important components of which are to identify where and when public health is most likely to be endangered, and to recommend ways to reduce or eliminate the threat (Collins and Koplan 2009). Short-term (daily) and long-term (annual) exposure to concentrations have been associated with increased daily and yearly health outcomes. The shape of the concentration–response relationship—particularly if there is a threshold—is critical for estimating public health impacts (Atkinson, Yu et al. 2012). This study investigated the concentration–response relationship between daily and yearly concentrations and their health impacts in Port of Brisbane for the calendar year 2013. Analysis of results showed the following:

- For the Port of Brisbane, long-term health end-points of $PM_{2.5}$ were projected to annually cause 0.39% of the adult population to suffer cardiopulmonary effects, 0.42% of the population to exhibit Ischaemic heart disease, and 0.39% to be affected by lung cancer. In addition, the life expectancy lost projection was 2e-3%. The long-term effect of $PM_{2.5}$ exposure also was projected to cause a 0.36% mortality rate in infants (<12 months of age).
- Short-term health end-points of $PM_{2.5}$ daily affected 2.8% of adults with non-trauma diseases and 4.7% with cardiovascular diseases. In addition, 0.8% hospitalised due to these cardiovascular diseases, 2.2% due to Cardiac failure as well as 1.0% for Ischaemic heart diseases. The daily concentrations also affected 1.69% with Myocardial infarction. In addition, 0.9% had to visit emergency departments for non-

fatal heart attacks, 1.28% for Minor restricted activity days and 1.24% due to some work lost days due to being affected. Also, 1.19% of 8-12-year-old children suffered from acute bronchitis and 1.058% from Lower respiratory symptoms.

- $PM_{10.0}$ affected 1.18% of the population from all-cause mortality due to its Long-term health endpoints annually as well as 16.4% affected from some years of lost life expectancy. This also caused 1.2% of the Infants (<12 months of age) with mortality. Also, 0.6% of population suffered from Airway inflammation.
- $PM_{10.0}$ short-term health endpoints were projected to cause 0.7% of the population to be subjected to cardiac hospitalization and 2.3% to experience cardiac failure, 0.6 % to suffer from pneumonia and acute bronchitis. In addition, 4.6% were projected to visit emergency departments for asthma and 25.8% were affected by shortness of breath.
- The projected results for NO_x long-term health endpoints are that 0.76% would experience asthma and 2.66% would experience airway inflammation annually. For NO_x short-term health endpoints, the projected results are greater, with 1.49% experiencing non-trauma mortality, 1.40% experiencing cardiovascular issues, and 3.43% experiencing respiratory issues. In addition, 0.8% of 15-64-year-olds and 0.02% of +65-year-olds were projected to be hospitalized due to cardiovascular issues, 0.8% due to cardiac issues, and 0.13% with cardiac failure issues. Short-term concentrations also made 0.91% visit the emergency department due to asthma and 0.01% due to lung malfunction.
- SO_x Long-term health endpoints also made 7.53% of the population visit the emergency departments for asthma issues as well as 3.86% with Bronchodilator use due to the Incidence of myocardial infarction.
- The analysis identified evidence of a threshold in the relationship between yearly concentrations of emissions and all-cause mortality, morbidity, emergency department visits and heart attacks. The daily concentration analyses also identified evidence of a threshold between short-term concentrations and all-cause mortality, hospitalisation, emergency department visits and minor morbidities.

This study indicates that the health of residents living near ports is most likely to be affected by different industrial activities. The obvious response is to minimise exposure for those living near ports when emissions from shipping operation activities are at their highest. This study is also one small part of what needs to be a comprehensive overview that incorporates all relevant

pathways and exposure scenarios, including occupational exposure, to enable a better understanding of the impacts of primary emissions on public health. A full Health Impact Assessment can identify where and when public health is most likely to be affected, and indicate strategies to reduce negative health impacts. Our preliminary results, indicating that people living near Port of Brisbane face significant health risks, warrant further study.

6.4.2. Short-term and long-term risk assessment of concentrations

The guidelines from Australia's National Environmental Management Plan (NEMP) and the World Health Organisation (WHO) were implemented to validate the results of the study (Table 6.4 and Table 6.5) (WHO 2000, Department of the Environment 2016). The maximum and average mean concentrations in the simulated air-shed in this study were less than the safety limit defined for short- and long-term inhalation exposure by NEMP and WHO. Assumptions underlie the offered “worst case” scenarios, one of which is the predicted flow of local-scale air pollution against the meteorological model that the Australian Bureau of Meteorology offers. The predicted flow incorporates the effects of sea breezes and land gradients. Meteorological data for the Port of Brisbane area is scarce, and the associated temporal resolution lacks the level of precision required to analyse a model developed from the data. The applied model, instead, offers an analytical framework that is more accurate and reliable. The Lagrangian Particle Model and Plume Rise Module (Hertwig, Soulhac et al. 2018, Teggi, Costanzini et al. 2018) are used in the simulation of this study to generate the flow at a higher level of accuracy, allowing predictions about the local meteorology that offer advantages over the use of available meteorological data.

6.4.3. Ecological effect risk assessment

Following the recognition of WHO that protecting the environment benefits human health, this study focused on the ecological effects of SO_x and NO_x. Some contaminants found in the atmosphere are also believed to cause environmental impacts including PM; however, practical approaches to measuring them have not yet been developed.

Since the publication of "Air Quality Guidelines for Europe" in 1987, emissions from SO_2 have fallen in many areas, and it is no longer viewed as the direct danger it once was (WHO 1987). However, it has a significant effect on plant life with minimal concentrations impacting on yield and growth, making plants more susceptible to other types of environmental stress (Bare

2008). The current WHO statistics (WHO 2000) suggest the yearly baseline estimate of 30 μg/m^3 as the standard average concentration; the measurement of SO_2 in this study, however, is much lower (Table 6.5). This is an annual average, however, and it is recommended that in the winter the concentration should be lower as its effect on winter crops is particularly severe. It has also been noted by WHO (WHO 1987) that an average daily guideline is not particularly useful as the cumulative effect is a more significant impact on plants. A baseline of 20 μg/m^3 is then currently recommended (Mcleod and Skeffington 1995). The level of SO_2 in this study is lower than the critical range as well (Table 6.5), and so the attention is mainly on the direct effects of exposure between one hour and one year long.

Table 6.4 *Maximum concentrations versus available guidelines*

Pollutants	Averaging time	Concentrations (μg/m^3)	NEPM	WHO
CO	10 minutes	1.87	n/a	100000 (μg/m^3)
CO	30 minutes	5.83	n/a	60000 (μg/m^3)
CO	1 hour	48.6	n/a	30000 (μg/m^3)
CO	8hours	22.3	9 ppm	10000 (μg/m^3)
SO_2	10 minutes	15.7	n/a	500 (μg/m^3)
SO_2	1 hour	93.8	0.2 ppm	n/a
SO_2	24 hours	36.2	0.08 ppm	20 (μg/m^3)
SO_2	1 year	9.98	0.02 ppm	n/a
NO_2	1 hour	25.3	0.12 ppm	200 (μg/m^3)
NO_2	1 year	10.4	0.03 ppm	40 (μg/m^3)
PM_{10}	24 hours	64.2	50 (μg/m^3)	50 (μg/m^3)
PM_{10}	1 year	8.3	25 (μg/m^3)	20 (μg/m^3)
$PM_{2.5}$	24 hours	40.3	25 (μg/m^3)	25 (μg/m^3)
$PM_{2.5}$	1 year	8.5	8 (μg/m^3)	10 (μg/m^3)

Table 6.5 *Average concentrations versus available guidelines*

Pollutant	Averaging time	Concentrations ($\mu g/m^3$)	NEPM	WHO
CO	10 minutes	0.96	n/a	100000 ($\mu g/m^3$)
CO	30 minutes	3.25	n/a	60000 ($\mu g/m^3$)
CO	1 hour	28.1	n/a	30000 ($\mu g/m^3$)
CO	8hours	17.5	9 ppm	10000 ($\mu g/m^3$)
SO_2	10 minutes	13.1	n/a	500 ($\mu g/m^3$)
SO_2	1 hour	75.8	0.2 ppm	n/a
SO_2	24 hours	19.8	0.08 ppm	20 ($\mu g/m^3$)
SO_2	1 year	7.5	0.02 ppm	n/a
NO_2	1 hour	19.63	0.12 ppm	200 ($\mu g/m^3$)
NO_2	1 year	9.84	0.03 ppm	40 ($\mu g/m^3$)
PM_{10}	24 hours	49.7	50 ($\mu g/m^3$)	50 ($\mu g/m^3$)
PM_{10}	1 year	6.12	25 ($\mu g/m^3$)	20 ($\mu g/m^3$)
$PM_{2.5}$	24 hours	23.74	25 ($\mu g/m^3$)	25 ($\mu g/m^3$)
$PM_{2.5}$	1 year	6.87	8 ($\mu g/m^3$)	10 ($\mu g/m^3$)

While there is an established guideline for acceptable levels of SO_2, elaborating critical standards for NH_3, NO_2, and NO is not so simple. In most parts of the world, these are the dominant forms of nitrogen deposition according to WHO (WHO 2000), but they have several significant effects that are not adequately considered by the acidity or critical loads for nitrogen, which has been based on the physiological and ecological impacts on plants, not on

biochemical changes (Camargo and Alonso 2005). Our survey considered that, ecologically, both stimulation and reduction in growth are negative responses to pollutants, and there is a need to comprehend more about prolonged biochemical effects on plants. There is insufficient data to establish the actual impact of critical levels for short-term exposure even with the formulation of a typical scenario. A value of approximately 75 $\mu g/m^3$ for NO_x as an hour mean has been suggested by WHO (WHO 1987). However, the values in our study are considerably lower (Table 6.5). Interactive effects involving NO_2 and SO_2 or ozone have also been reported but a review of recent literature reveals that the smallest efficient levels for combination effects are approximately the same to those for nitrogen (IV) oxide (Ito, Okano et al. 1986, Adaros, Weigel et al. 1991, Cape, Leith et al. 1991, Van de geijn 1993, Caporn, Hand et al. 1994). Measuring critical levels for a full year may cover relatively long-term effects. The annual level for NO_x is 30 $\mu g/m^3$; and as well, the values in this study are significantly lower (Table 6.5).

6.4.4. Carcinogenic risk assessment of concentrations

Receptors are also exposed to exhausts from diesel trains and ships, power generators, and other sources (Zeng, Jeppesen et al. 2018). There is already a large evidence to establish environmental standards for diesel exhaust emissions, and governments (mostly in North America and Europe) have established successively tighter emission standards for both diesel and gasoline engines (International Agency for Research on Cancer 2012). For diesel engines, however, standards tend to require a significant decrease in sulphur, changes to engine designs that will lead to more efficient burning, and improvements in exhaust control to reduce emissions (International Agency for Research on Cancer 2012).While these may reduce the quantity of particulates and chemicals, their effect on health is not yet clear. Particulate matter is of great concern specifically because it is carcinogenic and disrupts endocrine activity.

Our study has calculated the risk of exposure through inhalation utilising an equation of probabilistic risk assessment. For adults, the computed risk of cancer suggests that vulnerability via inhalation is 10e-6, which is the same for the young ones (WHO 2000). This value, called the Incremental Lifetime Cancer Risk (ILCR), considers the probability of any human getting cancer from exposure (to airborne pollutants). The way to validate this value in our study was to calculate the annual average concentration of $PM_{2.5}$ in the explained air-shed in section 6.2.3.2 and then to multiply it (for the air-shed and for any individual receptor locations) by (3.4 x 10e-5) ug/m^3 to calculate the individual ILCR for each person in that air-shed. A final ILCRs below 10e-6 is considered acceptable and in our study, the sequence of calculating the

cancer risk was “industrial sites > busy traffic sites > sensitive sites > residential sites. The individual danger through inhalation in our study (2.34e-04) is more than the recommended risk, therefore the risk of developing cancer from inhaling particles is not negligible. The potential for synergic or additive impact between toxic organic compounds and fine particles can also raise the vulnerability of cancer development through inhalation even though it accounts for a small percentage of the total intake of concentrations. Extensive research is required to improve the understanding of sources of airborne contaminants. Such studies can contribute to the formulation of adequate regulations to improve the standards for air quality in Australian ports.

Chapter 7: Conclusions and future work

This chapter presents the main summary and conclusions of this research and a number of recommendations for further work.

7.1. Conclusions

The following are the main conclusions from this PhD research study:

- *Real time in-vessel continuous emissions measurements of Particulate Matter (PM), NO_x, SO_x, CO_2, CO and HC measurements are demonstrated using portable gas instrumentation including PM size distributions.*
- *A comprehensive case study to identify the best vessel-specific inventory family predicting the primary emissions from ocean-going vessels when at berth, while manoeuvring and while cruising has been demonstrated and prediction deviations have been calculated.*
- *A generalized rational algorithm to rank inventory families based on the precision of their predictions for a given operational mode of a specific vessel has been created.*
- *The implications of the case study together with the developed algorithm to rank inventory families have been applied to offer a novel future policy for cost-effective and reliable emission estimation caused by shipping.*
- *Models for emission factor estimation methods and informed decision-making framework for ships operating in different conditions (fuel, operation, engine type, engine size, region) have been developed.*
- *A complex atmospheric dispersion modelling has been applied to assess the ground-level concentrations.*
- *Each resulting emission concentration has been assessed for its individual health impact, based on a calculated risk value.*

Based on the reported findings in this thesis, the following main conclusions can be drawn:

- The results from the measurement showed that fuel Sulphur content and the engine load are key factors in significant emission variations. For example, the auxiliary engine

emissions at berth were far more significant than main engine emissions due to a higher engine load, whereas primary emissions from the main engine became dominant when the vessel was manoeuvring and cruising.

- The measured emission rates were converted to instantaneous emission factors and eventually to total emission amounts. The latter were predicted with 13 families of emission inventories (Tier I–III, ENTEC, MEET, STEAM, MOPSEA, IMO, SMED, EMS, US EPA, NERI and Corbett) and prediction deviations have been calculated. A procedure was advised for estimating the prediction inventory deviations of the combined hourly emission amounts from the main engine plus the auxiliary engines. The best inventory families were identified using the minimal mean absolute deviation criterion. The best inventory method at berth happened to be MOPSEA (39.1% mean absolute deviation), for manoeuvring the best inventory family is US EPA (with 50.9% mean absolute deviation), and for cruising the best inventory family is MEET (with 53.4% mean absolute deviation). However, some of the other inventories produce unacceptably great deviation, well above 100%.
- A more rational procedure for inventory ranking was considered, where each inventory family has been formalized as a six-dimensional vector of prediction deviations for a given mode of operation, which treats the missing value problem and constructs a six-attribute value function. We proposed an algorithm to impute missing values in the vectors (in case some of the emission deviations were not calculated), and to construct a six-attribute value function. The calculation of the value function at the six-dimensional vectors of prediction deviations was in position more rationally to identify the best inventory family when the vessel is at-berth, during manoeuvring, and during cruising. The relation between the minimal mean absolute deviation criterion ranking and the maximal value function criterion was investigated. It was demonstrated that the former is a “quick and dirty” special case of the latter. The implications of the case study were used to advise novel future policy for cost-effective and reliable emission estimation caused by the shipping.
- The non-linear regression analysis applied to develop new sets of emission factor equations on each primary emission for engines at berth, manoeuvring, and at sea predicts emissions more accurately than current inventories. The updated estimations will help in developing emission models and inventory calculations that can be used to outline maximum continuous rate, shaft speed, and emission datasets more effectively than is currently achieved.

- A robust emissions inventory utilised to quantify the emissions of ocean-going vessels and incorporating CALPUFF for dispersion modelling. To demonstrate the effectiveness of methodology, it has been applied to Port of Brisbane and returns representative emissions results. This highlights the need for any assessment of the dispersion of in-port ship emissions to consider all emissions within port boundaries. This is particularly so in ports like Brisbane where long transit passages take place near densely populated suburbs. This also demonstrates that applying emission inventory results to detailed dispersion modelling of Port of Brisbane and completing an associated risk assessment provides a convincing demonstration of the need to combat the widespread effects of ship emissions.
- The study investigated the suitability of health risk frameworks for assessing shipping emissions within Australian ports. This shows that applying the emission inventory results to a detailed dispersion model of Port of Brisbane and completing the associated risk assessment provides a convincing argument to address the distribution, concentration, sources, and health vulnerability assessments of primary emissions in ports found in Australia.
- This research project led by the AMC demonstrate a continuous emission measurement system and analysis of emissions. The measurement campaign allowed for the fuel oil characteristics to be determined and assessed, and on-board measurements of the primary emissions were used in the development of emission factors. The auxiliary engine emissions at berth were far more significant than main engine emissions due to a higher engine load, whereas primary emissions from the main engine became dominant when the vessel was maneuvering and cruising.
- A procedure was advised for estimating the prediction inventory deviations of the combined hourly emission amounts from the main engine plus the auxiliary engines. The best inventory families were identified using the minimal mean absolute deviation criterion. The best inventory method at berth happened to be MOPSEA (32.2% mean absolute deviation), for maneuvering the best inventory family was MOPSEA (with 39.6% mean absolute deviation), and for cruising the best inventory family is MEET (with 59.2% mean absolute deviation). However, some of the other inventories produce unacceptably great deviation, well above 100%.
- This study highlights the need for any assessment of the dispersion of in-port ship emissions to consider all emissions within port boundaries. This is particularly so in

ports like Brisbane where long transit passages take place near densely populated suburbs.

- This study demonstrates that applying emission inventory results to detailed dispersion modelling of Port of Brisbane and completing an associated risk assessment provides a convincing demonstration of the need to combat the widespread effects of ship emissions.
- This study shows that applying the emission inventory results to a detailed dispersion model of Port of Brisbane and completing the associated risk assessment provides a convincing argument for the need to combat the widespread effects of ship emissions.
- To the best of our knowledge, this study is the initial comprehensive report addressing the distribution, concentration, sources, and health vulnerability assessments of primary emissions in ports found in Australia.

7.2. Areas of future development

There are several directions, in which this study can develop and expand in the future:

- It is recommended that further investigative studies and on-board measurements be carried out on different vessel types installed with different engine configurations to better understand ship emissions. PM and their size distribution are also a great concern for scientific environmental community. Further research is also needed to study the effect of the concentration of metals (in particular vanadium) on particulate emissions.
- Further study is needed to potentially reduce the uncertainties in current assessments of the effect of exposure to air emissions, to better direct efforts to prevent exposure, and to address the limitations identified in the risk assessment and emission inventories in this study.
- Further work may model shorter- and longer-term exposures and collect relevant data by area, residence, and personal exposure, with emphasis on peak short-term emissions.
- There is also a need to examine the toxicity of hydrocarbons, such as alkanes, and the health effects of mixtures of Hazardous Air Pollutants and other air pollutants associated with primary emissions. Emissions from specific emission sources may be characterised, and dispersion profiles of Hazardous Air Pollutants developed. These data, combined with those of local meteorological conditions and topography, will

provide guidance on the minimum distances between emissions sources and homes, schools, and businesses needed to protect human health.

- Of most interest in the future is the continued evaluation of results from ports over an extended period. Assessing long-term trends in the data with regard to both meteorological and shipping traffic fluctuations will add more context to the baseline results.
- Since also shipping exhaust emissions are the major source of pollution in ports, there is a need for further analysis using finer fractions of atmospheric aerosols. Source apportionments as well as dispersion modelling with higher number of samples can be performed to provide more information about emission sources and distribution. In addition, there is a need to conduct further research to characterise better those parameters that contribute most significantly to the risk estimates.
- It is recommended that further investigative studies and on-board measurements be carried out on different vessel types installed with different engine configurations to better understand ship emissions.
- Further study may reduce the uncertainties in current assessments of the effect of exposure to air emissions, to better direct efforts to prevent exposure, and to address the limitations identified in this risk assessment. Further work may model short- and longer-term exposures and collect relevant data by area, residence, and personal exposure, with emphasis on peak short-term emissions. There is also a need to examine the toxicity of hydrocarbons, such as alkanes, and the health effects of mixtures of HAPs and other air pollutants associated with primary emissions. Emissions from specific emission sources may be characterised, and dispersion profiles of HAPs developed. These data, combined with those of local meteorological conditions and topography, will provide guidance on the minimum distances between emissions sources and homes, schools, and businesses needed to protect human health. Of most interest in the future is the continued evaluation of results from ports over an extended period. Assessing long-term trends in the data with regard to both meteorological and shipping traffic fluctuations will add more context to the baseline results.
- Further study may reduce the uncertainties in current assessments of the effect of exposure to atmospheric emissions and improve the direct efforts to curb exposure as well as addressing the limitations identified in the risk assessment (McKenzie, Witter et al. 2012). Further work may model short- and longer-term exposures and collect relevant data by area, residence, and personal vulnerability, with emphasis on short-

term peak emissions. There is also a need to investigate the toxicity level of hydrocarbons like alkanes, and the health impacts they possess when mixed with other pollutants in the atmosphere associated with primary emissions.

- Further research can be conducted in several areas within the same topic. One of them includes an investigation and further analysis of shipping exhaust emissions using finer atmospheric aerosols. Source apportionments and dispersion modelling with an increased number of samples can be executed to offer extensive knowledge regarding emission distribution and sources. Moreover, more research on characterising parameters that contribute more crucially to the vulnerability's estimation must be conducted.

Bibliography

Abrutyte, E., A. Zukauskaite, R. Mickeviciene, V. Zabukas and T. Paulauskiene (2014). "Evaluation of NOx emission and dispersion from marine ships in Klaipeda sea port." Journal of Environmental Engineering and Landscape Management **22**(4): 264-273.

Acock, A. C. (2005). "Working with missing values." Journal of Marriage and Family **67**(4): 1012-1028.

Adaros, G., H. J. Weigel and H. J. Jager (1991). "Single and interactive effects of low levels of O3, SO2 and NO2 on the growth and yield of spring rape." Environ Pollut **72**(4): 269-286.

Agrawal, H., Q. G. J. Malloy, W. A. Welch, J. W. Miller and D. R. Cocker (2008). "In-use gaseous and particulate matter emissions from a modern ocean going container vessel." Atmospheric Environment **42**(21): 5504-5510.

Agrawal, H., W. A. Welch, S. Henningsen, J. W. Miller and D. R. Cocker (2010). "Emissions from main propulsion engine on container ship at sea." Journal of Geophysical Research-Atmospheres **115**(D23).

Agrawal, H., W. A. Welch, J. W. Miller and D. R. Cocker (2008). "Emission measurements from a crude oil tanker at sea." Environmental Science & Technology **42**(19): 7098-7103.

Aksoyoglu, S., U. Baltensperger and A. S. H. Prevot (2016). "Contribution of ship emissions to the concentration and deposition of air pollutants in Europe." Atmospheric Chemistry and Physics **16**(4): 1895-1906.

Amoatey, P., H. Omidvarborna and M. Baawain (2017). "Modeling of particulate matter dispersion from a cement plant: upwind-downwind case study." J Hum Ecol Risk Assess. **24**: 1181-96.

Anderson, H. R., S. A. Bremner, R. W. Atkinson, R. M. Harrison and S. Walters (2001). "Particulate matter and daily mortality and hospital admissions in the west midlands conurbation of the United Kingdom: associations with fine and coarse particles, black smoke and sulphate." Occup Environ Med **58**(8): 504-510.

Atkinson, R. W., D. Yu, B. G. Armstrong, S. Pattenden, P. Wilkinson, R. M. Doherty, M. R. Heal and H. R. Anderson (2012). "Concentration–Response Function for Ozone and Daily Mortality: Results from Five Urban and Five Rural U.K. Populations." Environmental Health Perspectives **120**(10): 1411-7

Auth, T., Tuv, Dtu, Ademe, Bmw, Tug, Infras, Kalivoda, Mira, Psa, Techne, Tno, Ulimerick and Vti (1999). Methodology for calculating transport emissions and energy consumption (MEET), Transport Research Fourth Framework Programme Strategic Research

Bailey, D. and G. Solomon (2004). "Pollution prevention at ports: clearing the air." Environmental Impact Assessment Review **24**(7-8): 749-774.

Barclay, J. and M. Borissova (2013). Potential problems using aermod to implement current odor regulations for wwtps. . International Water Association Conference on Odors and Air Emissions. , San Francisco, California, USA.

Bare, J. (2008). "The Tool for the Reduction and Assessment of Chemical and Other Environmental Impacts." Journal of Industrial Ecology **6**(3-4): 49-78.

Bell, M. L., K. Ebisu, R. D. Peng, J. Walker, J. M. Samet, S. L. Zeger and F. Dominici (2008). "Seasonal and regional short-term effects of fine particles on hospital admissions in 202 US counties, 1999-2005." Am J Epidemiol **168**(11): 1301-1310.

Blasco, J., V. Duran-Grados, M. Hampel and J. Moreno-Gutierrez (2014). "Towards an integrated environmental risk assessment of emissions from ships' propulsion systems." Environ Int **66**(1): 44-47.

Bluett, J., N. Gimson, G. Fisher, C. Heydenrych, T. Freeman and J. Godfrey (2004). Good practice guide for atmospheric dispersion modelling. Prepared by the National Institute of Water and Atmospheric Research, Aurora Pacific Limited and Earth Tech Incorporated for the Ministry for the Environment. Published in June 2004 by the Ministry for the Environment. This document is available on the Ministry for the Environment’s website: www.mfe.govt.nz

Brandt, J., J. D. Silver, J. H. Christensen, M. S. Andersen, J. H. Bonlokke, T. Sigsgaard, C. Geels, A. Gross, A. B. Hansen, K. M. Hansen, G. B. Hedegaard, E. Kaas and L. M. Frohn (2013). "Assessment of past, present and future health-cost externalities of air pollution in

Europe and the contribution from international ship traffic using the EVA model system." Atmospheric Chemistry and Physics **13**(15): 7747-7764.

Briggs, G. A. (1974). Diffusion estimation for small emissions. Annual Report, ATDL-106, USDOC-NOAA. Oak Ridge (Tennessee): US Atomic Energy Commission., Air Resources Atmospheric Turbulence and Diffusion Laboratory.

Broome, R. A., M. E. Cope, B. Goldsworthy, L. Goldsworthy, K. Emmerson, E. Jegasothy and G. G. Morgan (2016). "The mortality effect of ship-related fine particulate matter in the Sydney greater metropolitan region of NSW, Australia." Environ Int **87**(1): 85-93.

Browning, L. and K. Bailey (2006). Current Methodologies and Best Practices for Preparing Port Emission Inventories,. 15th International Emission Inventory Conference "Reinventing Inventories - New Ideas in New Orleans". US EPA. 1-20.

California Air Resources Board (2005). The California Almanac of Emissions and Air Quality. California, CARB.

California Air Resources Board (2006). Appendix A: Quantification of the Health Impacts and Economic Valuation of Air Pollution from Ports and Goods Movement in CA. California.

California Air Resources Board (2006). Proposed Emission Reduction Plan for Ports and Goods Movement in CA;. Sacramento, CA .

California Air Resources Board (2008). Emissions Estimation Methodology for Ocean-going Vessels. http://www.arb.ca.gov/regact/2008/fuelogv08/appdfuel.pdf. California.

Camargo, J. and A. Alonso (2005). "Ecological and toxicological effects of inorganic nitrogen pollution in aquatic ecosystems: A global assessment." Environment International **32**(6): 831-849.

Cape, J. N., I. D. Leith, D. Fowler, M. B. Murray, L. J. Sheppard, D. Eamus and R. H. F. Wilson (1991). "Sulfate and Ammonium in Mist Impair the Frost Hardening of Red Spruce Seedlings." New Phytologist **118**(1): 119-126.

Caporn, S. J. M., D. W. Hand, T. A. Mansfield and A. R. Wellburn (1994). "Canopy Photosynthesis of Co2-Enriched Lettuce (Lactuca-Sativa L) - Response to Short-Term Changes in Co2, Temperature and Oxides of Nitrogen." New Phytologist **126**(1): 45-52.

Cappa, C. D., E. J. Williams, D. A. Lack, G. M. Buffaloe, D. Coffman, K. L. Hayden, S. C. Herndon, B. M. Lerner, S. M. Li, P. Massoli, R. McLaren, I. Nuaaman, T. B. Onasch and P. K. Quinn (2014). "A case study into the measurement of ship emissions from plume intercepts of the NOAA ship Miller Freeman." Atmospheric Chemistry and Physics **14**(3): 1337-1352.

Carotenuto, F., G. Gualtieri, F. Miglietta, A. Riccio, P. Toscano, G. Wohlfahrt and B. Gioli (2018). "Industrial point source CO2 emission strength estimation with aircraft measurements and dispersion modelling." Environ Monit Assess **190**(3): 165.

Celo, V., E. Dabek-Zlotorzynska and M. McCurdy (2015). "Chemical characterization of exhaust emissions from selected canadian marine vessels: the case of trace metals and lanthanoids." Environ Sci Technol **49**(8): 5220-5226.

Cesari, D., A. Genga, P. Ielpo, M. Siciliano, G. Mascolo, F. M. Grasso and D. Contini (2014). "Source apportionment of PM2.5 in the harbour–industrialarea of Brindisi (Italy): identification and estimation of the contribution of in-port ship emissions." Sci. Total Environ., **497-498**(1): 392-400.

Chen, D., X. Wang, P. Nelson, Y. Li, N. Zhao and Y. Zhao (2017). "Ship emission inventory and its impact on the PM 2.5 air pollution in Qingdao Port, North China." Atmos. Environ., **166**(1): 351-366.

Chen, D., N. Zhao, J. Lang, Y. Zhou, X. Wang and Y. Li (2018). "Contribution of ship emissions to the concentration of PM2.5: a comprehensive study using AIS data and WRF/Chem model in Bohai Rim Region." China. Sci Total Environ, **610-611**(1): 1476-1486.

Chen, G., L. G. Huey, M. Trainer, D. Nicks, J. Corbett, T. Ryerson, D. Parrish, J. A. Neuman, J. Nowak, D. Tanner, J. Holloway, C. Brock, J. Crawford, J. R. Olson, A. Sullivan, R. Weber, S. Schauffler, S. Donnelly, E. Atlas, J. Roberts, F. Flocke, G. Hubler and F. Fehsenfeld (2005). "An investigation of the chemistry of ship emission plumes during ITCT 2002." Journal of Geophysical Research-Atmospheres **110**(D10).

Chen, J. H., W. P. Zhang, S. F. Li, F. W. Zhang, Y. H. Zhu and X. L. Huang (2018). "Identifying critical factors of oil spill in the tanker shipping industry worldwide." Journal of Cleaner Production **180**(1): 1-10.

Clarkson, D. (2015). Development of a risk-based methodology to assess the impact of vessel emissions within Australian ports, PhD thesis, University of Tasmania.

Cofala, J., M. Amann, C. Heyes, Z. Klimont, M. Posch, W. Schöpp, L. Tarasson, J. E. Jonson, C. Whall and A. Stavrakaki (2007). Final Report: Analysis of Policy Measures to Reduce Ship Emissions in the Context of the Revision of the National Emissions Ceilings Directive;. Laxenburg, Austria.

Cohan, A., J. Wu and D. Dabdub (2011). "High-resolution pollutant transport in the San Pedro Bay of California." Atmospheric Pollution Research **2**(3): 237-246.

Cohen, J., P. Cohen, S. West and L. Aiken (2003). Applied multiple regression/correction analysis for the behavioral sciences. Mahwah, NJ.

Collins, J. and J. P. Koplan (2009). "Health Impact Assessment A Step Toward Health in All Policies." Jama-Journal of the American Medical Association **302**(3): 315-317.

Committee on the medical effects of air pollutants (2006). Cardiovascular disease and air pollution. London, UK: Department of Health.

Committee on the medical effects of air pollutants (2009). Long-term exposure to air pollution: effect on mortality. London: Department of Health.

Committee on the medical effects of air pollutants (2010). The mortality effects of long-term exposure to pariculate air pollution in the United Kingdom. London: Department of Health.

Cooper, D., T. Gustafsson and SCB (2004). Methodology for calculating emissions from ships: 1. Update of emission factors (SMED). Assignment for Swedish Environmental Protection Agency. Publisher: SMHI Swedish Meteorological and Hydrological Institute.

Cooper, D. A. (2001). "Exhaust emissions from high speed passenger ferries." Atmospheric Environment **35**(24): 4189-4200.

Cooper, D. A. (2003). "Exhaust emissions from ships at berth." Atmospheric Environment **37**(27): 3817-3830.

Cooper, D. A. and K. Andreasson (1999). "Predictive NOx emission monitoring on board a passenger ferry." Atmospheric Environment **33**(28): 4637-4650.

Cooper, D. A., K. Peterson and D. Simpson (1996). "Hydrocarbon, PAH and PCB emissions from ferries: A case study in the Skagerak-Kattegatt-Oresund region." Atmospheric Environment **30**(14): 2463-2473.

Corbett, J. J., P. S. Fischbeck and S. N. Pandis (1999). "Global nitrogen and sulfur inventories for oceangoing ships." Journal of Geophysical Research-Atmospheres **104**(D3): 3457-3470.

Corbett, J. J. and H. W. Koehler (2003). "Updated emissions from ocean shipping." Journal of Geophysical Research-Atmospheres **108**(D20).

Corbett, J. J., J. J. Winebrake, E. H. Green, P. Kasibhatla, V. Eyring and A. Lauer (2007). "Mortality from ship emissions: a global assessment." Environ Sci Technol **41**(24): 8512-8518.

Dalsoren, S. B., M. S. Eide, O. Endresen, A. Mjelde, G. Gravir and I. S. A. Isaksen (2009). "Update on emissions and environmental impacts from the international fleet of ships: the contribution from major ship types and ports." Atmospheric Chemistry and Physics **9**(6): 2171-2194.

Davis, M. (2014). "Ship emissions from Australian ports " WIT Transactions on Ecology and The Environment **183**(1): 327 - 337.

DEFRA (2006). An economic analysis to inform the air quality strategy review consultation. London: An economic analysis to inform the air quality strategy review consultation.

Deniz, C. and A. Kilic (2010). "Estimation and Assessment of Shipping Emissions in the Region of Ambarli Port, Turkey." Environmental Progress & Sustainable Energy **29**(1): 107-115.

Department of the Environment (2016). National Environment Protection (Ambient Air Quality) Measure, National Environment Protection Council.

Dockery, D., C. Pope, X. Xu, J. Spengler, J. Ware, M. Fay, B. Ferris and F. Speizer (1993). "An association between air pollution and mortality in six US cities. ." N Engl J Med **329**(24): 1753-9.

Dockery, D. W., J. Cunningham, A. I. Damokosh, L. M. Neas, J. D. Spengler, P. Koutrakis, J. H. Ware, M. Raizenne and F. E. Speizer (1996). "Health effects of acid aerosols on North American children: respiratory symptoms." Environ Health Perspect **104**(5): 500-505.

Du, Y. Q., Q. S. Chen, X. W. Quan, L. Long and R. Y. K. Fung (2011). "Berth allocation considering fuel consumption and vessel emissions." Transportation Research Part E-Logistics and Transportation Review **47**(6): 1021-1037.

Ducruet, C. and L. Wang (2018). "China's Global Shipping Connectivity: Internal and External Dynamics in the Contemporary Era (1890–2016)." Chinese Geographical Science **28**(2): 202-216.

Endresen, O., E. Sorgard, H. L. Behrens, P. O. Brett and I. S. A. Isaksen (2007). "A historical reconstruction of ships' fuel consumption and emissions." Journal of Geophysical Research-Atmospheres **112**(D12): 1-17.

Endresen, O., E. Sorgard, J. K. Sundet, S. B. Dalsoren, I. S. A. Isaksen, T. F. Berglen and G. Gravir (2003). "Emission from international sea transportation and environmental impact." Journal of Geophysical Research-Atmospheres **108**(D17): 1-22.

EnHealth (2012). Environmental Health Risk Assessment - Guidelines for Assessing Human Health Risk Assessment, enHealth.

Entec (2007). Ship Emissions Inventory – Mediterranean Sea, Final Report for Concawe. London, UK.

ENTEC UK Limited (2002). Quantification of Emissions from Ships Associated with Ship Movements between Ports in the European Community, FS 13881. European Commission (Brussels, Belgium).

Environment protection and heritage council (2005). Expansion of the multi-city mortality and morbidity study: final report. EPHC. **1**.

Erbas, B., A. M. Kelly, B. Physick, C. Code and M. A. Edwards (2005). "Air pollution and childhood asthma emergency hospital admissions: estimating intra-city regional variations." Int J Environ Health Res. **15**(1): 11-20.

European commission (2005). Externalities of energy: methodology 2005 update. Luxemburg.

European Parliament (2005). Directive 2005/33/EC of the European Parliament and of the Council of 6 July 2005 amending Directive 1999/32/EC European Commission - Council of the European Union.

Eyring, V., I. S. A. Isaksen, T. Berntsen, W. J. Collins, J. J. Corbett, O. Endresen, R. G. Grainger, J. Moldanova, H. Schlager and D. S. Stevenson (2010). "Transport impacts on atmosphere and climate: Shipping." Atmospheric Environment **44**(37): 4735-4771.

Eyring, V., H. W. Kohler, J. van Aardenne and A. Lauer (2005). "Emissions from international shipping: 1. The last 50 years." Journal of Geophysical Research-Atmospheres **110**(D17): 1-12.

Fan, Q., Y. Zhang, W. Ma, H. Ma, J. Feng, Q. Yu, X. Yang, S. K. Ng, Q. Fu and L. Chen (2016). "Spatial and Seasonal Dynamics of Ship Emissions over the Yangtze River Delta and East China Sea and Their Potential Environmental Influence." Environ Sci Technol **50**(3): 1322-1329.

French, S. (1993). Decision theory: an introduction to the mathematics of rationality. UK: Ellis Horwood.

French, S. and D. R. Insua (2010). Statistical Decision Theory. Kendall's Library of Statistics 9, Wiley.

Frey, H. C., R. Bharvirkar and J. Zheng (1999). Quantitative Analysis of Variability and Uncertainty in Emissions Estimation. Prepared by. North Carolina State University for the U.S. Environmental Protection Agency, Research Triangle Park, NC.

Fu, M. L., Y. Ding, Y. S. Ge, L. X. Yu, H. Yin, W. T. Ye and B. Liang (2013). "Real-world emissions of inland ships on the Grand Canal, China." Atmospheric Environment **81**(1): 222-229.

Gariazzo, C., V. Papaleo, A. Pelliccioni, G. Calori, P. Radice and G. Tinarelli (2007). "Application of a Lagrangian particle model to assess the impact of harbour, industrial and urban activities on air quality in the Taranto area, Italy." Atmospheric Environment **41**(30): 6432-6444.

Gaston, C. J., P. K. Quinn, T. S. Bates, J. B. Gilman, D. M. Bon, W. C. Kuster and K. A. Prather (2013). "The impact of shipping, agricultural, and urban emissions on single particle chemistry observed aboard the R/V Atlantis during CalNex." Journal of Geophysical Research-Atmospheres **118**(10): 5003-5017.

Goldsworthy, L. and I. E. Galbally (2011). "Ship engine exhaust emissions in waters around Australia - an overview. ." Air Qual Clim Change **45**(4): 24-32.

Goldsworthy, L. and B. Goldsworthy (2015). "Modelling of ship engine exhaust emissions in ports and extensive coastal waters based on terrestrial AIS data - An Australian case study." Environmental Modelling & Software **63**(1): 45-60.

Goldsworthy, L. and M. Renilson (2013). "Ship engine exhaust emission estimates for Port of Brisbane." Air Qual. Climate Change **47**(2): 26-36.

Gommers, A., L. Verbeeck and E. V. Cleemput (2007). MOnitoring Programme on air pollution from SEA-going vessels EV/43 (MOPSEA)

Gonzalez, Y., S. Rodriguez, J. C. Garcia, J. L. Trujillo and R. Garcia (2011). "Ultrafine particles pollution in urban coastal air due to ship emissions." Atmospheric Environment **45**(28): 4907-4914.

Hallquist, A. M., E. Fridell, J. Westerlund and M. Hallquist (2013). "On-board measurements of nanoparticles from a SCR-equipped marine diesel engine." Environmental Science & Technology **47**(2): 773–780.

Harel, O. (2009). "The estimation of R2 and adjusted R2 in incomplete data sets using multiple imputation." Journal of Applied Statistics **36**(10): 1109-1118.

Hassellov, I. M., D. R. Turner, A. Lauer and J. J. Corbett (2013). "Shipping contributes to ocean acidification." Geophysical Research Letters **40**(11): 2731-2736.

Hertwig, D., L. Soulhac, V. Fuka, T. Auerswald, M. Carpentieri, P. Hayden, A. Robins, Z. T. Xie and O. Coceal (2018). "Evaluation of fast atmospheric dispersion models in a regular street network." Environmental Fluid Mechanics **18**(4): 1007-1044.

Hockstad, L. and L. Hanel. (2018). "Inventory of U.S. Greenhouse Gas Emissions and Sinks." U.S. Department of Energy Office of Scientific and Technical Information. OSTI Identifier: 1464240. Report Number(s): cdiac:EPA-EMISSIONS.

Holmes, N. S. and L. Morawska (2006). "A review of dispersion modelling and its application to the dispersion of particles: An overview of different dispersion models available." Atmospheric Environment **40**(30): 5902-5928.

House, D. J. (2007). Ship Handling. Publisher: Butterworth-Heinemann (an imprint of Elsevier). Oxford, UK. ISBN: 978-0-7506-8530-6

IMO (1997). International Convention for the Prevention of Pollution from Ships MARPOL 73/78: The Regulations for the Prevention of Air Pollution from Ships (Annex VI) London International Maritime Organization.

IMO (2008a). Resolution MEPC 176(58): Amendments to the annex of the protocol of 1997 to amend the international convention for the prevention of pollution from ships, 1973, as modified by the protocol of 1978 relating thereto, International Maritime Organization.

IMO (2008b). Resolution MEPC 177(58): Amendments to the technical code on control of emission of nitrogen oxides from marine diesel engines, International Maritime Organization.

IMO (2010). Report of the Marine Environment Protection Committee on its Sixty-First Session. London, UK, International Maritime Organisation.

IMO (2011). Resolution MEPC.203(62): Regulations on EEDI (Energy Efficiency Design Index) for new ships, and the SEEMP (Ship Energy Efficiency Management Plan) for all ships, International Maritime Organization.

IMO (2014). Reduction of GHG emissions from ships, Third IMO GHG study, Final Report.

International Agency for Research on Cancer (2012). Diesel Engine Exhaust Carcinogenic, World Health Organisation.

Isakov, V., T. Sax, A. Venkatram, D. Pankratz, J. Heumann and D. Fitz (2004). "Near-field dispersion modeling for regulatory applications." J Air Waste Manag Assoc **54**(4): 473-482.

Ito, O., K. Okano and T. Totsuka (1986). Effects of NO2 and O3 alone or in combination on kidney bean plants. II. Amino acid pool size and composition. Tokyo: National Institute of Environmental Studies.

Jalaludin, B., B. Khalaj, V. Sheppeard and G. G. Morgan (2008). Air pollution and ED visits for asthma in Australian children: a case-crossover analysis. . Int Arch Occup Environ Health **81**(8): 967-74.

Jalkanen, J. P., A. Brink, J. Kalli, H. Pettersson, J. Kukkonen and T. Stipa (2009). "A modelling system for the exhaust emissions of marine traffic and its application in the Baltic Sea area." Atmospheric Chemistry and Physics **9**(23): 9209-9223.

Jalkanen, J. P., L. Johansson and J. Kukkonen (2014). "A comprehensive inventory of the ship traffic exhaust emissions in the Baltic Sea from 2006 to 2009." Ambio **43**(3): 311-324.

Jalkanen, J. P., L. Johansson and J. Kukkonen (2016). "A comprehensive inventory of ship traffic exhaust emissions in the European sea areas in 2011." Atmospheric Chemistry and Physics **16**(1): 71-84.

Jalkanen, J. P., L. Johansson, J. Kukkonen, A. Brink, J. Kalli and T. Stipa (2012). "Extension of an assessment model of ship traffic exhaust emissions for particulate matter and carbon monoxide." Atmospheric Chemistry and Physics **12**(5): 2641-2659.

Jayaram, V., H. Agrawal, W. A. Welch, J. W. Miller and D. R. Cocker, 3rd (2011). "Real-time gaseous, PM and ultrafine particle emissions from a modern marine engine operating on biodiesel." Environ Sci Technol **45**(6): 2286-2292.

Johansson, L., J. P. Jalkanen and J. Kukkonen (2017). "Global assessment of shipping emissions in 2015 on a high spatial and temporal resolution." Atmospheric Environment **167**(1): 403-415.

Jun, P., M. Gillenwater and W. Barbour (2001). CO_2, CH_4, and N_2O emissions from transportation-water-borne navigation: Good Practice Guidance and Uncertainty Management in National Greenhouse Gas Inventories. Publisher: Intergovernmental Panel on Climate Chage.

Kaiser, J. (2005). "EPIDEMIOLOGY: Mounting Evidence Indicts FineParticle Pollution." Science **307**(5717): 1858a–1861.

Kasper, A., S. Aufdenblatten, A. Forss, M. Mohr and H. Burtscher (2007). "Particulate emissions from a low-speed marine diesel engine." Aerosol Science and Technology **41**(1): 24-32.

Keeney, R. L. and H. Raiffa (1993). Decisions with multiple objectives: preference and value tradeoffs. Cambridge University Press.

Khair, M. K. and H. Jääskeläinen (2011). Emission Formation in Diesel Engines. Dieselnet technology guide, Ecopoint Inc.

Khan, M. Y., S. Ranganathan, H. Agrawal, W. A. Welch, C. Laroo, J. W. Miller and D. R. Cocker, 3rd (2013). "Measuring in-use ship emissions with international and U.S. federal methods." J Air Waste Manag Assoc **63**(3): 284-291.

Khaniabadi, Y. O., P. Sicard, A. M. Taiwo, A. De Marco, S. Esmaeili and R. Rashidi (2018). "Modeling of particulate matter dispersion from a cement plant: Upwind-downwind case study." Journal of Environmental Chemical Engineering **6**(2): 3104-3110.

Kilic, A. and C. Deniz (2010). "Inventory of Shipping Emissions in Izmit Gulf, Turkey." Environmental Progress & Sustainable Energy **29**(2): 221-232.

Kim, S., J. W. Hwang and C. S. Lee (2010). "Experiments and modeling on droplet motion and atomization of diesel and bio-diesel fuels in a cross-flowed air stream." International Journal of Heat and Fluid Flow **31**(4): 667-679.

Krewski, D. E. A. (2009). Extended follow-up and spatial analysis of the American Cancer Society study linking particulate air pollution and mortality. Boston, MA: Health Effects Institute.

Kristensen, H. O. (2010). Energy demand and exhaust gas emissions of marine engines. Technical University of Denmark.

Kruse, C., L. DeSANTIS, S. Eaton and R. Billings (2018). Marine Transportation and the Environment: Trends and Issues, TR News January-February 2018: Marine Transportation and the Environment.

Lack, D. A., C. D. Cappa, J. Langridge, R. Bahreini, G. Buffaloe, C. Brock, K. Cerully, D. Coffman, K. Hayden, J. Holloway, B. Lerner, P. Massoli, S. M. Li, R. McLaren, A. M. Middlebrook, R. Moore, A. Nenes, I. Nuaaman, T. B. Onasch, J. Peischl, A. Perring, P. K. Quinn, T. Ryerson, J. P. Schwartz, R. Spackman, S. C. Wofsy, D. Worsnop, B. Xiang and E. Williams (2011). "Impact of fuel quality regulation and speed reductions on shipping emissions: implications for climate and air quality." Environ Sci Technol **45**(20): 9052-9060.

Lee, H. and Y. Jeong (2012). "The effect of dynamic operating conditions on nano-particle emissions from a light-duty diesel engine applicable to prime and auxiliary machines on marine vessels." International Journal of Naval Architecture and Ocean Engineering **4**(4): 403-411.

Li, C., J. Borken-Kleefeld, J. Y. Zheng, Z. B. Yuan, J. M. Ou, Y. Li, Y. L. Wang and Y. Q. Xu (2018). "Decadal evolution of ship emissions in China from 2004 to 2013 by using an integrated AIS-based approach and projection to 2040." Atmospheric Chemistry and Physics **18**(8): 6075-6093.

Liu, H., M. L. Fu, X. X. Jin, Y. Shang, D. Shindell, G. Faluvegi, C. Shindell and K. B. He (2016). "Health and climate impacts of ocean-going vessels in East Asia." Nature Climate Change **6**(11): 1037-1041.

LIyods (1990). Marine Exhaust Emissions Research Programme: Steady State Operation (including Slow Speed Addendum).

LIyods (1993). Transient Emissions and Air Quality Impact Evaluation, Industry Research Report.

LIyods (1995). Marine Exhaust Emissions Research Programme. Publisher: Lloyd's Register Engineering Services.

Lonati, G., S. Cernuschi and S. Sidi (2010). "Air quality impact assessment of at-berth ship emissions: Case-study for the project of a new freight port." Sci Total Environ **409**(1): 192-200.

Lu, G., J. R. Brook, M. R. Alfarra, K. Anlauf, W. R. Leaitch, S. Sharma, D. Wang, D. R. Worsnop and L. Phinney (2006). "Identification and characterization of inland ship plumes over Vancouver, BC." Atmospheric Environment **40**(15): 2767-2782.

Lucialli, P., P. Ugolini and E. Pollini (2007). "Harbour of Ravenna: The contribution of harbour traffic to air quality." Atmospheric Environment **41**(30): 6421-6431.

Lyyranen, J., J. Jokiniemi, E. I. Kauppinen and J. Joutsensaari (1999). "Aerosol characterisation in medium-speed diesel engines operating with heavy fuel oils." Journal of Aerosol Science **30**(6): 771-784.

Marelle, L., J. L. Thomas, J. C. Raut, K. S. Law, J. P. Jalkanen, L. Johansson, A. Roiger, H. Schlager, J. Kim, A. Reiter and B. Weinzierl (2016). "Air quality and radiative impacts of Arctic shipping emissions in the summertime in northern Norway: from the local to the regional scale." Atmospheric Chemistry and Physics **16**(4): 2359-2379.

Matthias, V., I. Bewersdorff, A. Aulinger and M. Quante (2010). "The contribution of ship emissions to air pollution in the North Sea regions." Environ Pollut **158**(6): 2241-2250.

McKenzie, L. M., R. Z. Witter, L. S. Newman and J. L. Adgate (2012). "Human health risk assessment of air emissions from development of unconventional natural gas resources." Sci Total Environ **424**(1): 79-87.

Mcleod, A. R. and R. A. Skeffington (1995). "The Liphook Forest Fumigation Project – an overview. ." Plant, cell and environment **18**(3): 327-336.

Merico, E., A. Gambaro, A. Argiriou, A. Alebic-Juretic, E. Barbaro, D. Cesari, L. Chasapidis, S. Dimopoulos, A. Dinoi, A. Donateo, C. Giannaros, E. Gregoris, A. Karagiannidis, A. G. Konstandopoulos, T. Ivosevic, N. Liora, D. Melas, B. Mifka, I. Orlic, A. Poupkou, K. Sarovic, A. Tsakis, R. Giua, T. Pastore, A. Nocioni and D. Contini (2017). "Atmospheric impact of ship traffic in four Adriatic-Ionian port-cities: Comparison and harmonization of different approaches." Transportation Research Part D-Transport and Environment **50**(1): 431-445.

Merk, O. (2014). Shipping Emissions in Ports. International Transport Forum Discussion Papers. No. 2014/20, OECD Publishing. Paris, France.

Miola, A. and B. Ciuffo (2011). "Estimating air emissions from ships: Meta-analysis of modelling approaches and available data sources." Atmospheric Environment **45**(13): 2242-2251.

Moldanova, J., E. Fridell, H. Winnes, S. Holmin-Fridell, J. Boman, A. Jedynska, V. Tishkova, B. Demirdjian, S. Joulie, H. Bladt, N. P. Ivleva and R. Niessner (2013). "Physical and chemical characterisation of PM emissions from two ships operating in European Emission Control Areas." Atmospheric Measurement Techniques **6**(12): 3577-3596.

Moreno-Gutierrez, J., F. Calderay, N. Saborido, M. Boile, R. R. Valero and V. Duran-Grados (2015). "Methodologies for estimating shipping emissions and energy consumption: A comparative analysis of current methods." Energy **86**(1): 603-616.

Mueller, L., G. Jakobi, H. Czech, B. Stengel, J. Orasche, J. M. Arteaga-Salas, E. Karg, M. Elsasser, O. Sippula, T. Streibel, J. G. Slowik, A. S. H. Prevot, J. Jokiniemi, R. Rabe, H. Harndorf, B. Michalke, J. Schnelle-Kreis and R. Zimmermann (2015). "Characteristics and temporal evolution of particulate emissions from a ship diesel engine." Applied Energy **155**(1): 204-217.

Nel, A. (2005). "ATMOSPHERE: Enhanced: Air Pollution-Related Illness: Effects of Particles." Science **308**(5723): 804-806.

Nikolova, N. D., K. Hirota, C. Kobashikawa and K. Tenekedjiev (2006). "Elicitation of non-monotonic preferences of a fuzzy rational decision maker." Information Technologies and Control **1**(36-50).

Nikolova, N. D., D. Toneva-Zheynova, D. Naydenov and K. I. Tenekedjiev (2012). Imputing missing values of environmental multi-dimensional vectors using a modified Roweis algorithm IFAC Workshop on Dynamics and Control in Agriculture and Food Processing, 3-16 June, Plovdiv, Bulgaria**:** 199-205.

NOAA. (2017). "GSHH—a global self-consistent, hierarchical, high-resolution geography database." Publisher: National Centers for Environmental Information.

NSWEPA (2005). Approved methods for the modelling and assessment of air pollutants in New South Wales. Publisher: State of NSW and Environment Protection Authority.

NSWEPA (2017). Approved Methods for the Modelling and Assessment of Air Pollutants in New South Wales. Publisher: State of NSW and Environment Protection Authority.

Olesen, H. R., M. Winther, T. Ellermann, J. Christensen and M. Plejdrup (2009). Ship Emissions and air pollution in Denmark (NERI). Publisher: Danish Ministry of the Environment. Environmental Protection Agency.

Olivié, D. J. J., D. Cariolle, H. Teyssèdre, D. Salas, A. Voldoire, H. Clark and D. Saint-Martin (2012). "Modeling the climate impact of road transport, maritime shipping and aviation over the period 1860–2100 with an AOGCM." Atmos. Chem. Phys., **12**(3): 1449-1480.

Ostro, B. D. (1987). "Air-Pollution and Morbidity Revisited - a Specification Test." Journal of Environmental Economics and Management **14**(1): 87-98.

Ostro, B. D. and S. Rothschild (1989). "Air pollution and acute respiratory morbidity: an observational study of multiple pollutants." Environ Res **50**(2): 238-247.

Pacific Environment (2017). Port of Brisbae $PM_{2.5}$ Air Quality Modelling. Document Control Number: AQU-QD-004-21193. Publisher: Pacific Environment Limited.

Pérez, N. and J. Pey (2011). APICE Intensive Air Pollution Monitoring Campaign at the Port of Barcelona.
http://www.apice-project.eu/img_web/pagine/files/%20Long%20monitoring%20campaign%20APICE.pdf.

Peters, A., D. W. Dockery, J. E. Muller and M. A. Mittleman (2001). "Increased particulate air pollution and the triggering of myocardial infarction." Circulation **103**(23): 2810-2815.

Petzold, A., P. Feldpausch, L. Fritzsche, A. Minikin, P. Lauer and H. Bauer (2004). Particle emissions from ship engines. European Aerosol Conference . 78-82. June 26 to 29, 2006, Oxford, UK.

Petzold, A., J. Hasselbach, P. Lauer, R. Baumann, K. Franke, C. Gurk, H. Schlager and E. Weingartner (2008). "Experimental studies on particle emissions from cruising ship, their characteristic properties, transformation and atmospheric lifetime in the marine boundary layer." Atmospheric Chemistry and Physics **8**(9): 2387-2403.

Pope, C. A., 3rd, R. T. Burnett, M. J. Thun, E. E. Calle, D. Krewski, K. Ito and G. D. Thurston (2002). "Lung cancer, cardiopulmonary mortality, and long-term exposure to fine particulate air pollution." JAMA **287**(9): 1132-1141.

Pope, C. A., M. J. Thun, M. M. Namboodiri, D. W. Dockery, J. S. Evans, F. E. Speizer and C. W. Heath (1995). "Particulate Air-Pollution as a Predictor of Mortality in a Prospective-Study of Us Adults." American Journal of Respiratory and Critical Care Medicine **151**(3): 669-674.

Poplawski, K., E. Setton, B. McEwen, D. Hrebenyk, M. Graham and P. Keller (2011). "Impact of cruise ship emissions in Victoria, BC, Canada." Atmospheric Environment **45**(4): 824-833.

Port of Brisbane (2015). Shipping Handbook.
https://www.portbris.com.au/getmedia/084724b5-e515-45f7-b00b-898e8f0d8d65/POB-1499-Shipping-handbook-2015-WEB.pdf.

Radischat, C., O. Sippula, B. Stengel, S. Klingbeil, M. Sklorz, R. Rabe, T. Streibel, H. Harndorf and R. Zimmermann (2015). "Real-time analysis of organic compounds in ship engine aerosol emissions using resonance-enhanced multiphoton ionisation and proton transfer mass spectrometry." Anal Bioanal Chem **407**(20): 5939-5951.

Raizenne, M., L. M. Neas, A. I. Damokosh, D. W. Dockery, J. D. Spengler, P. Koutrakis, J. H. Ware and F. E. Speizer (1996). "Health effects of acid aerosols on North American children: pulmonary function." Environ Health Perspect **104**(5): 506-514.

Rakopoulos, C. D. and E. G. Giakoumis (2009). Diesel engine transient operation: Principles of operation and simulation analysis. Publisher: Springer. ISBN 978-1-84882-375-4.

Reda, A. A., J. Schnelle-Kreis, J. Orasche, G. Abbaszade, J. Lintelmann, J. M. Arteaga-Salas, B. Stengel, R. Rabe, H. Harndorf, O. Sippula, T. Streibel and R. Zimmermann (2015). "Gas phase carbonyl compounds in ship emissions: Differences between diesel fuel and heavy fuel oil operation (vol 94, pg 467, 2014)." Atmospheric Environment **94**(1): 467-478.

Ring, A. M., T. P. Canty, D. C. Anderson, T. P. Vinciguerra, H. He, D. L. Goldberg, S. H. Ehrman, R. R. Dickerson and R. J. Salawitch (2018). "Evaluating commercial marine emissions and their role in air quality policy using observations and the CMAQ model." Atmospheric Environment **173**(1): 96-107.

Ristovski, Z. D., B. Miljevic, N. C. Surawski, L. Morawska, K. M. Fong, F. Goh and I. A. Yang (2012). "Respiratory health effects of diesel particulate matter." Respirology **17**(2): 201-212.

Roberts, A., R. Brooks and P. Shipway (2014). "Internal combustion engine cold-start efficiency: A review of the problem, causes and potential solutions." Energy Conversion and Management **82**(1): 327-350.

Russo, M. A., J. Leitao, C. Gama, J. Ferreira and A. Monteiro (2018). "Shipping emissions over Europe: A state-of-the-art and comparative analysis." Atmospheric Environment **177**(1): 187-194.

Saxe, H. and T. Larsen (2004). "Air pollution from ships in three Danish ports Atmospheric Environment." Atmospheric Environment **38**(24): 4057-4067.

Schrooten, L., I. De Vlieger, L. I. Panis, C. Chiffi and E. Pastori (2009). "Emissions of maritime transport: a European reference system." Sci Total Environ **408**(2): 318-323.

Schwartz, J. (1993). "Air pollution and daily mortality in Birmingham, Alabama." Am J Epidemiol **137**(10): 1136-1147.

Schwartz, J. and L. M. Neas (2000). "Fine particles are more strongly associated than coarse particles with acute respiratory health effects in schoolchildren." Epidemiology **11**(1): 6-10.

Scire, J. S., D. G. Strimaitis and R. J. Yamartino (2000). A user's guide for the CALPUFF dispersion model. Publisher: Earth Tech.

Siddiqui, A., M. Verma and V. Verter (2018). "An integrated framework for inventory management and transportation of refined petroleum products: Pipeline or marine?" Applied Mathematical Modelling **55**(1): 224-247.

Simpson, R., G. Williams, A. Petroeschevsky, T. Best, G. Morgan, L. Denison, A. Hinwood, G. Neville and A. Neller (2005). "The short-term effects of air pollution on daily mortality in four Australian cities." Aust N Z J Public Health **29**(3): 205-212.

Sinha, P., P. V. Hobbs, R. J. Yokelson, I. T. Bertschi, D. R. Blake, I. J. Simpson, S. Gao, T. W. Kirchstetter and T. Novakov (2003). "Emissions of trace gases and particles from savanna fires in southern Africa." Journal of Geophysical Research-Atmospheres **108**(D13): 1-32.

Sippula, O., B. Stengel, M. Sklorz, T. Streibel, R. Rabe, J. Orasche, J. Lintelmann, B. Michalke, G. Abbaszade, C. Radischat, T. Groger, J. Schnelle-Kreis, H. Harndorf and R. Zimmermann (2014). "Particle emissions from a marine engine: chemical composition and aromatic emission profiles under various operating conditions." Environ Sci Technol **48**(19): 11721-11729.

Skjølsvik, K. O., A. B. Andersen, J. J. Corbett and J. M. Skjelvik (2000). Study of greenhouse gas emissions from ships (report to International Maritime Organization on the outcome of the IMO Study on Greenhouse Gas Emissions from Ships). M. S. G. C. M. U. MEPC 45/8, Center for Economic Analysis/Det Norske Veritas, Trondheim, Norway.

Standards Australia (2009). Australia/New Zealand Standard. Risk management. Principles and guidelines AS/NZS ISO 31000:2009.

Port of Long Beach inventory of air emissions inventory (2005). Publisher: Starcrest Consulting Group.

Streets, D. G., T. C. Bond, G. R. Carmichael, S. D. Fernandes, Q. Fu, D. He, Z. Klimont, S. M. Nelson, N. Y. Tsai, M. Q. Wang, J. H. Woo and K. F. Yarber (2003). "An inventory of gaseous and primary aerosol emissions in Asia in the year 2000." Journal of Geophysical Research-Atmospheres **108**(D21).

Teggi, S., S. Costanzini, G. Ghermandi, C. Malagoli and M. Vinceti (2018). "A GIS-based atmospheric dispersion model for pollutants emitted by complex source areas." Sci Total Environ **610-611**(1): 175-190.

Trozzi, C. and R. DeLauretis (2013). International navigation, national navigation, national fishing. Publisher: EMEP/EEA air pollutant emission inventory guidebook.

Unctad (2014). Review of Maritime Transport, United Nations Conference on Trade and Development. United Nations Conference on Trade and Development. Publisher: United Nations.

USEPA (2000). Analysis of Commercial Marine Vessels Emissions and Fuel Consumption Data. Washington, DC US Environmental Protection Agency.

USEPA (2004). Control of Emissions of Air Pollution from Nonroad Diesel Engines and Fuel. Final Rule. Publisher: United States Environmental Protection Agency.

USEPA (2006). Regulatory impact analysis national ambient air quality standards for particle pollution. North Carolina: Research Triangle Park.

USEPA (2008). Inventory of US Greenhouse Gas Emissions and Sinks: 1990 - 2006. Publisher: United States Environmental Protection Agency.

USEPA (2009). Current Methodologies in Preparing Mobile Source Port-related Emission Inventories. Final Report. http://www.epa.gov/cleandiesel/documents/ports-emission-inv-april09.pdf.

USEPA (2010). Final regulatory impact analysis (RIA) for the NO2 National Ambient Air Quality Standards (NAAQS). NC. USA: Office of Air Quality Planning and Standards USEPA.

USEPA (2010). Quantitative health risk assessment for particulate matter. Publisher: United States Environmental Protection Agency.

USGS. (2017). "Shuttle radar topography mission (SRTM) 1 Arc-second global. USGS." United States Geological Survey.

Van de geijn, S. C. (1993). Problems and approaches to integrating the concurrent impacts of elevated CO_2, temperature, UVb radiation and O_3 on crop production. Crop Science of America. Chapter in a scientif book. Pages 333-338. Publisher: Theoretical Production Ecology.

Van der Gon, H. D., Tno. and J. Hulskotte (2010). Methodologies for estimating shipping emissions in Netherlands (EMS). Publisher: Netherlands Environmental Assessment Agency.

Viana, M., P. Hammingh, A. Colette, X. Querol, B. Degraeuwe, I. de Vlieger and J. van Aardenne (2014). "Impact of maritime transport emissions on coastal air quality in Europe." Atmospheric Environment **90**(1): 96-105.

Wang, C., J. J. Corbett and J. Firestone (2008). "Improving spatial representation of global ship emissions inventories." Environ Sci Technol **42**(1): 193-199.

Wang, C. F., J. J. Corbett and J. Firestone (2007). "Modeling energy use and emissions from North American shipping: Application of the ship traffic, energy, and environment model." Environmental Science & Technology **41**(9): 3226-3232.

Whall, C., D. Cooper, K. Archer, L. Twigger, N. Thurston, D. Ockwell, A. McIntyre and A. Ritchie (2002). Quantification of Emissions from Ships Associated with Ship Movements between Ports in the European Community. Final report for European Commission by ENTEC UK Limited.

Whall, C., T. Scarbrough, A. Stavrakaki, C. Green, J. Squire and R. Noden (2010). UK Ship Emission Inventory. London, UK Entec UK Limited.

WHO (1987). Air quality guidelines for Europe, WHO Regional Publications.

WHO (2000). Air quality guidelines for Europe, World Health Organisation Regional Publications.

WHO (2004). Health aspects of air pollution Results from the WHO project: systematic review of health aspects of air pollution in Europe. Copenhagen, Denmark.

Williams, G. E. A. (2012). Australian Child Health and Air Pollution Study (ACHAPS) final report. . University of Queensland: National Environment Protection Council.

Winnes, H. and E. Fridell (2009). "Particle emissions from ships: dependence on fuel type." J Air Waste Manag Assoc **59**(12): 1391-1398.

Winnes, H., L. Styhre and E. Fridell (2015). "Reducing GHG emissions from ships in port areas." Research in Transportation Business and Management **17**(1): 73-82.

Woodruff, T. J., J. Grillo and K. C. Schoendorf (1997). "The relationship between selected causes of postneonatal infant mortality and particulate air pollution in the United States." Environmental Health Perspectives **105**(6): 608-612.

Wright, A. (1997). "Marine Diesel Engine Particulate Emissions." Trans IMarE **109**(4): 345–364.

Zadakbar, O., R. Abbassi, F. Khan, K. Karimpour, M. Golshani and A. Vatani (2011). "Risk Analysis of Flare Flame-out Condition in a Gas Process Facility." Oil & Gas Science and Technology-Revue D Ifp Energies Nouvelles **66**(3): 521-530.

Zanobetti, A. and J. Schwartz (2009). "The effect of fine and coarse particulate air pollution on mortality: a national analysis." Environ Health Perspect **117**(6): 898-903.

Zeng, Q., E. Jeppesen, X. Gu, Z. Mao and H. Chen (2018). "Distribution, fate and risk assessment of PAHs in water and sediments from an aquaculture- and shipping-impacted subtropical lake, China." Chemosphere **201**(1): 612-620.

Zhang, J. J., J. Hodgson and E. Erkut (2000). "Using GIS to assess the risks of hazardous materials transport in networks." European Journal of Operational Research **121**(2): 316-329.

Zheng, J. Y., L. J. Zhang, W. W. Che, Z. Y. Zheng and S. S. Yin (2009). "A highly resolved temporal and spatial air pollutant emission inventory for the Pearl River Delta region, China and its uncertainty assessment." Atmospheric Environment **43**(32): 5112-5122.

Zhong, Z., J. Zheng, M. Zhu, Z. Huang, Z. Zhang, G. Jia, X. Wang, Y. Bian, Y. Wang and N. Li (2018). "Recent developments of anthropogenic air pollutant emission inventories in Guangdong province, China." Sci Total Environ **627**(1): 1080-1092.

Zmirou, D., J. Schwartz, M. Saez, A. Zanobetti, B. Wojtyniak, G. Touloumi, C. Spix, A. Ponce de Leon, Y. Le Moullec, L. Bacharova, J. Schouten, A. Ponka and K. Katsouyanni (1998). "Time-series analysis of air pollution and cause-specific mortality." Epidemiology **9**(5): 495-503.

Appendix A: Supplementary Data

- ## On-board measurement dataset

  This section explains the data processing of emissions applied i.e. SO_x, NO_x, CO_2, CO, HC and PM in different Auxiliary and Main Engines, in different shipping operation, and how mathematically they have been converted from the emission rates to the emissions in grams or kilograms.

```
function [total_E_v,final_EF_v,ave_SS_v,ave_SP_v,LFproc_v,AC_v,EMFR_v,SOC_v,Time_tot_v,N_v]=AEcalc_BE
    % AE at berth
    % constants
    R=8.3144598;              % in(kg.m^2)/(K.mol.s^2)
    T=309;                    % in K
    Patm=101325;              % in Pascals
    AirDens=1.225;            % in kg/m^3
    ACb=4968;                 % in kg/hour
    HOC=67.84;                % in kg/hour
    instSP=460;               % kW
    deltt=1/3600;             % in hours
    MolMass_NOx=46.01;        % in g/mol
    MolMass_SOx=64.066;       % in g/mol
    MolMass_CO2=44.01;        % in g/mol
    MolMass_CO=28.01;         % in g/mol
    % input data
    in_mat_file_name='data/At_Berth_AE';
    load(in_mat_file_name,'Date_Time_c','time_er_v','SS_er_v','SP_er_v','NOx_er_v','SOx_er_v','CO2_er_v','CO_er_v');
    disp(' ')
    disp('AE at Berth')
    disp(' ');
    % data processing NOx
    i_v=~isnan(NOx_er_v);
    Date_Time_NOx_c=Date_Time_c(i_v); %#ok<NASGU>
    time_NOx_v=time_er_v(i_v); %#ok<NASGU>
    SS_NOx_v=SS_er_v(i_v);
    SP_NOx_v=SP_er_v(i_v);
    ER_NOx_v=NOx_er_v(i_v);
    N_NOx=sum(i_v);
    Time_tot_NOx=N_NOx*deltt;   % in hours
    ave_SP_NOx=mean(abs(SP_NOx_v));
    ave_SS_NOx=mean(abs(SS_NOx_v));
    LFproc_NOx=100*ave_SP_NOx/instSP;
    [AC_NOx,SOC_NOx,EMFR_NOx] = CalcEMFR(ACb,LFproc_NOx,ave_SP_NOx,HOC);
    EF_NOx_v=ER_NOx_v*1e-6*Patm*EMFR_NOx/AirDens/R/T*MolMass_NOx./SP_NOx_v;
    ave_EF_NOx=mean(EF_NOx_v);
    E_NOx_v=EF_NOx_v.*SP_NOx_v*deltt/1000;
    total_E_NOx=sum(E_NOx_v);
    final_EF_NOx=total_E_NOx/Time_tot_NOx/ave_SP_NOx*1000;
    disp(' ');
    disp('NOx for AE at Berth')
    fprintf(1,'average  EF_NOx (g/kWh)=%.4f\n',ave_EF_NOx);
    fprintf(1,'total  E_NOx (kg)=%.5f\n',total_E_NOx);
    fprintf(1,'final  EF_NOx (g/kWh)=%.4f\n',final_EF_NOx);
    fprintf(1,'avarage  SS_NOx (RPM)=%7.3f\n',ave_SS_NOx);
    fprintf(1,'avarage  SP_NOx (kW)=%.3f\n',ave_SP_NOx);
    fprintf(1,'avarage  LF (%%)=%.3f\n',LFproc_NOx);
    fprintf(1,'avarage  AC_NOx (kg/hour)=%7.3f\n',AC_NOx);
    fprintf(1,'avarage  EMFR_NOx (kg/hour)=%7.3f\n',EMFR_NOx);
    fprintf(1,'avarage  SOC_NOx (g/kWh)=%7.3f\n',SOC_NOx);
    fprintf(1,'total time Time_tot_NOx (hour)=%8.5f\n',Time_tot_NOx);
    fprintf(1,'count of samples N_NOx (-)=%i\n',N_NOx);
    % data processing SOx
    i_v=~isnan(SOx_er_v);
    Date_Time_SOx_c=Date_Time_c(i_v); %#ok<NASGU>
```

NO_x emissions for auxiliary engines at berth

```
time_SOx_v=time_er_v(i_v); %#ok<NASGU>
SS_SOx_v=SS_er_v(i_v);
SP_SOx_v=SP_er_v(i_v);
ER_SOx_v=SOx_er_v(i_v);
N_SOx=sum(i_v);
Time_tot_SOx=N_SOx*deltt;    % in hours
ave_SP_SOx=mean(abs(SP_SOx_v));
ave_SS_SOx=mean(abs(SS_SOx_v));
LFproc_SOx=100*ave_SP_SOx/instSP;
[AC_SOx,SOC_SOx,EMFR_SOx] = CalcEMFR(ACb,LFproc_SOx,ave_SP_SOx,HOC);
EF_SOx_v=ER_SOx_v*1e-6*Patm*EMFR_SOx/AirDens/R/T*MolMass_SOx./SP_SOx_v;
ave_EF_SOx=mean(EF_SOx_v);
E_SOx_v=EF_SOx_v.*SP_SOx_v*deltt/1000;
total_E_SOx=sum(E_SOx_v);
final_EF_SOx=total_E_SOx/Time_tot_SOx/ave_SP_SOx*1000;
disp(' ');
disp('SOx for AE at Berth')
fprintf(1,'average  EF_SOx (g/kWh)=%.4f\n',ave_EF_SOx);
fprintf(1,'total  E_SOx (kg)=%.5f\n',total_E_SOx);
fprintf(1,'final  EF_SOx (g/kWh)=%.4f\n',final_EF_SOx);
fprintf(1,'avarage  SS_SOx (RPM)=%7.3f\n',ave_SS_SOx);
fprintf(1,'avarage  SP_SOx (kW)=%.3f\n',ave_SP_SOx);
fprintf(1,'avarage  LF (%%)=%.3f\n',LFproc_SOx);
fprintf(1,'avarage  AC_SOx (kg/hour)=%7.3f\n',AC_SOx);
fprintf(1,'avarage  EMFR_SOx (kg/hour)=%7.3f\n',EMFR_SOx);
fprintf(1,'avarage  SOC_SOx (g/kWh)=%7.3f\n',SOC_SOx);
fprintf(1,'total time Time_tot_SOx (hour)=%8.5f\n',Time_tot_SOx);
fprintf(1,'count of samples N_SOx (-)=%i\n',N_SOx);
% data processing CO2
i_v=~isnan(CO2_er_v);
Date_Time_CO2_c=Date_Time_c(i_v); %#ok<NASGU>
time_CO2_v=time_er_v(i_v); %#ok<NASGU>
SS_CO2_v=SS_er_v(i_v);
SP_CO2_v=SP_er_v(i_v);
ER_CO2_v=CO2_er_v(i_v);
N_CO2=sum(i_v);
Time_tot_CO2=N_CO2*deltt;    % in hours
ave_SP_CO2=mean(abs(SP_CO2_v));
ave_SS_CO2=mean(abs(SS_CO2_v));
LFproc_CO2=100*ave_SP_CO2/instSP;
[AC_CO2,SOC_CO2,EMFR_CO2] = CalcEMFR(ACb,LFproc_CO2,ave_SP_CO2,HOC);
EF_CO2_v=ER_CO2_v*1e-2*Patm*EMFR_CO2/AirDens/R/T*MolMass_CO2./SP_CO2_v;
ave_EF_CO2=mean(EF_CO2_v);
E_CO2_v=EF_CO2_v.*SP_CO2_v*deltt/1000;
total_E_CO2=sum(E_CO2_v);
final_EF_CO2=total_E_CO2/Time_tot_CO2/ave_SP_CO2*1000;
disp(' ');
disp('CO2 for AE at Berth')
fprintf(1,'average  EF_CO2 (g/kWh)=%.4f\n',ave_EF_CO2);
fprintf(1,'total  E_CO2 (kg)=%.5f\n',total_E_CO2);
fprintf(1,'final  EF_CO2 (g/kWh)=%.4f\n',final_EF_CO2);
fprintf(1,'avarage  SS_CO2 (RPM)=%7.3f\n',ave_SS_CO2);
fprintf(1,'avarage  SP_CO2 (kW)=%.3f\n',ave_SP_CO2);
fprintf(1,'avarage  LF (%%)=%.3f\n',LFproc_CO2);
fprintf(1,'avarage  AC_CO2 (kg/hour)=%7.3f\n',AC_CO2);
```

SO_x and CO_2 emissions for auxiliary engines at berth

```
fprintf(1,'avarage  EMFR_CO2 (kg/hour)=%7.3f\n',EMFR_CO2);
fprintf(1,'avarage  SOC_CO2 (g/kWh)=%7.3f\n',SOC_CO2);
fprintf(1,'total time Time_tot_CO2 (hour)=%8.5f\n',Time_tot_CO2);
fprintf(1,'count of samples N_CO2 (-)=%i\n',N_CO2);
% data processing CO
i_v=~isnan(CO_er_v);
Date_Time_CO_c=Date_Time_c(i_v); %#ok<NASGU>
time_CO_v=time_er_v(i_v); %#ok<NASGU>
SS_CO_v=SS_er_v(i_v);
SP_CO_v=SP_er_v(i_v);
ER_CO_v=CO_er_v(i_v);
N_CO=sum(i_v);
Time_tot_CO=N_CO*deltt;   % in hours
ave_SP_CO=mean(abs(SP_CO_v));
ave_SS_CO=mean(abs(SS_CO_v));
LFproc_CO=100*ave_SP_CO/instSP;
[AC_CO,SOC_CO,EMFR_CO] = CalcEMFR(ACb,LFproc_CO,ave_SP_CO,HOC);
EF_CO_v=ER_CO_v*1e-6*Patm*EMFR_CO/AirDens/R/T*MolMass_CO./SP_CO_v;
ave_EF_CO=mean(EF_CO_v);
E_CO_v=EF_CO_v.*SP_CO_v*deltt/1000;
total_E_CO=sum(E_CO_v);
final_EF_CO=total_E_CO/Time_tot_CO/ave_SP_CO*1000;
disp(' ');
disp('CO for AE at Berth')
fprintf(1,'average  EF_CO (g/kWh)=%.4f\n',ave_EF_CO);
fprintf(1,'total  E_CO (kg)=%.5f\n',total_E_CO);
fprintf(1,'final  EF_CO (g/kWh)=%.4f\n',final_EF_CO);
fprintf(1,'avarage  SS_CO (RPM)=%7.3f\n',ave_SS_CO);
fprintf(1,'avarage  SP_CO (kW)=%.3f\n',ave_SP_CO);
fprintf(1,'avarage  LF (%%)=%.3f\n',LFproc_CO);
fprintf(1,'avarage  AC_CO (kg/hour)=%7.3f\n',AC_CO);
fprintf(1,'avarage  EMFR_CO (kg/hour)=%7.3f\n',EMFR_CO);
fprintf(1,'avarage  SOC_CO (g/kWh)=%7.3f\n',SOC_CO);
fprintf(1,'total time Time_tot_CO (hour)=%8.5f\n',Time_tot_CO);
fprintf(1,'count of samples N_CO (-)=%i\n',N_CO);
% output
total_E_v=[total_E_NOx total_E_SOx total_E_CO2 total_E_CO];
final_EF_v=[final_EF_NOx final_EF_SOx final_EF_CO2 final_EF_CO];
ave_SS_v=[ave_SS_NOx ave_SS_SOx ave_SS_CO2 ave_SS_CO];
ave_SP_v=[ave_SP_NOx ave_SP_SOx ave_SP_CO2 ave_SP_CO];
LFproc_v=[LFproc_NOx LFproc_SOx LFproc_CO2 LFproc_CO];
AC_v=[AC_NOx AC_SOx AC_CO2 AC_CO];
EMFR_v=[EMFR_NOx EMFR_SOx EMFR_CO2 EMFR_CO];
SOC_v=[SOC_NOx SOC_SOx SOC_CO2 SOC_CO];
Time_tot_v=[Time_tot_NOx Time_tot_SOx Time_tot_CO2 Time_tot_CO];
N_v=[N_NOx N_SOx N_CO2 N_CO];
out_mat_file_name='data/EF_At_Berth_AE';
save(out_mat_file_name...
    ,'Date_Time_NOx_c','time_NOx_v','SS_NOx_v','SP_NOx_v','ER_NOx_v','EF_NOx_v','E_NOx_v'...
    ,'total_E_NOx','final_EF_NOx','ave_SS_NOx','ave_SP_NOx','LFproc_NOx','AC_NOx','EMFR_NOx','SOC_NOx','Time_tot_NOx','N_NOx'...
    ,'Date_Time_SOx_c','time_SOx_v','SS_SOx_v','SP_SOx_v','ER_SOx_v','EF_SOx_v','E_SOx_v'...
    ,'total_E_SOx','final_EF_SOx','ave_SS_SOx','ave_SP_SOx','LFproc_SOx','AC_SOx','EMFR_SOx','SOC_SOx','Time_tot_SOx','N_SOx'...
    ,'Date_Time_CO2_c','time_CO2_v','SS_CO2_v','SP_CO2_v','ER_CO2_v','EF_CO2_v','E_CO2_v'...
    ,'total_E_CO2','final_EF_CO2','ave_SS_CO2','ave_SP_CO2','LFproc_CO2','AC_CO2','EMFR_CO2','SOC_CO2','Time_tot_CO2','N_CO2'...
    ,'Date_Time_CO_c','time_CO_v','SS_CO_v','SP_CO_v','ER_CO_v','EF_CO_v','E_CO_v'...
    ,'total_E_CO','final_EF_CO','ave_SS_CO','ave_SP_CO','LFproc_CO','AC_CO','EMFR_CO','SOC_CO','Time_tot_CO','N_CO');
```

CO_2 and CO emissions for auxiliary engines at berth

101.00	11:07:12	3-11-2015 11:07:12 AM	900.000	265.000	2.000	21.000
102.00	11:07:13	3-11-2015 11:07:13 AM	900.000	265.000	2.000	21.000
103.00	11:07:14	3-11-2015 11:07:14 AM	900.000	265.000	2.000	21.000
104.00	11:07:15	3-11-2015 11:07:15 AM	900.000	265.000	1.000	21.000
105.00	11:07:16	3-11-2015 11:07:16 AM	900.000	265.000	1.000	21.000
106.00	11:07:17	3-11-2015 11:07:17 AM	900.000	265.000	1.000	21.000
107.00	11:07:18	3-11-2015 11:07:18 AM	900.000	265.000	1.000	21.000
108.00	11:07:19	3-11-2015 11:07:19 AM	900.000	265.000	1.000	21.000
109.00	11:07:20	3-11-2015 11:07:20 AM	900.000	265.000	2.000	21.000
110.00	11:07:21	3-11-2015 11:07:21 AM	900.000	265.000	2.000	21.000
111.00	11:07:22	3-11-2015 11:07:22 AM	900.000	265.000	2.000	21.000
112.00	11:07:23	3-11-2015 11:07:23 AM	900.000	265.000	2.000	21.000
113.00	11:07:24	3-11-2015 11:07:24 AM	900.000	265.000	2.000	21.000
114.00	11:07:25	3-11-2015 11:07:25 AM	900.000	265.000	46.000	27.000
115.00	11:07:26	3-11-2015 11:07:26 AM	900.000	265.000	46.000	27.000
116.00	11:07:27	3-11-2015 11:07:27 AM	900.000	265.000	321.000	207.000
117.00	11:07:28	3-11-2015 11:07:28 AM	900.000	265.000	321.000	207.000
118.00	11:07:29	3-11-2015 11:07:29 AM	900.000	265.000	498.000	715.000
119.00	11:07:30	3-11-2015 11:07:30 AM	900.000	265.000	498.000	715.000
120.00	11:07:31	3-11-2015 11:07:31 AM	900.000	265.000	498.000	715.000
121.00	11:07:32	3-11-2015 11:07:32 AM	900.000	265.000	-++++-	1298.000
122.00	11:07:33	3-11-2015 11:07:33 AM	900.000	265.000	-++++-	1298.000
123.00	11:07:34	3-11-2015 11:07:34 AM	900.000	265.000	-++++-	1586.000
124.00	11:07:35	3-11-2015 11:07:35 AM	900.000	265.000	-++++-	1586.000
125.00	11:07:36	3-11-2015 11:07:36 AM	900.000	265.000	-++++-	1586.000
126.00	11:07:37	3-11-2015 11:07:37 AM	900.000	265.000	-++++-	1305.000
127.00	11:07:38	3-11-2015 11:07:38 AM	900.000	265.000	-++++-	1305.000
128.00	11:07:39	3-11-2015 11:07:39 AM	900.000	265.000	-++++-	1305.000
129.00	11:07:40	3-11-2015 11:07:40 AM	900.000	265.000	-++++-	1305.000
130.00	11:07:41	3-11-2015 11:07:41 AM	900.000	265.000	227.000	1513.000
131.00	11:07:42	3-11-2015 11:07:42 AM	900.000	265.000	172.000	1050.000
132.00	11:07:43	3-11-2015 11:07:43 AM	900.000	265.000	172.000	1050.000
133.00	11:07:44	3-11-2015 11:07:44 AM	900.000	265.000	161.000	1050.000
134.00	11:07:45	3-11-2015 11:07:45 AM	900.000	265.000	161.000	1050.000
135.00	11:07:46	3-11-2015 11:07:46 AM	900.000	265.000	161.000	0.000
136.00	11:07:47	3-11-2015 11:07:47 AM	900.000	265.000	161.000	0.000
137.00	11:07:48	3-11-2015 11:07:48 AM	900.000	265.000	154.000	1.000
138.00	11:07:49	3-11-2015 11:07:49 AM	900.000	265.000	154.000	1.000
139.00	11:07:50	3-11-2015 11:07:50 AM	900.000	265.000	154.000	1.000
140.00	11:07:51	3-11-2015 11:07:51 AM	900.000	265.000	149.000	184.000
141.00	11:07:52	3-11-2015 11:07:52 AM	900.000	265.000	152.000	325.000
142.00	11:07:53	3-11-2015 11:07:53 AM	900.000	265.000	152.000	325.000
143.00	11:07:54	3-11-2015 11:07:54 AM	900.000	265.000	152.000	325.000
144.00	11:07:55	3-11-2015 11:07:55 AM	900.000	265.000	152.000	325.000
145.00	11:07:56	3-11-2015 11:07:56 AM	900.000	265.000	157.000	425.000
146.00	11:07:57	3-11-2015 11:07:57 AM	900.000	265.000	157.000	425.000

Raw emission rates measured for the auxiliary engines at berth

```
function [total_E_v,final_EF_v,ave_SS_v,ave_SP_v,LFproc_v,AC_v,EMFR_v,SOC_v,Time_tot_v,N_v]=MEcalc_BE
    % ME at berth
    % constants
    R=8.3144598;              % in(kg.m^2)/(K.mol.s^2)
    T=309;                    % in K
    Patm=101325;              % in Pascals
    AirDens=1.225;            % in kg/m^3
    ACb=79200;                % in kg/hour
    SOCb=208.597;             % in g/kWh
    instSP=6880;              % kW
    deltt=1/3600;             % in hours
    MolMass_NOx=46.01;        % in g/mol
    MolMass_SOx=64.066;       % in g/mol
    MolMass_CO2=44.01;        % in g/mol
    MolMass_CO=28.01;         % in g/mol
    % input data
    in_mat_file_name='data/At_Berth_ME';
    load(in_mat_file_name,'Date_Time_c','time_er_v','SS_er_v','SP_er_v','NOx_er_v','SOx_er_v','CO2_er_v','CO_er_v');
    disp(' ')
    disp('ME at Berth')
    disp(' ');
    % data processing NOx
    i_v=~isnan(NOx_er_v);
    Date_Time_NOx_c=Date_Time_c(i_v); %#ok<NASGU>
    time_NOx_v=time_er_v(i_v); %#ok<NASGU>
    SS_NOx_v=SS_er_v(i_v);
    SP_NOx_v=SP_er_v(i_v);
    ER_NOx_v=NOx_er_v(i_v);
    N_NOx=sum(i_v);
    Time_tot_NOx=N_NOx*deltt;   % in hours
    ave_SP_NOx=mean(abs(SP_NOx_v));
    ave_SS_NOx=mean(abs(SS_NOx_v));
    LFproc_NOx=100*ave_SP_NOx/instSP;
    [AC_NOx,SOC_NOx,EMFR_NOx] = CalcEMFR(ACb,LFproc_NOx,ave_SP_NOx,[],SOCb);
    EF_NOx_v=ER_NOx_v*1e-6*Patm*EMFR_NOx/AirDens/R/T*MolMass_NOx./SP_NOx_v;
    ave_EF_NOx=mean(EF_NOx_v);
    E_NOx_v=EF_NOx_v.*SP_NOx_v*deltt/1000;
    total_E_NOx=sum(E_NOx_v);
    final_EF_NOx=total_E_NOx/Time_tot_NOx/ave_SP_NOx*1000;
    disp(' ');
    disp('NOx for ME at Berth')
    fprintf(1,'average  EF_NOx (g/kWh)=%.4f\n',ave_EF_NOx);
    fprintf(1,'total  E_NOx (kg)=%.5f\n',total_E_NOx);
    fprintf(1,'final  EF_NOx (g/kWh)=%.4f\n',final_EF_NOx);
    fprintf(1,'avarage  SS_NOx (RPM)=%7.3f\n',ave_SS_NOx);
    fprintf(1,'avarage  SP_NOx (kW)=%.3f\n',ave_SP_NOx);
    fprintf(1,'avarage  LF (%%)=%.3f\n',LFproc_NOx);
    fprintf(1,'avarage  AC_NOx (kg/hour)=%7.3f\n',AC_NOx);
    fprintf(1,'avarage  EMFR_NOx (kg/hour)=%7.3f\n',EMFR_NOx);
    fprintf(1,'avarage  SOC_NOx (g/kWh)=%7.3f\n',SOC_NOx);
    fprintf(1,'total time Time_tot_NOx (hour)=%8.5f\n',Time_tot_NOx);
    fprintf(1,'count of samples N_NOx (-)=%i\n',N_NOx);
    % data processing SOx
    i_v=~isnan(SOx_er_v);
    Date_Time_SOx_c=Date_Time_c(i_v); %#ok<NASGU>
    time_SOx_v=time_er_v(i_v); %#ok<NASGU>
    SS_SOx_v=SS_er_v(i_v);
    SP_SOx_v=SP_er_v(i_v);
```

NO_x emissions for main engines at berth

```
ER_SOx_v=SOx_er_v(i_v);
N_SOx=sum(i_v);
Time_tot_SOx=N_SOx*deltt;    % in hours
ave_SP_SOx=mean(abs(SP_SOx_v));
ave_SS_SOx=mean(abs(SS_SOx_v));
LFproc_SOx=100*ave_SP_SOx/instSP;
[AC_SOx,SOC_SOx,EMFR_SOx] = CalcEMFR(ACb,LFproc_SOx,ave_SP_SOx,[],SOCb);
EF_SOx_v=ER_SOx_v*1e-6*Patm*EMFR_SOx/AirDens/R/T*MolMass_SOx./SP_SOx_v;
ave_EF_SOx=mean(EF_SOx_v);
E_SOx_v=EF_SOx_v.*SP_SOx_v*deltt/1000;
total_E_SOx=sum(E_SOx_v);
final_EF_SOx=total_E_SOx/Time_tot_SOx/ave_SP_SOx*1000;
disp(' ');
disp('SOx for ME at Berth')
fprintf(1,'average  EF_SOx (g/kWh)=%.4f\n',ave_EF_SOx);
fprintf(1,'total  E_SOx (kg)=%.5f\n',total_E_SOx);
fprintf(1,'final  EF_SOx (g/kWh)=%.4f\n',final_EF_SOx);
fprintf(1,'avarage  SS_SOx (RPM)=%7.3f\n',ave_SS_SOx);
fprintf(1,'avarage  SP_SOx (kW)=%.3f\n',ave_SP_SOx);
fprintf(1,'avarage  LF (%%)=%.3f\n',LFproc_SOx);
fprintf(1,'avarage  AC_SOx (kg/hour)=%7.3f\n',AC_SOx);
fprintf(1,'avarage  EMFR_SOx (kg/hour)=%7.3f\n',EMFR_SOx);
fprintf(1,'avarage  SOC_SOx (g/kWh)=%7.3f\n',SOC_SOx);
fprintf(1,'total time Time_tot_SOx (hour)=%8.5f\n',Time_tot_SOx);
fprintf(1,'count of samples N_SOx (-)=%i\n',N_SOx);
% data processing CO2
i_v=~isnan(CO2_er_v);
Date_Time_CO2_c=Date_Time_c(i_v); %#ok<NASGU>
time_CO2_v=time_er_v(i_v); %#ok<NASGU>
SS_CO2_v=SS_er_v(i_v);
SP_CO2_v=SP_er_v(i_v);
ER_CO2_v=CO2_er_v(i_v);
N_CO2=sum(i_v);
Time_tot_CO2=N_CO2*deltt;    % in hours
ave_SP_CO2=mean(abs(SP_CO2_v));
ave_SS_CO2=mean(abs(SS_CO2_v));
LFproc_CO2=100*ave_SP_CO2/instSP;
[AC_CO2,SOC_CO2,EMFR_CO2] = CalcEMFR(ACb,LFproc_CO2,ave_SP_CO2,[],SOCb);
EF_CO2_v=ER_CO2_v*1e-2*Patm*EMFR_CO2/AirDens/R/T*MolMass_CO2./SP_CO2_v;
ave_EF_CO2=mean(EF_CO2_v);
E_CO2_v=EF_CO2_v.*SP_CO2_v*deltt/1000;
total_E_CO2=sum(E_CO2_v);
final_EF_CO2=total_E_CO2/Time_tot_CO2/ave_SP_CO2*1000;
disp(' ');
disp('CO2 for ME at Berth')
fprintf(1,'average  EF_CO2 (g/kWh)=%.4f\n',ave_EF_CO2);
fprintf(1,'total  E_CO2 (kg)=%.5f\n',total_E_CO2);
fprintf(1,'final  EF_CO2 (g/kWh)=%.4f\n',final_EF_CO2);
fprintf(1,'avarage  SS_CO2 (RPM)=%7.3f\n',ave_SS_CO2);
fprintf(1,'avarage  SP_CO2 (kW)=%.3f\n',ave_SP_CO2);
fprintf(1,'avarage  LF (%%)=%.3f\n',LFproc_CO2);
fprintf(1,'avarage  AC_CO2 (kg/hour)=%7.3f\n',AC_CO2);
fprintf(1,'avarage  EMFR_CO2 (kg/hour)=%7.3f\n',EMFR_CO2);
fprintf(1,'avarage  SOC_CO2 (g/kWh)=%7.3f\n',SOC_CO2);
fprintf(1,'total time Time_tot_CO2 (hour)=%8.5f\n',Time_tot_CO2);
fprintf(1,'count of samples N_CO2 (-)=%i\n',N_CO2);
% data processing CO
i_v=~isnan(CO_er_v);
Date_Time_CO_c=Date_Time_c(i_v); %#ok<NASGU>
```

SO_x and CO_2 emissions for main engines at berth

```
time_CO_v=time_er_v(i_v); %#ok<NASGU>
SS_CO_v=SS_er_v(i_v);
SP_CO_v=SP_er_v(i_v);
ER_CO_v=CO_er_v(i_v);
N_CO=sum(i_v);
Time_tot_CO=N_CO*deltt;   % in hours
ave_SP_CO=mean(abs(SP_CO_v));
ave_SS_CO=mean(abs(SS_CO_v));
LFproc_CO=100*ave_SP_CO/instSP;
[AC_CO,SOC_CO,EMFR_CO] = CalcEMFR(ACb,LFproc_CO,ave_SP_CO,[],SOCb);
EF_CO_v=ER_CO_v*1e-6*Patm*EMFR_CO/AirDens/R/T*MolMass_CO./SP_CO_v;
ave_EF_CO=mean(EF_CO_v);
E_CO_v=EF_CO_v.*SP_CO_v*deltt/1000;
total_E_CO=sum(E_CO_v);
final_EF_CO=total_E_CO/Time_tot_CO/ave_SP_CO*1000;
disp(' ');
disp('CO for ME at Berth')
fprintf(1,'average  EF_CO (g/kWh)=%.4f\n',ave_EF_CO);
fprintf(1,'total  E_CO (kg)=%.5f\n',total_E_CO);
fprintf(1,'final  EF_CO (g/kWh)=%.4f\n',final_EF_CO);
fprintf(1,'avarage  SS_CO (RPM)=%7.3f\n',ave_SS_CO);
fprintf(1,'avarage  SP_CO (kW)=%.3f\n',ave_SP_CO);
fprintf(1,'avarage  LF (%%)=%.3f\n',LFproc_CO);
fprintf(1,'avarage  AC_CO (kg/hour)=%7.3f\n',AC_CO);
fprintf(1,'avarage  EMFR_CO (kg/hour)=%7.3f\n',EMFR_CO);
fprintf(1,'avarage  SOC_CO (g/kWh)=%7.3f\n',SOC_CO);
fprintf(1,'total time Time_tot_CO (hour)=%8.5f\n',Time_tot_CO);
fprintf(1,'count of samples N_CO (-)=%i\n',N_CO);
% output
total_E_v=[total_E_NOx total_E_SOx total_E_CO2 total_E_CO];
final_EF_v=[final_EF_NOx final_EF_SOx final_EF_CO2 final_EF_CO];
ave_SS_v=[ave_SS_NOx ave_SS_SOx ave_SS_CO2 ave_SS_CO];
ave_SP_v=[ave_SP_NOx ave_SP_SOx ave_SP_CO2 ave_SP_CO];
LFproc_v=[LFproc_NOx LFproc_SOx LFproc_CO2 LFproc_CO];
AC_v=[AC_NOx AC_SOx AC_CO2 AC_CO];
EMFR_v=[EMFR_NOx EMFR_SOx EMFR_CO2 EMFR_CO];
SOC_v=[SOC_NOx SOC_SOx SOC_CO2 SOC_CO];
Time_tot_v=[Time_tot_NOx Time_tot_SOx Time_tot_CO2 Time_tot_CO];
N_v=[N_NOx N_SOx N_CO2 N_CO];
out_mat_file_name='data/EF_At_Berth_ME';
save(out_mat_file_name...
    ,'Date_Time_NOx_c','time_NOx_v','SS_NOx_v','SP_NOx_v','ER_NOx_v','EF_NOx_v','E_NOx_v'...
    ,'total_E_NOx','final_EF_NOx','ave_SS_NOx','ave_SP_NOx','LFproc_NOx','AC_NOx','EMFR_NOx','SOC_NOx','Time_tot_NOx','N_NOx'...
    ,'Date_Time_SOx_c','time_SOx_v','SS_SOx_v','SP_SOx_v','ER_SOx_v','EF_SOx_v','E_SOx_v'...
    ,'total_E_SOx','final_EF_SOx','ave_SS_SOx','ave_SP_SOx','LFproc_SOx','AC_SOx','EMFR_SOx','SOC_SOx','Time_tot_SOx','N_SOx'...
    ,'Date_Time_CO2_c','time_CO2_v','SS_CO2_v','SP_CO2_v','ER_CO2_v','EF_CO2_v','E_CO2_v'...
    ,'total_E_CO2','final_EF_CO2','ave_SS_CO2','ave_SP_CO2','LFproc_CO2','AC_CO2','EMFR_CO2','SOC_CO2','Time_tot_CO2','N_CO2'...
    ,'Date_Time_CO_c','time_CO_v','SS_CO_v','SP_CO_v','ER_CO_v','EF_CO_v','E_CO_v'...
    ,'total_E_CO','final_EF_CO','ave_SS_CO','ave_SP_CO','LFproc_CO','AC_CO','EMFR_CO','SOC_CO','Time_tot_CO','N_CO');
```

CO emissions for main engines at berth

Time rel (in sec)	Time	Date/time	Shaft Speed [rpm]	Shaft Power [kW]	Time	Date / time
0.00	13:10:10	6-11-2015 1:10:10 PM	52.50	1085.00	13:10:10	6-11-2015 1:10:10 PM
5.00	13:10:15	6-11-2015 1:10:15 PM	51.00	974.00	13:10:11	6-11-2015 1:10:11 PM
10.00	13:10:20	6-11-2015 1:10:20 PM	49.40	868.00	13:10:12	6-11-2015 1:10:12 PM
15.00	13:10:25	6-11-2015 1:10:25 PM	48.40	813.00	13:10:13	6-11-2015 1:10:13 PM
20.00	13:10:30	6-11-2015 1:10:30 PM	47.40	765.00	13:10:14	6-11-2015 1:10:14 PM
25.00	13:10:35	6-11-2015 1:10:35 PM	46.60	731.00	13:10:15	6-11-2015 1:10:15 PM
30.00	13:10:40	6-11-2015 1:10:40 PM	46.00	707.00	13:10:16	6-11-2015 1:10:16 PM
35.00	13:10:45	6-11-2015 1:10:45 PM	45.50	683.00	13:10:17	6-11-2015 1:10:17 PM
40.00	13:10:50	6-11-2015 1:10:50 PM	45.40	678.00	13:10:18	6-11-2015 1:10:18 PM
45.00	13:10:55	6-11-2015 1:10:55 PM	45.70	706.00	13:10:19	6-11-2015 1:10:19 PM
50.00	13:11:00	6-11-2015 1:11:00 PM	45.90	732.00	13:10:20	6-11-2015 1:10:20 PM
55.00	13:11:05	6-11-2015 1:11:05 PM	46.20	754.00	13:10:21	6-11-2015 1:10:21 PM
60.00	13:11:10	6-11-2015 1:11:10 PM	46.50	778.00	13:10:22	6-11-2015 1:10:22 PM
65.00	13:11:15	6-11-2015 1:11:15 PM	46.70	790.00	13:10:23	6-11-2015 1:10:23 PM
70.00	13:11:20	6-11-2015 1:11:20 PM	46.80	799.00	13:10:24	6-11-2015 1:10:24 PM
75.00	13:11:25	6-11-2015 1:11:25 PM	46.80	802.00	13:10:25	6-11-2015 1:10:25 PM
80.00	13:11:30	6-11-2015 1:11:30 PM	46.90	819.00	13:10:26	6-11-2015 1:10:26 PM
85.00	13:11:35	6-11-2015 1:11:35 PM	47.10	829.00	13:10:27	6-11-2015 1:10:27 PM
90.00	13:11:40	6-11-2015 1:11:40 PM	47.00	822.00	13:10:28	6-11-2015 1:10:28 PM
95.00	13:11:45	6-11-2015 1:11:45 PM	47.10	827.00	13:10:29	6-11-2015 1:10:29 PM
100.00	13:11:50	6-11-2015 1:11:50 PM	47.10	828.00	13:10:30	6-11-2015 1:10:30 PM
105.00	13:11:55	6-11-2015 1:11:55 PM	47.20	830.00	13:10:31	6-11-2015 1:10:31 PM
110.00	13:12:00	6-11-2015 1:12:00 PM	47.20	831.00	13:10:32	6-11-2015 1:10:32 PM
115.00	13:12:05	6-11-2015 1:12:05 PM	47.20	830.00	13:10:33	6-11-2015 1:10:33 PM
120.00	13:12:10	6-11-2015 1:12:10 PM	47.20	831.00	13:10:34	6-11-2015 1:10:34 PM
125.00	13:12:15	6-11-2015 1:12:15 PM	47.20	826.00	13:10:35	6-11-2015 1:10:35 PM
130.00	13:12:20	6-11-2015 1:12:20 PM	47.30	829.00	13:10:36	6-11-2015 1:10:36 PM
135.00	13:12:25	6-11-2015 1:12:25 PM	47.40	830.00	13:10:37	6-11-2015 1:10:37 PM
140.00	13:12:30	6-11-2015 1:12:30 PM	47.20	824.00	13:10:38	6-11-2015 1:10:38 PM
145.00	13:12:35	6-11-2015 1:12:35 PM	47.10	820.00	13:10:39	6-11-2015 1:10:39 PM
150.00	13:12:40	6-11-2015 1:12:40 PM	47.20	820.00	13:10:40	6-11-2015 1:10:40 PM
155.00	13:12:45	6-11-2015 1:12:45 PM	47.20	819.00	13:10:41	6-11-2015 1:10:41 PM
160.00	13:12:50	6-11-2015 1:12:50 PM	47.10	823.00	13:10:42	6-11-2015 1:10:42 PM
165.00	13:12:55	6-11-2015 1:12:55 PM	47.10	818.00	13:10:43	6-11-2015 1:10:43 PM
170.00	13:13:00	6-11-2015 1:13:00 PM	46.80	812.00	13:10:44	6-11-2015 1:10:44 PM
175.00	13:13:05	6-11-2015 1:13:05 PM	46.70	810.00	13:10:45	6-11-2015 1:10:45 PM
180.00	13:13:10	6-11-2015 1:13:10 PM	46.60	817.00	13:10:46	6-11-2015 1:10:46 PM
185.00	13:13:15	6-11-2015 1:13:15 PM	46.60	827.00	13:10:47	6-11-2015 1:10:47 PM
190.00	13:13:20	6-11-2015 1:13:20 PM	46.60	836.00	13:10:48	6-11-2015 1:10:48 PM
195.00	13:13:25	6-11-2015 1:13:25 PM	46.70	846.00	13:10:49	6-11-2015 1:10:49 PM
200.00	13:13:30	6-11-2015 1:13:30 PM	46.90	861.00	13:10:50	6-11-2015 1:10:50 PM
205.00	13:13:35	6-11-2015 1:13:35 PM	47.00	867.00	13:10:51	6-11-2015 1:10:51 PM
210.00	13:13:40	6-11-2015 1:13:40 PM	47.10	880.00	13:10:52	6-11-2015 1:10:52 PM
215.00	13:13:45	6-11-2015 1:13:45 PM	47.30	882.00	13:10:53	6-11-2015 1:10:53 PM
220.00	13:13:50	6-11-2015 1:13:50 PM	47.30	883.00	13:10:54	6-11-2015 1:10:54 PM

Raw emission rates measured for the main engines at berth

```
function [total_E_v,final_EF_v,ave_SS_v,ave_SP_v,LFproc_v,AC_v,EMFR_v,SOC_v,Time_tot_v,N_v]=MEcalc_man
    % ME maneuvering
    % constants
    R=8.3144598;              % in(kg.m^2)/(K.mol.s^2)
    T=309;                    % in K
    Patm=101325;              % in Pascals
    AirDens=1.225;            % in kg/m^3
    ACb=79200;                % in kg/hour
    SOCb=208.597;             % in g/kWh
    instSP=6880;              % kW
    deltt=1/3600;             % in hours
    MolMass_NOx=46.01;        % in g/mol
    MolMass_SOx=64.066;       % in g/mol
    MolMass_CO2=44.01;        % in g/mol
    MolMass_CO=28.01;         % in g/mol
    % input data
    in_mat_file_name='data/Maneuvering_ME';
    load(in_mat_file_name,'Date_Time_c','time_er_v','SS_er_v','SP_er_v','NOx_er_v','SOx_er_v','CO2_er_v','CO_er_v');
    disp(' ')
    disp('ME maneuvering')
    disp(' ');
    % data processing NOx
    i_v=~isnan(NOx_er_v);
    Date_Time_NOx_c=Date_Time_c(i_v); %#ok<NASGU>
    time_NOx_v=time_er_v(i_v); %#ok<NASGU>
    SS_NOx_v=SS_er_v(i_v);
    SP_NOx_v=SP_er_v(i_v);
    ER_NOx_v=NOx_er_v(i_v);
    N_NOx=sum(i_v);
    Time_tot_NOx=N_NOx*deltt;   % in hours
    ave_SP_NOx=mean(abs(SP_NOx_v));
    ave_SS_NOx=mean(abs(SS_NOx_v));
    LFproc_NOx=100*ave_SP_NOx/instSP;
    [AC_NOx,SOC_NOx,EMFR_NOx] = CalcEMFR(ACb,LFproc_NOx,ave_SP_NOx,[],SOCb);
    EF_NOx_v=ER_NOx_v*1e-6*Patm*EMFR_NOx/AirDens/R/T*MolMass_NOx./SP_NOx_v;
    ave_EF_NOx=mean(EF_NOx_v);
    E_NOx_v=EF_NOx_v.*SP_NOx_v*deltt/1000;
    total_E_NOx=sum(E_NOx_v);
    final_EF_NOx=total_E_NOx/Time_tot_NOx/ave_SP_NOx*1000;
    disp(' ');
    disp('NOx for ME maneuvering')
    fprintf(1,'average  EF_NOx (g/kWh)=%.4f\n',ave_EF_NOx);
    fprintf(1,'total  E_NOx (kg)=%.5f\n',total_E_NOx);
    fprintf(1,'final  EF_NOx (g/kWh)=%.4f\n',final_EF_NOx);
    fprintf(1,'avarage  SS_NOx (RPM)=%7.3f\n',ave_SS_NOx);
    fprintf(1,'avarage  SP_NOx (kW)=%.3f\n',ave_SP_NOx);
    fprintf(1,'avarage  LF (%%)=%.3f\n',LFproc_NOx);
    fprintf(1,'avarage  AC_NOx (kg/hour)=%7.3f\n',AC_NOx);
    fprintf(1,'avarage  EMFR_NOx (kg/hour)=%7.3f\n',EMFR_NOx);
    fprintf(1,'avarage  SOC_NOx (g/kWh)=%7.3f\n',SOC_NOx);
    fprintf(1,'total time Time_tot_NOx (hour)=%8.5f\n',Time_tot_NOx);
    fprintf(1,'count of samples N_NOx (-)=%i\n',N_NOx);
    % data processing SOx
    i_v=~isnan(SOx_er_v);
    Date_Time_SOx_c=Date_Time_c(i_v); %#ok<NASGU>
    time_SOx_v=time_er_v(i_v); %#ok<NASGU>
    SS_SOx_v=SS_er_v(i_v);
    SP_SOx_v=SP_er_v(i_v);
```

NO_x *emissions for main engines at manoeuvring*

```
Date_Time_CO_c=Date_Time_c(i_v); %#ok<NASGU>
time_CO_v=time_er_v(i_v); %#ok<NASGU>
SS_CO_v=SS_er_v(i_v);
SP_CO_v=SP_er_v(i_v);
ER_CO_v=CO_er_v(i_v);
N_CO=sum(i_v);
Time_tot_CO=N_CO*deltt;   % in hours
ave_SP_CO=mean(abs(SP_CO_v));
ave_SS_CO=mean(abs(SS_CO_v));
LFproc_CO=100*ave_SP_CO/instSP;
[AC_CO,SOC_CO,EMFR_CO] = CalcEMFR(ACb,LFproc_CO,ave_SP_CO,[],SOCb);
EF_CO_v=ER_CO_v*1e-6*Patm*EMFR_CO/AirDens/R/T*MolMass_CO./SP_CO_v;
ave_EF_CO=mean(EF_CO_v);
E_CO_v=EF_CO_v.*SP_CO_v*deltt/1000;
total_E_CO=sum(E_CO_v);
final_EF_CO=total_E_CO/Time_tot_CO/ave_SP_CO*1000;
disp(' ');
disp('CO for ME maneuvering')
fprintf(1,'average  EF_CO (g/kWh)=%.4f\n',ave_EF_CO);
fprintf(1,'total  E_CO (kg)=%.5f\n',total_E_CO);
fprintf(1,'final  EF_CO (g/kWh)=%.4f\n',final_EF_CO);
fprintf(1,'avarage  SS_CO (RPM)=%7.3f\n',ave_SS_CO);
fprintf(1,'avarage  SP_CO (kW)=%.3f\n',ave_SP_CO);
fprintf(1,'avarage  LF (%%)=%.3f\n',LFproc_CO);
fprintf(1,'avarage  AC_CO (kg/hour)=%7.3f\n',AC_CO);
fprintf(1,'avarage  EMFR_CO (kg/hour)=%7.3f\n',EMFR_CO);
fprintf(1,'avarage  SOC_CO (g/kWh)=%7.3f\n',SOC_CO);
fprintf(1,'total time Time_tot_CO (hour)=%8.5f\n',Time_tot_CO);
fprintf(1,'count of samples N_CO (-)=%i\n',N_CO);
% output
total_E_v=[total_E_NOx total_E_SOx total_E_CO2 total_E_CO];
final_EF_v=[final_EF_NOx final_EF_SOx final_EF_CO2 final_EF_CO];
ave_SS_v=[ave_SS_NOx ave_SS_SOx ave_SS_CO2 ave_SS_CO];
ave_SP_v=[ave_SP_NOx ave_SP_SOx ave_SP_CO2 ave_SP_CO];
LFproc_v=[LFproc_NOx LFproc_SOx LFproc_CO2 LFproc_CO];
AC_v=[AC_NOx AC_SOx AC_CO2 AC_CO];
EMFR_v=[EMFR_NOx EMFR_SOx EMFR_CO2 EMFR_CO];
SOC_v=[SOC_NOx SOC_SOx SOC_CO2 SOC_CO];
Time_tot_v=[Time_tot_NOx Time_tot_SOx Time_tot_CO2 Time_tot_CO];
N_v=[N_NOx N_SOx N_CO2 N_CO];
out_mat_file_name='data/EF_maneuvering_ME';
save(out_mat_file_name...
    ,'Date_Time_NOx_c','time_NOx_v','SS_NOx_v','SP_NOx_v','ER_NOx_v','EF_NOx_v','E_NOx_v'...
    ,'total_E_NOx','final_EF_NOx','ave_SS_NOx','ave_SP_NOx','LFproc_NOx','AC_NOx','EMFR_NOx','SOC_NOx','Time_tot_NOx','N_NOx'...
    ,'Date_Time_SOx_c','time_SOx_v','SS_SOx_v','SP_SOx_v','ER_SOx_v','EF_SOx_v','E_SOx_v'...
    ,'total_E_SOx','final_EF_SOx','ave_SS_SOx','ave_SP_SOx','LFproc_SOx','AC_SOx','EMFR_SOx','SOC_SOx','Time_tot_SOx','N_SOx'...
    ,'Date_Time_CO2_c','time_CO2_v','SS_CO2_v','SP_CO2_v','ER_CO2_v','EF_CO2_v','E_CO2_v'...
    ,'total_E_CO2','final_EF_CO2','ave_SS_CO2','ave_SP_CO2','LFproc_CO2','AC_CO2','EMFR_CO2','SOC_CO2','Time_tot_CO2','N_CO2'...
    ,'Date_Time_CO_c','time_CO_v','SS_CO_v','SP_CO_v','ER_CO_v','EF_CO_v','E_CO_v'...
    ,'total_E_CO','final_EF_CO','ave_SS_CO','ave_SP_CO','LFproc_CO','AC_CO','EMFR_CO','SOC_CO','Time_tot_CO','N_CO');
```

SO_x and CO_2 and CO emissions for main engines at manoeuvring

Time rel (in sec)	Time	Date/time	Shaft Speed [rpm]	Shaft Power [kW]	Time	Date / time
0.00	11:19:30	6-11-2015 11:19:30 AM	81.800	3900.000	11:20:01	6-11-2015 11:20:01 AM
5.00	11:19:35	6-11-2015 11:19:35 AM	79.300	3577.000	11:20:02	6-11-2015 11:20:02 AM
10.00	11:19:40	6-11-2015 11:19:40 AM	77.800	3283.000	11:20:03	6-11-2015 11:20:03 AM
15.00	11:19:45	6-11-2015 11:19:45 AM	76.900	3238.000	11:20:04	6-11-2015 11:20:04 AM
20.00	11:19:50	6-11-2015 11:19:50 AM	77.400	3281.000	11:20:05	6-11-2015 11:20:05 AM
25.00	11:19:55	6-11-2015 11:19:55 AM	77.100	3299.000	11:20:06	6-11-2015 11:20:06 AM
30.00	11:20:00	6-11-2015 11:20:00 AM	77.500	3324.000	11:20:07	6-11-2015 11:20:07 AM
35.00	11:20:05	6-11-2015 11:20:05 AM	77.500	3289.000	11:20:08	6-11-2015 11:20:08 AM
40.00	11:20:10	6-11-2015 11:20:10 AM	77.500	3243.000	11:20:09	6-11-2015 11:20:09 AM
45.00	11:20:15	6-11-2015 11:20:15 AM	77.500	3240.000	11:20:10	6-11-2015 11:20:10 AM
50.00	11:20:20	6-11-2015 11:20:20 AM	78.000	3228.000	11:20:11	6-11-2015 11:20:11 AM
55.00	11:20:25	6-11-2015 11:20:25 AM	77.200	3196.000	11:20:12	6-11-2015 11:20:12 AM
60.00	11:20:30	6-11-2015 11:20:30 AM	77.700	3236.000	11:20:13	6-11-2015 11:20:13 AM
65.00	11:20:35	6-11-2015 11:20:35 AM	77.300	3237.000	11:20:14	6-11-2015 11:20:14 AM
70.00	11:20:40	6-11-2015 11:20:40 AM	77.500	3276.000	11:20:15	6-11-2015 11:20:15 AM
75.00	11:20:45	6-11-2015 11:20:45 AM	77.400	3328.000	11:20:16	6-11-2015 11:20:16 AM
80.00	11:20:50	6-11-2015 11:20:50 AM	77.600	3335.000	11:20:17	6-11-2015 11:20:17 AM
85.00	11:20:55	6-11-2015 11:20:55 AM	77.600	3360.000	11:20:18	6-11-2015 11:20:18 AM
90.00	11:21:00	6-11-2015 11:21:00 AM	77.800	3364.000	11:20:19	6-11-2015 11:20:19 AM
95.00	11:21:05	6-11-2015 11:21:05 AM	78.000	3355.000	11:20:20	6-11-2015 11:20:20 AM
100.00	11:21:10	6-11-2015 11:21:10 AM	77.300	3326.000	11:20:21	6-11-2015 11:20:21 AM
105.00	11:21:15	6-11-2015 11:21:15 AM	77.500	3323.000	11:20:22	6-11-2015 11:20:22 AM
110.00	11:21:20	6-11-2015 11:21:20 AM	77.400	3349.000	11:20:23	6-11-2015 11:20:23 AM
115.00	11:21:25	6-11-2015 11:21:25 AM	77.800	3360.000	11:20:24	6-11-2015 11:20:24 AM
120.00	11:21:30	6-11-2015 11:21:30 AM	77.300	3337.000	11:20:25	6-11-2015 11:20:25 AM
125.00	11:21:35	6-11-2015 11:21:35 AM	77.500	3384.000	11:20:26	6-11-2015 11:20:26 AM
130.00	11:21:40	6-11-2015 11:21:40 AM	77.700	3365.000	11:20:27	6-11-2015 11:20:27 AM
135.00	11:21:45	6-11-2015 11:21:45 AM	77.000	3318.000	11:20:28	6-11-2015 11:20:28 AM
140.00	11:21:50	6-11-2015 11:21:50 AM	77.400	3348.000	11:20:29	6-11-2015 11:20:29 AM
145.00	11:21:55	6-11-2015 11:21:55 AM	77.400	3328.000	11:20:30	6-11-2015 11:20:30 AM
150.00	11:22:00	6-11-2015 11:22:00 AM	77.600	3364.000	11:20:31	6-11-2015 11:20:31 AM
155.00	11:22:05	6-11-2015 11:22:05 AM	77.400	3353.000	11:20:32	6-11-2015 11:20:32 AM
160.00	11:22:10	6-11-2015 11:22:10 AM	77.300	3366.000	11:20:33	6-11-2015 11:20:33 AM
165.00	11:22:15	6-11-2015 11:22:15 AM	77.200	3389.000	11:20:34	6-11-2015 11:20:34 AM
170.00	11:22:20	6-11-2015 11:22:20 AM	77.600	3388.000	11:20:35	6-11-2015 11:20:35 AM
175.00	11:22:25	6-11-2015 11:22:25 AM	77.400	3383.000	11:20:36	6-11-2015 11:20:36 AM
180.00	11:22:30	6-11-2015 11:22:30 AM	77.300	3358.000	11:20:37	6-11-2015 11:20:37 AM
185.00	11:22:35	6-11-2015 11:22:35 AM	77.700	3402.000	11:20:38	6-11-2015 11:20:38 AM
190.00	11:22:40	6-11-2015 11:22:40 AM	77.300	3388.000	11:20:39	6-11-2015 11:20:39 AM
195.00	11:22:45	6-11-2015 11:22:45 AM	77.600	3393.000	11:20:40	6-11-2015 11:20:40 AM
200.00	11:22:50	6-11-2015 11:22:50 AM	78.000	3412.000	11:20:41	6-11-2015 11:20:41 AM
205.00	11:22:55	6-11-2015 11:22:55 AM	77.500	3390.000	11:20:42	6-11-2015 11:20:42 AM
210.00	11:23:00	6-11-2015 11:23:00 AM	77.500	3389.000	11:20:43	6-11-2015 11:20:43 AM
215.00	11:23:05	6-11-2015 11:23:05 AM	77.600	3398.000	11:20:44	6-11-2015 11:20:44 AM

Raw emission rates measured for the main engines at manoeuvring

```
function [total_E_v,final_EF_v,ave_SS_v,ave_SP_v,LFproc_v,AC_v,EMFR_v,SOC_v,Time_tot_v,N_v]=MEcalc_cruis
    % ME cruising
    % constants
    R=8.3144598;              % in(kg.m^2)/(K.mol.s^2)
    T=309;                    % in K
    Patm=101325;              % in Pascals
    AirDens=1.225;            % in kg/m^3
    ACb=79200;                % in kg/hour
    HOC=1150;                 % in kg/hour
    instSP=6880;              % kW
    deltt=1/3600;             % in hours
    MolMass_NOx=46.01;        % in g/mol
    MolMass_SOx=64.066;       % in g/mol
    MolMass_CO2=44.01;        % in g/mol
    MolMass_CO=28.01;         % in g/mol
    % input data
    in_mat_file_name='data/Cruising_ME';
    load(in_mat_file_name,'Date_Time_c','time_er_v','SS_er_v','SP_er_v','NOx_er_v','SOx_er_v','CO2_er_v','CO_er_v');
    disp(' ')
    disp('ME cruising')
    disp(' ');
    % data processing NOx
    i_v=~isnan(NOx_er_v);
    Date_Time_NOx_c=Date_Time_c(i_v); %#ok<NASGU>
    time_NOx_v=time_er_v(i_v); %#ok<NASGU>
    SS_NOx_v=SS_er_v(i_v);
    SP_NOx_v=SP_er_v(i_v);
    ER_NOx_v=NOx_er_v(i_v);
    N_NOx=sum(i_v);
    Time_tot_NOx=N_NOx*deltt;   % in hours
    ave_SP_NOx=mean(abs(SP_NOx_v));
    ave_SS_NOx=mean(abs(SS_NOx_v));
    LFproc_NOx=100*ave_SP_NOx/instSP;
    [AC_NOx,SOC_NOx,EMFR_NOx] = CalcEMFR(ACb,LFproc_NOx,ave_SP_NOx,HOC);
    EF_NOx_v=ER_NOx_v*1e-6*Patm*EMFR_NOx/AirDens/R/T*MolMass_NOx./SP_NOx_v;
    ave_EF_NOx=mean(EF_NOx_v);
    E_NOx_v=EF_NOx_v.*SP_NOx_v*deltt/1000;
    total_E_NOx=sum(E_NOx_v);
    final_EF_NOx=total_E_NOx/Time_tot_NOx/ave_SP_NOx*1000;
    disp(' ');
    disp('NOx for ME cruising')
    fprintf(1,'average  EF_NOx (g/kWh)=%.4f\n',ave_EF_NOx);
    fprintf(1,'total  E_NOx (kg)=%.5f\n',total_E_NOx);
    fprintf(1,'final  EF_NOx (g/kWh)=%.4f\n',final_EF_NOx);
    fprintf(1,'avarage  SS_NOx (RPM)=%7.3f\n',ave_SS_NOx);
    fprintf(1,'avarage  SP_NOx (kW)=%.3f\n',ave_SP_NOx);
    fprintf(1,'avarage  LF (%%)=%.3f\n',LFproc_NOx);
    fprintf(1,'avarage  AC_NOx (kg/hour)=%7.3f\n',AC_NOx);
    fprintf(1,'avarage  EMFR_NOx (kg/hour)=%7.3f\n',EMFR_NOx);
    fprintf(1,'avarage  SOC_NOx (g/kWh)=%7.3f\n',SOC_NOx);
    fprintf(1,'total time Time_tot_NOx (hour)=%8.5f\n',Time_tot_NOx);
    fprintf(1,'count of samples N_NOx (-)=%i\n',N_NOx);
    % data processing SOx
    i_v=~isnan(SOx_er_v);
    Date_Time_SOx_c=Date_Time_c(i_v); %#ok<NASGU>
    time_SOx_v=time_er_v(i_v); %#ok<NASGU>
    SS_SOx_v=SS_er_v(i_v);
    SP_SOx_v=SP_er_v(i_v);
    ER_SOx_v=SOx_er_v(i_v);
```

NO_x emissions for main engines at cruising

```
N_SOx=sum(i_v);
Time_tot_SOx=N_SOx*deltt;   % in hours
ave_SP_SOx=mean(abs(SP_SOx_v));
ave_SS_SOx=mean(abs(SS_SOx_v));
LFproc_SOx=100*ave_SP_SOx/instSP;
[AC_SOx,SOC_SOx,EMFR_SOx] = CalcEMFR(ACb,LFproc_SOx,ave_SP_SOx,HOC);
EF_SOx_v=ER_SOx_v*1e-6*Patm*EMFR_SOx/AirDens/R/T*MolMass_SOx./SP_SOx_v;
ave_EF_SOx=mean(EF_SOx_v);
E_SOx_v=EF_SOx_v.*SP_SOx_v*deltt/1000;
total_E_SOx=sum(E_SOx_v);
final_EF_SOx=total_E_SOx/Time_tot_SOx/ave_SP_SOx*1000;
disp(' ');
disp('SOx for ME cruising')
fprintf(1,'average  EF_SOx (g/kWh)=%.4f\n',ave_EF_SOx);
fprintf(1,'total  E_SOx (kg)=%.5f\n',total_E_SOx);
fprintf(1,'final  EF_SOx (g/kWh)=%.4f\n',final_EF_SOx);
fprintf(1,'avarage  SS_SOx (RPM)=%7.3f\n',ave_SS_SOx);
fprintf(1,'avarage  SP_SOx (kW)=%.3f\n',ave_SP_SOx);
fprintf(1,'avarage  LF (%%)=%.3f\n',LFproc_SOx);
fprintf(1,'avarage  AC_SOx (kg/hour)=%7.3f\n',AC_SOx);
fprintf(1,'avarage  EMFR_SOx (kg/hour)=%7.3f\n',EMFR_SOx);
fprintf(1,'avarage  SOC_SOx (g/kWh)=%7.3f\n',SOC_SOx);
fprintf(1,'total time Time_tot_SOx (hour)=%8.5f\n',Time_tot_SOx);
fprintf(1,'count of samples N_SOx (-)=%i\n',N_SOx);
% data processing CO2
i_v=~isnan(CO2_er_v);
Date_Time_CO2_c=Date_Time_c(i_v); %#ok<NASGU>
time_CO2_v=time_er_v(i_v); %#ok<NASGU>
SS_CO2_v=SS_er_v(i_v);
SP_CO2_v=SP_er_v(i_v);
ER_CO2_v=CO2_er_v(i_v);
N_CO2=sum(i_v);
Time_tot_CO2=N_CO2*deltt;   % in hours
ave_SP_CO2=mean(abs(SP_CO2_v));
ave_SS_CO2=mean(abs(SS_CO2_v));
LFproc_CO2=100*ave_SP_CO2/instSP;
[AC_CO2,SOC_CO2,EMFR_CO2] = CalcEMFR(ACb,LFproc_CO2,ave_SP_CO2,HOC);
EF_CO2_v=ER_CO2_v*1e-2*Patm*EMFR_CO2/AirDens/R/T*MolMass_CO2./SP_CO2_v;
ave_EF_CO2=mean(EF_CO2_v);
E_CO2_v=EF_CO2_v.*SP_CO2_v*deltt/1000;
total_E_CO2=sum(E_CO2_v);
final_EF_CO2=total_E_CO2/Time_tot_CO2/ave_SP_CO2*1000;
disp(' ');
disp('CO2 for ME cruising')
fprintf(1,'average  EF_CO2 (g/kWh)=%.4f\n',ave_EF_CO2);
fprintf(1,'total  E_CO2 (kg)=%.5f\n',total_E_CO2);
fprintf(1,'final  EF_CO2 (g/kWh)=%.4f\n',final_EF_CO2);
fprintf(1,'avarage  SS_CO2 (RPM)=%7.3f\n',ave_SS_CO2);
fprintf(1,'avarage  SP_CO2 (kW)=%.3f\n',ave_SP_CO2);
fprintf(1,'avarage  LF (%%)=%.3f\n',LFproc_CO2);
fprintf(1,'avarage  AC_CO2 (kg/hour)=%7.3f\n',AC_CO2);
fprintf(1,'avarage  EMFR_CO2 (kg/hour)=%7.3f\n',EMFR_CO2);
fprintf(1,'avarage  SOC_CO2 (g/kWh)=%7.3f\n',SOC_CO2);
fprintf(1,'total time Time_tot_CO2 (hour)=%8.5f\n',Time_tot_CO2);
fprintf(1,'count of samples N_CO2 (-)=%i\n',N_CO2);
% data processing CO
i_v=~isnan(CO_er_v);
Date_Time_CO_c=Date_Time_c(i_v); %#ok<NASGU>
```

SO_x and CO_2 emissions for main engines at cruising

```
time_CO_v=time_er_v(i_v); %#ok<NASGU>
SS_CO_v=SS_er_v(i_v);
SP_CO_v=SP_er_v(i_v);
ER_CO_v=CO_er_v(i_v);
N_CO=sum(i_v);
Time_tot_CO=N_CO*deltt;   % in hours
ave_SP_CO=mean(abs(SP_CO_v));
ave_SS_CO=mean(abs(SS_CO_v));
LFproc_CO=100*ave_SP_CO/instSP;
[AC_CO,SOC_CO,EMFR_CO] = CalcEMFR(ACb,LFproc_CO,ave_SP_CO,HOC);
EF_CO_v=ER_CO_v*1e-6*Patm*EMFR_CO/AirDens/R/T*MolMass_CO./SP_CO_v;
ave_EF_CO=mean(EF_CO_v);
E_CO_v=EF_CO_v.*SP_CO_v*deltt/1000;
total_E_CO=sum(E_CO_v);
final_EF_CO=total_E_CO/Time_tot_CO/ave_SP_CO*1000;
disp(' ');
disp('CO for ME cruising')
fprintf(1,'average  EF_CO (g/kWh)=%.4f\n',ave_EF_CO);
fprintf(1,'total  E_CO (kg)=%.5f\n',total_E_CO);
fprintf(1,'final  EF_CO (g/kWh)=%.4f\n',final_EF_CO);
fprintf(1,'avarage  SS_CO (RPM)=%7.3f\n',ave_SS_CO);
fprintf(1,'avarage  SP_CO (kW)=%.3f\n',ave_SP_CO);
fprintf(1,'avarage  LF (%%)=%.3f\n',LFproc_CO);
fprintf(1,'avarage  AC_CO (kg/hour)=%7.3f\n',AC_CO);
fprintf(1,'avarage  EMFR_CO (kg/hour)=%7.3f\n',EMFR_CO);
fprintf(1,'avarage  SOC_CO (g/kWh)=%7.3f\n',SOC_CO);
fprintf(1,'total time Time_tot_CO (hour)=%8.5f\n',Time_tot_CO);
fprintf(1,'count of samples N_CO (-)=%i\n',N_CO);
% output
total_E_v=[total_E_NOx total_E_SOx total_E_CO2 total_E_CO];
final_EF_v=[final_EF_NOx final_EF_SOx final_EF_CO2 final_EF_CO];
ave_SS_v=[ave_SS_NOx ave_SS_SOx ave_SS_CO2 ave_SS_CO];
ave_SP_v=[ave_SP_NOx ave_SP_SOx ave_SP_CO2 ave_SP_CO];
LFproc_v=[LFproc_NOx LFproc_SOx LFproc_CO2 LFproc_CO];
AC_v=[AC_NOx AC_SOx AC_CO2 AC_CO];
EMFR_v=[EMFR_NOx EMFR_SOx EMFR_CO2 EMFR_CO];
SOC_v=[SOC_NOx SOC_SOx SOC_CO2 SOC_CO];
Time_tot_v=[Time_tot_NOx Time_tot_SOx Time_tot_CO2 Time_tot_CO];
N_v=[N_NOx N_SOx N_CO2 N_CO];
out_mat_file_name='data/EF_cruising_ME';
save(out_mat_file_name...
    ,'Date_Time_NOx_c','time_NOx_v','SS_NOx_v','SP_NOx_v','ER_NOx_v','EF_NOx_v','E_NOx_v'...
    ,'total_E_NOx','final_EF_NOx','ave_SS_NOx','ave_SP_NOx','LFproc_NOx','AC_NOx','EMFR_NOx','SOC_NOx','Time_tot_NOx','N_NOx'...
    ,'Date_Time_SOx_c','time_SOx_v','SS_SOx_v','SP_SOx_v','ER_SOx_v','EF_SOx_v','E_SOx_v'...
    ,'total_E_SOx','final_EF_SOx','ave_SS_SOx','ave_SP_SOx','LFproc_SOx','AC_SOx','EMFR_SOx','SOC_SOx','Time_tot_SOx','N_SOx'...
    ,'Date_Time_CO2_c','time_CO2_v','SS_CO2_v','SP_CO2_v','ER_CO2_v','EF_CO2_v','E_CO2_v'...
    ,'total_E_CO2','final_EF_CO2','ave_SS_CO2','ave_SP_CO2','LFproc_CO2','AC_CO2','EMFR_CO2','SOC_CO2','Time_tot_CO2','N_CO2'...
    ,'Date_Time_CO_c','time_CO_v','SS_CO_v','SP_CO_v','ER_CO_v','EF_CO_v','E_CO_v'...
    ,'total_E_CO','final_EF_CO','ave_SS_CO','ave_SP_CO','LFproc_CO','AC_CO','EMFR_CO','SOC_CO','Time_tot_CO','N_CO');
```

CO emissions for main engines at cruising

Time rel (in sec)	Time	Date/time	Shaft Speed [rpm]	Shaft Power [kW]	Time	Date / time	ppm NOx	ppm SOx	% CO2	ppm CO
0.00	10:57:45	6-11-2015 10:57:45 AM	89.3600	5445.0000	10:57:49	6-11-2015 10:57:49 AM	66.0000	540.0000	2.9600	1.0000
5.00	10:57:50	6-11-2015 10:57:50 AM	89.3600	5352.0000	10:57:50	6-11-2015 10:57:50 AM	41.0000	39.0000	2.9600	1.0000
10.00	10:57:55	6-11-2015 10:57:55 AM	89.3600	5339.0000	10:57:51	6-11-2015 10:57:51 AM	41.0000	39.0000	2.9600	1.0000
15.00	10:58:00	6-11-2015 10:58:00 AM	89.3600	5375.0000	10:57:52	6-11-2015 10:57:52 AM	154.0000	17.0000	3.3600	8.0000
20.00	10:58:05	6-11-2015 10:58:05 AM	89.3600	5385.0000	10:57:53	6-11-2015 10:57:53 AM	154.0000	17.0000	3.3600	8.0000
25.00	10:58:10	6-11-2015 10:58:10 AM	89.3600	5401.0000	10:57:54	6-11-2015 10:57:54 AM	154.0000	17.0000	4.0000	25.0000
30.00	10:58:15	6-11-2015 10:58:15 AM	89.3600	5351.0000	10:57:55	6-11-2015 10:57:55 AM	433.0000	104.0000	4.0000	25.0000
35.00	10:58:20	6-11-2015 10:58:20 AM	89.3600	5375.0000	10:57:56	6-11-2015 10:57:56 AM	433.0000	104.0000	4.0000	25.0000
40.00	10:58:25	6-11-2015 10:58:25 AM	89.3600	5308.0000	10:57:57	6-11-2015 10:57:57 AM	740.0000	288.0000	4.4500	43.0000
45.00	10:58:30	6-11-2015 10:58:30 AM	89.3600	5254.0000	10:57:58	6-11-2015 10:57:58 AM	740.0000	288.0000	4.4500	43.0000
50.00	10:58:35	6-11-2015 10:58:35 AM	89.3600	5257.0000	10:57:59	6-11-2015 10:57:59 AM	740.0000	288.0000	4.5800	43.0000
55.00	10:58:40	6-11-2015 10:58:40 AM	89.3600	5228.0000	10:58:00	6-11-2015 10:58:00 AM	919.0000	475.0000	4.5800	58.0000
60.00	10:58:45	6-11-2015 10:58:45 AM	89.3600	5243.0000	10:58:01	6-11-2015 10:58:01 AM	919.0000	475.0000	4.5800	58.0000
65.00	10:58:50	6-11-2015 10:58:50 AM	89.3600	5261.0000	10:58:02	6-11-2015 10:58:02 AM	972.0000	586.0000	4.4700	73.0000
70.00	10:58:55	6-11-2015 10:58:55 AM	89.3600	5198.0000	10:58:03	6-11-2015 10:58:03 AM	972.0000	586.0000	4.4700	73.0000
75.00	10:59:00	6-11-2015 10:59:00 AM	89.3600	5194.0000	10:58:04	6-11-2015 10:58:04 AM	972.0000	586.0000	4.3700	73.0000
80.00	10:59:05	6-11-2015 10:59:05 AM	89.3600	5093.0000	10:58:05	6-11-2015 10:58:05 AM	980.0000	635.0000	4.3700	85.0000
85.00	10:59:10	6-11-2015 10:59:10 AM	89.3600	5065.0000	10:58:06	6-11-2015 10:58:06 AM	980.0000	635.0000	4.3700	85.0000
90.00	10:59:15	6-11-2015 10:59:15 AM	89.3600	5024.0000	10:58:07	6-11-2015 10:58:07 AM	993.0000	663.0000	4.4300	89.0000
95.00	10:59:20	6-11-2015 10:59:20 AM	89.3600	5034.0000	10:58:08	6-11-2015 10:58:08 AM	992.0000	663.0000	4.4300	89.0000
100.00	10:59:25	6-11-2015 10:59:25 AM	89.3600	5076.0000	10:58:09	6-11-2015 10:58:09 AM	992.0000	663.0000	4.5300	89.0000
105.00	10:59:30	6-11-2015 10:59:30 AM	89.3600	5064.0000	10:58:10	6-11-2015 10:58:10 AM	1001.0000	684.0000	4.5300	89.0000
110.00	10:59:35	6-11-2015 10:59:35 AM	89.3600	4983.0000	10:58:11	6-11-2015 10:58:11 AM	1001.0000	684.0000	4.5300	89.0000
115.00	10:59:40	6-11-2015 10:59:40 AM	89.3600	4957.0000	10:58:12	6-11-2015 10:58:12 AM	992.0000	691.0000	4.5100	90.0000
120.00	10:59:45	6-11-2015 10:59:45 AM	89.3600	4948.0000	10:58:13	6-11-2015 10:58:13 AM	992.0000	691.0000	4.5100	90.0000
125.00	10:59:50	6-11-2015 10:59:50 AM	89.3600	4927.0000	10:58:14	6-11-2015 10:58:14 AM	975.0000	686.0000	4.3900	94.0000
130.00	10:59:55	6-11-2015 10:59:55 AM	89.3600	4897.0000	10:58:15	6-11-2015 10:58:15 AM	975.0000	686.0000	4.3900	94.0000
135.00	11:00:00	6-11-2015 11:00:00 AM	89.3600	4948.0000	10:58:16	6-11-2015 10:58:16 AM	975.0000	686.0000	4.3700	98.0000
140.00	11:00:05	6-11-2015 11:00:05 AM	89.3600	4942.0000	10:58:17	6-11-2015 10:58:17 AM	974.0000	682.0000	4.3700	98.0000
145.00	11:00:10	6-11-2015 11:00:10 AM	89.3600	4911.0000	10:58:18	6-11-2015 10:58:18 AM	974.0000	682.0000	4.3700	98.0000
150.00	11:00:15	6-11-2015 11:00:15 AM	89.3600	4906.0000	10:58:19	6-11-2015 10:58:19 AM	974.0000	682.0000	4.3700	98.0000
155.00	11:00:20	6-11-2015 11:00:20 AM	89.3600	4796.0000	10:58:20	6-11-2015 10:58:20 AM	988.0000	685.0000	4.4700	102.0000
160.00	11:00:25	6-11-2015 11:00:25 AM	89.3600	4783.0000	10:58:21	6-11-2015 10:58:21 AM	988.0000	685.0000	4.4700	102.0000
165.00	11:00:30	6-11-2015 11:00:30 AM	89.3600	4787.0000	10:58:22	6-11-2015 10:58:22 AM	988.0000	685.0000	4.4900	107.0000
170.00	11:00:35	6-11-2015 11:00:35 AM	89.3600	4734.0000	10:58:23	6-11-2015 10:58:23 AM	1002.0000	690.0000	4.4900	107.0000
175.00	11:00:40	6-11-2015 11:00:40 AM	89.3600	4755.0000	10:58:24	6-11-2015 10:58:24 AM	1002.0000	690.0000	4.4900	107.0000
180.00	11:00:45	6-11-2015 11:00:45 AM	89.3600	4699.0000	10:58:25	6-11-2015 10:58:25 AM	1006.0000	690.0000	4.4500	111.0000
185.00	11:00:50	6-11-2015 11:00:50 AM	89.3600	4691.0000	10:58:26	6-11-2015 10:58:26 AM	1006.0000	690.0000	4.4500	111.0000
190.00	11:00:55	6-11-2015 11:00:55 AM	89.3600	4741.0000	10:58:27	6-11-2015 10:58:27 AM	1006.0000	690.0000	4.4100	111.0000
195.00	11:01:00	6-11-2015 11:01:00 AM	89.3600	4673.0000	10:58:28	6-11-2015 10:58:28 AM	999.0000	683.0000	4.4100	113.0000
200.00	11:01:05	6-11-2015 11:01:05 AM	89.3600	4607.0000	10:58:29	6-11-2015 10:58:29 AM	999.0000	683.0000	4.4100	113.0000
205.00	11:01:10	6-11-2015 11:01:10 AM	89.3600	4574.0000	10:58:30	6-11-2015 10:58:30 AM	988.0000	674.0000	4.3600	111.0000
210.00	11:01:15	6-11-2015 11:01:15 AM	89.3600	4520.0000	10:58:31	6-11-2015 10:58:31 AM	988.0000	674.0000	4.3600	111.0000
215.00	11:01:20	6-11-2015 11:01:20 AM	89.3600	4630.0000	10:58:32	6-11-2015 10:58:32 AM	988.0000	674.0000	4.4100	111.0000
220.00	11:01:25	6-11-2015 11:01:25 AM	89.3600	4601.0000	10:58:33	6-11-2015 10:58:33 AM	980.0000	669.0000	4.4100	107.0000

Raw emission rates measured for the main engines at cruising

```
function [final_EF_HC,total_E_HC,ave_SS_HC,ave_SP_HC,LFproc,AC_HC,EMFR_HC,SOC_HC,Time_tot_HC,N_HC]=HCcalc_BE
    % HC at berth
    % constants
    R=8.3144598;              % in(kg.m^2)/(K.mol.s^2)
    T=309;                    % in K
    Patm=101325;              % in Pascals
    AirDens=1.225;            % in kg/m^3
    ACb=79200;                % in kg/hour
    SOCb=208.597;             % in g/kWh
    instSP=6880;              % kW
    deltt=300/3600;           % in hours
    MolMass=44;               % in g/mol
    % measurements
    time_c={
        '6/11/2015 13:15'
        '6/11/2015 13:20'
        '6/11/2015 13:25'
        '6/11/2015 13:30'};
    SS_v=[33;47.1;33.2;33.2]; % in RPM
    SP_v=[291;906;304;305];   % in kW
    HC_er_v=[23;22;22;29];    % in ppm
    % data processing
    N_HC=length(SP_v);
    Time_tot_HC=N_HC*deltt;
    ave_SP_HC=mean(abs(SP_v));
    LFproc=100*ave_SP_HC/instSP;
    [AC_HC,SOC_HC,EMFR_HC] = CalcEMFR(ACb,LFproc,ave_SP_HC,[],SOCb);
    ave_SS_HC=mean(abs(SS_v));
    EF_HC_v=HC_er_v*1e-6*Patm*EMFR_HC/AirDens/R/T*MolMass./SP_v;
    ave_EF_HC=mean(EF_HC_v);
    E_HC_v=EF_HC_v.*SP_v*deltt/1000;
    total_E_HC=sum(E_HC_v);
    final_EF_HC=total_E_HC/Time_tot_HC/ave_SP_HC*1000;
    % typing the output
    disp(' ')
    disp('HC at Berth')
    disp(' ');
    fprintf(1,'date&time          SS (RPM)   SP (kW)     ER_HC (ppm)   EF_HC (g/kWh)      E_HC (kg)\n');
    for i=1:length(time_c)
        fprintf(1,'%15s   %6.1f      %6.1f     %6.2f        %6.4f           %7.4f\n',time_c{i},SS_v(i),SP_v(i),HC_er_v(i),EF_HC_v(i),E_HC_v(i));
    end
    disp(' ');
    fprintf(1,'average  EF_HC (g/kWh)=%.4f\n',ave_EF_HC);
    fprintf(1,'total  E_HC (kg)=%.5f\n',total_E_HC);
    fprintf(1,'final  EF_HC (g/kWh)=%.4f\n',final_EF_HC);
    fprintf(1,'avarage  SS_HC (RPM)=%7.3f\n',ave_SS_HC);
    fprintf(1,'avarage  SP_HC (kW)=%.3f\n',ave_SP_HC);
    fprintf(1,'avarage  LF (%%)=%.3f\n',LFproc);
    fprintf(1,'avarage  AC_HC (kg/hour)=%7.3f\n',AC_HC);
    fprintf(1,'avarage  EMFR_HC (kg/hour)=%7.3f\n',EMFR_HC);
    fprintf(1,'avarage  SOC_HC (g/kWh)=%7.3f\n',SOC_HC);
    fprintf(1,'total time Time_tot_HC (hour)=%8.5f\n',Time_tot_HC);
    fprintf(1,'count of samples N_HC (-)=%i\n',N_HC);
end
```

```
HC at Berth

date&time          SS (RPM)   SP (kW)     ER_HC (ppm)   EF_HC (g/kWh)      E_HC (kg)
6/11/2015 13:15      33.0        291.0       23.00          0.5950           0.0144
6/11/2015 13:20      47.1        906.0       22.00          0.1828           0.0138
6/11/2015 13:25      33.2        304.0       22.00          0.5448           0.0138
6/11/2015 13:30      33.2        305.0       29.00          0.7157           0.0182

average  EF_HC (g/kWh)=0.5096
total  E_HC (kg)=0.06022
final  EF_HC (g/kWh)=0.4001
avarage  SS_HC (RPM)= 36.625
avarage  SP_HC (kW)=451.500
avarage  LF (%)=6.563
avarage  AC_HC (kg/hour)=5197.500
avarage  EMFR_HC (kg/hour)=5313.849
avarage  SOC_HC (g/kWh)=257.694
total time Time_tot_HC (hour)= 0.33333
count of samples N_HC (-)=4

ans =

    0.4001
```

HC emissions for main engines at berth

```
function [final_EF_HC,total_E_HC,ave_SS_HC,ave_SP_HC,LFproc,AC_HC,EMFR_HC,SOC_HC,Time_tot_HC,N_HC]=HCcalc_man
    % HC at maneuvering
    % constants
    R=8.3144598;              % in(kg.m^2)/(K.mol.s^2)
    T=309;                    % in K
    Patm=101325;              % in Pascals
    AirDens=1.225;            % in kg/m^3
    ACb=79200;                % in kg/hour
    SOCb=208.597;             % in g/kWh
    instSP=6880;              % kW
    deltt=300/3600;           % in hours
    MolMass=44;               % in g/mol
    % measurements
    time_c={
        '6/11/2015 11:00'
        '6/11/2015 11:05'
        '6/11/2015 11:10'
        '6/11/2015 11:15'
        '6/11/2015 11:20'};
    SS_v=[81.8;81.8;81.8;81.8;77.5]; % in RPM
    SP_v=[3900;3900;3900;3900;3324]; % in kW
    HC_er_v=[14;14;14;15;15];        % in ppm
    % data processing
    N_HC=length(SP_v);
    Time_tot_HC=N_HC*deltt;
    ave_SP_HC=mean(abs(SP_v));
    LFproc=100*ave_SP_HC/instSP;
    [AC_HC,SOC_HC,EMFR_HC] = CalcEMFR(ACb,LFproc,ave_SP_HC,[],SOCb);
    ave_SS_HC=mean(abs(SS_v));
    EF_HC_v=HC_er_v*1e-6*Patm*EMFR_HC/AirDens/R/T*MolMass./SP_v;
    ave_EF_HC=mean(EF_HC_v);
    E_HC_v=EF_HC_v.*SP_v*deltt/1000;
    total_E_HC=sum(E_HC_v);
    final_EF_HC=total_E_HC/Time_tot_HC/ave_SP_HC*1000;
    % typing the output
    disp(' ')
    disp('HC maneuvering')
    disp(' ');
    fprintf(1,'date&time          SS (RPM)   SP (kW)     ER_HC (ppm)   EF_HC (g/kWh)      E_HC (kg)\n');
    for i=1:length(time_c)
        fprintf(1,'%15s   %6.1f      %6.1f     %6.2f        %6.4f           %7.4f\n',time_c{i},SS_v(i),SP_v(i),HC_er_v(i),EF_HC_v(i),E_HC_v(i));
    end
    disp(' ');
    fprintf(1,'average  EF_HC (g/kWh)=%.4f\n',ave_EF_HC);
    fprintf(1,'total  E_HC (kg)=%.4f\n',total_E_HC);
    fprintf(1,'final  EF_HC (g/kWh)=%.5f\n',final_EF_HC);
    fprintf(1,'avarage  SS_HC (RPM)=%7.3f\n',ave_SS_HC);
    fprintf(1,'avarage  SP_HC (kW)=%.3f\n',ave_SP_HC);
    fprintf(1,'avarage  LF (%%)=%.3f\n',LFproc);
    fprintf(1,'avarage  AC_HC (kg/hour)=%7.3f\n',AC_HC);
    fprintf(1,'avarage  EMFR_HC (kg/hour)=%7.3f\n',EMFR_HC);
    fprintf(1,'avarage  SOC_HC (g/kWh)=%7.3f\n',SOC_HC);
    fprintf(1,'total time Time_tot_HC (hour)=%8.5f\n',Time_tot_HC);
    fprintf(1,'count of samples N_HC (-)=%i\n',N_HC);
end
```

```
HC maneuvering

date&time          SS (RPM)   SP (kW)     ER_HC (ppm)   EF_HC (g/kWh)      E_HC (kg)
6/11/2015 11:00      81.8       3900.0      14.00          0.2257            0.0733
6/11/2015 11:05      81.8       3900.0      14.00          0.2257            0.0733
6/11/2015 11:10      81.8       3900.0      14.00          0.2257            0.0733
6/11/2015 11:15      81.8       3900.0      15.00          0.2418            0.0786
6/11/2015 11:20      77.5       3324.0      15.00          0.2837            0.0786

average  EF_HC (g/kWh)=0.2405
total  E_HC (kg)=0.3772
final  EF_HC (g/kWh)=0.23919
avarage  SS_HC (RPM)= 80.940
avarage  SP_HC (kW)=3784.800
avarage  LF (%)=55.012
avarage  AC_HC (kg/hour)=43569.209
avarage  EMFR_HC (kg/hour)=44380.113
avarage  SOC_HC (g/kWh)=214.253
total time Time_tot_HC (hour)= 0.41667
count of samples N_HC (-)=5

ans =

    0.2392
```

HC emissions for main engines at manoeuvring

```
function [final_EF_HC,total_E_HC,ave_SS_HC,ave_SP_HC,LFproc,AC_HC,EMFR_HC,SOC_HC,Time_tot_HC,N_HC]=HCcalc_cruis
    % HC at cruising
    % constants
    R=8.3144598;              % in(kg.m^2)/(K.mol.s^2)
    T=309;                    % in K
    Patm=101325;              % in Pascals
    AirDens=1.225;            % in kg/m^3
    ACb=79200;                % in kg/hour
    HOC=1150;                 % in kg/hour
    instSP=6880;              % kW
    deltt=300/3600;           % in hours
    MolMass=44;               % in g/mol
    % measurements
    time_c={
        '4/11/2015 3:30'
        '4/11/2015 3:35'
        '4/11/2015 3:40'
        '4/11/2015 3:40'
        '4/11/2015 3:50'
        '4/11/2015 3:55'
        '4/11/2015 4:00'
        '4/11/2015 4:05'
        '4/11/2015 4:10'
        '4/11/2015 4:15'
        '4/11/2015 4:20'
        '4/11/2015 4:25'
        '4/11/2015 4:30'
        '4/11/2015 4:35'
        '4/11/2015 4:40'
        '4/11/2015 4:45'
        '4/11/2015 4:50'
        '4/11/2015 4:55'
        '4/11/2015 5:00'
        '4/11/2015 5:05'
        '4/11/2015 5:10'
        '4/11/2015 5:15'
        '4/11/2015 5:20'
        '4/11/2015 5:25'
        '5/11/2015 12:15'
        '5/11/2015 12:20'
        '5/11/2015 12:25'
        '5/11/2015 12:30'
        '5/11/2015 12:35'
        '5/11/2015 12:40'
        '5/11/2015 12:45'
        '5/11/2015 12:50'
        '5/11/2015 12:55'
        '5/11/2015 13:00'
        '5/11/2015 13:05'
        '5/11/2015 13:10'
        '5/11/2015 13:15'
        '5/11/2015 13:20'
        '5/11/2015 13:25'
        '5/11/2015 13:30'
        '5/11/2015 13:35'
        '5/11/2015 13:40'
        '5/11/2015 13:45'
        '5/11/2015 13:50'
        '5/11/2015 13:55'
        '5/11/2015 14:00'
        '5/11/2015 14:05'
        '5/11/2015 14:10'
        '5/11/2015 14:15'
        '5/11/2015 14:20'
        '5/11/2015 14:25'
        '5/11/2015 14:30'
        '5/11/2015 14:35'
        '5/11/2015 14:40'
        '5/11/2015 14:45'
        '5/11/2015 14:50'
        '5/11/2015 14:55'
        '5/11/2015 15:00'
        '5/11/2015 15:05'
        '5/11/2015 15:10'
        '5/11/2015 15:15'
        '6/11/2015 11:00'
        '6/11/2015 11:05'
        '6/11/2015 11:10'};
    SS_v=[88.5;88.3;88.3;88.0;88.4;88.4;88.4;88.2;88.3;88.1;88.2;88.3;88.2 ...
        ;88.2;89.3;90.4;90.3;90.3;90.3;90.5;90.5;90.3;90.3;90.4;89.36;89.36  ...
        ;89.36;89.36;89.36;89.36;89.36;89.36;89.36;89.36;89.36;89.36;89.36 ...
        ;89.36;89.36;89.36;89.36;89.36;89.36;89.36;89.36;89.36;89.36;89.36 ...
        ;89.36;89.36;89.36;89.36;89.36;89.36;89.36;89.36;89.36;89.36;89.36 ...
        ;89.36;89.36;89.36;89.36];                                  % in RPM
    SP_v=[5651;5760;5553;5654;5714;5827;5892;5831;5861;5476;5803;5460;5758 ...
        ;5870;6193;6404;6241;5998;5909;5813;5876;5744;5716;5672;5840;5835;5788 ...
        ;5747;5803;5805;5805;5805;5805;5805;5638;5638;5638;5638;5609;5519;5518 ...
        ;5559;5478;5625;5588;5585;5472;5554;5514;5564;5618;5487;5585;5617;5465 ...
        ;5592;5701;5631;5682;5617;5615;4948;4544;4497];              % in kW
    HC_er_v=[2;4;5;5;3;3;3;3;3;4;4;4;4;5;4;4;5;3;4;6;4;7;5;5;17;15;15;14;12 ...
        ;13;13;11;11;10;12;10;12;11;12;12;11;12;11;11;10;11;11;10;11;12;11;11;11 ...
        ;11;12;9;11;9;9;9;8;14;14;14];                              % in ppm
    % data processing
    N_HC=length(SP_v);
    Time_tot_HC=N_HC*deltt;
    ave_SP_HC=mean(abs(SP_v));
    LFproc=100*ave_SP_HC/instSP;
    [AC_HC,SOC_HC,EMFR_HC] = CalcEMFR(ACb,LFproc,ave_SP_HC,HOC);
    ave_SS_HC=mean(abs(SS_v));
    EF_HC_v=HC_er_v*1e-6*Patm*EMFR_HC/AirDens/R/T*MolMass./SP_v;
    ave_EF_HC=mean(EF_HC_v);
    E_HC_v=EF_HC_v.*SP_v*deltt/1000;
    total_E_HC=sum(E_HC_v);
    final_EF_HC=total_E_HC/Time_tot_HC/ave_SP_HC*1000;
    % typing the output
    disp(' ')
    disp('HC cruising')
    disp(' ');
    fprintf(1,'date&time           SS (RPM)   SP (kW)     ER_HC (ppm)   EF_HC (g/kWh)      E_HC (kg)\n');
    for i=1:length(time_c)
        fprintf(1,'%15s   %6.1f       %6.1f     %6.2f         %6.4f            %7.4f\n',time_c{i},SS_v(i),SP_v(i),HC_er_v(i),EF_HC_v(i),E_HC_v(i));
    end
    disp(' ');
    fprintf(1,'average  EF_HC (g/kWh)=%.4f\n',ave_EF_HC);
    fprintf(1,'total  E_HC (kg)=%.4f\n',total_E_HC);
    fprintf(1,'final  EF_HC (g/kWh)=%.5f\n',final_EF_HC);
```

HC cruising

date&time	SS (RPM)	SP (kW)	ER_HC (ppm)	EF_HC (g/kWh)	E_HC (kg
4/11/2015 3:30	88.5	5651.0	2.00	0.0333	0.0157
4/11/2015 3:35	88.3	5760.0	4.00	0.0653	0.0313
4/11/2015 3:40	88.3	5553.0	5.00	0.0846	0.0392
4/11/2015 3:40	88.0	5654.0	5.00	0.0831	0.0392
4/11/2015 3:50	88.4	5714.0	3.00	0.0493	0.0235
4/11/2015 3:55	88.4	5827.0	3.00	0.0484	0.0235
4/11/2015 4:00	88.4	5892.0	3.00	0.0479	0.0235
4/11/2015 4:05	88.2	5831.0	3.00	0.0484	0.0235
4/11/2015 4:10	88.3	5861.0	3.00	0.0481	0.0235
4/11/2015 4:15	88.1	5476.0	4.00	0.0686	0.0313
4/11/2015 4:20	88.2	5803.0	4.00	0.0648	0.0313
4/11/2015 4:25	88.3	5460.0	4.00	0.0689	0.0313
4/11/2015 4:30	88.2	5758.0	4.00	0.0653	0.0313
4/11/2015 4:35	88.2	5870.0	5.00	0.0801	0.0392
4/11/2015 4:40	89.3	6193.0	4.00	0.0607	0.0313
4/11/2015 4:45	90.4	6404.0	4.00	0.0587	0.0313
4/11/2015 4:50	90.3	6241.0	5.00	0.0753	0.0392
4/11/2015 4:55	90.3	5998.0	3.00	0.0470	0.0235
4/11/2015 5:00	90.3	5909.0	4.00	0.0636	0.0313
4/11/2015 5:05	90.5	5813.0	6.00	0.0970	0.0470
4/11/2015 5:10	90.5	5876.0	4.00	0.0640	0.0313
4/11/2015 5:15	90.3	5744.0	7.00	0.1145	0.0548
4/11/2015 5:20	90.3	5716.0	5.00	0.0822	0.0392
4/11/2015 5:25	90.4	5672.0	5.00	0.0828	0.0392
5/11/2015 12:15	89.4	5840.0	17.00	0.2736	0.1331
5/11/2015 12:20	89.4	5835.0	15.00	0.2416	0.1175
5/11/2015 12:25	89.4	5788.0	15.00	0.2436	0.1175
5/11/2015 12:30	89.4	5747.0	14.00	0.2289	0.1096
5/11/2015 12:35	89.4	5803.0	12.00	0.1943	0.0940
5/11/2015 12:40	89.4	5805.0	13.00	0.2105	0.1018
5/11/2015 12:45	89.4	5805.0	13.00	0.2105	0.1018
5/11/2015 12:50	89.4	5805.0	11.00	0.1781	0.0861
5/11/2015 12:55	89.4	5805.0	11.00	0.1781	0.0861
5/11/2015 13:00	89.4	5805.0	10.00	0.1619	0.0783
5/11/2015 13:05	89.4	5638.0	12.00	0.2000	0.0940
5/11/2015 13:10	89.4	5638.0	10.00	0.1667	0.0783
5/11/2015 13:15	89.4	5638.0	12.00	0.2000	0.0940
5/11/2015 13:20	89.4	5638.0	11.00	0.1834	0.0861
5/11/2015 13:25	89.4	5609.0	12.00	0.2011	0.0940
5/11/2015 13:30	89.4	5519.0	12.00	0.2043	0.0940
5/11/2015 13:35	89.4	5518.0	11.00	0.1873	0.0861
5/11/2015 13:40	89.4	5559.0	12.00	0.2029	0.0940
5/11/2015 13:45	89.4	5478.0	11.00	0.1887	0.0861
5/11/2015 13:50	89.4	5625.0	11.00	0.1838	0.0861
5/11/2015 13:55	89.4	5588.0	10.00	0.1682	0.0783
5/11/2015 14:00	89.4	5585.0	11.00	0.1851	0.0861
5/11/2015 14:05	89.4	5472.0	11.00	0.1889	0.0861
5/11/2015 14:10	89.4	5554.0	10.00	0.1692	0.0783
5/11/2015 14:15	89.4	5514.0	11.00	0.1875	0.0861
5/11/2015 14:20	89.4	5564.0	12.00	0.2027	0.0940
5/11/2015 14:25	89.4	5618.0	11.00	0.1840	0.0861
5/11/2015 14:30	89.4	5487.0	11.00	0.1884	0.0861
5/11/2015 14:35	89.4	5585.0	11.00	0.1851	0.0861
5/11/2015 14:40	89.4	5617.0	11.00	0.1840	0.0861
5/11/2015 14:45	89.4	5465.0	12.00	0.2064	0.0940
5/11/2015 14:50	89.4	5592.0	9.00	0.1513	0.0705
5/11/2015 14:55	89.4	5701.0	11.00	0.1813	0.0861
5/11/2015 15:00	89.4	5631.0	9.00	0.1502	0.0705
5/11/2015 15:05	89.4	5682.0	9.00	0.1489	0.0705
5/11/2015 15:10	89.4	5617.0	9.00	0.1506	0.0705
5/11/2015 15:15	89.4	5615.0	8.00	0.1339	0.0627
6/11/2015 11:00	89.4	4948.0	14.00	0.2659	0.1096
6/11/2015 11:05	89.4	4544.0	14.00	0.2896	0.1096
6/11/2015 11:10	89.4	4497.0	14.00	0.2926	0.1096

```
average  EF_HC (g/kWh)=0.1477
total  E_HC (kg)=4.4014
final  EF_HC (g/kWh)=0.14572
avarage  SS_HC (RPM)= 89.262
avarage  SP_HC (kW)=5663.281
avarage  LF (%)=82.315
avarage  AC_HC (kg/hour)=65193.586
avarage  EMFR_HC (kg/hour)=66343.586
avarage  SOC_HC (g/kWh)=203.062
total time Time_tot_HC (hour)= 5.33333
count of samples N_HC (-)=64

ans =

    0.1457
```

HC emissions for main engines at cruising

```
    CO2_deluted_2_5_v=CO2_deluted_v(ind_2_5_v);
    CO2_background_2_5_v=CO2_background_v(ind_2_5_v);
    deluted_PM_2_5_er_v=PM_2_5_er_v.*(CO2_raw_2_5_v-CO2_background_2_5_v)./(CO2_deluted_2_5_v-CO2_background_2_5_v);
    EF_PM_2_5_v=EMFR_2_5*deluted_PM_2_5_er_v./SP_2_5_v/1000/AirDens;
    % typing the PM1.0-2.5 output
    disp(' ')
    disp('PM1.0-2.5 at Berth')
    disp(' ')
    fprintf(1,'date&time           SP (kW)     ER_PM (mg/m^3)  Deluted_ER_PM (mg/m^3)    EF_PM_1.0-2.5 (g/kWh)\n');
    for i=1:length(time_2_5_c)
        fprintf(1,'%15s    %6.1f       %.3f           %6.2f                    %.3f\n',time_2_5_c{i},SP_2_5_v(i),PM_2_5_er_v(i),deluted_PM_2_5_er_v(i),EF_PM_2_5_v(i));
    end
    disp(' ')
    ave_EF_PM_2_5=mean(EF_PM_2_5_v);
    fprintf(1,'average  EF_PM_1.0-2.5 (g/kWh)=%.3f\n',ave_EF_PM_2_5);
    fprintf(1,'avarage  AC_PM_1.0-2.5 (kg/hour)=%7.3f\n',AC_2_5);
    fprintf(1,'average  EMFR_1.0-2.5 (kg/hour)=%.3f\n',EMFR_2_5);
    fprintf(1,'avarage  SOC_1.0-2.5 (g/kWh)=%7.3f\n',SOC_2_5);
    % data processing General
    N_PM=length(SP_v);
    Time_tot_PM=N_PM*deltt;
    ave_SP_PM=mean(abs(SP_v));
    LFproc=100*ave_SP_PM/instSP;
    [AC_PM,SOC_PM,EMFR_PM] = CalcEMFR(ACb,LFproc,ave_SP_PM,[],SOCb);
    ave_SS_PM=mean(abs(SS_v));
    EF_PM_v=[EF_PM_1_0_v+ave_EF_PM_2_5;EF_PM_2_5_v+ave_EF_PM_1_0];
    EF_PM_v=EF_PM_v/.8;
    ave_EF_PM=mean(EF_PM_v);
    E_PM_v=EF_PM_v.*SP_v*deltt/1000;
    total_E_PM=sum(E_PM_v);
    final_EF_PM=total_E_PM/Time_tot_PM/ave_SP_PM*1000;
    % typing the General output
    disp(' ')
    disp('PM at Berth')
    disp(' ')
    fprintf(1,'date&time           SS (RPM) SP (kW)   EF_PM (g/kWh)     E_PM (kg)\n');
    for i=1:length(time_c)
        fprintf(1,'%15s   %6.1f     %6.1f    %.3f             %.3f\n',time_c{i},SS_v(i),SP_v(i),EF_PM_v(i),E_PM_v(i));
    end
    disp(' ');
    fprintf(1,'average  EF_PM (g/kWh)=%.4f\n',ave_EF_PM);
    fprintf(1,'total  E_PM (kg)=%.5f\n',total_E_PM);
    fprintf(1,'final  EF_PM (g/kWh)=%.4f\n',final_EF_PM);
    fprintf(1,'avarage  SS_PM (RPM)=%7.3f\n',ave_SS_PM);
    fprintf(1,'avarage  SP_PM (kW)=%.3f\n',ave_SP_PM);
    fprintf(1,'avarage  LF (%%)=%.3f\n',LFproc);
    fprintf(1,'avarage  AC_PM (kg/hour)=%7.3f\n',AC_PM);
    fprintf(1,'avarage  EMFR_PM (kg/hour)=%7.3f\n',EMFR_PM);
    fprintf(1,'avarage  SOC_PM (g/kWh)=%7.3f\n',SOC_PM);
    fprintf(1,'total time Time_tot_PM (hour)=%8.5f\n',Time_tot_PM);
    fprintf(1,'count of samples N_PM (-)=%i\n',N_PM);
end
```

```
function [final_EF_PM,total_E_PM,ave_SS_PM,ave_SP_PM,LFproc,AC_PM,EMFR_PM,SOC_PM,Time_tot_PM,N_PM]=PMcalc_BE
    % PM at berth
    % constants
    AirDens=1.225;                          % in kg/m^3
    ACb=79200;                              % in kg/hour
    SOCb=208.597;                           % in g/kWh
    instSP=6880;                            % kW
    deltt=300/3600;                         % in hours
    % measurements
    time_c={
        '6/11/2015 13:10'
        '6/11/2015 13:15'
        '6/11/2015 13:20'
        '6/11/2015 13:25'
        '6/11/2015 13:30'};
    SS_v=[52.5;33.0;47.1;33.2;33.2];        % in RPM
    SP_v=[1085;291;906;304;305];            % in kW
    CO2_raw_v=2.85*ones(5,1);               % in %
    CO2_deluted_v=[0.23;0.25;0.12;0.14;0.13];  % in %
    CO2_background_v=0.03*ones(5,1);        % in %
    %
    % Data Procesing PM1.0
    PM_1_0_er_v=[1.49;3.2;3.54];            % in mg/m^3
    ind_1_0_v=[1 1 1 0 0]'==1;
    ave_SP_1_0=mean(SP_v(ind_1_0_v));
    LFproc_1_0=100*ave_SP_1_0/instSP;
    [AC_1_0,SOC_1_0,EMFR_1_0] = CalcEMFR(ACb,LFproc_1_0,ave_SP_1_0,[],SOCb);
    time_1_0_c=time_c(ind_1_0_v);
    SP_1_0_v=SP_v(ind_1_0_v);
    CO2_raw_1_0_v=CO2_raw_v(ind_1_0_v);
    CO2_deluted_1_0_v=CO2_deluted_v(ind_1_0_v);
    CO2_background_1_0_v=CO2_background_v(ind_1_0_v);
    deluted_PM_1_0_er_v=PM_1_0_er_v.*(CO2_raw_1_0_v-CO2_background_1_0_v)./(CO2_deluted_1_0_v-CO2_background_1_0_v);
    EF_PM_1_0_v=EMFR_1_0*deluted_PM_1_0_er_v./SP_1_0_v/1000/AirDens;
    % typing the PM1.0 output
    disp(' ')
    disp('PM1.0 at Berth')
    disp(' ')
    fprintf(1,'date&time         SP (kW)       ER_PM (mg/m^3)  Deluted_ER_PM (mg/m^3)    EF_PM_1.0 (g/kWh)\n');
    for i=1:length(time_1_0_c)
        fprintf(1,'%15s   %6.1f       %.3f           %6.2f                    %.3f\n',time_1_0_c{i},SP_1_0_v(i),PM_1_0_er_v(i),deluted_PM_1_0_er_v(i),EF_PM_1_0_v(i));
    end
    disp(' ')
    ave_EF_PM_1_0=mean(EF_PM_1_0_v);
    fprintf(1,'average  EF_PM_1_0 (g/kWh)=%.3f\n',ave_EF_PM_1_0);
    fprintf(1,'avarage  AC_PM_1.0 (kg/hour)=%7.3f\n',AC_1_0);
    fprintf(1,'average  EMFR_1.0 (kg/hour)=%.3f\n',EMFR_1_0);
    fprintf(1,'avarage  SOC_1.0 (g/kWh)=%7.3f\n',SOC_1_0);
    % Data Procesing PM1.0-2.5
    PM_2_5_er_v=[5.5;3.87];                 % in mg/m^3
    ind_2_5_v=[0 0 0 1 1]'==1;
    ave_SP_2_5=mean(SP_v(ind_2_5_v));
    LFproc_2_5=100*ave_SP_2_5/instSP;
    [AC_2_5,SOC_2_5,EMFR_2_5] = CalcEMFR(ACb,LFproc_2_5,ave_SP_2_5,[],SOCb);
    time_2_5_c=time_c(ind_2_5_v);
    SP_2_5_v=SP_v(ind_2_5_v);
    CO2_raw_2_5_v=CO2_raw_v(ind_2_5_v);
```

PM1.0 at Berth

date&time	SP (kW)	ER_PM (mg/m^3)	Deluted_ER_PM (mg/m^3)	EF_PM_1.0 (g/kWh)
6/11/2015 11:00	3900.0	1.620	17.86	0.128
6/11/2015 11:05	3900.0	1.530	16.01	0.115
6/11/2015 11:10	3900.0	1.110	12.58	0.090
6/11/2015 11:15	3900.0	1.470	17.64	0.127
6/11/2015 11:20	3324.0	1.630	20.15	0.170
6/11/2015 11:25	3388.0	1.540	18.48	0.153
6/11/2015 11:30	3456.0	1.550	18.60	0.151
6/11/2015 12:05	1282.0	5.900	96.16	2.101
6/11/2015 12:10	2188.0	2.370	37.58	0.481
6/11/2015 12:15	4170.0	1.100	17.24	0.116
6/11/2015 12:20	2050.0	1.030	24.64	0.337
6/11/2015 13:05	876.0	3.110	64.21	2.053
6/11/2015 13:10	1690.0	1.490	27.94	0.463

average EF_PM_1_0 (g/kWh)=0.499
avarage AC_PM_1.0 (kg/hour)=33670.626
average EMFR_1.0 (kg/hour)=34317.603
avarage SOC_1.0 (g/kWh)=221.194

PM1.0-2.5 at Berth

date&time	SP (kW)	ER_PM (mg/m^3)	Deluted_ER_PM (mg/m^3)	EF_PM_1.0-2.5 (g/kWh)
6/11/2015 11:35	1863.0	2.140	41.49	0.427
6/11/2015 11:40	650.0	2.140	41.49	1.224
6/11/2015 11:45	773.0	6.700	85.39	2.118
6/11/2015 11:50	2266.0	2.150	27.40	0.232
6/11/2015 11:55	775.0	6.070	98.93	2.448
6/11/2015 12:00	799.0	7.040	114.74	2.754
6/11/2015 12:25	3764.0	1.170	18.40	0.094
6/11/2015 12:30	3626.0	1.050	28.63	0.151
6/11/2015 12:35	3596.0	1.250	26.91	0.143
6/11/2015 12:40	1890.0	2.680	47.66	0.484

average EF_PM_1.0-2.5 (g/kWh)=1.007
avarage AC_PM_1.0-2.5 (kg/hour)=23025.558
average EMFR_1.0-2.5 (kg/hour)=23489.542
avarage SOC_1.0-2.5 (g/kWh)=231.969

PM2.5-10 at Berth

date&time	SP (kW)	ER_PM (mg/m^3)	Deluted_ER_PM (mg/m^3)	EF_PM_2.5-10 (g/kWh)
6/11/2015 12:45	3796.0	1.620	28.81	0.247
6/11/2015 12:50	2306.0	1.730	41.62	0.588
6/11/2015 12:55	3348.0	5.150	61.95	0.602
6/11/2015 13:00	4151.0	1.640	26.83	0.210

average EF_PM_2.5-10 (g/kWh)=0.412
avarage AC_PM_2.5-10 (kg/hour)=39142.413
average EMFR_2.5-10 (kg/hour)=39880.235
avarage SOC_2.5-10 (g/kWh)=216.991

PM emissions for main engines at berth

```
function [final_EF_PM,total_E_PM,ave_SS_PM,ave_SP_PM,LFproc,AC_PM,EMFR_PM,SOC_PM,Time_tot_PM,N_PM]=PMcalc_man
    % PM maneuvering
    % constants
    AirDens=1.225;                              % in kg/m^3
    ACb=79200;                                  % in kg/hour
    SOCb=208.597;                               % in g/kWh
    instSP=6880;                                % kW
    deltt=300/3600;                             % in hours
    % measurements
    time_c={
        '6/11/2015 11:00'
        '6/11/2015 11:05'
        '6/11/2015 11:10'
        '6/11/2015 11:15'
        '6/11/2015 11:20'
        '6/11/2015 11:25'
        '6/11/2015 11:30'
        '6/11/2015 11:35'
        '6/11/2015 11:40'
        '6/11/2015 11:45'
        '6/11/2015 11:50'
        '6/11/2015 11:55'
        '6/11/2015 12:00'
        '6/11/2015 12:05'
        '6/11/2015 12:10'
        '6/11/2015 12:15'
        '6/11/2015 12:20'
        '6/11/2015 12:25'
        '6/11/2015 12:30'
        '6/11/2015 12:35'
        '6/11/2015 12:40'
        '6/11/2015 12:45'
        '6/11/2015 12:50'
        '6/11/2015 12:55'
        '6/11/2015 13:00'
        '6/11/2015 13:05'
        '6/11/2015 13:10'};
    SS_v=[81.8;81.8;81.8;81.8;77.5;77.6;77.2;63;46;45.1;63.8;47.1;46.8;53.2 ...
        ;63.6;78.1;63.5;78.1;78.1;78.2;63.9;78.1;67.8;74.2;78.2;46.5;58.9]; % in RPM
    SP_v=[3900;3900;3900;3900;3900;3324;3388;3456;1863;650;773;2266;775;799;1282 ...
        ;2188;4170;2050;3764;3626;3596;1890;3796;2306;3348;4151;876;1690];  % in kW
    CO2_raw_v=4.12*ones(27,1);                                              % in %
    CO2_deluted_v=[.4;.42;.39;.37;.36;.37;.37;.24;.24;.35;.35;.28;.28;.28 ...
        ;.287;.29;.2;.29;.18;.22;.26;.26;.2;.37;.28;.23;.25];               % in %
    CO2_background_v=[.029*ones(17,1);.03*ones(8,1);.032;.032];             % in %    %
    % Data Procesing PM1.0
    PM_1_0_er_v=[1.62;1.53;1.11;1.47;1.63;1.54;1.55 ...
        ;5.9;2.37;1.1;1.03;3.11;1.49];                                      % in mg/m^3
    ind_1_0_v=[1 1 1 1 1 1 1 0 0 0 0 0 0 1 1 1 1 0 0 0 0 0 0 0 0 1 1]'==1;
    ave_SP_1_0=mean(SP_v(ind_1_0_v));
    LFproc_1_0=100*ave_SP_1_0/instSP;
    [AC_1_0,SOC_1_0,EMFR_1_0] = CalcEMFR(ACb,LFproc_1_0,ave_SP_1_0,[],SOCb);
    time_1_0_c=time_c(ind_1_0_v);
    SP_1_0_v=SP_v(ind_1_0_v);
    CO2_raw_1_0_v=CO2_raw_v(ind_1_0_v);
    CO2_deluted_1_0_v=CO2_deluted_v(ind_1_0_v);
    CO2_background_1_0_v=CO2_background_v(ind_1_0_v);
```

```
deluted_PM_1_0_er_v=PM_1_0_er_v.*(CO2_raw_1_0_v-CO2_background_1_0_v)./(CO2_deluted_1_0_v-CO2_background_1_0_v);
EF_PM_1_0_v=EMFR_1_0*deluted_PM_1_0_er_v./SP_1_0_v/1000/AirDens;
% typing the PM1.0 output
disp(' ')
disp('PM1.0 at Berth')
disp(' ')
fprintf(1,'date&time         SP (kW)       ER_PM (mg/m^3)  Deluted_ER_PM (mg/m^3)    EF_PM_1.0 (g/kWh)\n');
for i=1:length(time_1_0_c)
    fprintf(1,'%15s   %6.1f        %.3f           %6.2f                    %.3f\n',time_1_0_c{i},SP_1_0_v(i),PM_1_0_er_v(i),deluted_PM_1_0_er_v(i),EF_PM_1_0_v(i));
end
disp(' ')
ave_EF_PM_1_0=mean(EF_PM_1_0_v);
fprintf(1,'average  EF_PM_1_0 (g/kWh)=%.3f\n',ave_EF_PM_1_0);
fprintf(1,'avarage  AC_PM_1.0 (kg/hour)=%7.3f\n',AC_1_0);
fprintf(1,'average  EMFR_1.0 (kg/hour)=%.3f\n',EMFR_1_0);
fprintf(1,'avarage  SOC_1.0 (g/kWh)=%7.3f\n',SOC_1_0);
% Data Procesing PM1.0-2.5
PM_2_5_er_v=[2.14;2.14;6.7;2.15;6.07;7.04;1.17;1.05;1.25;2.68];         % in mg/m^3
ind_2_5_v=[0 0 0 0 0 0 0 1 1 1 1 1 1 1 0 0 0 0 0 1 1 1 1 1 0 0 0 0 0 0]'==1;
ave_SP_2_5=mean(SP_v(ind_2_5_v));
LFproc_2_5=100*ave_SP_2_5/instSP;
[AC_2_5,SOC_2_5,EMFR_2_5] = CalcEMFR(ACb,LFproc_2_5,ave_SP_2_5,[],SOCb);
time_2_5_c=time_c(ind_2_5_v);
SP_2_5_v=SP_v(ind_2_5_v);
CO2_raw_2_5_v=CO2_raw_v(ind_2_5_v);
CO2_deluted_2_5_v=CO2_deluted_v(ind_2_5_v);
CO2_background_2_5_v=CO2_background_v(ind_2_5_v);
deluted_PM_2_5_er_v=PM_2_5_er_v.*(CO2_raw_2_5_v-CO2_background_2_5_v)./(CO2_deluted_2_5_v-CO2_background_2_5_v);
EF_PM_2_5_v=EMFR_2_5*deluted_PM_2_5_er_v./SP_2_5_v/1000/AirDens;
% typing the PM1.0-2.5 output
disp(' ')
disp('PM1.0-2.5 at Berth')
disp(' ')
fprintf(1,'date&time          SP (kW)     ER_PM (mg/m^3)  Deluted_ER_PM (mg/m^3)    EF_PM_1.0-2.5 (g/kWh)\n');
for i=1:length(time_2_5_c)
    fprintf(1,'%15s    %6.1f       %.3f           %6.2f                    %.3f\n',time_2_5_c{i},SP_2_5_v(i),PM_2_5_er_v(i),deluted_PM_2_5_er_v(i),EF_PM_2_5_v(i));
end
disp(' ')
ave_EF_PM_2_5=mean(EF_PM_2_5_v);
fprintf(1,'average  EF_PM_1.0-2.5 (g/kWh)=%.3f\n',ave_EF_PM_2_5);
fprintf(1,'avarage  AC_PM_1.0-2.5 (kg/hour)=%7.3f\n',AC_2_5);
fprintf(1,'average  EMFR_1.0-2.5 (kg/hour)=%.3f\n',EMFR_2_5);
fprintf(1,'avarage  SOC_1.0-2.5 (g/kWh)=%7.3f\n',SOC_2_5);
% Data Procesing PM2.5-10
PM_10_0_er_v=[1.62;1.73;5.15;1.64];                                     % in mg/m^3
ind_10_0_v=[0 0 0 0 0 0 0 0 0 0 0 0 0 0 0 0 0 0 0 0 0 0 0 1 1 1 1 1 0 0]'==1;
ave_SP_10_0=mean(SP_v(ind_10_0_v));
LFproc_10_0=100*ave_SP_10_0/instSP;
[AC_10_0,SOC_10_0,EMFR_10_0] = CalcEMFR(ACb,LFproc_10_0,ave_SP_10_0,[],SOCb);
time_10_0_c=time_c(ind_10_0_v);
SP_10_0_v=SP_v(ind_10_0_v);
CO2_raw_10_0_v=CO2_raw_v(ind_10_0_v);
CO2_deluted_10_0_v=CO2_deluted_v(ind_10_0_v);
CO2_background_10_0_v=CO2_background_v(ind_10_0_v);
deluted_PM_10_0_er_v=PM_10_0_er_v.*(CO2_raw_10_0_v-CO2_background_10_0_v)./(CO2_deluted_10_0_v-CO2_background_10_0_v);
EF_PM_10_0_v=EMFR_10_0*deluted_PM_10_0_er_v./SP_10_0_v/1000/AirDens;
% typing the PM2.5-10 output
disp(' ')
```

```
    disp('PM2.5-10 at Berth')
    disp(' ')
    fprintf(1,'date&time          SP (kW)     ER_PM (mg/m^3)  Deluted_ER_PM (mg/m^3)    EF_PM_2.5-10 (g/kWh)\n');
    for i=1:length(time_10_0_c)
        fprintf(1,'%15s    %6.1f       %.3f           %6.2f                    %.3f\n',time_10_0_c{i},SP_10_0_v(i),PM_10_0_er_v(i),deluted_PM_10_0_er_v(i),EF_PM_10_0_v(i));
    end
    disp(' ')
    ave_EF_PM_10_0=mean(EF_PM_10_0_v);
    fprintf(1,'average  EF_PM_2.5-10 (g/kWh)=%.3f\n',ave_EF_PM_10_0);
    fprintf(1,'avarage  AC_PM_2.5-10 (kg/hour)=%7.3f\n',AC_10_0);
    fprintf(1,'average  EMFR_2.5-10 (kg/hour)=%.3f\n',EMFR_10_0);
    fprintf(1,'avarage  SOC_2.5-10 (g/kWh)=%7.3f\n',SOC_10_0);
    % data processing General
    N_PM=length(SP_v);
    Time_tot_PM=N_PM*deltt;
    ave_SP_PM=mean(abs(SP_v));
    LFproc=100*ave_SP_PM/instSP;
    [AC_PM,SOC_PM,EMFR_PM] = CalcEMFR(ACb,LFproc,ave_SP_PM,[],SOCb);
    ave_SS_PM=mean(abs(SS_v));
    EF_PM_v=[(EF_PM_1_0_v+ave_EF_PM_2_5)/.8;(EF_PM_2_5_v+ave_EF_PM_1_0);EF_PM_10_0_v+ave_EF_PM_1_0+ave_EF_PM_2_5];
    ave_EF_PM=mean(EF_PM_v);
    E_PM_v=EF_PM_v.*SP_v*deltt/1000;
    total_E_PM=sum(E_PM_v);
    final_EF_PM=total_E_PM/Time_tot_PM/ave_SP_PM*1000;
    % typing the General output
    disp(' ')
    disp('PM maneuvering')
    disp(' ')
    fprintf(1,'date&time          SS (RPM) SP (kW)   EF_PM (g/kWh)     E_PM (kg)\n');
    for i=1:length(time_c)
        fprintf(1,'%15s   %6.1f     %6.1f    %.3f            %.3f\n',time_c{i},SS_v(i),SP_v(i),EF_PM_v(i),E_PM_v(i));
    end
    disp(' ');
    fprintf(1,'average  EF_PM (g/kWh)=%.4f\n',ave_EF_PM);
    fprintf(1,'total  E_PM (kg)=%.5f\n',total_E_PM);
    fprintf(1,'final  EF_PM (g/kWh)=%.4f\n',final_EF_PM);
    fprintf(1,'avarage  SS_PM (RPM)=%7.3f\n',ave_SS_PM);
    fprintf(1,'avarage  SP_PM (kW)=%.3f\n',ave_SP_PM);
    fprintf(1,'avarage  LF (%%)=%.3f\n',LFproc);
    fprintf(1,'avarage  AC_PM (kg/hour)=%7.3f\n',AC_PM);
    fprintf(1,'avarage  EMFR_PM (kg/hour)=%7.3f\n',EMFR_PM);
    fprintf(1,'avarage  SOC_PM (g/kWh)=%7.3f\n',SOC_PM);
    fprintf(1,'total time Time_tot_PM (hour)=%8.5f\n',Time_tot_PM);
    fprintf(1,'count of samples N_PM (-)=%i\n',N_PM);
end
```

```
PM maneuvering

date&time          SS (RPM) SP (kW)   EF_PM (g/kWh)     E_PM (kg)
6/11/2015 11:00     81.8     3900.0    1.420             0.461
6/11/2015 11:05     81.8     3900.0    1.403             0.456
6/11/2015 11:10     81.8     3900.0    1.372             0.446
6/11/2015 11:15     81.8     3900.0    1.418             0.461
6/11/2015 11:20     77.5     3324.0    1.472             0.408
6/11/2015 11:25     77.6     3388.0    1.450             0.409
6/11/2015 11:30     77.2     3456.0    1.448             0.417
6/11/2015 11:35     63.0     1863.0    3.886             0.603
6/11/2015 11:40     46.0      650.0    1.861             0.101
6/11/2015 11:45     45.1      773.0    1.404             0.090
6/11/2015 11:50     63.8     2266.0    1.680             0.317
6/11/2015 11:55     47.1      775.0    3.826             0.247
6/11/2015 12:00     46.8      799.0    1.838             0.122
6/11/2015 12:05     53.2     1282.0    0.926             0.099
6/11/2015 12:10     63.6     2188.0    1.723             0.314
6/11/2015 12:15     78.1     4170.0    2.617             0.909
6/11/2015 12:20     63.5     2050.0    0.731             0.125
6/11/2015 12:25     78.1     3764.0    2.947             0.924
6/11/2015 12:30     78.1     3626.0    3.253             0.983
6/11/2015 12:35     78.2     3596.0    0.593             0.178
6/11/2015 12:40     63.9     1890.0    0.650             0.102
6/11/2015 12:45     78.1     3796.0    0.642             0.203
6/11/2015 12:50     67.8     2306.0    0.982             0.189
6/11/2015 12:55     74.2     3348.0    1.753             0.489
6/11/2015 13:00     78.2     4151.0    2.094             0.724
6/11/2015 13:05     46.5      876.0    2.109             0.154
6/11/2015 13:10     58.9     1690.0    1.717             0.242

average  EF_PM (g/kWh)=1.7487
total  E_PM (kg)=10.17525
final  EF_PM (g/kWh)=1.7047
avarage  SS_PM (RPM)= 67.841
avarage  SP_PM (kW)=2652.852
avarage  LF (%)=38.559
avarage  AC_PM (kg/hour)=30538.643
avarage  EMFR_PM (kg/hour)=31132.904
avarage  SOC_PM (g/kWh)=224.008
total time Time_tot_PM (hour)= 2.25000
count of samples N_PM (-)=27

ans =

    1.7047
```

PM emissions for main engines at manoeuvring

```
function [final_EF_PM,total_E_PM,ave_SS_PM,ave_SP_PM,LFproc,AC_PM,EMFR_PM,SOC_PM,Time_tot_PM,N_PM]=PMcalc_cruis
    % PM cruising
    % constants
    AirDens=1.225;                          % in kg/m^3
    ACb=79200;                              % in kg/hour
    HOC=1150;                               % in kg/hour
    instSP=6880;                            % kW
    deltt=300/3600;                         % in hours
    % measurements
    time_c={
        '4/11/2015 3:30'
        '4/11/2015 3:35'
        '4/11/2015 3:40'
        '4/11/2015 3:40'
        '4/11/2015 3:50'
        '4/11/2015 3:55'
        '4/11/2015 4:00'
        '4/11/2015 4:05'
        '4/11/2015 4:10'
        '4/11/2015 4:15'
        '4/11/2015 4:20'
        '4/11/2015 4:25'
        '4/11/2015 4:30'
        '4/11/2015 4:35'
        '4/11/2015 4:40'
        '4/11/2015 4:45'
        '4/11/2015 4:50'
        '4/11/2015 4:55'
        '4/11/2015 5:00'
        '4/11/2015 5:05'
        '4/11/2015 5:10'
        '4/11/2015 5:15'
        '4/11/2015 5:20'
        '4/11/2015 5:25'
        '5/11/2015 12:15'
        '5/11/2015 12:20'
        '5/11/2015 12:25'
        '5/11/2015 12:30'
        '5/11/2015 12:35'
        '5/11/2015 12:40'
        '5/11/2015 12:45'
        '5/11/2015 12:50'
        '5/11/2015 12:55'
        '5/11/2015 13:00'
        '5/11/2015 13:05'
        '5/11/2015 13:10'
        '5/11/2015 13:15'
        '5/11/2015 13:20'
        '5/11/2015 13:25'
        '5/11/2015 13:30'
        '5/11/2015 13:35'
        '5/11/2015 13:40'
        '5/11/2015 13:45'
        '5/11/2015 13:50'
        '5/11/2015 13:55'
        '5/11/2015 14:00'
        '5/11/2015 14:05'
        '5/11/2015 14:10'
        '5/11/2015 14:15'
        '5/11/2015 14:20'
        '5/11/2015 14:25'
        '5/11/2015 14:30'
        '5/11/2015 14:35'
        '5/11/2015 14:40'
        '5/11/2015 14:45'
        '5/11/2015 14:50'
        '5/11/2015 14:55'
        '5/11/2015 15:00'
        '5/11/2015 15:05'
        '5/11/2015 15:10'
        '5/11/2015 15:15'
        '6/11/2015 11:00'
        '6/11/2015 11:05'
        '6/11/2015 11:10'};
    SS_v=[88.5;88.3;88.3;88.0;88.4;88.4;88.4;88.2;88.3;88.1;88.2;88.3;88.2 ...
        ;88.2;89.3;90.4;90.3;90.3;90.3;90.5;90.5;90.3;90.3;90.4;89.36;89.36    ...
        ;89.36;89.36;89.36;89.36;89.36;89.36;89.36;89.36;89.36;89.36;89.36   ...
        ;89.36;89.36;89.36;89.36;89.36;89.36;89.36;89.36;89.36;89.36;89.36  ...
        ;89.36;89.36;89.36;89.36;89.36;89.36;89.36;89.36;89.36;89.36;89.36   ...
        ;89.36;89.36;89.36;89.36;89.3600];                                  % in RPM
    SP_v=[5651.0;5760.0;5553.0;5654.0;5714.0;5827.0;5892.0;5831.0;5861.0  ...
        ;5476.0;5803.0;5460.0;5758.0;5870.0;6193.0;6404.0;6241.0;5998.0;5909.0 ...
        ;5813.0;5876.0;5744.0;5716.0;5672.0;5840.0;5835.0;5788.0;5747.0;5803.0  ...
        ;5805.0;5805.0;5805.0;5805.0;5805.0;5638.0;5638.0;5638.0;5638.0;5609.0  ...
        ;5519.0;5518.0;5559.0;5478.0;5625.0;5588.0;5585.0;5472.0;5554.0;5514.0  ...
        ;5564.0;5618.0;5487.0;5585.0;5617.0;5465.0;5592.0;5701.0;5631.0;5682.0  ...
        ;5617.0;5615.0;4948.0;4544.0;4497.0];                               % in kW
    CO2_raw_v=4.53*ones(64,1);                                              % in %
    CO2_deluted_v=[0.39;0.38;0.38;0.37;0.37;0.35;0.35;0.35;0.35;0.37;0.37 ...
        ;0.37;0.37;0.36;0.38;0.38;0.37;0.36;0.35;0.34;0.34;0.32;0.31;0.31;0.32 ...
        ;0.34;0.37;0.38;0.38;0.37;0.36;0.36;0.36;0.36;0.36;0.36;0.37;0.36;0.37 ...
        ;0.36;0.36;0.34;0.36;0.35;0.37;0.36;0.36;0.33;0.35;0.36;0.35;0.34;0.35 ...
        ;0.36;0.34;0.35;0.36;0.36;0.36;0.36;0.36;0.40;0.42;0.39];           % in %
    CO2_background_v=[.029*ones(16,1);.03*ones(21,1);.028*ones(6,1);.029*ones(6,1) ...
        ;.027*ones(6,1);.028*ones(6,1);.029*ones(3,1)];                     % in %
    % Data Procesing PM1.0
    PM_1_0_er_v=[1.24;1.41;1.67;1.22;1.16;1.15;1.16;1.15;1.23;1.01;0.85;0.93 ...
        ;0.93;0.91;0.85;0.94;1.62;1.53;1.11];                               % in mg/m^3
    ind_1_0_v=[0 0 0 0 0 0 0 0 0 0 0 0 0 0 0 0 0 0 0 0 0 0 0 0 1 1 1 1 1 1 1 1 1 1 1 ...
        0 0 0 0 0 0 0 0 0 0 0 0 1 1 1 1 1 1 0 0 0 0 0 0 0 0 0 0 0 0 0 0 0 1 1 1]'==1;
    ave_SP_1_0=mean(SP_v(ind_1_0_v));
    LFproc_1_0=100*ave_SP_1_0/instSP;
    [AC_1_0,SOC_1_0,EMFR_1_0] = CalcEMFR(ACb,LFproc_1_0,ave_SP_1_0,HOC);
    time_1_0_c=time_c(ind_1_0_v);
    SP_1_0_v=SP_v(ind_1_0_v);
    CO2_raw_1_0_v=CO2_raw_v(ind_1_0_v);
    CO2_deluted_1_0_v=CO2_deluted_v(ind_1_0_v);
    CO2_background_1_0_v=CO2_background_v(ind_1_0_v);
    deluted_PM_1_0_er_v=PM_1_0_er_v.*(CO2_raw_1_0_v-CO2_background_1_0_v)./(CO2_deluted_1_0_v-CO2_background_1_0_v);
    EF_PM_1_0_v=EMFR_1_0*deluted_PM_1_0_er_v./SP_1_0_v/1000/AirDens;
    % typing the PM1.0 output
    disp(' ')
    disp('PM1.0 at Berth')
    disp(' ')
```

```
    fprintf(1,'date&time          SP (kW)       ER_PM (mg/m^3)  Deluted_ER_PM (mg/m^3)    EF_PM_1.0 (g/kWh)\n');
    for i=1:length(time_1_0_c)
        fprintf(1,'%15s   %6.1f        %.3f           %6.2f                    %.3f\n',time_1_0_c{i},SP_1_0_v(i),PM_1_0_er_v(i),deluted_PM_1_0_er_v(i),EF_PM_1_0_v(i));
    end
    disp(' ')
    ave_EF_PM_1_0=mean(EF_PM_1_0_v);
    fprintf(1,'average  EF_PM_1_0 (g/kWh)=%.3f\n',ave_EF_PM_1_0);
    fprintf(1,'avarage  AC_PM_1.0 (kg/hour)=%7.3f\n',AC_1_0);
    fprintf(1,'average  EMFR_1.0 (kg/hour)=%.3f\n',EMFR_1_0);
    fprintf(1,'avarage  SOC_1.0 (g/kWh)=%7.3f\n',SOC_1_0);
    % Data Procesing PM1.0-2.5
    PM_2_5_er_v=[1.69;1.72;1.59;1.44;1.53;1.57;1.57;1.57;1.57;1.52;1.52;1.52 ...
        ;1.52;1.56;1.53;1.57;1.20;1.14;1.15;1.12;1.17;1.15;0.95;0.99;0.96 ...
        ;0.94;0.92;0.91];                                                   % in mg/m^3
    ind_2_5_v=[1 1 1 1 1 1 1 1 1 1 1 1 1 1 1 1 0 0 0 0 0 0 0 0 0 0 0 0 0 0 0 0 0 0 ...
        1 1 1 1 1 1 0 0 0 0 0 0 0 0 0 0 0 0 1 1 1 1 1 1 0 0 0 0 0 0 0 0 0 0]'==1;
    ave_SP_2_5=mean(SP_v(ind_2_5_v));
    LFproc_2_5=100*ave_SP_2_5/instSP;
    [AC_2_5,SOC_2_5,EMFR_2_5] = CalcEMFR(ACb,LFproc_2_5,ave_SP_2_5,HOC);
    time_2_5_c=time_c(ind_2_5_v);
    SP_2_5_v=SP_v(ind_2_5_v);
    CO2_raw_2_5_v=CO2_raw_v(ind_2_5_v);
    CO2_deluted_2_5_v=CO2_deluted_v(ind_2_5_v);
    CO2_background_2_5_v=CO2_background_v(ind_2_5_v);
    deluted_PM_2_5_er_v=PM_2_5_er_v.*(CO2_raw_2_5_v-CO2_background_2_5_v)./(CO2_deluted_2_5_v-CO2_background_2_5_v);
    EF_PM_2_5_v=EMFR_2_5*deluted_PM_2_5_er_v./SP_2_5_v/1000/AirDens;
    % typing the PM1.0-2.5 output
    disp(' ')
    disp('PM1.0-2.5 at Berth')
    disp(' ')
    fprintf(1,'date&time          SP (kW)     ER_PM (mg/m^3)  Deluted_ER_PM (mg/m^3)    EF_PM_1.0-2.5 (g/kWh)\n');
    for i=1:length(time_2_5_c)
        fprintf(1,'%15s    %6.1f       %.3f           %6.2f                    %.3f\n',time_2_5_c{i},SP_2_5_v(i),PM_2_5_er_v(i),deluted_PM_2_5_er_v(i),EF_PM_2_5_v(i));
    end
    disp(' ')
    ave_EF_PM_2_5=mean(EF_PM_2_5_v);
    fprintf(1,'average  EF_PM_1.0-2.5 (g/kWh)=%.3f\n',ave_EF_PM_2_5);
    fprintf(1,'avarage  AC_PM_1.0-2.5 (kg/hour)=%7.3f\n',AC_2_5);
    fprintf(1,'average  EMFR_1.0-2.5 (kg/hour)=%.3f\n',EMFR_2_5);
    fprintf(1,'avarage  SOC_1.0-2.5 (g/kWh)=%7.3f\n',SOC_2_5);
    % Data Procesing PM2.5-10
    PM_10_0_er_v=[1.67;1.64;1.43;1.40;1.50;1.03;1.14;1.13;0.96;1.07;1.02 ...
        ;0.92;0.96;0.94;0.94;0.93;0.93];                                    % in mg/m^3
    ind_10_0_v=[0 0 0 0 0 0 0 0 0 0 0 0 0 0 0 0 1 1 1 1 1 0 0 0 0 0 0 0 0 0 0 0 ...
        0 0 0 0 0 1 1 1 1 1 0 0 0 0 0 0 0 0 0 0 0 0 1 1 1 1 1 1 0 0 0]'==1;
    ave_SP_10_0=mean(SP_v(ind_10_0_v));
    LFproc_10_0=100*ave_SP_10_0/instSP;
    [AC_10_0,SOC_10_0,EMFR_10_0] = CalcEMFR(ACb,LFproc_10_0,ave_SP_10_0,HOC);
    time_10_0_c=time_c(ind_10_0_v);
    SP_10_0_v=SP_v(ind_10_0_v);
    CO2_raw_10_0_v=CO2_raw_v(ind_10_0_v);
    CO2_deluted_10_0_v=CO2_deluted_v(ind_10_0_v);
    CO2_background_10_0_v=CO2_background_v(ind_10_0_v);
    deluted_PM_10_0_er_v=PM_10_0_er_v.*(CO2_raw_10_0_v-CO2_background_10_0_v)./(CO2_deluted_10_0_v-CO2_background_10_0_v);
    EF_PM_10_0_v=EMFR_10_0*deluted_PM_10_0_er_v./SP_10_0_v/1000/AirDens;
    % typing the PM2.5-10 output
    disp(' ')
    disp('PM2.5-10 at Berth')
```

```
    disp(' ')
    fprintf(1,'date&time          SP (kW)     ER_PM (mg/m^3)  Deluted_ER_PM (mg/m^3)    EF_PM_2.5-10 (g/kWh)\n');
    for i=1:length(time_10_0_c)
        fprintf(1,'%15s    %6.1f       %.3f           %6.2f                    %.3f\n',time_10_0_c{i},SP_10_0_v(i),PM_10_0_er_v(i),deluted_PM_10_0_er_v(i),EF_PM_10_0_v(i));
    end
    disp(' ')
    ave_EF_PM_10_0=mean(EF_PM_10_0_v);
    fprintf(1,'average  EF_PM_2.5-10 (g/kWh)=%.3f\n',ave_EF_PM_10_0);
    fprintf(1,'avarage  AC_PM_2.5-10 (kg/hour)=%7.3f\n',AC_10_0);
    fprintf(1,'average  EMFR_2.5-10 (kg/hour)=%.3f\n',EMFR_10_0);
    fprintf(1,'avarage  SOC_2.5-10 (g/kWh)=%7.3f\n',SOC_10_0);
    % data processing General
    N_PM=length(SP_v);
    Time_tot_PM=N_PM*deltt;
    ave_SP_PM=mean(abs(SP_v));
    LFproc=100*ave_SP_PM/instSP;
    [AC_PM,SOC_PM,EMFR_PM] = CalcEMFR(ACb,LFproc,ave_SP_PM,HOC);
    ave_SS_PM=mean(abs(SS_v));
    EF_PM_v=[(EF_PM_1_0_v+ave_EF_PM_2_5)/.8;(EF_PM_2_5_v+ave_EF_PM_1_0);EF_PM_10_0_v+ave_EF_PM_1_0+ave_EF_PM_2_5];
    ave_EF_PM=mean(EF_PM_v);
    E_PM_v=EF_PM_v.*SP_v*deltt/1000;
    total_E_PM=sum(E_PM_v);
    final_EF_PM=total_E_PM/Time_tot_PM/ave_SP_PM*1000;
    % typing the General output
    disp(' ')
    disp('PM cruising')
    disp(' ')
    fprintf(1,'date&time          SS (RPM) SP (kW)   EF_PM (g/kWh)     E_PM (kg)\n');
    for i=1:length(time_c)
        fprintf(1,'%15s   %6.1f     %6.1f    %.3f            %.3f\n',time_c{i},SS_v(i),SP_v(i),EF_PM_v(i),E_PM_v(i));
    end
    disp(' ');
    fprintf(1,'average  EF_PM (g/kWh)=%.4f\n',ave_EF_PM);
    fprintf(1,'total  E_PM (kg)=%.5f\n',total_E_PM);
    fprintf(1,'final  EF_PM (g/kWh)=%.4f\n',final_EF_PM);
    fprintf(1,'avarage  SS_PM (RPM)=%7.3f\n',ave_SS_PM);
    fprintf(1,'avarage  SP_PM (kW)=%.3f\n',ave_SP_PM);
    fprintf(1,'avarage  LF (%%)=%.3f\n',LFproc);
    fprintf(1,'avarage  AC_PM (kg/hour)=%7.3f\n',AC_PM);
    fprintf(1,'avarage  EMFR_PM (kg/hour)=%7.3f\n',EMFR_PM);
    fprintf(1,'avarage  SOC_PM (g/kWh)=%7.3f\n',SOC_PM);
    fprintf(1,'total time Time_tot_PM (hour)=%8.5f\n',Time_tot_PM);
    fprintf(1,'count of samples N_PM (-)=%i\n',N_PM);
end
```

PM1.0 at Berth

date&time	SP (kW)	ER_PM (mg/m^3)	Deluted_ER_PM (mg/m^3)	EF_PM_1.0 (g/kWh)
4/11/2015 5:15	5744.0	1.240	19.24	0.177
4/11/2015 5:20	5716.0	1.410	22.66	0.210
4/11/2015 5:25	5672.0	1.670	26.84	0.250
5/11/2015 12:15	5840.0	1.220	18.93	0.172
5/11/2015 12:20	5835.0	1.160	16.84	0.153
5/11/2015 12:25	5788.0	1.150	15.22	0.139
5/11/2015 12:30	5747.0	1.160	14.91	0.137
5/11/2015 12:35	5803.0	1.150	14.79	0.135
5/11/2015 12:40	5805.0	1.230	16.28	0.148
5/11/2015 12:45	5805.0	1.010	13.77	0.126
5/11/2015 13:50	5625.0	0.850	11.92	0.112
5/11/2015 13:55	5588.0	0.930	12.28	0.116
5/11/2015 14:00	5585.0	0.930	12.65	0.120
5/11/2015 14:05	5472.0	0.910	12.37	0.120
5/11/2015 14:10	5554.0	0.850	12.71	0.121
5/11/2015 14:15	5514.0	0.940	13.18	0.126
6/11/2015 11:00	4948.0	1.620	19.65	0.210
6/11/2015 11:05	4544.0	1.530	17.61	0.205
6/11/2015 11:10	4497.0	1.110	13.84	0.163

average EF_PM_1_0 (g/kWh)=0.155
avarage AC_PM_1.0 (kg/hour)=63666.573
average EMFR_1.0 (kg/hour)=64816.573
avarage SOC_1.0 (g/kWh)=207.933

PM1.0-2.5 at Berth

date&time	SP (kW)	ER_PM (mg/m^3)	Deluted_ER_PM (mg/m^3)	EF_PM_1.0-2.5 (g/kWh)
4/11/2015 3:30	5651.0	1.690	21.07	0.204
4/11/2015 3:35	5760.0	1.720	22.06	0.210
4/11/2015 3:40	5553.0	1.590	20.39	0.201
4/11/2015 3:40	5654.0	1.440	19.01	0.184
4/11/2015 3:50	5714.0	1.530	20.20	0.194
4/11/2015 3:55	5827.0	1.570	22.01	0.207
4/11/2015 4:00	5892.0	1.570	22.01	0.205
4/11/2015 4:05	5831.0	1.570	22.01	0.207
4/11/2015 4:10	5861.0	1.570	22.01	0.206
4/11/2015 4:15	5476.0	1.520	20.06	0.201
4/11/2015 4:20	5803.0	1.520	20.06	0.189
4/11/2015 4:25	5460.0	1.520	20.06	0.201
4/11/2015 4:30	5758.0	1.520	20.06	0.191
4/11/2015 4:35	5870.0	1.560	21.21	0.198
4/11/2015 4:40	6193.0	1.530	19.62	0.173
4/11/2015 4:45	6404.0	1.570	20.13	0.172
5/11/2015 12:50	5805.0	1.200	16.36	0.154
5/11/2015 12:55	5805.0	1.140	15.55	0.147
5/11/2015 13:00	5805.0	1.150	15.68	0.148
5/11/2015 13:05	5638.0	1.120	15.27	0.148
5/11/2015 13:10	5638.0	1.170	15.95	0.155
5/11/2015 13:15	5638.0	1.150	15.22	0.148
5/11/2015 14:20	5564.0	0.950	12.85	0.126
5/11/2015 14:25	5618.0	0.990	13.80	0.135
5/11/2015 14:30	5487.0	0.960	13.81	0.138
5/11/2015 14:35	5585.0	0.940	13.10	0.128
5/11/2015 14:40	5617.0	0.920	12.44	0.121
5/11/2015 14:45	5465.0	0.910	13.09	0.131

average EF_PM_1.0-2.5 (g/kWh)=0.172
avarage AC_PM_1.0-2.5 (kg/hour)=65933.671
average EMFR_1.0-2.5 (kg/hour)=67083.671
avarage SOC_1.0-2.5 (g/kWh)=200.783

PM2.5-10 at Berth

date&time	SP (kW)	ER_PM (mg/m^3)	Deluted_ER_PM (mg/m^3)	EF_PM_2.5-10 (g/kWh)
4/11/2015 4:50	6241.0	1.670	22.10	0.193
4/11/2015 4:55	5998.0	1.640	22.36	0.203
4/11/2015 5:00	5909.0	1.430	20.11	0.186
4/11/2015 5:05	5813.0	1.400	20.32	0.191
4/11/2015 5:10	5876.0	1.500	21.77	0.202
5/11/2015 13:20	5638.0	1.030	13.97	0.135
5/11/2015 13:25	5609.0	1.140	15.01	0.146
5/11/2015 13:30	5519.0	1.130	15.32	0.151
5/11/2015 13:35	5518.0	0.960	13.02	0.129
5/11/2015 13:40	5559.0	1.070	15.44	0.152
5/11/2015 13:45	5478.0	1.020	13.83	0.138
5/11/2015 14:50	5592.0	0.920	12.86	0.125
5/11/2015 14:55	5701.0	0.960	13.02	0.125
5/11/2015 15:00	5631.0	0.940	12.75	0.123
5/11/2015 15:05	5682.0	0.940	12.75	0.122
5/11/2015 15:10	5617.0	0.930	12.61	0.122
5/11/2015 15:15	5615.0	0.930	12.61	0.123

average EF_PM_2.5-10 (g/kWh)=0.151
avarage AC_PM_2.5-10 (kg/hour)=65681.286
average EMFR_2.5-10 (kg/hour)=66831.286
avarage SOC_2.5-10 (g/kWh)=201.555

PM cruising

date&time	SS (RPM)	SP (kW)	EF_PM (g/kWh)	E_PM (kg)
4/11/2015 3:30	88.5	5651.0	0.437	0.206
4/11/2015 3:35	88.3	5760.0	0.477	0.229
4/11/2015 3:40	88.3	5553.0	0.528	0.244
4/11/2015 3:40	88.0	5654.0	0.430	0.202
4/11/2015 3:50	88.4	5714.0	0.406	0.193
4/11/2015 3:55	88.4	5827.0	0.389	0.189
4/11/2015 4:00	88.4	5892.0	0.387	0.190
4/11/2015 4:05	88.2	5831.0	0.384	0.186
4/11/2015 4:10	88.3	5861.0	0.401	0.196
4/11/2015 4:15	88.1	5476.0	0.372	0.170
4/11/2015 4:20	88.2	5803.0	0.355	0.172
4/11/2015 4:25	88.3	5460.0	0.361	0.164
4/11/2015 4:30	88.2	5758.0	0.365	0.175
4/11/2015 4:35	88.2	5870.0	0.365	0.178
4/11/2015 4:40	89.3	6193.0	0.367	0.189
4/11/2015 4:45	90.4	6404.0	0.373	0.199
4/11/2015 4:50	90.3	6241.0	0.478	0.249
4/11/2015 4:55	90.3	5998.0	0.472	0.236
4/11/2015 5:00	90.3	5909.0	0.419	0.206
4/11/2015 5:05	90.5	5813.0	0.359	0.174
4/11/2015 5:10	90.5	5876.0	0.364	0.178
4/11/2015 5:15	90.3	5744.0	0.356	0.170

4/11/2015 5:20	90.3	5716.0	0.339	0.161
4/11/2015 5:25	90.4	5672.0	0.348	0.165
5/11/2015 12:15	89.4	5840.0	0.362	0.176
5/11/2015 12:20	89.4	5835.0	0.359	0.175
5/11/2015 12:25	89.4	5788.0	0.361	0.174
5/11/2015 12:30	89.4	5747.0	0.360	0.173
5/11/2015 12:35	89.4	5803.0	0.355	0.172
5/11/2015 12:40	89.4	5805.0	0.344	0.166
5/11/2015 12:45	89.4	5805.0	0.356	0.172
5/11/2015 12:50	89.4	5805.0	0.346	0.167
5/11/2015 12:55	89.4	5805.0	0.353	0.171
5/11/2015 13:00	89.4	5805.0	0.328	0.159
5/11/2015 13:05	89.4	5638.0	0.327	0.154
5/11/2015 13:10	89.4	5638.0	0.309	0.145
5/11/2015 13:15	89.4	5638.0	0.301	0.142
5/11/2015 13:20	89.4	5638.0	0.303	0.142
5/11/2015 13:25	89.4	5609.0	0.303	0.142
5/11/2015 13:30	89.4	5519.0	0.310	0.142
5/11/2015 13:35	89.4	5518.0	0.303	0.139
5/11/2015 13:40	89.4	5559.0	0.281	0.130
5/11/2015 13:45	89.4	5478.0	0.289	0.132
5/11/2015 13:50	89.4	5625.0	0.293	0.137
5/11/2015 13:55	89.4	5588.0	0.283	0.132
5/11/2015 14:00	89.4	5585.0	0.276	0.128
5/11/2015 14:05	89.4	5472.0	0.286	0.130
5/11/2015 14:10	89.4	5554.0	0.520	0.241
5/11/2015 14:15	89.4	5514.0	0.530	0.244
5/11/2015 14:20	89.4	5564.0	0.513	0.238
5/11/2015 14:25	89.4	5618.0	0.518	0.242
5/11/2015 14:30	89.4	5487.0	0.529	0.242
5/11/2015 14:35	89.4	5585.0	0.462	0.215
5/11/2015 14:40	89.4	5617.0	0.473	0.221
5/11/2015 14:45	89.4	5465.0	0.478	0.218
5/11/2015 14:50	89.4	5592.0	0.456	0.212
5/11/2015 14:55	89.4	5701.0	0.478	0.227
5/11/2015 15:00	89.4	5631.0	0.465	0.218
5/11/2015 15:05	89.4	5682.0	0.452	0.214
5/11/2015 15:10	89.4	5617.0	0.452	0.211
5/11/2015 15:15	89.4	5615.0	0.450	0.211
6/11/2015 11:00	89.4	4948.0	0.449	0.185
6/11/2015 11:05	89.4	4544.0	0.449	0.170
6/11/2015 11:10	89.4	4497.0	0.449	0.168

PM emissions for main engines at cruising

Security Clearances and Approvals

This section explains the number of approvals that was required to undertake any work within ports or on-board vessels within Australia.

Several approvals is required to undertake any work within ports or on-board vessels within Australia. Due to the number of stakeholders involved, understanding the complexities of these approvals is quite difficulty. The following approvals have been obtained:

- Maritime Security Identification Cards (MSIC)
- Port of Brisbane General Induction
- Stevedore operation (AAT, Patricks, DP World) inductions
- Maritime Safety Queensland approval
- Stevedore operation approval
- Approval from vessel owner/operators

A large amount of the effort thus far was dedicated to receiving the required approvals to gain access to the restricted landside and waterside zones as shown in the below figure. In Australia, a Maritime Security Identification Card (MSIC) is required to access work in a maritime security zone. The introduction of MSIC cards was part of a larger system to secure the maritime transport sector. MSIC cards are nationally recognized and are required to be carried at all times while located within these areas. These were obtained for all team members involved in the study.

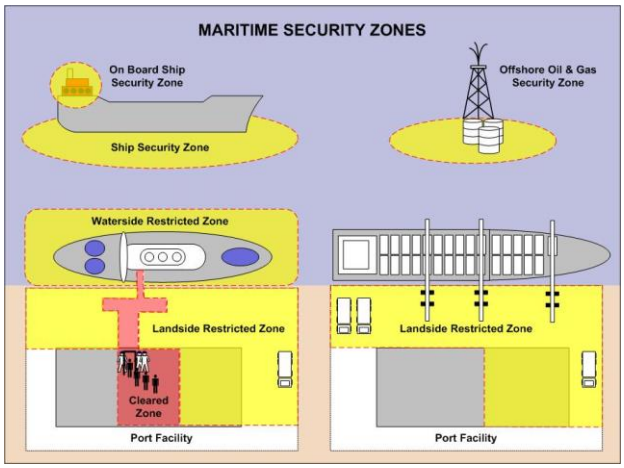

Types of maritime security zones on Australian facilities

Approval has been given from both the Port of Brisbane as well as three of the stevedore operations (DP World, AAT, Patricks) on Fisherman Islands at the Port of Brisbane to conduct work within their facilities. In addition to the requirement of MSIC cards to access these areas of the Port, individual inductions were required to be completed for each facility for all involved in the project. Strong collaboration with the Port of Brisbane has meant they have agreed to provide adequate space for conducting required analysis at their offices. Obtaining all the required permits to gain access to the restricted Port areas has taken in excess of 2 months even with the assistance of the Port of Brisbane. It is evident that the restrictions in place severely hinder the progress of research and are no doubt partially accountable for the lack of other similar studies.

Main Engine developed equations and figures

The section accompanies Chapter 3 to presents all the developed emission factor equations and the detailed results and figures produced accordingly:

Developed EF equations with the adjusted R_a^2 factor

Mode	EF equations (g)	R_a^2
At berth	$SO_x = 9.0 + 0.9\ x_1^a - 0.04\ x_2^b$	0.7672
	$NO_x = 11.4 + 1.4\ x_1 - 0.05\ x_2 - 0.004\ x_2\text{^}2$	0.9504
	$CO_2 = 220.6 + 34.8\ x_1 + 3.9\ x_2$	0.7163
	$CO = - 6.2 - 22.5 / x_1 + 403.3 / x_2$	0.7649
Manoeuvring	$SO_x = 3623.9 + 40.9\ x_1 - 122.1\ x_2 + 0.3\ x_1\text{^}2 + 1.1\ x_2\text{^}2 - 0.9\ x_1\ x_2$	0.9495
	$NO_x = - 184.8 - 1.8\ x_1 + 4.2\ x_2$	0.8793
	$CO_2 = - 9763.9 + 239.6\ x_1 + 181.2\ x_2 - 9.4\ x_1\text{^}2 + 0.08\ x_1\text{^}3$	0.7844
	$CO = 1097.7 + 12.5\ x_1 - 35.8\ x_2 + 0.03\ x_1\text{^}2 + 0.3\ x_2\text{^}2 - 0.2\ x_1\ x_2$	0.7689
Cruising	$SO_x = 3049.8 - 17.7\ x_1 - 50.6\ x_2 + 0.03\ x_1\text{^}2 + 0.2\ x_2\text{^}2 + 0.1\ x_1\ x_2$	0.9686
	$NO_x = 161.0 - 0.8\ x_1 - 0.07\ x_2$	0.9464
	$CO_2 = 4980.2 - 31.5\ x_1 + 31.7\ x_2$	0.9355
	$CO = 108.3 - 2.2\ x_1 - 0.2\ x_2 + 0.01\ x_1\text{^}2$	0.7204

[a] Maximum Continuous Rate (MCR)

[b] Shaft Speed (SS)

Results of actual on-board estimation predicted emission inventory and available inventories

At berth	On-board Estimation	Predicted Inventory	TIER III	Entec	MEET	STEAM	MOPSEA	NERI	USEPA	SMED	IMO
SO_x	1059	1059	358	1071	1041	1041	537	1041	1236	N/S [a]	448
NO_x	1308	1340	1662	1425	804	2018	1729	2018	3711	N/S [a]	2018
CO_2	32728	32908	N/S [a]	38177	34716	35008	33739	34609	89699	N/S [a]	33783
CO	12	13	38	N/S [a]	46	N/S [a]	53	42	22	N/S [a]	14
Manoeuvring											
SO_x	4444	4445	1221	3661	3571	3567	1832	3571	4238	3124	1527
NO_x	12643	12635	18528	15881	19937	22498	19269	22498	14528	19190	22498
CO_2	626420	627221	N/S [a]	644219	583902	588854	567479	582113	724477	644219	568209
CO	433	432	316	N/S [a]	385	N/S [a]	445	354	185	221	118
Cruising											
SO_x	5483	5469	1554	4204	4518	4513	2332	4518	5362	3604	1943
NO_x	3482	3503	5271	4518	5083	5120	4385	5120	3210	5451	5120
CO_2	236570	236631	N/S [a]	248648	249062	251202	242075	248299	284392	248648	242368
CO	297	297	479	N/S [a]	479	N/S [a]	671	534	279	167	179

[a] Not Specified

Comparison of S value for the predicted inventories and existing inventories

At berth	SO_x	NO_x	CO_2	CO
Predicted Emission Inventory	0.8	1.2	53.0	0.1
TIER III	8.8	4.0	-	1.3
Entec	1.6	3.0	149.2	-
MEET	1.6	3.7	98.7	1.7
STEAM	1.6	-	102.8	-
MOPSEA	6.6	4.4	87.9	2.0
NERI	1.6	-	97.4	1.5
US EPA	2.7	17.6	954.0	0.6
SMED	-	-	-	-
IMO	7.7	6.1	88.4	0.2
Manoeuvring	SO_x	NO_x	CO_2	CO
Predicted Emission Inventory	4.8	2.3	151.4	0.8
TIER III	65.6	29.9	-	4.1
Entec	17.5	17.6	426.1	-
MEET	19.0	36.5	541.2	2.6
STEAM	19.1	-	523.0	-
MOPSEA	53.3	33.4	609.2	2.3
NERI	-	-	548.1	3.2
US EPA	9.1	11.4	653.5	7.9
SMED	27.6	33.0	426.1	6.8
IMO	59.8	48.7	606	10.0
Cruising	SO_x	NO_x	CO_2	CO
Predicted Emission Inventory	3.2	3.08	80.4	0.7
TIER III	92.7	52.1	-	-
Entec	30.3	32.3	383.5	-
MEET	22.8	46.9	373.3	7.8
STEAM	22.9	-	408.4	-
MOPSEA	74.4	28.9	277.9	15.6
NERI	-	-	360.9	10.0
US EPA	4.6	11.9	1114.1	0.8
SMED	44.4	56.9		4.9
IMO	83.6	48.1	280.9	4.5

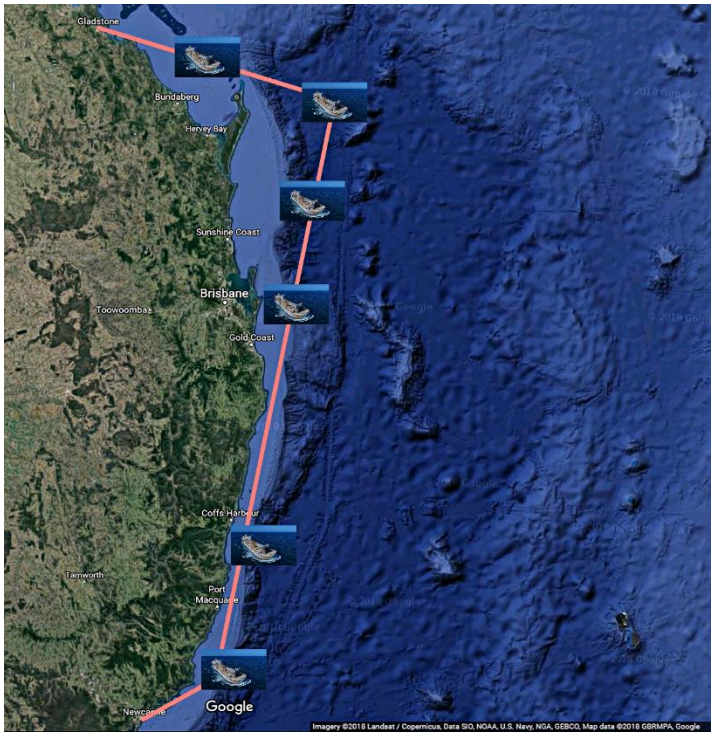

Routes of Vessels I and II between Newcastle, Brisbane and Gladstone ports

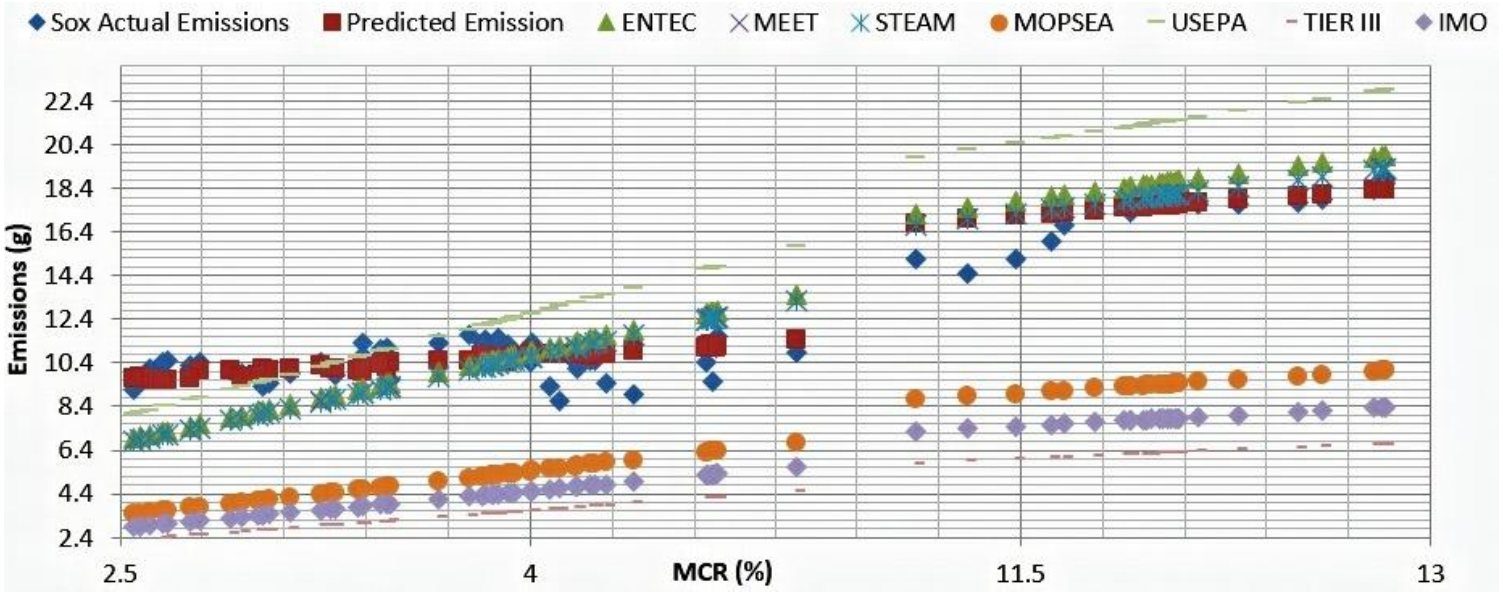
Sox Actual Emissions
Predicted Emission
ENTEC
MEET
STEAM
MOPSEA
USEPA
TIER III
IMO
Emissions (g)
22.4
20.4
18.4
16.4
14.4
12.4
10.4
8.4
6.4
4.4
2.4
2.5
4
MCR (%)
11.5
13

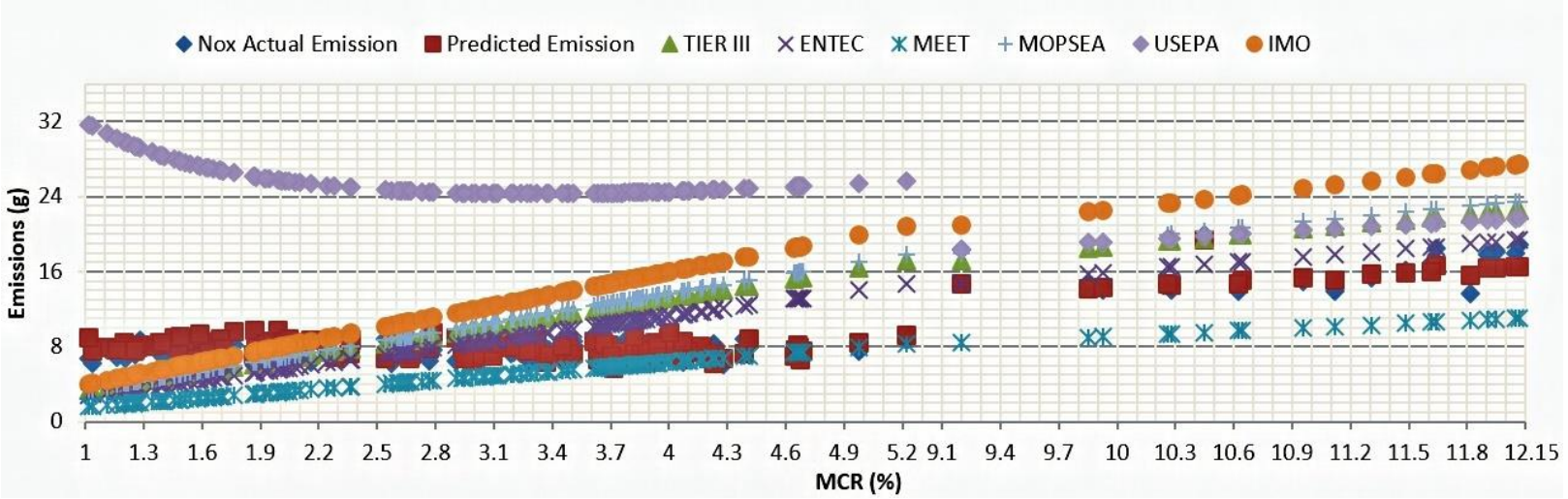
Nox Actual Emission
Predicted Emission
TIER III
ENTEC
MEET
MOPSEA
USEPA
IMO
Emissions (g)
32
24
16
8
0
1
1.3
1.6
1.9
2.2
2.5
2.8
3.1
3.4
3.7
4
4.3
4.6
4.9
5.2
9.1
9.4
9.7
10
10.3
10.6
10.9
11.2
11.5
11.8
12.15
MCR (%)

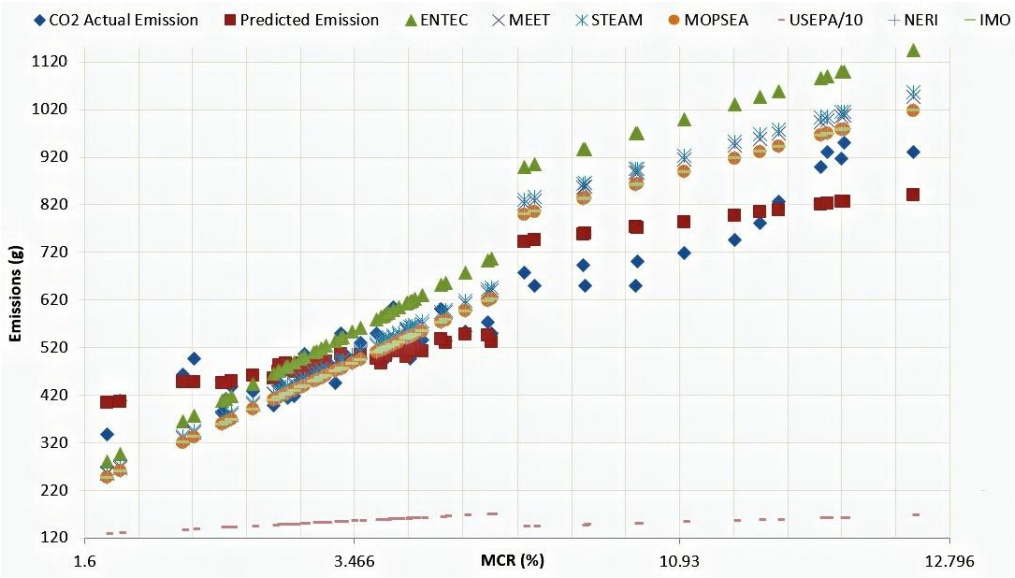

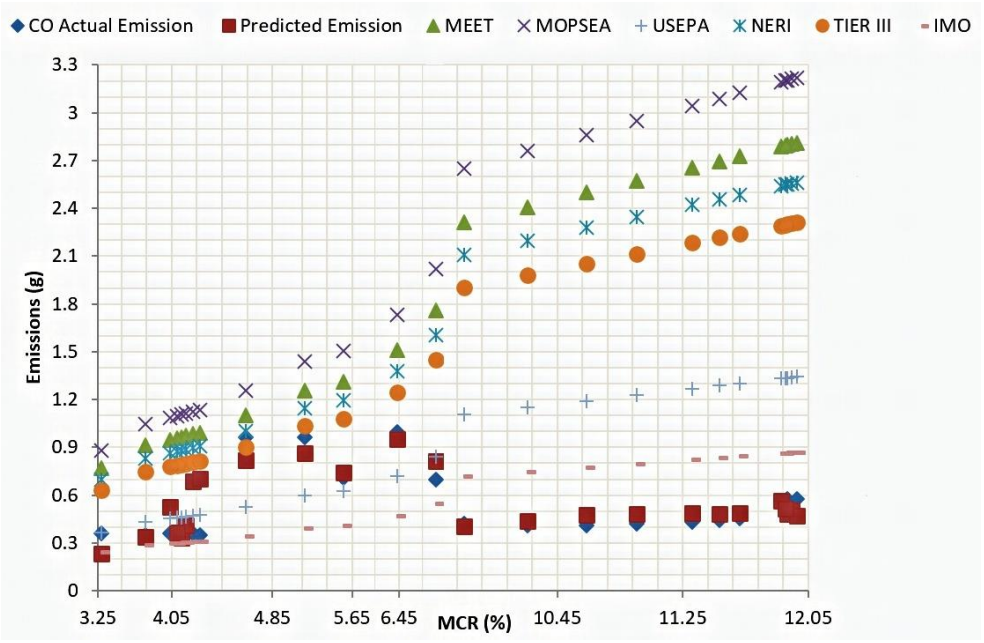

Trends of predicted and available inventory emissions (g) at berth

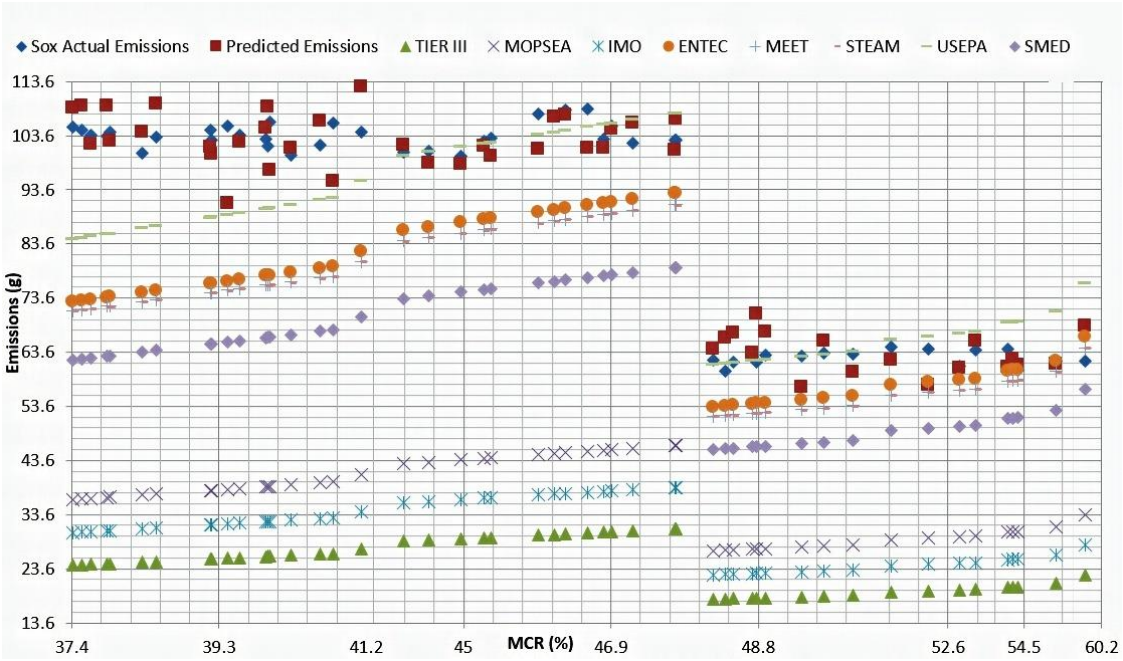
Sox Actual Emissions
Predicted Emissions
TIER III
MOPSEA
IMO
ENTEC
MEET
STEAM
USEPA
SMED
Emissions (g)
113.6
103.6
93.6
83.6
73.6
63.6
53.6
43.6
33.6
23.6
13.6
37.4
39.3
41.2
45
MCR (%)
46.9
48.8
52.6
54.5
60.2

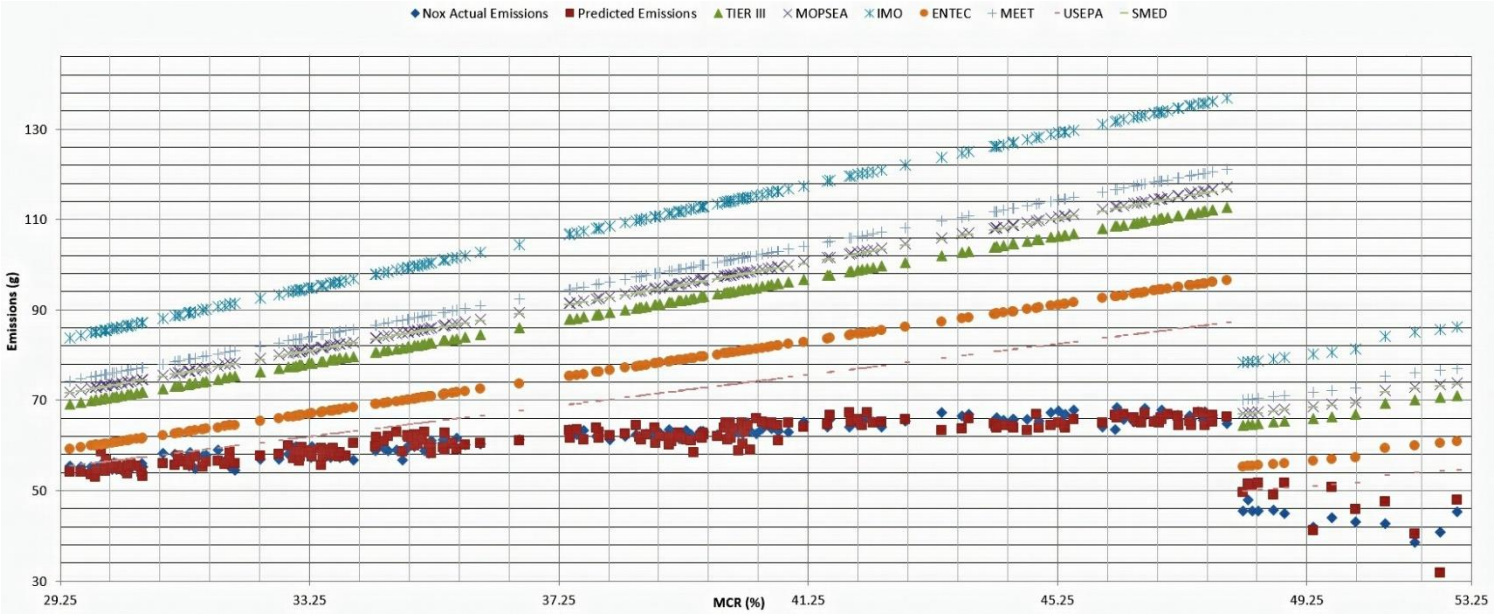
Nox Actual Emissions
Predicted Emissions
TIER III
MOPSEA
IMO
ENTEC
MEET
USEPA
SMED
Emissions (g)
130
110
90
70
50
30
29.25
33.25
37.25
MCR (%)
41.25
45.25
49.25
53.25

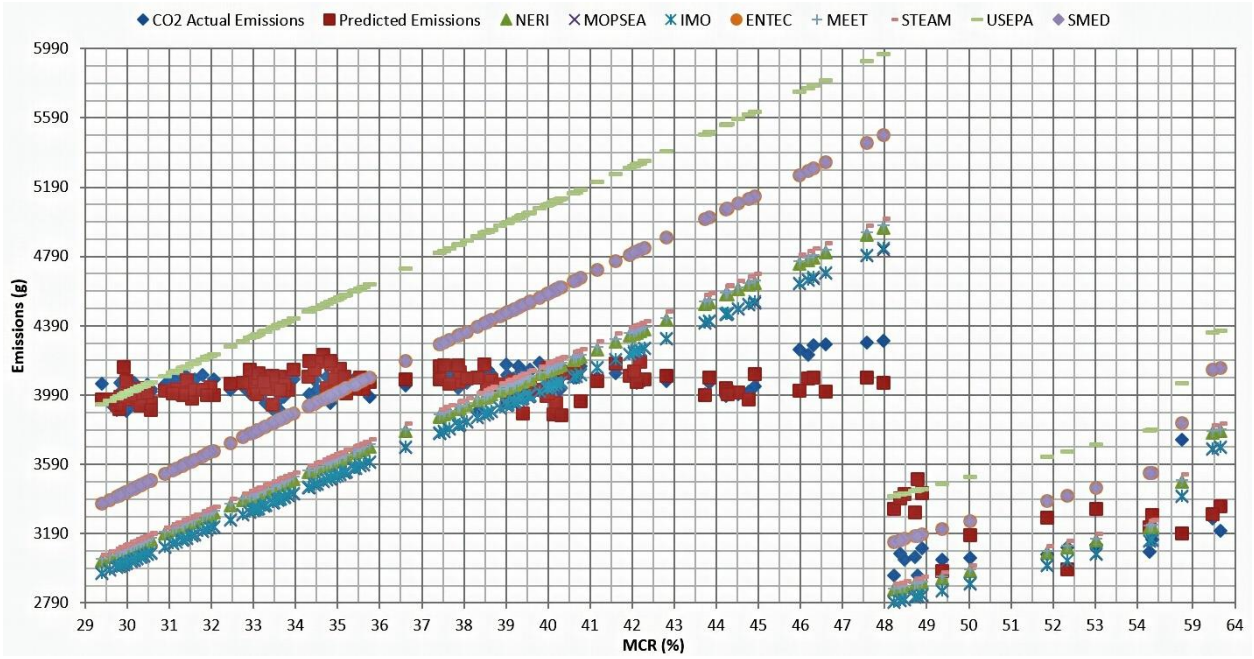

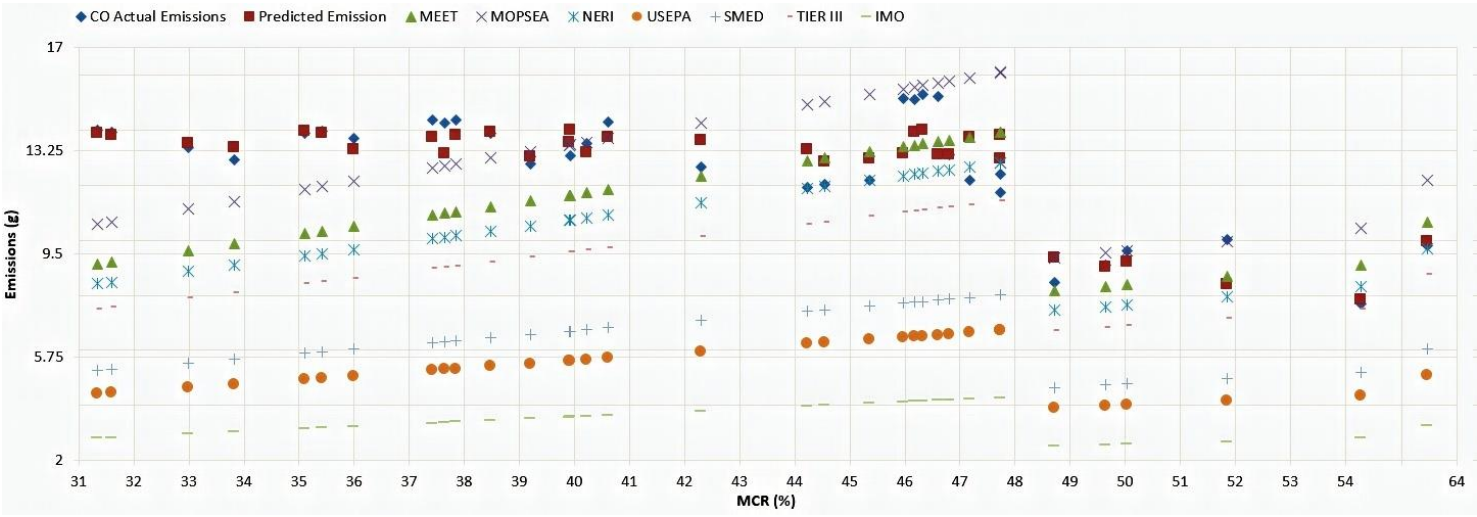

Trends of predicted and available inventory emissions (g) during manoeuvring

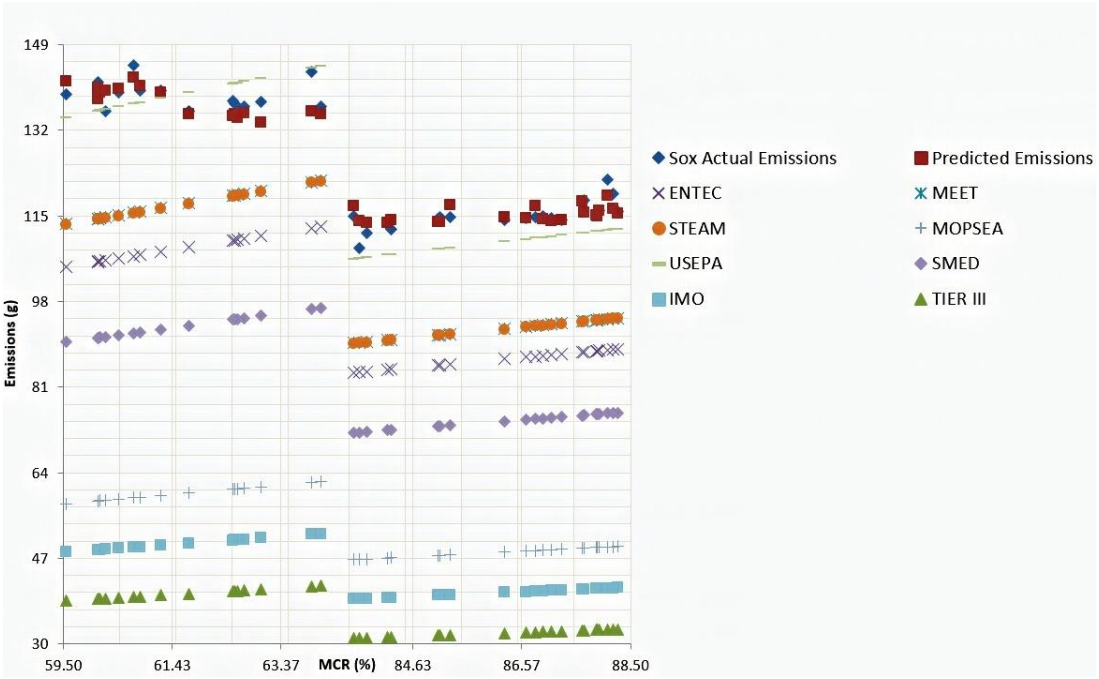
Sox Actual Emissions
Predicted Emissions
ENTEC
MEET
STEAM
MOPSEA
USEPA
SMED
IMO
TIER III
Emissions (g)
149
132
115
98
81
64
47
30
59.50
61.43
63.37
MCR (%)
84.63
86.57
88.50

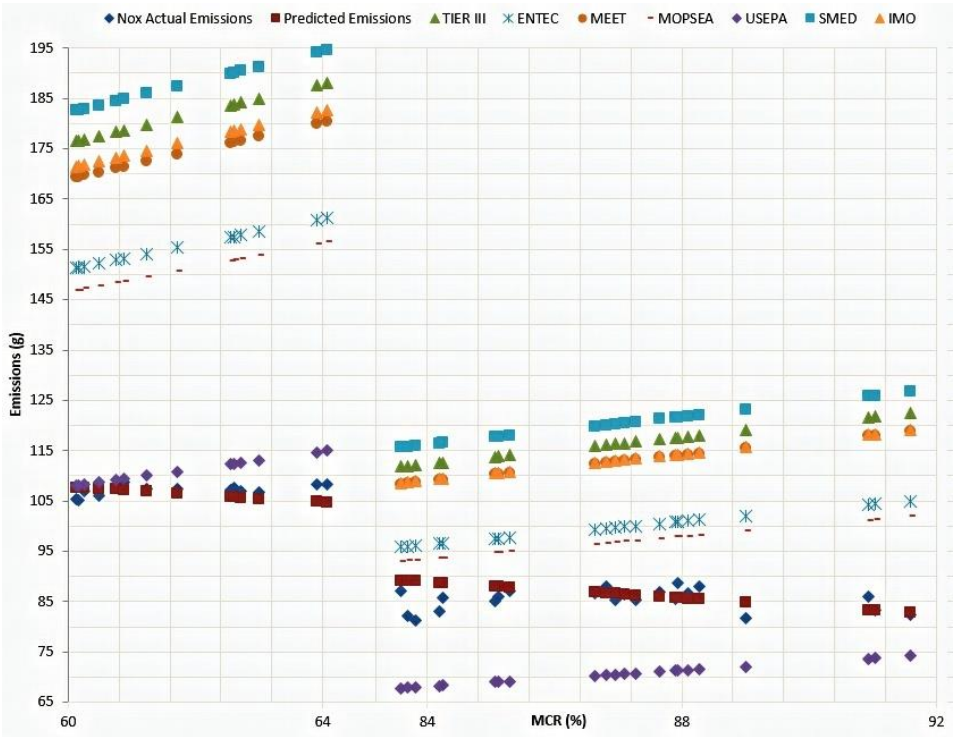
Nox Actual Emissions
Predicted Emissions
TIER III
ENTEC
MEET
MOPSEA
USEPA
SMED
IMO
Emissions (g)
195
185
175
165
155
145
135
125
115
105
95
85
75
65
60
64
84
MCR (%)
88
92

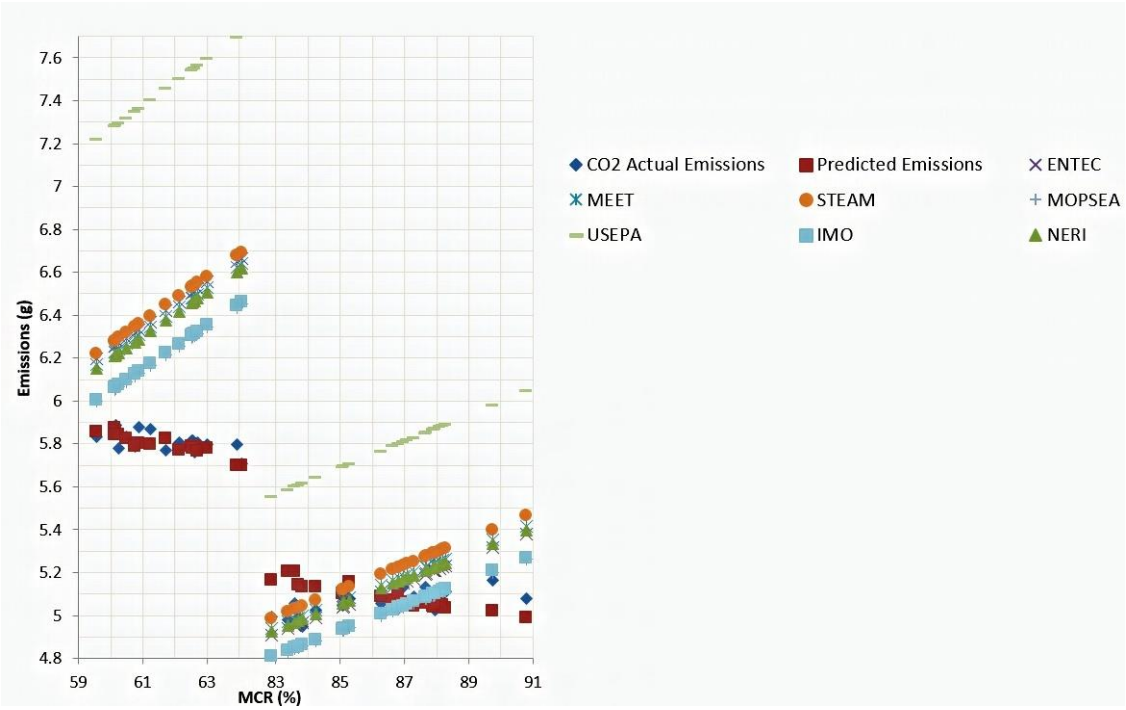

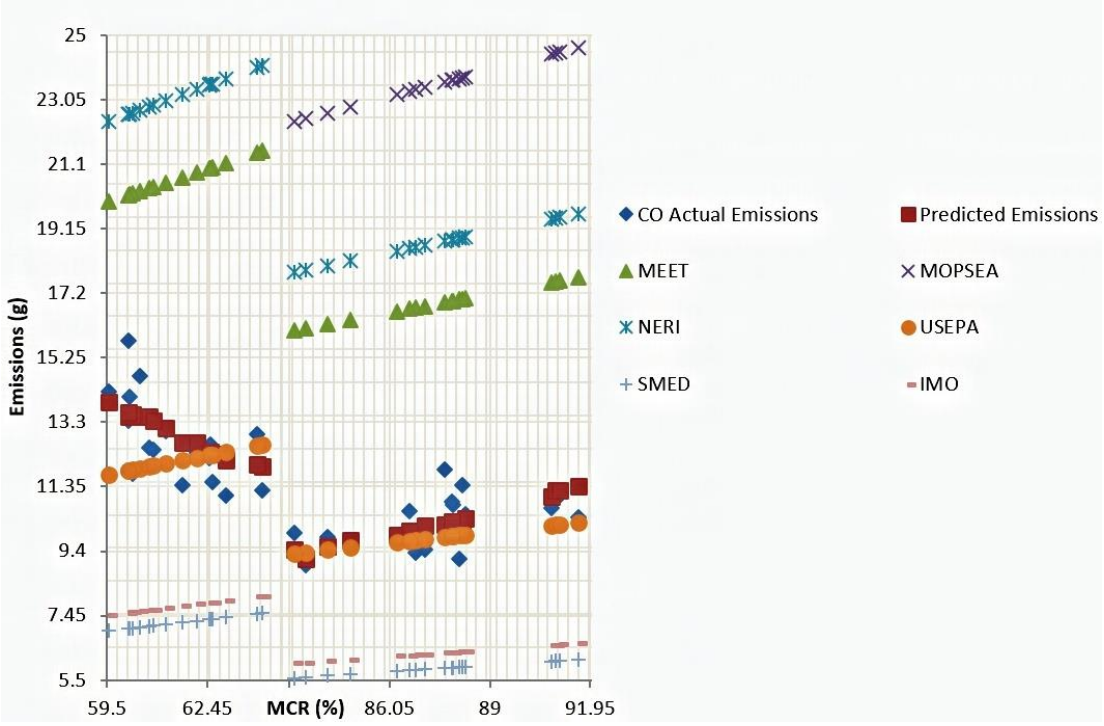

Trends of predicted and available inventory emissions (g) during cruising

Dispersion Modelling dataset

This section outlines setting up and running the CALPUFF model using CALApps GUI accompanying Chapter 5. Setting up and running the model using CALApps GUI and the selection of CALMET critical parameters in observation mode are also mentioned in this appendix.

CALApps v2.10.1 (CALPUFF's newest graphical feature) is a beta version with few functional issues. Tips for getting around the two most common are:

1. CALApps crashes after clicking RUN.

Immediately before crashing, a window should appear containing a file called 'run'. Double click on this and the desired process will run.

2. CALApps Viewer crashes or generates error messages.

Use CALView rather than CALApps Viewer to plot results. (CALView was distributed with CALPro Plus, the precursor to CALApps).

Required files are summarised in the below table.

Summary of the data files used in the CALPUFF model

Data file description	File name
Land use	AUSPACIF.LU
Elevation	S27E152.hgt S27E153.hgt S28E152.hgt S28E153.hgt
Coastline	gshhs_f.b gshhs_f.b
Surface	SURF.DAT
Precipitation	PRECIP.DAT
Upper air	UP.DAT

Project information

CALApps allows the user to apply project information settings to all steps in the modelling process. The following lists the various steps to take, using this study's Brisbane project as an example. Brisbane-specific information is *italicised*.

1. Select **PROJECT INFORMATION** in the CALApps navigation window.

2. Under **GENERAL INFORMATION -> PROJECT NAME** enter a name for the project.

3. Under **GENERAL INFORMATION -> PROJECT NAME**, deselect the **APPLY STANDARD NAMING TO ALL OUTPUT FILES** tick-box.

4. Under **GENERAL INFORMATION -> PROJECT FOLDER**, select **Project** as the directory for saving files associated with the project.

5. Under **MODELING PERIOD** select a beginning and end date for the modelling run. To use the entire meteorological data set provided, the beginning and end dates should be set to **January 01 2013 00:00:00** and **January 01 2014 00:00:00** respectively. For test runs, it is advisable to use a shorter modelling period in order to reduce processing time.

6. Under **MODELLING PERIOD -> TIME ZONE**, select ***UTC+10:00 Brisbane***.

7. Under **MAP PROJECTION -> PROJECTION** select **UTM**.

8. Under **MAP PROJECTION -> DATUM** select **WGS-84**.

9. Under **UTM -> ZONE**, select ***56***.

10. Under **UTM -> HEMISPHERE**, select **SOUTHERN**.

11. Under **MODELING GRID -> SOUTHWEST CORNER OF DOMAIN**, enter the *south west UTM coordinates*.

12. Under **MODELING GRID -> NUMBER OF GRID CELLS**, enter **100** for the number of grid cells in both the X and Y directions. This number can be increased if a higher-resolution modelling run is required. Note that increasing resolution will increase computation time.

13. Under **MODELING GRID -> GRID SPACING**, set the grid spacing to **1 km**. For higher resolution runs, the grid spacing must be reduced.

14. Under **MODELING GRID -> NUMBER OF VERTICAL LAYERS**, select the default value of **11**. This number can be increased if a higher resolution modelling run is required.

15. Under **MODELING GRID -> VERTICAL LAYER CELL FACE HEIGHTS**, use the default values.

16. Click the **APPLY TO ALL** button at the bottom of the window.

17. Click the **save** icon at the bottom of the window and save the project under **Project name**.

Geophysical

CTGPROC

CTGPROC processes land-use data to generate a lu.dat file that can be processed by MAKEGEO. To run CTGPROC in the CALApps GUI, follow these steps:

1. Select **CTGPROC** in the CALApps navigation window.

2. Under **LAND USE DATA FILES -> TYPE**, select **USGS Global (Lambert Azimuthal) for Australia-Pacific [GLAZAP]**.

3. Under **LAND USE DATA FILES -> DATA FILES**, select the provided land-use data file **AUSPACIF.LU**. This land-use data file can also be used for other sites in Australia.

4. Under **MAP PROJECTION**, select the same settings used under **PROJECT INFORMATION**. These settings should populate automatically if **APPLY TO ALL** was selected under **PROJECT INFORMATION**.

5. Under **MODELING DOMAIN**, select the same settings used under **PROJECT INFORMATION**. These settings should populate automatically if **APPLY TO ALL** was selected under **PROJECT INFORMATION**.

6. Under **COASTLINE PROCESSING**, select the **Process coastline data** tick-box.

7. Under **COASTLINE PROCESSING -> COASTLINE DATA FILE**, select the provided coastline data file **gshhs_f.b**. This file can also be used for other coastal sites in Australia.

8. Under **COASTLINE PROCESSING -> COASTLINE DATA FILE**, select the binary format option.

9. Under **OUTPUT FILES -> OUTPUT FOLDER**, select **Project/CTGPROC/** as the directory for saving CTGPROC output files.

10. Click the save icon at the bottom of the window. Click ‘save’ again when the dialogue box appears.

11. Click the **RUN CTGPROC** button at the bottom of the window. A command prompt window will appear with an output similar to the following:

```
C:\CALApps\Project\CTGPROC>"C:\Program Files
(x86)\Exponent\CALApps\EXE Files\TNG\ctgproc_v7.0.0.exe"
Project_ctgproc.inp
 SETUP PHASE

 Processing coastline data


Note: # shoreline polygons found:  76

 COMPUTATIONAL PHASE
 Processing: 6 2 1  c:\calapps\project\ctgproc\auspacif.lu
Land Use Processing Complete -- Check LIST file for Run
Summary and QA Warning Messages.
 TERMINATION PHASE

C:\CALApps\Project\CTGPROC>pause
Press any key to continue . . .
```

12. Navigate to **Project/CTGPROC/** and open **ctgproc.lst** in a text editor. Scroll to the end of the file and check to see if any error or warning messages are present. If error messages are present, address them and re-run CTGPROC. If CTGPROC runs successfully, the end of **ctgproc.lst** should look like this:

```
POTENTIAL ERROR: Number of Grid Cells with no defined land
use =         65
 This should NOT be your LAST run unless these cells are
PROPERLY filled in
 with the missing value (IMISS) used in the next
processing step (MAKEGEO).
 Consult the gridded table printed above to identify the
cells.

 Coastline processing - empty cells filled with
 "OCEAN" in the following number of cells :        48



 Land Use Processing Complete.


  End of run -- Clock time: 14:35:53
                    Date: 19-Sep-2017
```

The warning messages above occur because land-use data is not available over water. These warning messages can be ignored because MAKEGEO will automatically assign water surface properties to cells with missing land-use data.

13. Navigate to **Project/CTGPROC/** and locate **lu.dat**. This is the processed land-use data file that is required by MAKEGEOTERREL

TERREL processes elevation data to generate a terr.dat file that can be processed by MAKEGEO. To run TERREL in the CALApps GUI, follow these steps:

1. Select **TERREL** in the CALApps navigation window.

2. Under **TERRAIN DATA FILES -> TYPE**, select **1-sec Shuttle RADAR Topo Mission files (~30m**) [SRTM1].

3. Under **TERRAIN DATA FILES -> DATA FILES**, select the four provided elevation data files **Project/TERREL/*.hgt**. These elevation data files cover only the selected modelling domain. To model other sites in Australia, the corresponding elevation data files can be obtained free of charge from http://dwtkns.com/srtm30m/.

4. Under **MAP PROJECTION**, select the same settings used under **PROJECT INFORMATION.** These settings should populate automatically if **APPLY TO ALL** was selected under **PROJECT INFORMATION**.

5. Under **MODELING DOMAIN**, select the same settings used under **PROJECT INFORMATION**). These settings should populate automatically if **APPLY TO ALL** was selected under **PROJECT INFORMATION**.

6. Under **COASTLINE PROCESSING**, select the Process coastline data tick-box.

7. Under **COASTLINE PROCESSING -> COASTLINE DATA FILE**, select the provided coastline data file **Project/TERREL/gshhs_f.b**. This file can also be used for other coastal sites in Australia.

8. Under **COASTLINE PROCESSING -> COASTLINE DATA FILE**, select the binary format option.

9. Under **OUTPUT FILES -> OUTPUT FOLDER**, select **Project/TERREL/** as the directory for saving TERREL output files.

10. Click the save icon at the bottom of the window. Click ‘save’ again when the dialogue box appears.

11. Click the **RUN TERREL** button at the bottom of the window. This step will take a few minutes to run. A command prompt window will appear with an output similar to the following:

```
C:\CALApps\Project\TERREL>"C:\Program Files
(x86)\Exponent\CALApps\EXE Files\TNG\terrel_v7.0.0.exe"
Project_terrel.inp
 SETUP PHASE

 Processing coastline data

Note: # shoreline polygons found:  76

 COMPUTATIONAL PHASE


Processing data file:
c:\calapps\project\terrel\s27e152.hgt
Finished Sheet #  1
Finished Sheets in Panel #  1

Processing data file:
c:\calapps\project\terrel\s27e153.hgt
Finished Sheet #  1
Finished Sheets in Panel #  1

Processing data file:
c:\calapps\project\terrel\s28e152.hgt
Finished Sheet #  1
Finished Sheets in Panel #  1

Processing data file:
c:\calapps\project\terrel\s28e153.hgt
Finished Sheet #  1
Finished Sheets in Panel #  1
 TERMINATION PHASE

C:\CALApps\Project\TERREL>pause
Press any key to continue . . .
```

12. Navigate to **Project/TERREL/** and open **terrel.lst** in a text editor. Scroll to the end of the file and check to see if any error or warning messages are present. If error messages are present, addressed them and re-run TERREL. Once TERREL runs successfully, the end of **terrel.lst** should look like this:

```
Summary Information for cells with data:
 --              Number of cells with data      10201
 --        Average number of hits per cell       1183
 --           0 cells have fewer hits than        887
 --           0 cells have  more hits than       1479


  End of run -- Clock time: 14:51:10
                      Date: 19-Sep-2017

         Elapsed Clock Time:          399 (seconds)

                   CPU Time:          398 (seconds)
```

13. Navigate to **Project/TERREL/** and locate **terr.dat**. This is the processed elevation data file that is required by MAKEGEO

MAKEGEO

MAKEGEO processes land-use and elevation data to generate a geo.dat file that can be processed by CALMET. To run MAKEGEO in the CALApps GUI, follow these steps:

1. Select **MAKEGEO** in the CALApps navigation window.

2. Under **TERR.DAT** and **LU.DAT** FILES in **TERR.DAT FILE**, select **Project/TERREL/terr.dat**. This is the terrain file that was generated by TERREL.

3. Under **TERR.DAT** and **LU.DAT FILES** in **LU.DAT FILE**, select **Project/CTGPROC/lu.dat**. This is the land-use file that was generated by CTGPROC.

4. Under **MAP PROJECTION**, select the same settings used under **PROJECT INFORMATION**. These settings should populate automatically if **APPLY TO ALL** was selected under **PROJECT INFORMATION**.

5. Under **MODELING DOMAIN**, select the same settings used under **PROJECT INFORMATION**. These settings should populate automatically if **APPLY TO ALL** was selected under **PROJECT INFORMATION**.

6. Under **OUTPUT FILES -> OUTPUT FOLDER**, select **Project/MAKEGEO/** as the directory for saving the MAKEGEO output files.

7. Click the save icon at the bottom of the window. Click ‘save’ again when the dialogue box appears.

8. Click the **RUN MAKEGEO** button at the bottom of the window. A command prompt window will appear with an output like this:

```
C:\CALApps\Project\MAKEGEO>"C:\Program Files
(x86)\Exponent\CALApps\EXE Files\TNG\makegeo_v3.2.exe"
Project_makegeo.inp
 SETUP PHASE
 COMPUTATIONAL PHASE
 Warning -- LU coverage is less than  0.001 in         65
cell(s)
 Missing LU fraction filled with LU =  55
 TERMINATION PHASE

C:\CALApps\Project\MAKEGEO>pause
Press any key to continue . . .
```

9. Navigate to **Project/MAKEGEO/** and open **makegeo.lst** in a text editor. Scroll to the end of the file and check to see if any error or warning messages are present. If error messages are

present, address them and re-run MAKEGEO. If MAKEGEO has run successfully, the end of **makegeo.lst** should look like the following:

```
Warning -- LU coverage is less than  0.001 in         65
cell(s)
Missing LU fraction filled with LU =  55


  End of run -- Clock time: 14:57:51
                      Date: 19-Sep-2017

        Elapsed Clock Time:            0 (seconds)

                  CPU Time:            0 (seconds)
```

This warning above has occurred because land-use data is not available over water. This message can be ignored because MAKEGEO automatically assigns water surface properties to cells with missing land-use data.

10. Navigate to **Project/MAKEGEO/** and locate **geo.dat**. This is the processed geophysical data file required by CALMET, as will be described in later sections.

Meteorological

SURFGEN

SURFGEN processes raw surface meteorological data to generate SURF.DAT and PRECIP.DAT files that can be processed by CALMET. SURFGEN has not been used in this model because the SURF.DAT and PRECIP.DAT files have been generated separately using SMERGE and PMERGE respectively.

SMERGE

SMERGE processes raw surface meteorological data to generate a SURF.DAT file that can be processed by CALMET. For this model, SMERGE has been used to generate a SURF.DAT file. For other sites in Australia, local surface meteorological data must be purchased.

PMERGE

PMERGE processes raw precipitation data to generate a PRECIP.DAT file that can be processed by CALMET. In this model, PMERGE has been used to generate a PRECIP.DAT file. For other sites in Australia, local precipitation data must be purchased.

READ62

READ62 processes raw upper air data to generate an UP.DAT file that can be processed by CALMET. In this model, READ62 has been used to generate an UP.DAT file. For modelling sites in Australia, local upper air data must be purchased and repaired if necessary. If no suitable upper air data is available, then 3D gridded prognostic data may be used instead.

BUOY

BUOY processes raw overwater data to generate SEA.DAT files that can be processed by CALMET. For this model, no suitable overwater is available. As such, observational overwater data is not included in the model. For other overwater locations in Australia, it is advisable to include overwater data where available.

Main

CALMET

CALMET processes land-use, elevation, surface meteorology, precipitation, upper air, overwater and 3D gridded prognostic data, to generate a calmet.dat file that can be processed by CALPUFF. To run CALMET, follow these steps:

1. Select **CALMET** in the CALApps navigation window.

2. Under **RUN TYPE**, click on **OBS-ONLY**. This will select observation mode; that is, CALMET will use observed meteorological data to initialise the Initial Guess wind field. For modelling sites in Australia, it may be necessary to use the no-observation or hybrid mode if suitable observed metrological data is not available.

3. Under **MODELING PERIOD**, select the same settings used under **PROJECT INFORMATION**. These settings should populate automatically if **APPLY TO ALL** was selected under **PROJECT INFORMATION**.

4. Under **MAP PROJECTION**, select the same settings used under **PROJECT INFORMATION**. These settings should populate automatically if **APPLY TO ALL** was selected under **PROJECT INFORMATION**.

5. Under **MODELING DOMAIN**, select the same settings used under **PROJECT INFORMATION**. These settings should populate automatically if **APPLY TO ALL** was selected under **PROJECT INFORMATION**.

6. Under **CRITICAL PARAMETERS**, enter the values for **RMAX1**, **RMAX2**, **R1**, **R2** and **TERRAD** from the table 'Recommended values for critical parameters'. Note that for some sites in Australia, manual tuning of these parameters may be required.

7. Under **CRITICAL PARAMETERS -> IEXTRP**, select **Similarity Theory**.

8. Under **CRITICAL PARAMETERS -> IEXTRP**, select the **Ignore Layer 1 data at upper air stations** tick-box.

9. Under **CRITICAL PARAMETERS -> BIAS**, use the default values.

10. Under **GEO.DAT FILE**, select **Project/MAKEGEO/geo.dat**. This is the geo.dat file that was generated using MAKEGEO.

11. Under **MM5/WRF/3D.DAT FILES**, leave the selection field blank. This field is not required when running CALMET in observation mode.

12. Under **SURFACE STATION DATA -> SURFACE STATION DATA FILE**, select the provided surface meteorology file **Project/SMERGE/SURF.DAT**. For modelling sites in Australia, a local **SURF.DAT** file must be obtained.

13. Under **SURFACE STATION DATA -> SURFACE STATION PARAMETERS**, enter the station parameters. Stations must be entered in the same order that they appear in the **SURF.DAT** file. For modelling sites in Australia, surface station parameters should be entered for the stations that appear in the relevant local **SURF.DAT** file.

14. Under **UPPER AIR STATION DATA -> UPPER AIR STATION DATA FILE**, select the provided upper air file **Project/READ62/UP.DAT** file. For modelling sites in Australia, a local **UP.DAT** file should be obtained if available.

15. Under **UPPER AIR STATION DATA -> UPPER AIR STATION PARAMETERS**, enter the station parameters. Stations must be entered in the same order that they appear in the **UP.DAT** file. For modelling sites in Australia, upper air station parameters should be entered for the stations that appear in the relevant local **UP.DAT** file.

16. Under **PRECIPITATION STATION DATA -> PRECIPITATION STATION DATA FILE**, select the provided precipitation files **Project/PMERGE/PRECIP.DAT** file. For modelling sites in Australia, a local **PRECIP.DAT** file must be obtained.

17. Under **PRECIPITATION STATION DATA -> PRECIPITATION STATION PARAMETERS**, enter the station parameters. Stations must be entered in the same order that they appear in the **PRECIP.DAT** file. For modelling sites in Australia, precipitation station parameters should be entered for the stations that appear in the relevant local **PRECIP.DAT** file.

18. Leave **OVERWATER STATION DATA -> OVERWATER STATION PARAMETERS** blank. For modelling sites in Australia, **SEA.DAT** overwater files processed using BUOY should be selected here if available.

19. Leave **OVERWATER STATION DATA -> RMAX3** blank. For modelling sites in Australia, an appropriate value for RMAX3 should be chosen if overwater data is to be included in the model (see the table 'Recommended values for critical parameters').

20. Under **TEMPERATURE AND RELATIVE HUMIDITY PARAMETERS -> ITPROG**, select **Use surface and upper air observations [0]**.

21. Under **TEMPERATURE AND RELATIVE HUMIDITY PARAMETERS -> IRHPROG**, select **Use surface observations [0]**.

22. Under **OUTPUT FILES -> OUTPUT FOLDER**, select **Project/CALMET/** as the directory for saving CALMET output files.

23. Click the **CALMET.INP** tab near the top of the window. This will allow manual edits to the **CALMET.INP** file.

24. Locate **JWAT1** and **JWAT2** and set both equal to **9999**:

```
Beginning (JWAT1) and ending (JWAT2)
land use categories for temperature        ! JWAT1 = 9999 !
interpolation over water -- Make           ! JWAT2 = 9999 !
bigger than largest land use to disable
```

25. Locate **ICLDOUT** and set equal to **0**:

```
Output option - output a CLOUD.DAT file (yes or no)
       0=no, 1=yes
               (ICLDOUT) Default:999       ! ICLDOUT = 0  !
```

26. Locate **SIGMAP** and set equal to **100**.

```
Radius of Influence
(SIGMAP)          Default: 100.0          ! SIGMAP = 100. !
         (0.0 => use half dist. btwn          Units: km
          nearest stns w & w/out
          precip when NFLAGP = 3)
```

27. Click the save icon at the bottom of the window. Click ‘save’ again when the dialogue box appears.

28. Before running CALMET, make sure that enough storage space is available for generating the **calmet.dat** file, which typically is larger than 20GB.

29. Click the **RUN CALMET** button at the bottom of the window. This might take a while. A command prompt window will appear with an output like this:

```
C:\CALApps\Project\CALMET>"C:\Program Files
(x86)\Exponent\CALApps\EXE Files\TNG\calmet_v6.5.0.exe"
Project_calmet.inp
ENTERING SETUP PHASE
WARNINGS are found in the CONTROL file
Review messages written to the LIST file
ENTERING COMPUTATIONAL PHASE
Processing Year, Day, Hour, Sec from: 2013 365 23    0
to:2013 365 23 3600
ENTERING TERMINATION PHASE

C:\CALApps\Project\CALMET>pause
Press any key to continue . . .
```

30. Navigate to **Project/CALMET/** and open **calmet.lst** in a text editor. Scroll to the end of the file and check to see if any error or warning messages are present. If so, address them and re-run CALMET. If CALMET has run successfully, the end of **calmet.lst** should look like this:

```
LAST PERIOD PROCESSED ENDS AT:
       Year: 2014  Month:  1   Day:  1   Julian day:   1
Hour:  0   Second:    0


  End of run -- Clock time: 13:49:40
                     Date: 20-Sep-2017

        Elapsed clock time:     9844.0 (seconds)

                  CPU time:     9819.6 (seconds)
```

31. Navigate to **Project/CALMET/** and locate **calmet.dat**. This is the processed CALMET data file that is required to run CALPUFF, as described next.

CALPUFF

CALPUFF models emissions dispersion, using site specific geophysical and meteorological data, to predict air quality impacts. To run CALPUFF, follow these steps:

1. Select **CALPUFF** in the CALApps navigation window.

2. Under **CALMET.DAT FILES**, select the **Project/CALMET/calmet.dat** file that was generated by CALMET.

3. Under **MODELING PERIOD**, select the same settings used under **PROJECT INFORMATION**. These settings should populate automatically if **APPLY TO ALL** was selected there. Alternatively, select **RUN ALL PERIODS FOUND IN INPUT METEOROLOGICAL DATA** to automatically run CALPUFF for the entire period included in the **calmet.dat** file.

4. Under **MAP PROJECTION**, select the same settings used under **PROJECT INFORMATION**. These settings should populate automatically if **APPLY TO ALL** was selected there.

5. Under **METEOROLOGICAL GRID**, select the same settings used under **PROJECT INFORMATION**. These settings should populate automatically if **APPLY TO ALL** was selected there.

6. Under **COMPUTATIONAL GRID**, use the default values.

7. Under **MODELED SPECIES -> LIBRARY**, select **SO2, NOX, CO, PM2.5** and **PM10,** then click **ADD**.

8. Under **MODELED SPECIES -> MODELED**, select **SO2, NOX, CO, PM2.5** and **PM10**, then click **APPLY**.

9. Under **TECHNICAL OPTIONS -> DISPERSION COEFFICIENTS**, select **Turbulence-based dispersion [2]**.

10. Under **TECHNICAL OPTIONS -> PDF**, select **PDF used for dispersion under convective conditions [1]**.

11. Under **TECHNICAL OPTIONS -> CHEMICAL MECHANISM**, select **Chemical transformation not modelled [0]**. The other modelling options available here should only be used if species reaction is to be modelled; this is not required for most applications.

12. Under **TECHNICAL OPTIONS -> AQUEOUS PHASE TRANSFORMATION**, select **Aqueous phase transformation not modelled [0]**.

13. Under **DEPOSITION -> TYPES**, select the **DRY DEPOSITION** and **WET DEPOSITION** tick-boxes.

14. Under **DEPOSITION -> DRY DEPOSITION**, select the species for which dry deposition is to be modelled.

15. Under **DEPOSITION -> DRY DEPOSITION -> CHEMICAL PARAMETERS FOR DRY DEPOSITION OF GASES**, use the default values (this table will be blank if no gaseous species have been selected for dry deposition modelling).

16. Under **DEPOSITION -> DRY DEPOSITION -> SIZE PARAMETERS FOR DRY DEPOSITION OF PARTICLES**, use the default values (this table will be blank if no particulate species have been selected for dry deposition modelling).

17. Under **DEPOSITION -> WET DEPOSITION**, use the default values.

18. Under **POINT SOURCE PARAMETERS -> NUMBER OF POINT SOURCES**, select **10**.

19. Under **POINT SOURCE PARAMETERS**, enter the appropriate values. Set **Building Downwash** equal to **0** and **Vertical Momentum Flux Factor** equal to **1**.

20. Under **POINT SOURCE PARAMETERS -> VARIABLE EMISSIONS FILE**, leave the field blank unless temporally or spatially varying sources are to be modelled.

21. Under **POINT SOURCE PARAMETERS -> BUILDING DOWNWASH**, use the default settings.

22. Under **AREA SOURCE PARAMETERS -> NUMBER OF AREA SOURCES**, select **0**.

23. Under **LINE SOURCE PARAMETERS -> NUMBER OF LINES SOURCES**, select **0**.

24. Under **VOLUME SOURCE PARAMETERS -> NUMBER OF VOLUME SOURCES**, select **0**.

25. Under **ROAD SOURCE PARAMETERS -> NUMBER OF ROAD SOURCES**, select **0**.

26. Under **RECEPTORS -> TYPES**, select the **GRIDDED RECEPTORS** tick-box. Leave the **DISCRETE RECEPTORS** tick-box deselected.

27. Under **RECEPTORS -> GRIDDED RECEPTORS** use the values that will appear automatically if **APPLY TO ALL** was selected under **PROJECT INFORMATION.**

28. Under **OUTPUT OPTIONS**, select all the available tick-boxes.

29. Under **OUTPUT FILES -> OUTPUT FOLDER**, select **Project/CALPUFF/** as the directory for saving CALPUFF output files.

30. Click the save icon at the bottom of the window. Click 'save' again when the dialogue box appears.

31. Click the **RUN CALPUFF** button at the bottom of the window. This might take a while. A command prompt window will appear with an output similar to this:

```
C:\CALApps\Project\CALPUFF>"C:\Program Files
(x86)\Exponent\CALApps\EXE Files\TNG\calpuff_v7.2.1.exe"
Project_calpuff.inp
 SETUP PHASE
 COMPUTATIONAL PHASE
   --- Advection Step Starting:
   --- YYYYJJJHH SSSS   # Old  # Emitted

      201336523    0    41553       26      -  299871
inactive puffs removed
 TERMINATION PHASE

C:\CALApps\Project\CALPUFF>pause
Press any key to continue . . .
```

32. Navigate to **Project/CALPUFF/** and open **calpuff.lst** in a text editor. Scroll to the end of the file and check to see if any error or warning messages are present. Address errors and re-run CALPUFF. If CALPUFF has run successfully, the end of **calpuff.lst** should look like this:

```
LAST PERIOD PROCESSED ENDS AT:
       Year: 2014  Month:  1   Day:  1   Julian day:   1
Hour:  0   Second:    0


  End of run -- Clock time: 15:29:30
                     Date: 09-20-2017

        Elapsed Clock Time:     5384.0 (seconds)

                  CPU Time:     5370.9 (seconds)
```

33. Navigate to **Project/CALPUFF/** and locate the result files ending with ***.CON**, ***.DRY**, ***.RHO**, ***.T2D**, ***.VIS** and ***.WET**. These are the CALPUFF concentration, dry flux, density, temperature, relative humidity and wet flux result files, and are required to run CALPOST as described in the next section.

34. Navigate to **Project/CALPUFF/** and copy **luse.clr**, **qaluse.grd** and **qaterr.grd** to **~/Project/Plotting/**. Overwrite existing files if necessary.

CALPOST

CALPOST processes CALPUFF result files to generate time-averaged results that can be plotted using visualisation software such as Surfer. To run CALPOST, follow these steps:

1. Select **CALPOST** in the CALApps navigation window.

2. Under **CALPUFF DATA FILE** select the result file that was generated by CALPUFF **Project/CALPUFF/*.CON**.

3. Under **TYPE OF PROCESSING**, select **Concentrations**.

4. Under **MODELING PERIOD**, select the same settings used under **PROJECT INFORMATION**, which should populate automatically if **APPLY TO ALL** was selected under **PROJECT INFORMATION**. Alternatively, select **RUN ALL PERIODS IN CALPUFF DATA** to run CALPOST automatically for the entire period included in the CALPUFF result file.

5. Under **CONCENTRATION/DEPOSITION PROCESSING -> SPECIES 1**, enter **SO2** for the **SPECIES NAME** and **CO, NOx, PM2.5** and **PM10.0** for other species accordingly. Use the default settings for **UNITS FOR OUTPUT**, **SCALING FACTORS** and **AVERAGING PERIODS**.

6. Under **CONCENTRATION/DEPOSITION PROCESSING -> COMPUTE DAILY MAXIMUM VALUES**, select **NO**.

7. Under **CONCENTRATION/DEPOSITION PROCESSING -> RANKS TO PROCESS**, select all the tick-boxes except **CUSTOM**.

8. Under **CONCENTRATION/DEPOSITION PROCESSING -> NOx to NO2 CALCULATIONS**, select **Use NO2 directly from CALPUFF file with no scaling**.

9. Under **CONCENTRATION/DEPOSITION PROCESSING -> OUTPUT OPTIONS**, select all tick boxes plus **.GRD under PLOT FILE FORMAT**.

10. Under **RECEPTORS -> TYPES**, select the **GRIDDED RECEPTORS** tick-box and deselect the **DISCRETE RECEPTORS** tick-box.

11. Under **RECEPTORS -> GRIDDED RECEPTORS**, select **ALL**.

12. Under **OUTPUT FILES -> OUTPUT FOLDER**, select **Project/CALPOST/** as the directory for saving CALPOST output files.

13. Click the save icon at the bottom of the window. Click 'save' again when the dialogue box appears.

14. Click the **RUN CALPOST** button at the bottom of the window. A command prompt window will appear with an output similar to this:

15. Navigate to **Project/CALPOST/** and open **calpost.lst** in a text editor. Scroll to the end of the file and check for error or warning messages. Address errors and re-run CALPOST. If CALPOST has run successfully, the end of **calpost.lst** should look like this:

```
  CALPOST Application Completed
  Last Period Processed ENDS at:
  Year: 2013  Month: 12   Day: 31   Julian day: 365
Hour: 24   Second:    0

 End of run -- Clock time: 15:58:02
                    Date: 20-Sep-2017

       Elapsed clock time:          168 (seconds)

                 CPU time:          140 (seconds)
```

16. Navigate to **Project/CALPOST/** and locate the files ending with ***.grd**. These are the processed result files that can be plotted using Surfer.

18. Navigate to **Project/CALPOST/** and copy all of the ***.grd** files to **~/Project/Plotting/**.

Selecting CALMET critical parameters in observation mode

When processing data in observation mode, CALMET uses an inverse-distance method at each grid-point to interpolate between observational data and the Step 1 wind field. The interpolation method allows observational data to be weighted depending on proximity to observational stations, as follows (Equation 1):

Equation 1 $$(\mathrm{u},\mathrm{v})_2' = \frac{\frac{(\mathrm{u},\mathrm{v})_1}{\mathrm{R}^2} + \sum_k \frac{(u_{obs},v_{obs})_k}{R_k^2}}{\frac{1}{R^2} + \sum \frac{1}{R_k^2}}$$

where $(u_{obs}, v_{obs})_k$, $(\mathrm{u},\mathrm{v})_1$, $(\mathrm{u},\mathrm{v})_2'$, R_k, and R are the observed wind components at station k, the Step 1 wind components at the grid-point, the initial Step 2 wind components, distance from observational station k to the grid-point and the weighting parameter, respectively. The weighting parameter is the distance from the observational station at which the observation data and the Step 1 wind field are weighted equally. A higher weighting parameter will give observational data greater influence, and vice versa. Separate weighting parameters must be specified for the surface layer (R1) and the above-surface layers (R2).

```
C:\CALApps\Project\CALPOST>"C:\Program Files
(x86)\Exponent\CALApps\EXE Files\TNG\calpost_v7.1.0.exe"
Project_calpost.inp



 CALPOST Application Completed
 Last Period Processed ENDS at:
 Year: 2013  Month: 12   Day: 31   Julian day: 365   Hour:
24   Second:    0


 End of run -- Clock time: 15:58:02
                    Date: 20-Sep-2017

       Elapsed clock time:          168 (seconds)

                  CPU time:          140 (seconds)

C:\CALApps\Project\CALPOST>pause
Press any key to continue . . .
```

Additionally, maximum distances for interpolation must be specified: that is, a station further than a specified distance from a particular grid-point will be excluded from the interpolation. Separate maximum distance parameters must be specified for the surface layer (RMAX1) and above surface layers (RMAX2) and for interpolation over water (RMAX3).

CALMET accounts for the thermodynamic blocking effects of terrain features by adjusting wind direction to be tangential to the terrain if a critical Froude number is exceeded. The Froude number at a particular grid-point is computed as follows (Equation 2):

Equation 2 $$Fr = \frac{V}{N\,(h_{max} - z)}$$

where *Fr, V, N,* h_{max} and *z are* Froude number, wind speed at the grid-point, Brun-Vaisala frequency, highest gridded terrain height within a specified radius of the grid-point and height of the grid-point, respectively. The radius for determining the highest grid-point (TERRAD) must be specified by the user.

When interpolating to compute the Step 1 wind field, CALMET enables users to apply a bias (BIAS) to each vertical layer. The bias weights the significance of surface and upper air data as follows:

- BIAS = 0: surface and upper air data are interpolated with equal weighting;
- BIAS = -1: only surface data are used for interpolations;
- BIAS = +1: only upper air data are used for interpolation.

For most applications, it will be sufficient to use the default BIAS (0) for interpolating surface and upper air data. An exception to this is when terrain is complex and the upper air data have been obtained at a location far from the complex terrain.

Critical parameters values recommended are provided in the below table. It is advisable to plot processed CALMET wind data to visually verify that the processed field is representative of the area being modelled. Some manual tuning of the critical parameters may be required.

Recommended values for critical parameters

Critical parameter	Recommended value (USEPA 2009)
R1	50
R2	100
RMAX1	100
RMAX2	200
RMAX3	200
TERRAD	15
BIAS	0 (at all levels)

Health Risk Assessment dataset

This section accompanies Chapter 6 to present the comprehensive ground and higher-level concentrations of the primary emissions as well as the short- and long-term health endpoints and concentration-response functions.

Different PG Stability Classes

PG Stability Classes	A	B	D	F
R_y	0.4	0.36	0.32	0.31
r_y	0.91	0.86	0.78	0.71
R_z	0.4	0.33	0.22	0.06
r_z	0.91	0.86	0.78	0.71
$\sigma y\ (m) = R_y \times X^{ry}$	26.42774	18.89307	11.6185	8.153831
$\sigma z\ (m) = R_z \times X^{rz}$	26.42774	17.31865	7.987717	1.578161

Plume Rise Calculations

PG	$Z^{'}$ (m)	Option No.	Notes
A, B, D	$54.57 = (1.6 \times ((Fo \times X)^2)^{1/3}) / U$	1	
F	$6.05 = MIN((1.6\times((Fo \times (X)^2)^{1/3}) / U); (2.4 \times (Fo / (9.81 \times 2.5/ Ta))^{1/3})/U^{1/3}; Fo^{1/4}\times(G \times 2.5/ Ta)^{-3/8})$	1	Assuming F<55 and x<F*
		2	For F choose smallest of 1, 2 and 3
		3	For F choose smallest of 1, 2 and 3
F*	$425.26 = 49 \times Fo^{5/8}$	1	Buoyancy Flux plume rise parameter F* = 49*F^(5/8)

A 1-hour $PM_{2.5}$ considering different stability classes and shipping operations

Z (m)	PG: A – Cruising (µg/m^3)	PG: A – Manoeuvring (µg/m^3)	PG: A – At Berth (µg/m^3)	PG: B – Cruising (µg/m^3)	PG: B – Manoeuvring (µg/m^3)	PG: B – At Berth (µg/m^3)	PG: D – Cruising (µg/m^3)	PG: D – Manoeuvring (µg/m^3)	PG: D – At Berth (µg/m^3)
0	5.40e+08	4.34e+08	3.26e+08	5.82e+08	4.68e+08	3.52e+08	2.59e+07	2.08e+07	1.57e+07
3	0.0056	0.0045	0.0034	0.0001	0.0001	0.0001	4.03e-09	3.24e-09	2.44e-09
6	0.0064	0.0051	0.0039	0.0001	0.0001	0.0001	1.09e-09	8.72e-09	6.56e-09
9	0.0076	0.0061	0.0046	0.0002	0.0002	0.0001	2.54e-09	2.04e-09	1.54e-09
12	0.0095	0.0076	0.0057	0.0005	0.0004	0.0003	5.17e-09	4.15e-09	3.12e-09
15	0.0119	0.0095	0.0072	0.0008	0.0007	0.0005	9.14e-09	7.34e-09	5.52e-09
18	0.0149	0.0120	0.0090	0.0015	0.0012	0.0009	1.40e-09	1.13e-09	8.46e-09
21	0.0188	0.0151	0.0113	0.0026	0.0021	0.0016	1.87e-09	1.50e-09	1.13e-09
24	0.0233	0.0187	0.0141	0.0043	0.0035	0.0026	2.16e-09	1.73e-09	1.30e-09
27	0.0287	0.0231	0.0173	0.0071	0.0057	0.0043	2.17e-08	1.74e-08	1.31e-08
30	0.0350	0.0281	0.0211	0.0113	0.0090	0.0068	1.89e-07	1.52e-07	1.14e-07
33	0.0420	0.0337	0.0254	0.0173	0.0139	0.0105	1.43e-06	1.15e-06	8.66e-07
36	0.0499	0.0401	0.0301	0.0259	0.0208	0.0156	9.43e-06	7.57e-06	5.70e-06
39	0.0585	0.0470	0.0353	0.0375	0.0301	0.0226	5.39e-05	4.33e-05	3.25e-05
42	0.0677	0.0544	0.0409	0.0527	0.0423	0.0318	0.0003	0.0002	0.0002
45	0.0774	0.0621	0.0467	0.0719	0.0577	0.0434	0.0012	0.0009	0.0007
48	0.0873	0.0701	0.0527	0.0952	0.0764	0.0575	0.0043	0.0035	0.0026
51	0.0972	0.0780	0.0587	0.1223	0.0982	0.0739	0.0140	0.0113	0.0085
54	0.1068	0.0858	0.0645	0.1525	0.1225	0.0921	0.0395	0.0318	0.0239
57	0.1160	0.0931	0.0700	0.1846	0.1482	0.1115	0.0969	0.0778	0.0585
60	0.1243	0.0998	0.0750	0.2167	0.1741	0.1309	0.2064	0.1657	0.1246
63	0.1310	0.1060	0.0790	0.2470	0.1980	0.1490	0.3810	0.3060	0.2300
66	0.1370	0.1100	0.0830	0.2730	0.2190	0.1650	0.6120	0.4920	0.3700
69	0.1000	0.1000	0.1000	0.3000	0.2000	0.2000	0.9000	0.7000	0.5000

72	0.1000	0.1000	0.1000	0.3000	0.2000	0.2000	1.0000	0.8000	0.6000
75	0.1000	0.1000	0.1000	0.3000	0.2000	0.2000	1.1000	0.9000	0.7000
78	0.1000	0.1000	0.1000	0.3000	0.2000	0.2000	1.0000	0.8000	0.6000

A 24-hour $PM_{2.5}$ considering different stability classes and shipping operations

Z (m)	PG: A – Cruising (µg/m^3)	PG: A – Manoeuvring (µg/m^3)	PG: A – At Berth (µg/m^3)	PG: B – Cruising (µg/m^3)	PG: B – Manoeuvring (µg/m^3)	PG: B – At Berth (µg/m^3)	PG: D – Cruising (µg/m^3)	PG: D – Manoeuvring (µg/m^3)	PG: D – At Berth (µg/m^3)
0	2.25e+08	1.81e+08	1.36e+08	3.52e+08	3.52e+08	3.52e+08	1.08e+07	8.68e+07	6.53e+07
3	0.0002	0.0002	0.0001	0.0001	0.0001	0.0001	1.68e-09	1.35e-09	1.01e-09
6	0.0003	0.0002	0.0002	0.0001	0.0001	0.0001	4.53e-09	3.63e-09	2.73e-09
9	0.0003	0.0003	0.0002	0.0001	0.0001	0.0001	1.06e-09	8.51e-09	6.40e-09
12	0.0004	0.0003	0.0002	0.0003	0.0003	0.0003	2.16e-09	1.73e-09	1.30e-09
15	0.0005	0.0004	0.0003	0.0005	0.0005	0.0005	3.81e-09	3.06e-09	2.30e-09
18	0.0006	0.0005	0.0004	0.0009	0.0009	0.0009	5.84e-09	4.69e-09	3.53e-09
21	0.0008	0.0006	0.0005	0.0016	0.0016	0.0016	7.78e-09	6.24e-09	4.70e-09
24	0.0010	0.0008	0.0006	0.0026	0.0026	0.0026	8.99e-09	7.22e-09	5.43e-09
27	0.0012	0.0010	0.0007	0.0043	0.0043	0.0043	9.04e-09	7.26e-09	5.46e-09
30	0.0015	0.0012	0.0009	0.0068	0.0068	0.0068	7.88e-09	6.33e-09	4.76e-09
33	0.0018	0.0014	0.0011	0.0105	0.0105	0.0105	5.97e-08	4.80e-08	3.61e-08
36	0.0021	0.0017	0.0013	0.0156	0.0156	0.0156	3.93e-07	3.16e-07	2.37e-07
39	0.0024	0.0020	0.0015	0.0226	0.0226	0.0226	2.25e-06	1.80e-06	1.36e-06
42	0.0028	0.0023	0.0017	0.0318	0.0318	0.0318	1.11e-05	8.95e-06	6.73e-06
45	0.0032	0.0026	0.0019	0.0434	0.0434	0.0434	4.80e-05	3.86e-05	2.90e-05
48	0.0036	0.0029	0.0022	0.0575	0.0575	0.0575	0.00018	0.000144	0.000108
51	0.0040	0.0033	0.0024	0.0739	0.0739	0.0739	0.000584	0.000469	0.000353
54	0.0045	0.0036	0.0027	0.0921	0.0921	0.0921	0.001648	0.001323	0.000995
57	0.0048	0.0039	0.0029	0.1115	0.1115	0.1115	0.004039	0.003244	0.002439
60	0.0052	0.0042	0.0031	0.1309	0.1309	0.1309	0.008598	0.006905	0.005193
63	0.0050	0.0040	0.0030	0.1490	0.1490	0.1490	0.0160	0.012764	0.009599

66	0.0060	0.0050	0.0030	0.1650	0.1650	0.1650	0.0260	0.020491	0.01541
69	0.0000	0.0000	0.0000	0.2000	0.2000	0.2000	0.0000	0.028568	0.021484
72	0.0000	0.0000	0.0000	0.2000	0.2000	0.2000	0.0000	0.034589	0.026012
75	0.0000	0.0000	0.0000	0.2000	0.2000	0.2000	0.0000	0.036369	0.027351
78	0.0000	0.0000	0.0000	0.2000	0.2000	0.2000	0.0000	0.03321	0.024975

A 1-hour $PM_{10.0}$ considering different stability classes and shipping operations

Z (m)	PG: A – Cruising (µg/m^3)	PG: A – Manoeuvring (µg/m^3)	PG: A – At Berth (µg/m^3)	PG: B – Cruising (µg/m^3)	PG: B – Manoeuvring (µg/m^3)	PG: B – At Berth (µg/m^3)	PG: D – Cruising (µg/m^3)	PG: D – Manoeuvring (µg/m^3)	PG: D – At Berth (µg/m^3)
0	5.56e+08	4.47e+08	3.37e+08	5.99e+08	4.82e+08	3.63e+08	2.67e+07	2.15e+07	1.62e+07
3	0.0058	0.0047	0.0035	0.0001	0.0001	0.0001	4.15e-09	3.34e-09	2.51e-09
6	0.0066	0.0053	0.0040	0.0001	0.0001	0.0001	1.12e-09	8.98e-09	6.77e-09
9	0.0079	0.0063	0.0048	0.0002	0.0002	0.0002	2.62e-09	2.10e-09	1.59e-09
12	0.0097	0.0078	0.0059	0.0005	0.0004	0.0003	5.32e-09	4.28e-09	3.23e-09
15	0.0122	0.0098	0.0074	0.0009	0.0007	0.0005	9.40e-09	7.56e-09	5.70e-09
18	0.0154	0.0124	0.0093	0.0015	0.0012	0.0009	1.44e-09	1.16e-09	8.74e-09
21	0.0193	0.0155	0.0117	0.0027	0.0021	0.0016	1.92e-09	1.54e-09	1.16e-09
24	0.0240	0.0193	0.0145	0.0045	0.0036	0.0027	2.22e-09	1.79e-09	1.35e-09
27	0.0295	0.0238	0.0179	0.0073	0.0059	0.0044	2.23e-08	1.79e-08	1.35e-08
30	0.0359	0.0289	0.0218	0.0116	0.0093	0.0070	1.95e-07	1.56e-07	1.18e-07
33	0.0432	0.0348	0.0262	0.0178	0.0143	0.0108	1.47e-06	1.19e-06	8.94e-07
36	0.0513	0.0413	0.0311	0.0266	0.0214	0.0161	9.70e-06	7.80e-06	5.88e-06
39	0.0602	0.0484	0.0365	0.0385	0.0310	0.0234	5.54e-05	4.46e-05	3.36e-05
42	0.0696	0.0560	0.0422	0.0542	0.0436	0.0329	0.0003	0.0002	0.0002
45	0.0796	0.0640	0.0482	0.0739	0.0595	0.0448	0.0012	0.0010	0.0007
48	0.0897	0.0722	0.0544	0.0979	0.0787	0.0594	0.0044	0.0036	0.0027
51	0.1000	0.0804	0.0606	0.1258	0.1012	0.0763	0.0144	0.0116	0.0087
54	0.1099	0.0884	0.0666	0.1569	0.1262	0.0951	0.0407	0.0327	0.0247
57	0.1193	0.0959	0.0723	0.1898	0.1527	0.1151	0.0997	0.0802	0.0605

60	0.1278	0.1028	0.0775	0.2229	0.1793	0.1352	0.2122	0.1707	0.1287
63	0.1352	0.1087	0.0820	0.2540	0.2043	0.1540	0.3923	0.3155	0.2379
66	0.1411	0.1135	0.0856	0.2809	0.2260	0.1704	0.6298	0.5065	0.3819
69	0.1455	0.1170	0.0882	0.3015	0.2425	0.1828	0.8781	0.7062	0.5324
72	0.1481	0.1191	0.0898	0.3140	0.2526	0.1904	1.0631	0.8550	0.6447
75	0.1487	0.1196	0.0902	0.3174	0.2553	0.1925	1.1178	0.8990	0.6778
78	0.1475	0.1186	0.0894	0.3113	0.2504	0.1888	1.0207	0.8209	0.6190

A 24-hour $PM_{10.0}$ considering different stability classes and shipping operations

Z (m)	PG: A – Cruising ($\mu g/m^3$)	PG: A – Manoeuvring ($\mu g/m^3$)	PG: A – At Berth ($\mu g/m^3$)	PG: B – Cruising ($\mu g/m^3$)	PG: B – Manoeuvring ($\mu g/m^3$)	PG: B – At Berth ($\mu g/m^3$)	PG: D – Cruising ($\mu g/m^3$)	PG: D – Manoeuvring ($\mu g/m^3$)	PG: D – At Berth ($\mu g/m^3$)
0	2.31e+08	1.86e+08	1.40e+08	2.49e+08	2.01e+08	1.51e+08	1.11e+07	8.94e+07	6.74e+07
3	0.0002	0.0002	0.0001	0.00001	0.00001	0.00001	1.73e-09	1.39e-09	1.05e-09
6	0.0003	0.0002	0.0002	0.00001	0.00001	0.00001	4.65e-09	3.74e-09	2.82e-09
9	0.0003	0.0003	0.0002	0.00001	0.00001	0.00001	1.09e-09	8.77e-09	6.61e-09
12	0.0004	0.0003	0.0002	0.00002	0.00002	0.00001	2.22e-09	1.78e-09	1.34e-09
15	0.0005	0.0004	0.0003	0.00004	0.00003	0.00002	3.91e-09	3.15e-09	2.37e-09
18	0.0006	0.0005	0.0004	0.00006	0.00005	0.00004	6.00e-09	4.83e-09	3.64e-09
21	0.0008	0.0006	0.0005	0.00011	0.00009	0.00007	8.00e-09	6.43e-09	4.85e-09
24	0.0010	0.0008	0.0006	0.00019	0.00015	0.00011	9.25e-09	7.44e-09	5.61e-09
27	0.0012	0.0010	0.0007	0.00030	0.00024	0.00018	9.29e-09	7.47e-09	5.63e-09
30	0.0015	0.0012	0.0009	0.00048	0.00039	0.00029	8.11e-09	6.52e-09	4.92e-09
33	0.0018	0.0014	0.0011	0.00074	0.00060	0.00045	6.14e-08	4.94e-08	3.72e-08
36	0.0021	0.0017	0.0013	0.00111	0.00089	0.00067	4.04e-07	3.25e-07	2.45e-07
39	0.0025	0.0020	0.0015	0.00161	0.00129	0.00097	2.31e-06	1.86e-06	1.40e-06
42	0.0029	0.0023	0.0018	0.00226	0.00182	0.00137	1.15e-05	9.21e-06	6.95e-06
45	0.0033	0.0027	0.0020	0.00308	0.00248	0.00187	4.94e-05	3.97e-05	2.99e-05
48	0.0037	0.0030	0.0023	0.00408	0.00328	0.00247	0.0002	0.0001	0.0001
51	0.0042	0.0033	0.0025	0.00524	0.00422	0.00318	0.0006	0.0005	0.0004

54	0.0046	0.0037	0.0028	0.00654	0.00526	0.00396	0.0017	0.0014	0.0010
57	0.0050	0.0040	0.0030	0.00791	0.00636	0.00480	0.0042	0.0033	0.0025
60	0.0053	0.0043	0.0032	0.00929	0.00747	0.00563	0.0088	0.0071	0.0054
63	0.0056	0.0045	0.0034	0.01058	0.00851	0.00642	0.0163	0.0131	0.0099
66	0.0059	0.0047	0.0036	0.01171	0.00941	0.00710	0.0262	0.0211	0.0159
69	0.0061	0.0049	0.0037	0.01256	0.01010	0.00762	0.0366	0.0294	0.0222
72	0.0062	0.0050	0.0037	0.01309	0.01052	0.00793	0.0443	0.0356	0.0269
75	0.0062	0.0050	0.0038	0.01323	0.01064	0.00802	0.0466	0.0375	0.0282
78	0.0061	0.0049	0.0037	0.01297	0.01043	0.00787	0.0425	0.0342	0.0258

$PM_{2.5}$ long-term health endpoints and concentration-response function (95%CI) – annual average concentrations

Health outcomes	**Australian**	**UK**	**Europe**	**US EPA**	**WHO**	**Recommended**	**This Study**
Mortality							
Cardiopulmonary	n/a	1.09 (1.03-1.16) per 10 µg/m^3 (Pope, Burnett et al. 2002, Committee on the medical effects of air pollutants 2009) Age: 30+ years	n/a	1.14 (1.11-1.17 per 10 µg/m^3 (Krewski 2009, USEPA 2010) ICD9: 401-440, 460-519; Age: 30+ years.	n/a	Recommended CRF: 1.14 (1.11-1.17) per 10 µg/m^3	0.39
Ischaemic heart disease	n/a	n/a	n/a	1.24 (1.19-1.28) per 10 µg/m^3 (Krewski 2009, USEPA 2010) ICD9: 410-414; Age: 30+ years	n/a	Recommended CRF: 1.24 (1.19-1.28) per 10 µg/m^3	0.42
Lung cancer	n/a	1.08 (1.01-1.16) per 10 µg/m^3 (Pope, Burnett et al. 2002, Committee on the medical effects of air pollutants 2009); Age: 30+ years.	n/a	1.14 (1.06-1.123) per 10 µg/m^3 (Krewski 2009, USEPA 2010); ICD9: 162; Age: 30+ years.	n/a	Recommended CRF: 1.14 (1.06-1.123) per 10 µg/m^3	0.39
Infant (<12 months of age)	n/a	n/a	n/a	1.07 (0.93-1.24) for	n/a	Recommended CRF: 1.07 (0.93-1.24) per 10 µg/m^3	0.36

Health outcomes	Australian	UK	Europe	US EPA	WHO	Recommended	This Study
				10 µg/m^3 (Woodruff, Grillo et al. 1997, USEPA 2006), All ICD9; Age: <12 months			
Life expectancy lost (years of life lost; YOLL)	n/a	6 months of life expectancy lost in the UK at current levels of anthropogenic $PM_{2.5}$ (~9 µg/m^3) (Committee on the medical effects of air pollutants 2010)	6.02E-04 YOLL/ (person/year/µg/m^3) (Leksell, 2001)	n/a	n/a	Recommended CRF: 6.02E^{-04} YOLL/ (person/year/µg/m^3)	2e-3

$PM_{2.5}$ short-term health endpoints and concentration-response function (95%CI) – daily average concentrations

Health Outcomes	Australian	UK	Europe	US EPA	WHO	Recommended	This Study
Mortality							
Non-trauma	0.9% (0.2-1.6%) per 3.78 µg/m^3 (Environment protection and heritage council 2005)	n/a	n/a	0.98% (0.75 to 1.22%) per 10 µg/m^3 (Zanobetti and Schwartz 2009, USEPA 2010)	1.00339 (0.99150-1.01542) per 10 µg/m^3 (Anderson, Bremner et al. 2001, WHO 2004)	Recommended CRF: 0.9% (0.2-1.6%) per 3.78 µg/m^3	2.82%
Cardiovascular	1.0439 (1.0090- 1.0800) increase per 1-unit bsp (10-4. m-1) (Simpson, Williams et al. 2005) Pooled CRF from 4 cities (Sydney, Perth, Melbourne, Brisbane)	1.4% (0.7-2.2%) per 10 µg/m3 (Committee on the medical effects of air pollutants 2006); All ages.	n/a	0.85% (0.46 to 1.25%) per 10 µg/m3 (Zanobetti and Schwartz 2009); Ages: All ages.	1.00507 (0.98808-1.02236) per 10 µg/m3 (Anderson, Bremner et al. 2001); Age: All ages.	Recommended CRF: 1.5% (0.7-2.3%) per 3.78 µg/m3	4.7%

	1.5% (0.7-2.3%) per 3.78 µg/m3 (Environment protection and heritage council 2005); Age: All ages; All year; No heterogeneity; Meta-analysis of 4 cities - Brisbane, Melbourne, Perth Sydney.						
Hospitalisation							
Cardiovascular	15-64 years: No effect 65+ years: 1.3% (0.6-2.0) increase per 3.78 µg/m^3 (Environment protection and heritage council 2005)	n/a	n/a	0.80% (0.59-1.10%) per 10 µg/m^3 (Bell, Ebisu et al. 2008)		Recommended CRF: 65+ years: 1.3% (0.6-2.0) increase per 3.78 µg/m^3	0.8%
Cardiac failure	15-64 years: No effect 65 years: 3.6% (1.8-5.4%) per 3.78 µg/m^3 24-hour average (Environment protection and heritage council 2005); Moderate heterogeneity for 65+ years; Meta-analysis of 4 cities – Brisbane, Melbourne, Perth	n/a	n/a	n/a	n/a	Recommended CRF: 65+ years: 3.6% (1.8-5.4%) increase per 3.78 µg/m3	2.2%
Ischaemic heart disease	15-64 years: No effect 65+ years: 1.6% (0.7-2.4%) per 3.78 µg/m^3 (Environment protection and heritage council 2005); 24-hour	n/a	n/a	n/a	n/a	Recommended CRF: 65+ years: 1.6% (0.7-2.4%)	1.0%

	average. Lag 01; Low heterogeneity; Meta-analysis of 4 cities: Brisbane, Melbourne, Perth Sydney.					increase per 3.78 µg/m3	
Myocardial infarction	15-64 years: No effect. 65+ years: 2.7% (1.3-4.2%) per 3.78 µg/m^3 (Environment protection and heritage council 2005); 24-hour average; Lag 01; Low heterogeneity for 65+ years; Meta-analysis of 4 cities: Brisbane, Melbourne, Perth Sydney.	n/a	n/a	n/a	n/a	Recommended CRF: 65+ years: 2.7% (1.3-4.2%) increase per 3.78 µg/m3	1.69%
Emergency department visits							
Incidence of myocardial infarction (heart attacks)							
Non-fatal heart attacks (24-hr PM)	n/a	n/a	n/a	1.62 (1.13-2.34) per 20 µg/m3 (Peters, Dockery et al. 2001); Age: 18+ years		Recommended CRF: 1.62 (1.132.34) per 20 µg/m3	0.9
Minor morbidity							
Minor restricted activity days (MRAD)	n/a	n/a	0.74% (0.60-0.88%) per 1 µg/m^3 (Ostro and	1.0769 (1.0622-1.0918) per 10 µg/m^3 (Ostro and Rothschild		Recommended CRF: 1.0769 (1.0622-1.0918) per 10 µg/m3	1.28

				Rothschild 1989); Age: 18-64 years.	1989); Age: 18-64 years.			
Work lost days (WLD)	n/a			n/a	0.46% (0.39-0.53%) per 1 µg/m^3 (Ostro 1987); Age: 15-64 years.	1.0471 (1.0397-1.0545) per 10 µg/m3 (Ostro 1987); Age: 18-64 years.		Recommended CRF: 1.0471 (1.0397-1.0545) per 10 µg/m3	1.24
Acute bronchitis (incidence, 8-12 years)	n/a			n/a	n/a	1.5 (0.91-2.47) per 14.9 lag/m3 (Dockery, Cunningham et al. 1996)		Recommended CRF: 1.5 (0.91-2.47) per 14.9 µg/m3	1.19
Lower respiratory symptoms	n/a	n/a	n/a	1.33 (1.11-1.58) per 15 µg/m^3 (Schwartz and Neas 2000); Age: 7-14 years.		n/a	Recommended CRF: 1.33 (1.11-1.58) per 15 µg/m^3		1.058

$PM_{10.0}$ long-term health endpoints and concentration-response function (95%CI) – annual average concentrations							
Health outcomes	**Australian**	**UK**	**Europe**	**US EPA**	**WHO**	**Recommended**	**This Study**
Long-term outcomes (annual average concentration)							
Mortality							
All cause	n/a	n/a	0.386% (0.295- 0.477%) per 1 µg/m^3 (Pope, Thun et al. 1995); All Age: 30+ years	n/a	1.10 (1.03-1.18) per 10 µg/m^3 (Dockery, Pope et al. 1993)	Recommended CRF: 0.386% (0.295-0.477%) per 1 µg/m^3	1.18%
Infant all cause (<12 months age)	n/a	n/a	4% (2-7%) per 10 µg/m3 (Woodruff, Grillo et al. 1997)	n/a	n/a	Recommended CRF: 4% (2-7%) per 10 µg/m^3	1.2%
Life expectancy (Years of life lost; YOLL)	n/a	2-6 months per death brought forward (DEFRA 2006)	2.69E-04 YOLL / (person/yr/µg/m^3) (European commission 2005); Applies to whole population.	n/a	n/a	Recommended CRF: 2.69E-04 YOLL / (person/yr/µg/m3)	16.4
Morbidity							
Airway inflammation	1.04 (1.01-1.06) per 1 µg/m^3 in single pollutant model (Williams 2012); Six cities –	n/a	n/a	n/a	n/a	Recommended CRF: 1.04 (1.01-1.06) per 1 µg/m3	0.6

	Adelaide, Brisbane, Canberra, Melbourne, Perth, Sydney.						

$PM_{10.0}$ short-term health endpoints and concentration-response function (95%CI) – daily average concentrations							
Health outcomes	**Australian**	**UK**	**Europe**	**US EPA**	**WHO**	**Recommended**	**This Study**
Hospitalisation							
Cardiac	2.4% (1.5-3.4%) per 10 µg/m^3 (Simpson, 2005); Pooled estimate from 3 cities (Sydney, Melbourne, Brisbane); Age: All ages. 15-64 years: No effect and 65+ years: 1.4%	n/a	n/a	n/a	n/a	Recommended CRF: 65+ years: 1.4% (0.5-2.2%) per 7.53 µg/m^3	0.7%
Cardiac failure	15-64 years: No effect 65+ years: 3.6% (2.0-5.2%) per 7.53 µg/m3 (Environment protection and heritage council 2005) for 65+ years; Meta-analysis of 4 cities - Brisbane, Melbourne, Perth	n/a	n/a	n/a	n/a	Recommended CRF: 65+ years: 3.6% (2.0-5.2%) per 7.53 µg/m3	2.3%
Pneumonia and acute bronchitis	0 years: No effect 1-4 years: No effect 15-64 years: No effect 65+ years: 1.0% (0.2-3.8%) per 7.53 µg/m^3 (Environment protection and heritage council 2005)	n/a	n/a	n/a	n/a	Recommended CRF: 65+ years: 1.0% (0.2-3.8%) per 7.53 µg/m^3 per 7.53 µg/m^3	0.6%
Emergency department visits							
Asthma	1.4% (0.8-2.0%) per 7.6 µg/m3 (Jalaludin, Khalaj et al. 2008) – Sydney	n/a	1.0374 (1.0121-1.0633) per 10 µg/m^3 (Schwartz 1993); Age: All ages.	n/a	n/a	Recommended CRF: 1.4% (0.82.0%) per 7.6 µg/m3	4.6%

Lung function							
Change in forced expiratory volume in 1 second (FEW litres)	-0.0043 (-0.0078 to -0.0008) per 1 µg/m^3 and 24-hour average Lag 2 (Williams 2012); Six cities – Adelaide, Brisbane, Canberra, Melbourne, Perth, Sydney; Age: mean age 10.0 years. 270 children with current asthma.		n/a	n/a	-1.2% (-2.3 to -0.1%) per 10 µg/m^3 (Raizenne, Neas et al. 1996)	Recommended CRF: -0.0043 (-0.0078 to -0.0008) per 1 µg/m3	-0.10
Change in peak expiratory flow rate (PEF; litres per minute)	No effect	n/a	n/a	n/a	-0.13% (-0.17 to -0.09%) per 10 µg/m3 (WHO 2000)	Recommended CRF: -0.8187 (-1.3325 to -0.3048) per 1 µg/m^3	-20.3
Minor morbidity							
Shortness of breath	Day SOB: No effect Night SOB: 1.0417 (1.0031-1.0819) per 1 µg/m^3 (Williams 2012); Six cities – Adelaide, Brisbane, Canberra, Melbourne, Perth, Sydney; Age: mean 10.0 years.	n/a	n/a	n/a	n/a	Recommended CRF: 1.0417 (1.0031-1.0819) per 1 µg/m3	25.8

NO_x long-term health endpoints and concentration-response function (95%CI) – annual average concentrations

Health outcomes	Australian	UK	Europe	US EPA	WHO	Recommended	This Study
Mortality							
Incidence of asthma	1.27 (1.041.56) per 4.31 ppb (Williams 2012); Six cities -Adelaide, Brisbane, Canberra, Melbourne, Perth, Sydney; Age: mean age10.0 years. 2,860 children.	n/a	n/a	n/a	n/a	Recommended CRF for asthma incidence: 1.27 (1.04-1.56) per 4.31ppb	0.76
Airway inflammation	1.03 (1.01-1.05) per 1 ppb in single pollutant model. Remains significant in 2-pollutant models with $PM_{2.5}$, PM_{10}, O_3 and SO_2 and CO (Williams 2012); Six cities - Adelaide, Brisbane, Canberra, Melbourne, Perth, Sydney; Average hourly NO_2 over lifetime. Age: mean age10.0 years. 2,860 children.	n/a	n/a	n/a	n/a	Recommended CRF: 1.03 (1.01-1.05) per 1 ppb	2.66

NO_x Short-term health endpoints and concentration-response function (95%CI) – Daily Average Concentrations

Health outcomes	Australian	UK	Europe	US EPA	WHO	Recommended	This Study
Mortality							
Non-trauma	1.7% (0.3-3.2%) per 8.98 ppb (European commission 2005); Age: All; All year. 5 cities-Brisbane, Canberra, Melbourne, Perth, Sydney.	n/a	n/a	n/a	n/a	Recommended CRF: 1.7% (0.3-3.2%) per 8.98 ppb	1.49%
Cardiovascular	3.9% (0.6-7.4%) per 8.98 ppb (European commission 2005); Age: All ages; All year; 5 cities-Brisbane, Canberra, Melbourne, Perth, Sydney.	1.0% (0.8-1.3%) per 10 ug/m^3 (Committee on the medical effects of air pollutants 2006)	n/a	n/a	n/a	Recommended CRF: 1.6% (0.4-2.8%) per 8.98 ppb	1.40%
Respiratory	3.9% (0.6-7.4%) per 8.98 ppb (European commission 2005); Age: All ages; All year; 5 cities-Brisbane, Canberra, Melbourne, Perth, Sydney.	No effect (Zmirou, Schwartz et al. 1998)	n/a	n/a	n/a	Recommended CRF: 3.9% (0.6-7.4%) per 8.98 ppb	3.43%
Hospitalisation							
Cardiovascular	1.0022 (1.0016- 1.0028) per 1 ppb (Simpson, Williams et al. 2005) in Sydney, Perth, Melbourne.	1.3% (1.0-1.7%) per 10 ug/m3 (Committee on the medical effects of air pollutants 2006)	n/a	n/a	n/a	Recommended CRF: 1.3% (0.32.3%) per 8.98 ppb in 15-64 years; 2.6% (1.8-3.3%) per 8.98 ppb in 65+ years	15-64 years: 0.8% +65 years:

							0.02%
Cardiac	15-64 years: No effect 65+ years: 7.5% (5.3-9.7%) per 8.98 ppb	1.3% (0.4-2.3%) change per 10 ug/m^3 (Committee on the medical effects of air pollutants 2006)	n/a	n/a		Recommended CRF: 15-64 years: 1.2% (0.0-2.4%) per 8.98 ppb in 15-64 years; 3.3% (2.4-4.3%) per 8.98 ppb in 15-64 years	0.8%
Cardiac failure	65+ years: 1.0016 (1.0006-1.0026) (European commission 2005) per 1 ppb - Sydney, Perth, Melbourne, Brisbane.	No effect (Zmirou, Schwartz et al. 1998)	n/a	n/a	n/a	Recommended CRF: 7.5% (5.39.7%) per 8.98 ppb in 65+ years	0.13%
Emergency department visits							
Asthma	Single pollutant model: 2.3% (1.4, 3.2%) per 9.5 ppb Two pollutant model with $PM_{2.5}$: 1.1% (0.6-1.6%) per 9.5 ppb (Jalaludin, Khalaj et al. 2008) in Sydney	n/a	n/a	n/a	n/a	Recommended CRF: Two pollutant model with $PM_{2.5}$: 1.1% (0.6-1.6%) per 9.5 ppb	0.91%
Lung function							
Change in forced expiratory volume in 1 second (FEW litres)	-0.4042 (-0.7318 to -0.0767) per 1 ppb (Jalaludin, Khalaj et al. 2008)	n/a	n/a	n/a	n/a	Recommended CRF: Morning FEW 0.0025 (-0.0047 to 0.0002) per 1 ppb	0.01

Change in peak expiratory flow rate (PEF; litres per minute)			n/a	n/a	n/a	Recommended CRF: Morning PEF: -0.4042 (-0.7318 to -0.0767) per 1 ppb (Williams 2012)	-3.1

SO_x long-term health endpoints and concentration-response function (95%CI) – annual average concentrations

Health outcomes	Australian	UK	Europe	US EPA	WHO	Recommended	This Study
Mortality							
Change in forced expiratory volume	No effect in single pollutant model.	n/a	n/a	n/a	n/a	Recommended CRF: -6.62 mls (-12.3 to -0.96 mls) per 0.74 ppb in 2-pollutant model with NO2 (Williams 2012)	-12.7mls
Change in forced vital capacity	No effect in single pollutant model.					Recommended CRF: -8.92 mls (-16.0 to -1.84 mls) per 0.74 ppb in 2-pollutant model with NO_2 (Williams 2012)	-17.1mls
Emergency department visits							
Asthma	Not assessed (Erbas, Kelly et al. 2005)	n/a	n/a	n/a	n/a	Recommended CRF: 1.6% (0.72.4%) per 0.8 ppb (Bell, Ebisu et al. 2008)	7.53%
Incidence of myocardial infarction (heart attacks)							
Bronchodilator use	1-hour maximum Night use: 1.0247 (1.0021-1.0478) per 1 (Williams 2012) - Adelaide, Brisbane,	n/a	n/a	n/a	n/a	Recommended CRF for night bronchodilator use: 1.0247 (1.0021-1.0478) per 1 ppb	3.86

Appendix B: Full Papers Published

Paper 1 – *Jahangiri S, Nikolova N and Tenekedjiev K. Emission Inventories for Ship Operations; Methodological Comparison with On-board Measurements. AGA 2018 / IAMU Student - International Association of Maritime Universities (IAMU). ISBN 978-84-947311-7-4. Pages 33-40. October 2018.*

This article has been removed for copyright or proprietary reasons.

Paper 2 – *Jahangiri S, Nikolova N and Tenekedjiev K. Empirical Testing of Inventories Applying On-board Measurements of Exhaust Emissions at Port and at Sea. Journal of Sustainable Development of Transport and Logistics. Volume 3, Issue 2. Pages 6-33. Doi: https://dx.doi.org/10.14254/jsdtl.2018.3-2.1. December 2018.*

Journal of Sustainable Development of Transport and Logistics
journal home page: https://jsdtl.sciview.net

Jahangiri, S., Nikolova, N., & Tenekedjiev, K. (2018). Empirical testing of inventories applying on-board measurements of exhaust emissions at port and at sea. *Journal of Sustainable Development of Transport and Logistics, 3*(2), 6-33. doi:10.14254/jsdtl.2018.3-2.1.

ISSN 2520-2979

Empirical testing of inventories applying on-board measurements of exhaust emissions at port and at sea

Sanaz Jahangiri [1], **Natalia Nikolova** [1,2], **Kiril Tenekedjiev** [1,2]

[1] *Australian Maritime College, University of Tasmania, Launceston, Tasmania, Australia*
[2] *Nikola Vaptsarov Naval Academy, Varna, Bulgaria*

Article history:

Received: June 10, 2018
1st Revision: August 20, 2018
Accepted: October 25, 2018

DOI:
10.14254/jsdtl.2018.3-2.1

Abstract: We present a comprehensive case study to identify the best vessel-specific inventory family that predicts the primary emissions from an ocean-going vessel when at berth, while maneuvering and while cruising. The main purpose of the paper is to generalize the implication of the case study by advising a novel policy, which will allow different authorities to estimate the shipping emissions in a cost-effective and reliable way. The emissions rates of nitrogen oxides, sulphur oxides, carbon dioxide, carbon monoxide, hydrocarbon, and particulate matter from the main engine and from the auxiliary engines are measured for different modes of ship operations in an on-board experiment campaign. The measured total emission amounts were predicted with 13 families of emission inventories and prediction deviations have been calculated. A procedure was advised for estimating the prediction inventory deviations of the combined hourly emission amounts from the main engine plus the auxiliary engines. Each inventory family has been formalized as a six-dimensional vector of prediction deviations for any mode of operation. The best vessel-specific inventory families were identified using the minimal mean absolute deviation criteria. A more rational procedure to rank inventories is considered, which treats the missing value problem and constructs a six-attribute value function. The use of preferential analysis and value functions further clarifies the recommended choice of inventory method. In this case study we demonstrated that the most suitable inventory families will provide reliable predictions with acceptable deviations from the measured emissions. At berth and for maneuvering, the best inventory family turned out to be MOPSEA (with 32.2% and 39.6% mean absolute deviations respectively). For cruising, the most precise inventory family is MEET (with 59.2% mean absolute deviation), whereas MOPSEA being the third best. However, some of the other inventories produce unacceptably high deviation, well above 100%. The practical implication is that while inventory methods can produce precise and cost-effective predictions, they should never be used without experimental verification. That is why, we provide an algorithm to use on-board experimental measurements to identify the best vessel-specific inventory family, which predicts the primary emission of a ship at a given mode of operation. The proposed algorithm and the implications of the case study are utilized to motivate a proposal for a novel future policy for a cost-effective and reliable emission estimation from shipping.

Keywords: Emission pollution in ports, Emission inventory, On-board measurement, Experimental ranking of inventory procedures, Additive value functions.

Corresponding author: *Sanaz Jahangiri*
E-mail: Sanaz.jahangiri@utas.edu.au

1. Introduction

1.1. Sea transport and its environmental sustainability

Transportation of freight and unrefined oil by ships is a critical operation in the transit of petroleum from the Middle East to global users (Michaelowa, 2000), and sea transport is currently recognized as the best method of transport (Wang, Corbett, & Firestone, 2008). Marine transportation of petroleum and other goods is economical, and ships can transport bulky goods better than other means of transport (Deniz & Kilic, 2010). Furthermore, sea transport is considered secure (Martínez de Osés & La Castells, 2010) and improves environmental sustainability as it produces fewer pollutants than land transport (OECD, 1997). The rising popularity of shipping is also expected to increase the number of oceangoing vessels (UNCTAD, 2014).

Even though sea transport is less polluting than land transport, the growing number of shipping activities means that pollution from ships is a significant danger to health. The growing number of shipping activities causes increased pollution levels both globally and in the ports because most shipping companies use low-quality fuel (Deniz & Kilic, 2010). Therefore, tracing all emissions and determining their possible effects on the environment is a growing necessity. While there is strict regulation and close monitoring of land-related emissions, the sea transport sector lacks adequate mechanisms to monitor and determine the rate of emissions, hindering steps to foster environmental protection and sustainability (Corbett & Fischbeck, 1997; Corbett et al., 2007).

1.2. State-of-the-art in emission monitoring for maritime transport

Shipping operations emit a significant amount of primary emissions including nitrogen oxides (NO_2, NO, N_2O denoted as a whole with NO_x), sulphur oxides (SO_2, SO_3, SO denoted as a whole with SO_x), carbon dioxide (CO_2), carbon monoxide (CO), volatile organic compounds, in particular hydrocarbon (HC), and particulate matter (PM) (Eyring, Kohler, Van Aardenne, & Lauer, 2005). Studies have noted that such emissions have adverse consequences on human health and the environment (Corbett et al., 2007; Goldsworthy & Goldsworthy, 2015). For instance, NO_2 and CO emissions cause flu-like symptoms, while SO_x-pollutants lead to breathing difficulties and PM emissions result in premature deaths (EPA, 2010). Various empirical studies have linked asthma and cardiovascular illnesses to some of those pollutants (Kim, Hwang, & Lee, 2010; Lu et al., 2006), and some researchers and scientists (Corbett et al., 2007) have reported lung cancer deaths and heart-related diseases connected to PM pollutants in ports in Europe, East Asia and South Asia. Shipping emissions pose various public health consequences for people living near ports, and finding solutions to the situation and taking practical steps to identify and measure emissions precisely require that better procedures and plans to control pollutants need to be developed.

Several studies (Kilic & Deniz, 2010; Moreno-Gutierrez et al., 2015; Merk, 2014) have considered emissions caused by shipping operations and their effects on distinct scales, such as different seaports and nations. There are some estimates that ocean-going vessels generate 17–31% of worldwide emissions of NO_x, and 4–10% of SO_x (Eyring et al., 2005; Kilic & Deniz, 2010; Moreno-Gutierrez et al., 2015). A recent study (Merk, 2014) assessed that CO_2 from shipping emissions as accounting for approximately 2–3% of world emissions, which is higher than the amount of non-greenhouse emissions. As the operations of the global fleet of ocean-going vessels increase, emissions are expected to also increase. It is argued in (Eyring et al., 2005) that by the year 2050 the number of vessels will triple, the primary emissions will quadruple, and the emission of CO_2 may rise by 50% of current emissions (Radischat et al., 2015). Approximating and assessing potential amount of and danger caused by shipping emissions is an increasing concern.

Several approaches to estimating shipping emissions have been developed. One such solution is online computer-based monitoring of shipping pollution, which utilizes measurement system as part of the fixed ship equipment. Online monitoring mechanisms provide data over an extended period, but it is very expensive to obtain and maintain because of the aggressive ship environment and the lack of expertise on-board. On top, the measurement results are with low precision and sometimes unreliable (Radischat et al., 2015). Another method is the ship plumes-related measurement, where the measurement equipment is portable and owned by different party. The on-board measurement is conducted on a specified ship whenever it is demanded by the ship owner or by the authorities. The mechanism provides an exact emissions information of a specific vessel. Multiple previously conducted studies applied on-board measurement (Cooper & Andreasson, 1999; Endresen et al., 2003; Petzold et al., 2006; Sinha et al., 2003). Petzold et al. (2008) focused on a 4-stroke marine engine, while in (Kasper,

Aufdenblatten, Forss, Mohr, & Burtscher, 2007) the PM emissions of a 2-stroke marine engine were investigated. Corbett & Koehler (2003) focused on various pollutants in several types of engine. Others (Cooper, 2001, 2003; Cooper, Peterson, & Simpson, 1996) evaluated the emissions from the main engines (ME)s and auxiliary engines (AE)s of ferries. Some studies (Kasper et al., 2007; Lyyranen, Jokiniemi, Kauppinen, & Joutsensaari, 1999; Petzold et al., 2008; Wright, 1997) considered slow speed diesel (SSD) and medium speed diesel (MSD) engines on test rigs. This research focuses on the measurement of emission rates related to marine diesel engines during different stages of operation, both at mooring and while cruising, to provide insights into the emissions produced under different sailing conditions.

Because the utilization of inbuilt measurements proves to be difficult, time-consuming and resource-demanding, it is difficult to convince ship-owners to purchase and install recommended measurement devices (Cappa et al., 2014; Chen et al., 2005). Therefore, emission inventories are utilized, which are mathematical models to estimate emissions discharged into the atmosphere (Dalsoren et al., 2009; Endresen, Sorgard, Behrens, Brett, & Isaksen, 2007; Skjølsvik, Andersen, Corbett, & Skjelvik, 2000). We will be analyzing such emission inventories made during shipping operations. Several factors are taken into account when developing emission inventories, such as the type of fuels, the place to conduct the study, the nature of the vessel, the engine models, etc. Most existing emission inventories are affected by weak quantifications and application of traditional emission elements to measure both regional and global air quality, such as US EPA discussed in (Browning & Bailey, 2006).

Various methodologies exist that can utilize shipping emission inventories as a way to make accurate estimations of the level of emissions from shipping. The thirteen methods used in this study are: Tier I–III (Trozzi & De Lauretis, 2013), ENTEC (ENTEC. 2007), MEET (Hickman, Hassel, Joumard, Samaraz & Sorensen, 1999), STEAM (Jalkanen et al., 2009), MOPSEA (Gommers, Verbeeck, Cleemput, Schrooten & De Vlieger, 2007), IMO (IMO. 2014), SMED (Cooper & Gustafsson, 2004), EMS (Van der Gon & Hulskotte, 2010), US EPA (Hockstad & Hanel, 2018), NERI (Olesen, Winther, Ellermann, Christensen, & Plejdrup, 2009) and Corbett (Corbett et al., 2003). These approaches can be categorized into three groups: a full bottom-up approach, a comprehensive top-down approach, and a mixed approach, as postulated by Miola and Ciuffo (2011). The categorization is according to the emissions evaluation and the geographical characterization.

A full bottom-up approach assesses the levels and types of emissions generated by a single ship, considering the nature of the vessel, which includes ship type, date of construction, quality of engine and the specific fuel oil consumption (SFOC) at a given point (Moreno-Gutierrez et al., 2015). This allows the underlying factors of the emissions to be identified and evaluated, leading to an explicit understanding of the consequences they may have. ENTEC, Corbett, STEAM, MOPSEA, NERI, EMS, US EPA, and SMED belong to this category in our study.

An entirely top-down methodology observes emissions from a more global perspective and utilizes generalized factors, such as fuel consumption data for given fuel types and the types of engines used in particular ships as determinants of emissions (Miola & Ciuffo, 2011).

Some of the methods discussed in this paper follow a mixed approach. Tier I–III displays some top-down characteristics regarding emission inventories, but tends to be bottom-up regarding geographical distribution. The MEET and IMO approximate a bottom-up emissions inventory and a top-down geographic distribution.

Whichever approach is adopted, each inventory method predicts a set of emission factors (EF)s that will deviate from the experimental measurement values. The main reason for the observed discrepancies between the observed and predicted EFs is that most of the inventories are developed under specific assumptions that include fuel type, consumption units of fuel, ship navigation locations, types of ships, the nature of engines, type of the vessels, etc., which in any particular case will be different from the actual one. It is therefore important to determine a good-enough emission inventory mechanism that is premised on the factors and assumptions which are as close as possible to the actual factors and assumptions for the vessel whose EFs are to be predicted.

1.3. Objectives of the study

The first objective of this paper is to present a comprehensive case study to identify the best vessel-specific inventory family predicting the primary emissions from ocean-going vessels when at berth, while maneuvering and while cruising. In the case study, the primary emission rates of NO_x, SO_x, CO_2, CO, HC, and PM were measured during on-board experimental measurement campaign for the three modes of the vessel's operation. The emissions were predicted with 13 families of emission inventories (Tier I–III, ENTEC, MEET, STEAM, MOPSEA, IMO, SMED, EMS, US EPA, NERI and Corbett) and prediction deviations have been calculated.

Another objective is to create generalized rational algorithm to rank inventory families based on the precision of their predictions for a given operational mode of a specific vessel.

The third objective is to use the implications of the case study together with the developed algorithm to rank inventory families to offer a novel future policy for a cost-effective and reliable emission estimation caused by shipping.

In what follows, section 2 explains the conditions and the procedures in the on-board measurement campaign. The results of the comparison analysis between the measured and predicted emissions are described in section 3. In section 4, a six-attribute value function is discussed as a rational alternative for the minimal mean absolute deviation criterion and general algorithm for identifying the best vessel-specific inventory families for a given mode of operation. Based on the case study implications, a possible future policy for ship emission evaluation is advised. Section 5 concludes the paper.

2. On-board campaign measurement

2.1. General description of on-board measurements campaign

Measurements were taken on-board a large hauler ship as it approached Newcastle from Gladstone, Australia. This vessel, manufactured in 2002, is 187.5m in length, with a 27198 GRT capacity and an average steaming speed of 11.6 knots. The vessel has a MAN B&W 6S50MC main engine, which is 6880-kW, two-stroke, six-cylinder, slow speed diesel (SSD). Each of the auxiliary engines is Wartsila 20, which is 460-kW, four-stroke, four-cylinder, medium speed diesel (MSD).

Measurements of emissions were taken on-board following the procedures elaborated in ISO 8178-2:2008 (Jalkanen et al., 2012) and ISO 8178-1:2006 (MEET, 1999). The on-board emission measurement campaign was divided into 4 separate experiments. The first one was to measure the NO_x, SO_x, CO_2, and CO emissions from the AE when the vessel was at berth. The second, third, and fourth experiment were to measure the NO_x, SO_x, CO_2, CO, HC, and PM emissions from the ME when the vessel was at berth, maneuvering, and cruising respectively.

For the main engine experiments the probes of the exhaust gas were sampled between the turbocharger and the economizer of the ME. The emission rates of SO_x, CO_2, CO, and HC were measured with main gas analyzer Testo 350 XL. The emission rates HC were measured with Horiba MEXA 584L 5-gas analyzer. The mass concentration of PM was measured with Dust Trak Aerosol Monitor 8530 (TSI) separately for $PM_{2.5\text{-}10}$ (with aerodynamic diameters between 2.5 and 10 μm), $PM_{1.0\text{-}2.5}$ (with aerodynamic diameters between 1.0 and 2.5 μm), and $PM_{1.0}$ (with aerodynamic diameters less than 1.0 μm). To cool the probe for PM measurement, the sample was diluted with air. The rates of the samples' dilution were estimated by comparing the CO_2 emission rate in the initial sample with, the CO_2 emission rate of the diluted sample measured with Sable CA-10 CO_2 monitor. Simultaneously the shaft speed (SS) and the actual engine power (P_{act}) were measured every 5 sec. The specific oil consumption (SOC) was determined as a quadratic function of the engine load factor LF (the actual engine power measured in % of the maximum continues rating of the engine). The average air consumption (AC) was assessed as a linear function of the load factor. The instantaneous exhaust mass flow rate (EMFR) was assessed as the sum of AC with the product of SOC and P_{act}.

For the auxiliary engine experiments, the probes of the exhaust gas were sampled after the turbocharger. The measurement equipment was Testo 350 XL only. In this experiment, HC and PM were not measured. The SS, P_{act}, SOC, AC and EMFR were obtained as in the ME experiments.

For each of the experiments the probes were taken at equal inter-sample interval Δt. If the duration of the experiment is T, then the count of the probes sampled for measurement is $N=T/\Delta t$. The time when the i-th probe was sampled is $t_i=(i\text{-}0.5)\Delta t$ for $i=1,2,\ldots,N$. The parameters of the measurement process for each of the experiments are given in Table 1.

Table 1: Measurement process parameters

Experiment	Inter-sample Interval (h)	Count of Samples	Duration (h)	Duration (h, min, s)
ME at berth for NO_x	1/3600	1569	0.4358	26 min, 9 s
ME at berth for SO_x, CO	1/3600	1577	0.4381	26 min, 17 s
ME at berth for CO_2	1/3600	1521	0.4225	25 min, 22 s
ME at berth for HC	300/3600	4	0.3333	20 min
ME at berth for PM	300/3600	5	0.4167	25 min
AE at berth for NOx, SO_x, CO_2, CO	1/3600	9476	2.632	2 h, 37 min, 56 s
ME maneuvering for NO_x	1/3600	6553	1.820	1 h, 49 min, 13 s
ME maneuvering for SO_x	1/3600	6558	1.822	1 h, 49 min, 18 s
ME maneuvering for CO_2	1/3600	6522	1.812	1 h, 48 min, 42 s
ME maneuvering for CO	1/3600	6542	1.817	1 h, 49 min, 2 s
ME maneuvering for HC	300/3600	5	0.4167	25 min
ME maneuvering for PM	300/3600	27	2.250	2 h, 15 min
ME cruising for NO_x, SO_x, CO_2, CO	1/3600	15305	4.251	4 h, 15 min, 5 s
ME cruising for HC, PM	300/3600	64	5.333	5 h, 20 min

2.2. On-board measurements

For the five gases (NO_x, SO_x, CO_2, CO, and HC) the measured instantaneous emission rates at time t_i were converted into instantaneous emission factors (EFs) using the atmospheric pressure, the exhaust gas temperature, the exhaust flow rate (which is the total fuel and air consumption divided by the mass density of the exhaust gas), the molar mass of the gas, the air density, and the engine power. The later was linearly interpolated for each t_i from the measured engine power data. For each of the three types of PM ($PM_{2.5\text{-}10}$, $PM_{1.0\text{-}2.5}$, and $PM_{1.0}$) the mass concentrations were converted into instantaneous emission factors (EFs) using the exhaust flow rate, the dilution rate (calculated from the difference of the CO_2 measured before and after the dilution of the hot probe with cold air), the air density, and the actual engine power (P_{act}). The EF of the PM is calculated as the sum of the EFs for $PM_{2.5\text{-}10}$, $PM_{1.0\text{-}2.5}$, and $PM_{1.0}$. When not measured, the EF for $PM_{2.5\text{-}10}$ is assessed as 20% of the EF of PM (Hockstad & Hanel, 2018). In the same way when not measured, the EFs for $PM_{1.0\text{-}2.5}$, and $PM_{1.0}$ are substituted with the mean of the respective measured EFs. The micro emission in the interval Δt centered around time t_i was calculated as the instantaneous emission factor multiplied by P_{act} and by Δt. The total emission during any experiment was estimated as sum of the micro emissions measured. The measured average emission factors given in Tables 2 were calculated as the total emissions divided by the product of the average engine power with the experimental time T. The average shaft speed, the average actual power of the engine, the average load factor, the average air consumption, and the average exhaust mass flow rate for each of the experiments are also given in Table 2.

Table 2: Experimental condition and measured EFs

Experiment	Ave. SS (rpm)	Ave. P_{act} (kW)	Ave. LF (%)	Ave. AC (kg/h)	Ave. EMFR (kg/h)	Ave. SOC (g/kWh)	Average Measured Emission Factors in (g/kWh) NO_x	SO_x	CO_2	CO	HC	PM
ME at berth for NO_x	38.11	509.0	7.399	5860	5990	256.6	10.1					
ME at berth for SO_x, CO	38.15	510.5	7.421	5877	6008	256.5		9.10		1.48		
ME at berth for CO_2	38.25	507.5	7.376	5842	5972	256.6			476			
ME at berth for HC	36.62	451.5	6.563	5197	5313	257.7					0.400	
ME at berth for PM	39.8	578.2	8.404	6656	6804	255.2						2.23
AE at berth for NO_x, SO_x, CO_2, CO	900.0	265.0	57.61	2862	2930	256.0	11.2	26.2	1140	1.74		
ME maneuvering for NO_x	65.31	2444	35.53	28140	28690	226.4	11.5					
ME maneuvering for SO_x	65.30	2442	35.51	28120	28670	226.4		13.8				
ME maneuvering for CO_2	65.45	2453	35.65	28240	28790	226.3			687			
ME maneuvering for CO	65.29	2443	35.50	28120	28670	226.4				2.43		
ME maneuvering for HC	80.94	3785	55.01	43570	44380	214.3					0.239	
ME maneuvering for PM	67.84	2653	38.56	30540	31130	224.0						1.70
ME cruising for NO_x, SO_x, CO_2, CO	89.50	5595	81.33	64410	65560	205.5	19.0	18.1	764	1.12		
ME cruising for HC, PM	89.26	5663	82.31	65190	66340	203.1					0.146	0.391

While at berth, the AEs run to generate the required auxiliary power (Hickman et al., 1999) and can be said to be the key emission producer (Du et al., 2011). Major activities include, but are not limited to, light supply to the ship, refrigeration, heating, ventilation, and electric equipment electric loads (Hickman et al., 1999). The AEs operate with greater load factor (LF) than ME and therefore produce higher EFs (Table 2).

The main engine runs on heavy fuel oil (HFO) with 3.13% sulphur mass content that was adopted for the fuel type in this study. HFO is a fuel type preferred for most ship's boilers and engines (Goldsworthy & Galbally, 2011), with a sulphur content ranging from 2% to 3.5% with a 2.6% average globally (IMO, 2010). The properties of the HFO used in our study are given in Table 3. For most ships sailing to Australia, the average fuel sulphur content of the HFO may be higher than this average (Goldsworthy & Goldsworthy, 2015). Also, HFO combustion is very complex and may emit primary gases (Goldsworthy & Galbally, 2011).

Table 3: Properties of the heavy fuel oil used

Density at 15° C	986 kg/m^3
Viscosity at 50° C	377 mm^2/s
Micro - carbon residue	14.6% mass
Sulphur (S)	3.13% mass
Ash	0.0640% mass
Vanadium (V)	141 mg/kg

Since NO_x and CO emissions are combustion dependent, service history and individual maintenance are a concern (Cooper, 2003). Higher amounts of nitrogen in fuels can produce NO_x emissions (Cooper, 2003). For this study, nitrogen content was 0.68% of the total mass. Thermally, greater nitrogen fixation during combustion is required if temperature periods are long and the engine is slow. The level of PM in marine diesel emissions may vary with fuel type or combustion conditions and more will be generated by higher amounts of fuel sulphur plus ash content. Dependency on PM fuel emissions becomes less conspicuous compared to CO_2 and SO_2 emissions due to induced PM combustion emissions (Cooper, 2003). According to Agrawal et al. (2008), the higher the quantity of ash content, the higher the PM EFs, although, in a general sense, there is insufficient data on the measurement of PM and differences in engine models, fuel used, instrumentations and working conditions (Hallquist, Fridell, Westerlund, & Hallquist, 2013).

Variations in engine power and speed may result in poor combustion, which can lead to increased HC and PM emission rates. PM concentration is largely dependent on the conditions of engine load, which is higher at low LFs and vice-versa (Winnes & Fridell, 2009): if the average power is considered with LFs remaining at their lowest in berth, the EF results for PM produce greater amounts. However, EF averages for NO_x, CO_2 and SO_x in cruising mode are higher than when maneuvering at berth. All NO_x emissions are temperature dependent, increasing with a rise in temperature. Hence, the rate of emission of NO_x is dependent on a ship's engine power and engine LF (Sinha et al., 2003). If the engine is steady, with a speed higher than its power, while in operation it may run for longer and at higher temperatures, producing higher NO_x emissions. Pollution rates, then, increase with increased engine power. The demand of engine power, air consumption and mass flow of exhaust emissions increase during cruising. Moreover, an elevated engine load increases the average engine power, which in turn additionally increases the influence of the fuel's carbon and sulphur content (Table 3) on the EFs of SO_x and CO_2 for cruising modes compared with other operating modes (Table 2). Generally, the CO emissions recorded were low, a result of high oxygen surplus concentrations and an adequate combustion process, but if engines are poorly maintained at small power ranges, CO proportions may increase expectedly due to considerable relative concentration (Kristensen, 2010). In this study, generally the EFs for CO are low but they increase at the maneuvering phase. Variable engine speed and power may lead to poor combustion during the maneuvering phase leading to increased CO emission rates (Fu et al., 2013).

3. Comparison analysis between measured and predicted EFs

In this section the on-board experimental measurements are compared with the predictions of the inventory methods introduced in section 1.2. As described in section 2.1 the primary emission rates (or the mass concentration for PM) of the main engine were measured at berth, while maneuvering, and while cruising. For the auxiliary engines the only rates measured were NO_x, SO_x, CO_2 and CO emissions at berth. In section 2.2, the

measured emission rates were converted to EFs and the results were shown in Table 2. The total emission amount of given type released in the atmosphere during one experiment (e.g. CO emission of the ME during the maneuvering experiment) can be calculated by integrating the time curve of the instantaneous emissions for the time span of the experiment (e.g. 1 h, 49 min, 2 sec for CO emission of the ME during the maneuvering). The instantaneous emission in g/h at time *t* is the EF at time *t*, multiplied by the actual engine power at time *t*. The total emission amount measured for each "pollutant" (inclusive of CO_2, which technically is not a pollutant) from the four experiment types are given in kg on the first row of Tables 4, 5, 7, and 8. For each total emission amount measured, we have tried to predict the results with as many inventories as possible from the list of inventories given in Section 1.2. Each of the inventories is predicting the EF generally as a function of the load factor, the type of the fuel, the sulphur content of the fuel, the type of the engine, the operation mode, the built date of the engine, the shaft rotational speed, specific fuel consumption, etc. The inventory-predicted emission factor for any emission has been converted into inventory-predicted total emission amount by multiplying with the average engine power and the experiment time *T*. We opted to calculate the total predicted emissions in that simplified way instead of integrating the instantaneous emission curves in order to mimic more closely the real utilization of the inventory prediction. The inventory deviations of the predicted total emission amount in % from the experimentally measured total emission amounts can be calculated for all "pollutants" (note that CO_2 is not a pollutant), and for any inventory method that can predict that pollutant. Those inventory deviations from the four experiment types are given in Tables 4, 5, 7, and 8 (from the second row onward, excluding the last columns of Tables 7 and 8).

Example 1: MEET inventory prediction for CO emission of the auxiliary engine is

$$\mathrm{EF}_{\mathrm{CO}}^{\mathrm{MEET}} = \left[20.7 - 0.218(\mathrm{LF}) - 0.0231\mathrm{P}_{act} + 0.000345\mathrm{P}_{act}(\mathrm{LF})\right]\mathrm{SOC}/1000$$

For the auxiliary engine at berth the average load factor LF is 57.6%, the average engine power P_{act} is 265 kW, the average specific oil consumption SOC is 256 g/kWh (see Table 2). So,

$$\mathrm{EF}_{\mathrm{CO}}^{\mathrm{MEET}} = \left[20.7 - 0.218(57.6) - 0.0231(265) + 0.000345(265)(57.6)\right](256.0)/1000 \approx 1.87 \text{ g/kWh}$$

For CO emission from the auxiliary engine at berth the experimental time is 2.632 h (see Table 1). The MEET predicted total CO emission amount is

$$\mathrm{CO}^{\mathrm{MEET}} = \mathrm{EF}_{\mathrm{CO}}^{\mathrm{MEET}}\mathrm{P}_{\mathrm{act}}T = 1.87(265)(2.632)/1000 \approx 1.304 \text{ kg}$$

The MEET inventory deviation in % from 1.214 kg, which is the experimentally measured total CO emission amount for the auxiliary engine at berth (see Table 5) is

$$\Delta\mathrm{CO}^{\mathrm{MEET}} = 100\left(\mathrm{CO}^{\mathrm{MEET}} - \mathrm{CO}^{\mathrm{mes}}\right)/\mathrm{CO}^{\mathrm{mes}} = 100(1.304 - 1.214)/1.214 \approx 7.43\%$$

That result is shown in Table 5.

Example 2: The ENTEC prediction for the NO_x emission factor from the main engine when the vessel is maneuvering was $\mathrm{EF}_{\mathrm{NO_x}}^{\mathrm{ENTEC}} = 12.0$ g/kWh . The latter value considers that the vessel is at maneuvering, that the main engine is post-2000 SSD, and that the fuel is HFO. For NO_x emission from the main engine when maneuvering the experimental time is 1.820 h (see Table 1), and the average engine power P_{act} is 2444 kW (see Table 2). The ENTEC predicted total NO_x emission amount is,

$$\mathrm{NO}_{\mathrm{x}}^{\mathrm{ENTEC}} = \mathrm{EF}_{\mathrm{NO_x}}^{\mathrm{ENTEC}}\mathrm{P}_{\mathrm{act}}T = 12.0(2444)(1.820)/1000 \approx 53.4 \text{ kg}$$

The ENTEC inventory deviation in % from 51.17 kg, which is the experimentally measured total NO_x emission amount for the main engine at maneuvering (see Table 7) is,

$$\Delta\mathrm{NO}_{\mathrm{x}}^{\mathrm{ENTEC}} = 100\left(\mathrm{NO}_{\mathrm{x}}^{\mathrm{ENTEC}} - \mathrm{NO}_{\mathrm{x}}^{\mathrm{mes}}\right)/\mathrm{NO}_{\mathrm{x}}^{\mathrm{mes}} = 100(53.4 - 51.17)/51.17 \approx 4.33\%$$

That result is shown in Table 7.

Example 3: US EPA inventory prediction for SO_x emission of the main engine is

$$\mathrm{EF}_{\mathrm{SO_x}}^{\mathrm{US\ EPA}} = 2.3735(\mathrm{SOC})(\mathrm{FSF}) - 0.4792$$

For SO_x emission of the main engine at berth the specific oil consumption SOC=256.5 g/kWh (see Table 2), and the fuel sulphur fraction in the HFO is FSF=0.0313 (see Table 3). So,

$$\mathrm{EF}_{\mathrm{SO_x}}^{\mathrm{US\ EPA}} = 2.3735(256.5)(0.0313) - 0.4792 \approx 18.54 \text{ g/kWh}$$

For SO_x emission of the main engine the experimental time T is 0.4381 h (see Table 1), and the average engine power P_{act} is 510.5 kW (see Table 1). The US EPA predicted total SO_x emission amount is,

$$SO_x^{US\ EPA} = EF_{SO_x}^{US\ EPA} P_{act} T = 18.54(510.5)(0.4381)/1000 \approx 4.147 \text{ kg}$$

The US EPA inventory deviation in % from 2.035 kg, which is the experimentally measured SO_x emission amount for the main engine at berth (see Table 4) is,

$$\Delta SO_x^{US\ EPA} = 100\left(SO_x^{US\ EPA} - SO_x^{mes}\right)/SO_x^{mes} = 100(4.147 - 2.035)/2.035 \approx 104\%$$

That result is shown in Table 4.

3.1. Inventories Performance when the Vessel is at Berth

The experimentally measured total emission amounts and the inventory predictions for the main engine at berth are shown in Figure 1. The experimentally measured total emission amounts and the inventory deviations in % from the experimental values for the main engine at berth are given in Table 4.

Most methods systemically over-predict the on-board measured total emission amounts of NO_x, CO_2, CO, and HC from the main engine at berth. The SO_x inventories' predictions are well scattered around the measured total emission amounts. The PM inventories' predictions are somewhat scattered around the measured total emission amount, although some under-prediction is obvious. The inventory predictions for NO_x, CO_2, and PM are somewhat satisfactory because the absolute deviations does not exceed 68.8%, 72.6%, and 86.3% respectively. However, the inventory predictions for SO_x, CO, and HC are completely unreliable with maximal absolute deviations reaching 104%, 1610%, and 1390% respectively.

Table 4: Inventory deviations from the experimentally measured total emission amounts in % for the main engine at berth. The experimental measurements are given in the second row in kg per time equal to the experiment duration according to the third column of Table 1

Inventory	NO_x	SO_x	CO_2	CO	HC	PM
Experiment	2.248	2.035	102.0	0.3319	0.06022	0.5373
Tier III	38.1	37.4	NaN	-0.276	350	7.62
ENTEC	18.4	27.5	43.4	NaN	350	7.62
MEET	-11.4	76.9	72.6	1610	1390	-86.3
STEAM	114	-34.2	31.0	NaN	NaN	NaN
MOPSEA	68.8	-34.1	30.8	6.46	-41.0	-47.5
NERI	18.4	-56.0	34.1	7.81	25.0	-83.9
EMS	77.7	18.7	33.5	79.2	45.0	-41.7
US EPA	64.8	104	162	668	987	-77.7
IMO	64.8	-49.1	21.1	-65.5	42.5	-39.5

The inventories, which produce least absolute deviations for the main engine at berth are MEET for NO_x with -11.4% deviation, EMS for SO_x with 18.7% deviation, IMO for CO_2 with 21.1% deviation, MOPSEA for CO with 6.46% deviation, NERI for HC with 25.0% deviation, and jointly TIER III & ENTEC for PM with 7.62% deviation.

The experimentally measured total emission amounts and the inventory predictions for the auxiliary engines at berth are shown in Figure 2. The experimentally measured total emission amounts and the inventory deviations in % from the experimental values for the auxiliary engines at berth are given in Table 5.

Most methods systemically over-predict the on-board measured total emission amounts of NO_x, whereas at the same time systemically under-predict the on-board measured total emission amounts of SO_x and CO_2 from the auxiliary engines at berth. The CO inventories' predictions are somewhat scattered around the measured CO total emission amount, although some under-prediction can be detected. The CO_2 is more or less well predicted by every inventory method, with absolute deviations less than 45.4%. The inventory predictions for NO_x, SO_x, and CO also are somewhat satisfactory because their respective absolute deviations do not exceed 81.8%, 98.5%, and 54.0%.

Figure 1: Total emission amounts' measurement and inventory prediction at berth for the main engine

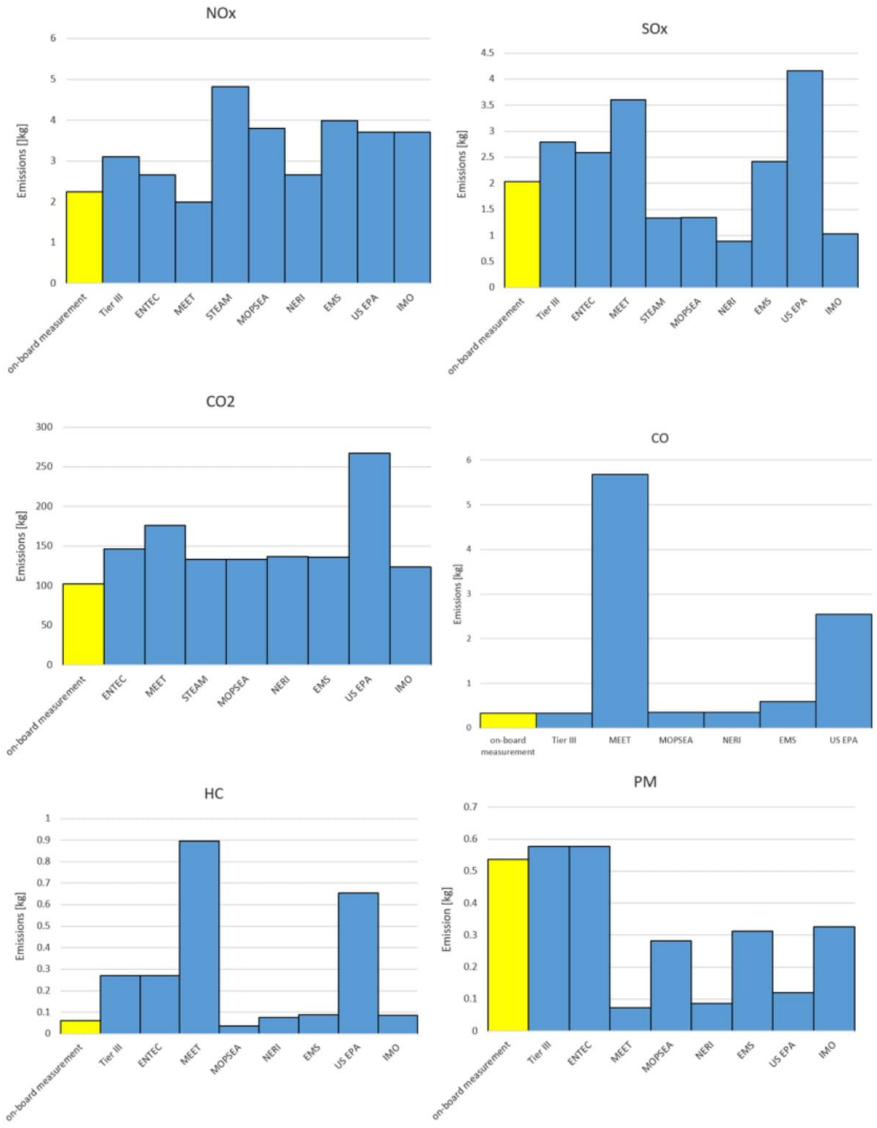

The inventories, which produce least absolute deviations for the auxiliary engines at berth, are MEET for SO_x, and CO_2 with -38.8%, and -28.2% deviations respectively, NERI for NO_x with -1.50% deviation, and MOPSEA for CO with -5.79% deviation.

The experimentally measured total emission amounts for the main engine and the auxiliary engines at berth were converted to hourly emission amounts, by dividing the former with the respective experimental time in hours. The combined hourly emission amount from all engines at berth has been calculated as the sum of the hourly emission amounts from main engine and from auxiliary engines. The experimentally measured combined hourly emission amounts are given in on the first row of Table 6, except for the HC and PM column where the

hourly emission amount are from the main engine, only (see section 2.1). The inventory deviation in % for any hourly emission amount prediction is the same as that of the total emission amount prediction. The combined hourly emission amount prediction can be calculated as the sum of two independent hourly amount predictions: one for the main engine and one for the auxiliary engines. It is trivial to prove that the inventory deviation from the experimentally measured combined hourly emission amount in % is a weighted average of the two inventory deviations from total emission amounts in % (one for the main engine and one for the auxiliary engines). The weight coefficients are the experimentally measured hourly emission amounts from the main engine and auxiliary engines respectively.

Table 5: Inventory deviations from the experimentally measured total emission amounts in % for the auxiliary engines at berth. The experimental measurements are given in the second row in kg per time equal to the experiment duration according to the third column of Table 1

Inventory	NO_x	SO_x	CO_2	CO
Experiment	7.790	18.26	795.5	1.214
Tier III	27.1	-47.3	NaN	-6.36
ENTEC	9.24	-53.0	-36.7	NaN
MEET	94.3	-38.9	-28.2	7.43
STEAM	2.97	-77.1	-45.4	NaN
MOPSEA	-21.2	-74.8	-40.0	-5.79
NERI	-1.50	-98.5	-38.4	-8.08
EMS	34.3	-54.5	-38.8	54.0
US EPA	31.6	-54.2	-36.6	-36.8
SMED	25.4	-60.3	-36.7	-48.3
IMO	81.8	-78.5	-38.5	-64.2

Example 4: Let us concentrate on NO_x emission at berth. The measured total emission amount for NO_x from the main engine at berth is 2.248 kg for T=0.4358 h (see Table 4). It follows that the measured hourly emission amount for NO_x from the main engine at berth is 2.248/0.4358=5.158 kg/h. The measured total emission amount for NO_x from the auxiliary engines at berth is 7.790 kg for T=2.632 (see Table 5). It follows that the measured hourly emission amount for NO_x from the auxiliary engines at berth is 7.790/2.632=2.960 kg/h. So, the measured combined hourly emission amount for NO_x from all engines at berth will be 5.158+2.960=8.117 kg/h (see Table 6).

Let us use the NERI inventory for NO_x at berth. The NERI inventory deviation from the experimentally measured 2.248 kg total NO_x emission amount from main engine at berth is 18.4% (see Table 4). It follows that NERI inventory deviation from the experimentally measured 5.158 kg/h hourly NO_x emission amount from ME at berth will be also 18.4%. The NERI inventory deviation from the experimentally measured 7.790 kg total NO_x emission amount from the auxiliary engines at berth is -1.50% (see Table 5). It follows that NERI inventory deviation from the experimentally measured 2.960 kg/h hourly NO_x emission amount from the auxiliary engines at berth will be also -1.50%. So, the NERI inventories deviation from the experimentally measured 8.117 kg/h combined hourly NO_x emission amount from all engines at berth will be, [18.4(5.158) -1.50 (2.960)]/8.117 ≈11.2%

That result is shown in Table 6.

The experimentally measured combined hourly emission amounts and the inventory predictions for all engines at berth are shown in Figure 3. The experimentally measured combined hourly emission amounts and the inventory deviations in % from the experimental values for all engines at berth are given in Table 6. The deviations in the last two columns of Table 6 are the same as the deviations in last two columns of Table 4 because there were no measurements of the HC and PM emissions from the auxiliary engines berth (see Table 1).

Most methods systemically over-predict the on-board measured combined hourly emission amounts of NO_x and HC, whereas systemically under-predict the on-board measured combined hourly emission amounts of SO_x and CO_2 when the vessel is at berth. The CO and PM inventories' predictions are somewhat scattered around the measured combined hourly emission amounts, although some under-prediction is present. The inventory predictions for NO_x, SO_x, CO_2 and PM are somewhat satisfactory because the absolute deviations do not exceed 73.6%, 81.5%, 51.6%, and 86.3% respectively. However, the inventory predictions for CO, and HC are completely unreliable with maximal absolute deviations reaching 1000%, and 1390% respectively.

Figure 2: Total Emission amounts' measurement and inventory prediction at berth for auxiliary engines

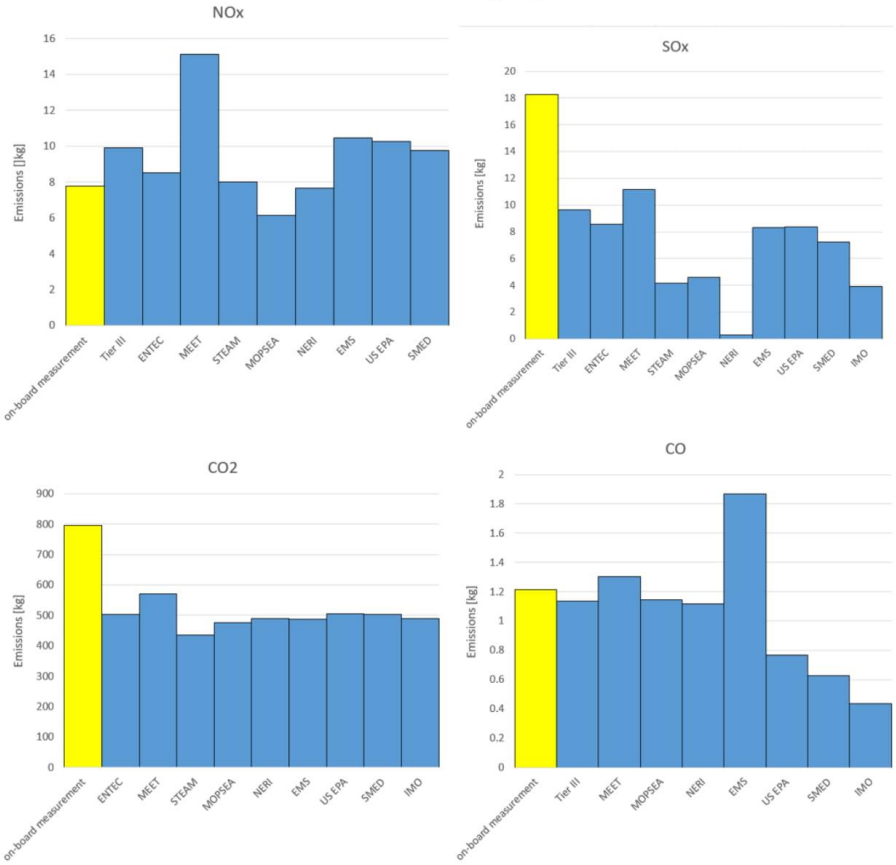

Table 6: Inventory deviations from the experimentally measured combined hourly emission amounts in % for the main engine plus the auxiliary engines at berth. The experimentally measured combined hourly emission amounts are given in the first row in kg/h. The mean absolute deviations in % are shown in the last column

Inventory	NO_x	SO_x	CO_2	CO	HC	PM	MAD
Experiment	8.117	11.58	543.6	1.219	0.1806	1.289	0.000
Tier III	34.2	-13.3	NaN	-2.58	350	7.62	81.5
ENTEC	15.1	-20.7	-1.13	NaN	350	7.62	78.9
MEET	27.2	7.56	16.6	1000	1390	-86.3	422
STEAM	73.6	-59.9	-11.5	NaN	NaN	NaN	**48.3**
MOPSEA	36.0	-58.5	-8.58	1.83	-41.0	-47.5	32.2
NERI	11.2	-81.5	-6.21	1.80	25.0	-83.9	34.9
EMS	61.9	-25.2	-6.69	69.7	45.0	-41.7	41.7
US EPA	52.7	9.43	51.6	401	987	-77.7	263
IMO	71.0	-66.7	-12.0	-65.0	42.5	-39.5	49.5

Figure 3: Combined hourly emission amounts' measurement and inventory prediction at berth for the main engine plus the auxiliary engines

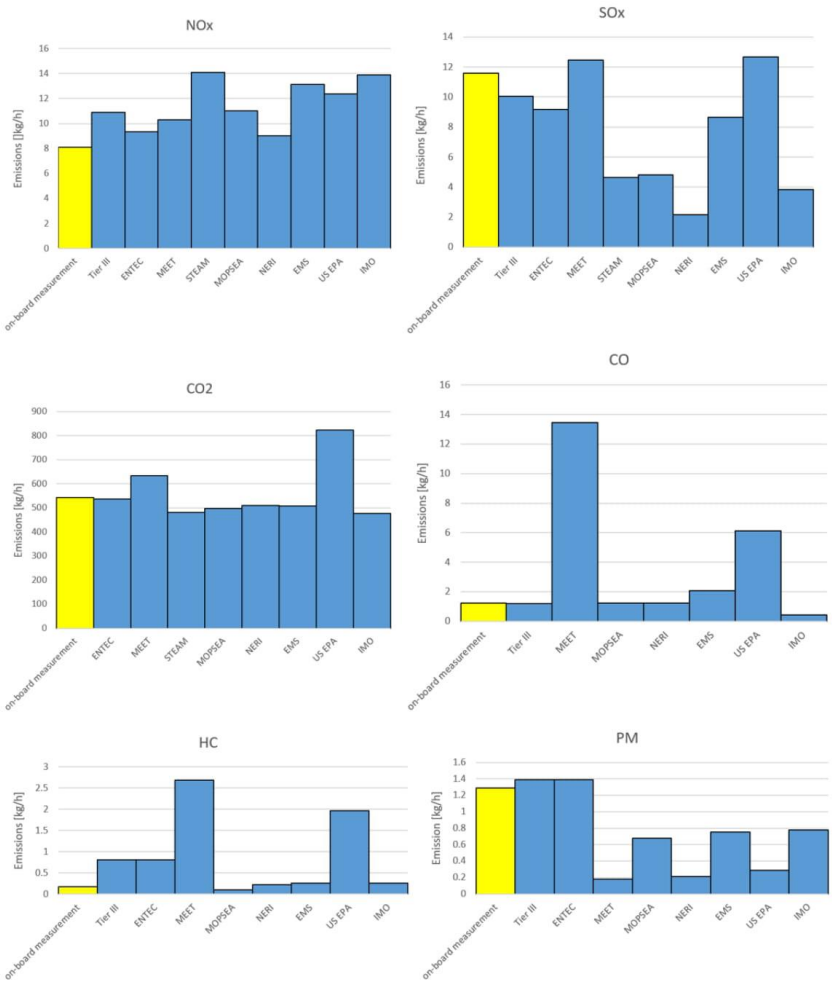

The inventories, which produce least absolute deviations from the experimentally measured combined hourly emission amounts at berth, are NERI for NO_x, CO, and HC with 11.2%, 1.80%, and 25.0% deviations respectively, MEET for SO_x with 7.56% deviation, and ENTEC for CO_2, and PM with -1.13%, and 7.62%. Tier III for PM has the same result as ENTEC.

For each inventory family the mean value of its absolute deviations from the experimentally measured combined hourly emission amounts is shown in the last column of Table 6. With all its imperfections these values can serve as a "quick and dirty" marginalization of the 6-dimensional preference problem into a 1-dimensional ranking problem in ascending order of the Mean Absolute Deviation (MAD). All inventory families, which do not predict at least five of the six combined hourly emission amounts, are disqualified and their MADs are shown bolded in Table 6. According to the minimal MAD criterion the best inventory family at berth is MOPSEA with the 32.2% MAD. That family predicts all six of the emissions. The other inventory families, which predict all six of the combined hourly emission amounts, are MEET, NERI, EMS, US EPA, and IMO.

3.2. Inventories Performance when the Vessel is Maneuvering

The experimentally measured total emission amounts and the inventory predictions for the main engine when the vessel is maneuvering are shown in Figure 4. The experimentally measured total emission amounts and the inventory deviations in % from the experimental values for the main engine when maneuvering are given in Table 7.

Table 7: Inventory deviations from the experimentally measured total emission amounts in % for the main engine at maneuvering. The experimental measurements are given in the second row in kg per time equal to the experiment duration according to the third column of Table 1. The mean absolute deviations in % are shown in the last column

Inventory	NO_x	SO_x	CO_2	CO	HC	PM	MAD
Experiment	51.17	61.28	3051	10.79	0.3772	10.18	0.000
Tier III	21.7	-9.26	NaN	-39.1	653	40.8	153
ENTEC	4.33	-15.8	-0.607	NaN	653	40.8	143
MEET	53.9	3.09	5.45	161	222	-84.2	88.3
STEAM	69.5	-56.5	-9.26	NaN	NaN	NaN	**45.1**
MOPSEA	75.6	-56.4	-9.41	29.1	59.3	-7.90	39.6
NERI	69.5	1.63	-7.08	-34.2	109	36.1	42.9
US EPA	57.4	0.907	4.86	-42.4	151	-67.9	54.1
SMED	18.2	-28.1	-0.670	-59.2	149	52.5	51.3
IMO	45.2	-66.4	-16.1	-78.9	138	-20.8	61.0

Most methods systemically over-predict the on-board measured total emission amounts of NO_x, and HC, whereas under-predict the CO_2 emission amounts. The SO_x, CO, and PM inventories' predictions are somewhat scattered around the measured total emission amounts for the main engine when the vessel is maneuvering. The CO_2 is well predicted by every inventory method, with absolute deviations less than 16.1%. The inventory predictions for NO_x, SO_x, and PM are somewhat satisfactory because the absolute deviations do not exceed 69.55, 66.4%, and 84.2% respectively. However, the inventory predictions for CO, and HC are very unreliable with maximal absolute deviations reaching 161%, and 653% respectively.

The inventories, which produced least absolute deviations for the main engine when maneuvering, are MOPSEA for CO, HC, and PM with 29.1%, 59.3%, and -7.9% deviations respectively, ENTEC for NO_x, and CO_2 with 4.33%, and -0.607% deviations respectively, and NERI for SO_x with 1.63% deviation.

For each inventory family the MAD criterion is shown in the last column of Table 7. All inventories, which do not predict at least five of the six total emission amounts, are disqualified and their mean values are shown with red in Table 7.

According to the minimal MAD criterion, the best inventory family for the main engine, when the vessel is maneuvering, is MOPSEA with the 39.6% MAD. That family predicts all six of the emissions. The other inventory families which predict all six of the total emission amounts are MEET, NERI, US EPA, SMED, and IMO.

3.3. Inventories Performance when the Vessel is Cruising

In comparison to the other two operational modes (at berth and during maneuvering), more inventories are available for prediction of total emission amounts while the vessel is on cruising mode. The experimentally measured total emission amounts and the inventory predictions for the main engine when the vessel is cruising are shown in Figure 5. The experimentally measured total emission amounts and the inventory deviations in % from the experimental values for the main engine when cruising are given in Table 8.

Figure 4: Total emission amounts' measurement and inventory prediction when maneuvering for the main engine

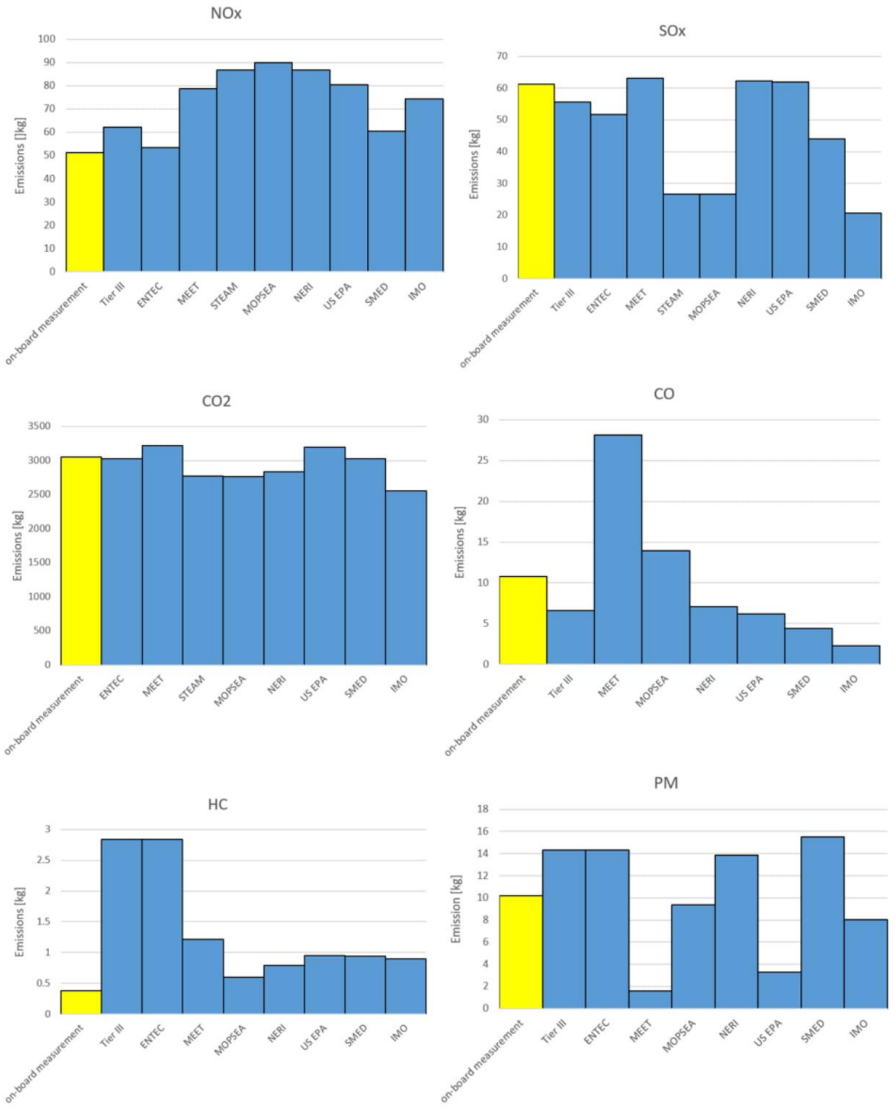

Most methods systemically under-predict the on-board measured total emission amounts of NO_x, SO_x, and CO_2, whereas at the same time systemically over-predict the on-board measured total emission amounts of CO, HC, and PM from the main engine when the vessel is cruising. The NO_x and CO_2 are well predicted by every inventory method, with absolute deviations less than 21.0% and 24.6% respectively. The inventory predictions for SO_x and CO also are somewhat satisfactory because the absolute deviations do not exceed 74.4% and 55.9% respectively. However, the inventory predictions for HC and PM are completely unreliable with maximal absolute deviations reaching 312% and 335% respectively.

The inventories, which produce least absolute deviations for the main engine at cruising, are MEET for SO_x, CO_2, and PM with -28.7%, -13.9%, and -37.6% deviations respectively, STEAM for NO_x with -3.67% deviation, SMED for HC with 104% deviation, and jointly NERI & US EPA for CO with 24.5% deviation.

For each inventory family the MAD criterion is shown in the last column of Table 8. All inventories, which do not predict at least five of the six total emission amounts, are disqualified and their mean values are shown bolded in Table 8.

According to the minimal MAD criterion the best inventory family for the main engine, when the vessel is cruising is MEET with the 59.2% MAD. That family predicts all six of the emissions. The other inventory families which predict all six of the total emission amounts, are MOPSEA, NERI, US EPA, SMED, and IMO.

Table 8. Inventory deviations from the experimentally measured total emission amounts in % for the main engine at cruising. The experimental measurements are given in the first row in kg per time equal to the experiment duration according to the third column of Table 1. The mean absolute deviations in % are shown in the last column

Inventory	NO_x	SO_x	CO_2	CO	HC	PM	MAD
Experiment	451.9	430.3	18180	26.76	4.401	11.80	0.000
Tier I	-16.8	-30.9	NaN	31.6	271	187	107
Tier II	-5.78	-30.9	NaN	31.6	312	299	136
Tier III	-7.89	-30.9	NaN	31.6	312	335	143
Corbett	-10.5	-44.7	-14.3	NaN	312	220	120
ENTEC	-21.0	-42.0	-18.9	NaN	312	335	146
MEET	-5.78	-28.7	-13.9	35.1	234	-37.6	59.2
STEAM	-3.67	-66.9	-18.5	NaN	NaN	NaN	**29.7**
MOPSEA	-6.31	-66.8	-18.6	36.0	79.1	276	80.5
NERI	-4.73	-30.3	-14.4	24.5	312	268	109
US EPA	-4.73	-30.3	-14.4	24.5	312	268	109
SMED	-10.5	-50.2	-18.9	-55.9	104	233	78.7
IMO	-12.1	-74.4	-24.6	-54.5	291	245	117

Figure 5. Total emission amounts' measurement and inventory prediction when cruising for the main engine

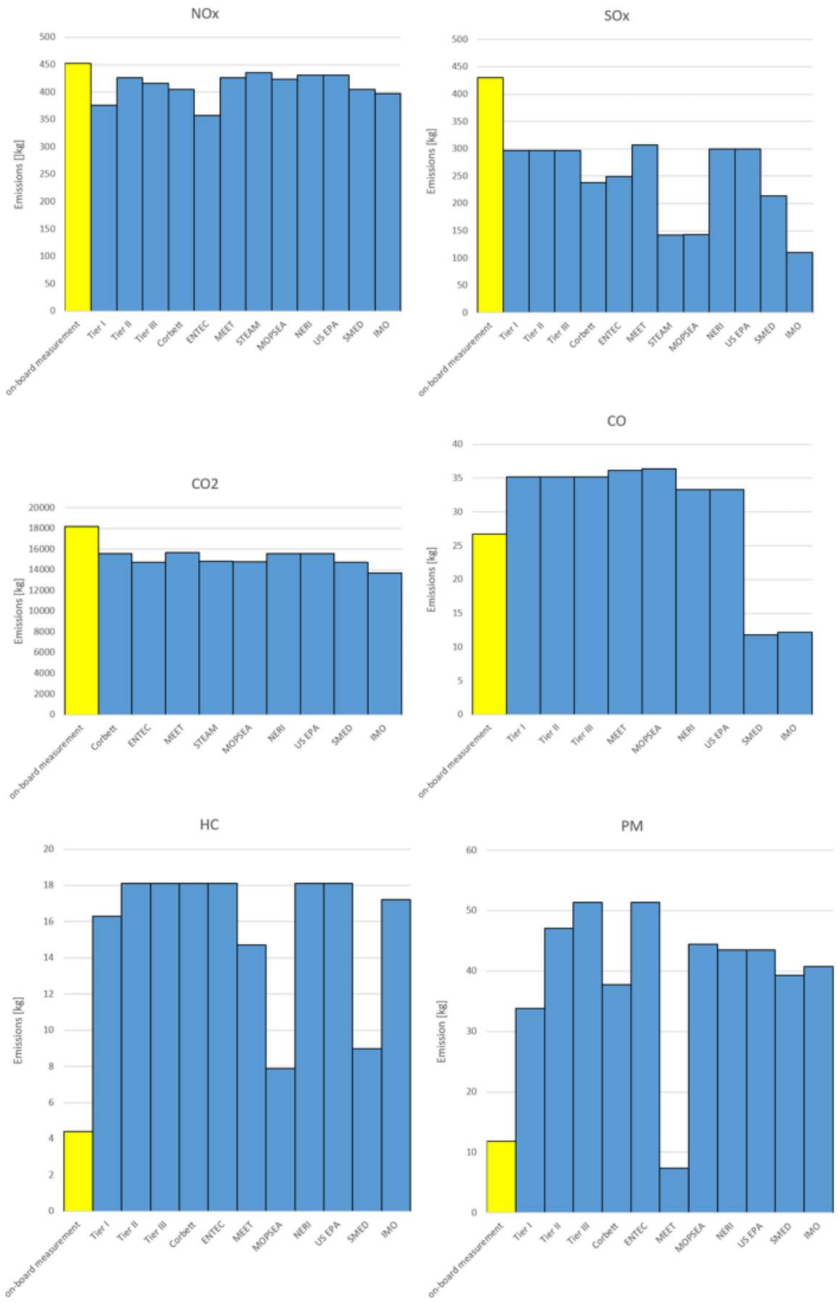

4. Discussion

4.1. Improvement of the Minimal Mean Absolute Deviation Criterion

A problem related to the case study described in sections 2 and 3 is the application of the minimal mean absolute deviation criterion to rank the inventory families under specific operational mode of the vessel. That criterion is not entirely rational, as it was pointed in the text. In this section we will discuss a more elaborate and rational method for ranking.

In section 3, we arranged the possible inventory methods according to preference three times (for each mode of operation). The preferences of any decision maker (DM) over a specific inventory family for a selected operational mode of a given vessel will depend only on the deviations of the inventory prediction emissions from the six emissions measured in the on-board experiment. Let us denote those deviations (in %) as follows: $\Delta_1 = \Delta\mathrm{NO_x}$, $\Delta_2 = \Delta\mathrm{SO_x}$, $\Delta_3 = \Delta\mathrm{CO_2}$, $\Delta_4 = \Delta\mathrm{CO}$, $\Delta_5 = \Delta\mathrm{HC}$ and $\Delta_6 = \Delta\mathrm{PM}$. The six values can be organized in a 6-dimensional vector of deviations $\vec{\Delta}$ as follows:

$$\vec{\Delta} = \left(\Delta_1, \Delta_2, \ldots, \Delta_6\right) = \left(\Delta\mathrm{NO_x}, \Delta\mathrm{SO_x}, \Delta\mathrm{CO_2}, \Delta\mathrm{CO}, \Delta\mathrm{HC}, \Delta\mathrm{PM}\right)$$

The parameters $\Delta_1, \Delta_2, \ldots, \Delta_6$ in the terminology of decision analysis are called attributes. Some of the vectors can have one attribute missing (because some inventory families do not predict all six of the emissions). We need to rank those vectors for each of the operational modes of a vessel.

Example 5. In our case study during maneuvering, according to Table 7, we have six vectors (for MEET, MOPSEA, NERI, US EPA, SMED and IMO) with all 6 deviations:

$\vec{\Delta}^{MEET}_{maneuvering}$ =(53.9,3.09,5.45,161,222, -84.2)

$\vec{\Delta}^{MOPSEA}_{maneuvering}$ =(75.6,-56.4,-9.41,29.1,59.3,-7.90)

$\vec{\Delta}^{NERI}_{maneuvering}$ =(69.5,1.63,-7.08,-34.2,109,36.1)

$\vec{\Delta}^{US\ EPA}_{maneuvering}$ =(57.4,0.907,4.86,-42.4,151,-67.9)

$\vec{\Delta}^{SMED}_{maneuvering}$ =(18.2,-28.1,-0.670,-59.2,149,52.5)

$\vec{\Delta}^{IMO}_{maneuvering}$ =(45.1,-66.4,-16.1,-78.9,138,-20.8)

During maneuvering we also have two other vectors with missing values, but with at least four emission deviations calculated (for Tier III, and ENTEC):

$\vec{\Delta}^{Tier\ III}_{maneuvering}$ =(21.7,-9.26,NaN,-39.1,653,40.8)

$\vec{\Delta}^{ENTEC}_{maneuvering}$ =(4.33,-15.8,-0.607,NaN,653,40.8)

In Section 3, we implicitly substituted the missing values with the mean of the known absolute deviations (that is with MAD). There are other more elaborate methods to impute missing values (Acock, 2005; Cohen, Cohen, West, & Aiken, 2003), but this problem goes beyond the scope of the paper (see (Nikolova, Toneva-Zheynova, Naydenov, & Tenekedjiev, 2012) for further discussion).

In section 3 we used the mean absolute deviation criterion to marginalize the stated six-dimensional preference problem into a one-dimensional ranking problem. However, it has been stated in this paper that the criterion in question is “quick and dirty”. Completely rational decisions can be obtained if a value function is built, which accurately reflects the preferences of the DM. The function will be additive because the DM holds the mutual preferential independence over the 6 attributes: from two inventories, the DM will prefer the one that has more favorable deviation for any attribute, if the rest of the attributes are pair-wise equal, and the decision will never depend on the equal deviations (French & Insua, 2010). That is why, it is possible to construct a value function over the vector of deviations in the form:

$$v\left(\vec{\Delta}\right) = v\left(\Delta\mathrm{NO_x}, \Delta\mathrm{SO_x}, \Delta\mathrm{CO_2}, \Delta\mathrm{CO}, \Delta\mathrm{HC}, \Delta\mathrm{PM}\right) =$$
$$= a_1 v_1\left(\Delta\mathrm{NO_x}\right) + a_2 v_2\left(\Delta\mathrm{SO_x}\right) + a_3 v_3\left(\Delta\mathrm{CO_2}\right) + a_4 v_4\left(\Delta\mathrm{CO}\right) + a_5 v_5\left(\Delta\mathrm{HC}\right) + a_6 v_6\left(\Delta\mathrm{PM}\right)$$

The inventories have to be ranked in descending order of the value function. The value function is normalized in the closed interval [0; 1] in a sense that it should be 1 if all deviations are 0% (the best-case scenario) and it should be 0, if all deviations are -100% (the worst-case scenario). In the above equation, the constants a_i, for i=1, 2, ..., 6 are the weight coefficients, which reflect the importance of each attribute into the overall preference of the DM over the six-dimensional vectors $\vec{\Delta}$. Each of the six constants should be non-negative and they should sum to one. The one-dimensional functions $v_i(.)$, for i=1, 2, ..., 6 are the attribute value functions over each of the emission deviations (which are value-difference functions (French & Insua, 2010)). Each of $v_i(.)$ is normalized so that v_i(-100%)=0, v_i(0%)=1, and $\lim_{\Delta_i \to \infty} v_i\left(\Delta_i\right) = 0$. The function should increase from -100% to 0% and decrease from 0% to "plus infinity" %. An example of such a function is given on Figure 6.

It is perfectly rational that the attribute value functions are different for each of the attributes and for each of the vessel modes of operation. Alternatively, the DM may use one and the same function over each attribute for each mode, since they all measure the opinion of the DM regarding the precision of predictions. The form of the attribute value functions depends solely on the preferences of the DM. There is not much discussion in literature regarding the rational construction of value functions. However, as far as value functions are a special case of utility functions under risk, then the techniques for construction of such functions may be adopted for the case of value functions. The single attribute utility function is constructed usually by eliciting several nodes of their function and then applying either an analytical non-linear function to approximate the utility on the elicited nodes, or linear function to interpolate over the elicited nodes. We will demonstrate how to elicit several nodes of the one-dimensional function $v_i(.)$. It is already known that $v_i(-100\%)=0$, $v_i(0\%)=1$, and $\lim_{\Delta_i \to \infty} v_i\left(\Delta_i\right) = 0$. The DM can select a set of M additional deviation values $\left\{\Delta_{i,1}, \Delta_{i,2}, \ldots, \Delta_{i,M}\right\}$ for the i^{th} emission. In order to find the value of the one-dimensional function $v_i\left(\Delta_{i,j}\right)$ at the deviation $\Delta_{i,j}$ the DM has to identify the probability p_j where he/she is indifferent between:

A) the option of getting $\Delta_{i,best} = 0\%$ with probability p_j or getting $\Delta_{i,worst} = -100\%$ with probability $(1-p_j)$. This option is denoted as $< \Delta_{i,best}\left(p_j\right)\Delta_{i,worst} >$.

B) the option of getting a deviation $\Delta_{i,j}$ for sure.

If p_j is identified by the DM so that the latter is indifferent between the two stated options, then $v_i\left(\Delta_{i,j}\right) = p_j$. In fact, the DM has to solve M preferential equations of the type $< \Delta_{i,best}\left(p_j\right)\Delta_{i,worst} > \sim \Delta_{i,j}$ where the symbol $\sim$ stands for indifference. The recommended method to elicit such nodes is called probability equivalence method, but there are other more complicated methods (see French & Insua, 2010 as well as Nikolova, Hirota, Kobashikawa & Tenekedjiev, 2006) for discussion on methods to elicit nodes of one-dimensional value functions).

The weight coefficients in the value function measure the importance of each pollutant in the overall assessment of preferences over emission inventories. It is only natural to expect that pollution levels have different significance depending on the regime – pollution close or in ports are causing more direct harm than emissions while at sea, while still the pollution is of global importance. There are elaborate methods to elicit the weight coefficients, which are nothing else but scaling constants in the utility theory. Scaling constants are elicited subjectively, where the DM has to identify the probability p_i, which makes him/her indifferent when comparing:

A) the option of getting $\vec{\Delta}_{best} = (0,0,0,0,0,0)$ with probability p_i or getting $\vec{\Delta}_{worst} = (-100,-100,-100,-100,-100,-100)$ with probability $(1-p_i)$. This option is denoted as $< \vec{\Delta}_{best}\left(p_i\right)\vec{\Delta}_{worst} >$.

B) the option of getting for sure a deviation vector, where only the i-th deviation is set to its best level 0%, and the others are at their worst level of -100%:

$\vec{\Delta}_{corner,i} = \left(\Delta_1 = -100, \ldots, \Delta_{i-1} = -100, \Delta_i = 0, \Delta_{i+1} = -100, \ldots, \Delta_n = -100\right)$. Such vector is a.k.a. corner vector.

If p_i is identified by the DM so that the latter is indifferent between the two stated options, then $a_i = p_i$. In fact, the DM has to solve six preferential equations of the type $< \vec{\Delta}_{best}\left(p_i\right)\vec{\Delta}_{worst} > \sim \vec{\Delta}_{corner,i}$ (see Keeney & Raiffa, 1993) for detailed discussion on multi-dimensional utility functions and identification of scaling constants).

Figure 6: Example of the value functions $v_i(.)$ over an emission deviation (continues line). The function $v_{quick}(\Delta_i) = 1 - |\Delta_i|/100$ is shown for reference (dashed line)

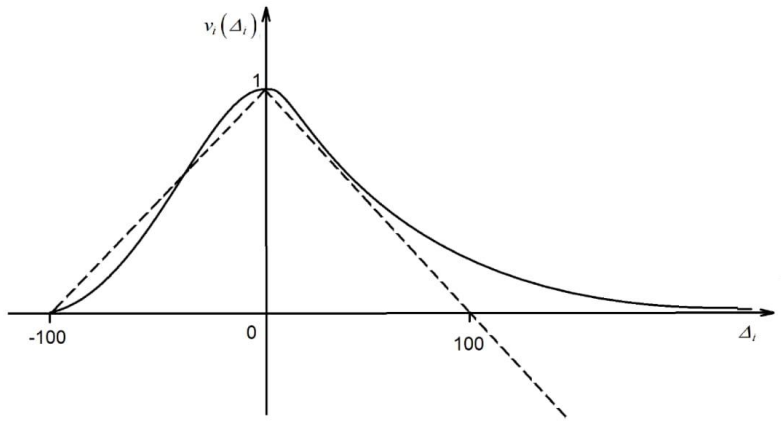

4.2. Choosing the Best Inventory Family for a Given Type of Operation

Constructing the value functions, we will be able to choose which inventory method is the best (most preferred) for each operational mode. The following algorithm can be utilized to select the best inventory method for a given type of ship operation:

Algorithm to select the best inventory method for a selected type of operation:

1. Define the vector of deviations $\vec{\Delta} = \left(\Delta NO_x, \Delta SO_x, \Delta CO_2, \Delta CO, \Delta HC, \Delta PM\right)$ for each inventory method (with at least five emission deviations calculated).
2. Impute missing values in the vector of deviations by replacing them with the mean of the known deviations' absolute values.
3. Construct the attribute value functions $v_i(.)$ for the selected type of operation.
4. Elicit the scaling constants a_i for i=1, 2, ..., 6 for the selected type of operation.
5. Construct the value function v as function of six attributes and their scaling constants.
6. Calculate $v\left(\vec{\Delta}\right)$ for each of the deviation vectors from step 1).
7. Choose the inventory family that has the highest value, calculated in step 6).

While our algorithm assumes we need at least five calculated deviations (in step 1), this requirement may be modified and is prescriptive, not mandatory. If all six deviations are calculated, then step 2 of the above algorithm will be obsolete. We will demonstrate the application of this algorithm in an example.

Example 6. Let us select the best inventory method for operation during maneuvering. There are eight vectors that satisfy step 1 of the Algorithm (that at least five pollution deviations are calculated) and they were given in Example 5.

Following step 2 of the Algorithm, we identify the following imputed values for the two vectors containing missing values. For the inventory Tier III, the deviation in CO_2 will be:

$$\Delta_3 = \left(\left|\Delta_1\right| + \left|\Delta_2\right| + \left|\Delta_4\right| + \left|\Delta_5\right| + \left|\Delta_6\right|\right) / 5 = \left(21.7 + 9.26 + 39.1 + 653 + 40.8\right) / 5 \approx 153 = \text{MAD}^{TIER\ III}$$

Then $\vec{\Delta}^{Tier\ III}_{maneuvering}$ =(21.7,-9.26,153,-39.1,653,40.8).

For the inventory family ENTEC, the deviation in CO will be:

$$\Delta_4 = \left(\left|\Delta_1\right| + \left|\Delta_2\right| + \left|\Delta_3\right| + \left|\Delta_5\right| + \left|\Delta_6\right|\right) / 5 = \left(4.33 + 15.8 + 0.607 + 653 + 40.8\right) / 5 \approx 143 = \text{MAD}^{ENTEC}$$

Then $\vec{\Delta}^{ENTEC}_{maneuvering}$ =(4.33,-15.8,-0.607,143,653,40.8).

Following step 3 of the Algorithm, let the DM believe that all attribute value functions are the same and are equal to $v_{sa}(.)$:

$$v_1(.) \equiv v_2(.) \equiv \ldots \equiv v_6(.) \equiv v_{sa}(.).$$

The following preferential equations were solved in order to elicit additional nodes from $v_{sa}(.)$:

<0% (0.17) -100%> ~ –75% => $v_{sa}(-75\%) = 0.17$

<0% (0.40) -100%> ~ –50% => $v_{sa}(-50\%) = 0.40$

<0% (0.75) -100%> ~ –25% => $v_{sa}(-25\%) = 0.75$,

<0% (0.75) -100%> ~ 25% => $v_{sa}(25\%) = 0.75$

<0% (0.60) -100%> ~ 50% => $v_{sa}(50\%) = 0.60$

<0% (0.50) -100%> ~ 75% => $v_{sa}(75\%) = 0.50$

<0% (0.429) -100%> ~ 100% => $v_{sa}(100\%) = 0.429 \approx 0.43$

<0% (0.273) -100%> ~ 200% => $v_{sa}(200\%) = 0.273 \approx 0.27$

<0% (0.20) -100%> ~ 300% => $v_{sa}(300\%) = 0.20$

The function $v_{sa}(.)$ is then approximated with the following analytical form:

$$v_{sa}(x) = \begin{cases} \dfrac{100 + x}{75 - x} & \text{for } -100 \le x \le -25 \\ \dfrac{2500 - x^2}{2500} & \text{for } -25 < x < 25 \\ \dfrac{75}{x + 75} & \text{for } x \ge 25 \end{cases}$$

Figure 7 presents the approximated function $v_{sa}(x)$, for $x \in [-100; \infty)$ (we can see the similarities of this function to the example one presented on Figure 6).

Figure 7: Graphics of the single attribute function $v_{sa}(x)$

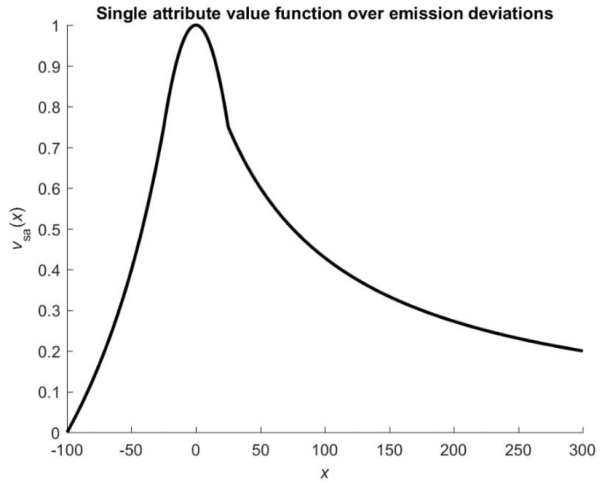

The DM has also elicited the following scaling constants:

$< \vec{\Delta}_{best}\ (0.10)\ \vec{\Delta}_{worst} > \sim\ \vec{\Delta} = (-100,0,0,0,0,0)$ => a_1=0.10

$< \vec{\Delta}_{best}\ (0.25)\ \vec{\Delta}_{worst} > \sim\ \vec{\Delta} = (0,-100,0,0,0,0)$ => a_2=0.25

$< \vec{\Delta}_{best}\ (0.05)\ \vec{\Delta}_{worst} > \sim\ \vec{\Delta} = (0,0,-100,0,0,0)$ => a_3=0.05

$< \vec{\Delta}_{best}\ (0.30)\ \vec{\Delta}_{worst} > \sim\ \vec{\Delta} = (0,0,0,-100,0,0)$ => a_4=0.30

$< \vec{\Delta}_{best}\ (0.10)\ \vec{\Delta}_{worst} > \sim\ \vec{\Delta} = (0,0,0,0,-100,0)$ => a_5=0.10

$< \vec{\Delta}_{best}\ (0.20)\ \vec{\Delta}_{worst} > \sim\ \vec{\Delta} = (0,0,0,0,0,-100)$ => a_6=0.20

Following step 4 of the Algorithm, the six-attribute value function is constructed:

$$v(\vec{\Delta}) = v(\Delta\mathrm{NO_x}, \Delta\mathrm{SO_x}, \Delta\mathrm{CO_2}, \Delta\mathrm{CO}, \Delta\mathrm{HC}, \Delta\mathrm{PM}) =$$

$$= 0.10 v_{sa}(\Delta\mathrm{NO_x}) + 0.25 v_{sa}(\Delta\mathrm{SO_x}) + 0.05 v_{sa}(\Delta\mathrm{CO_2}) + 0.30 v_{sa}(\Delta\mathrm{CO}) + 0.10 v_{sa}(\Delta\mathrm{HC}) + 0.20 v_{sa}\Delta\mathrm{PM}$$

Following step 5 of the Algorithm, we can calculate the value function over each of the inventories. For example, for MEET we have:

$$v(\vec{\Delta}^{MEET}_{maneuvering}) = v(53.9, 3.09, 5.45, 161, 222, -84.2)$$

$$= 0.10 v_{sa}(53.9) + 0.25 v_{sa}(3.09) + 0.05 v_{sa}(5.45) + 0.30 v_{sa}(161) + 0.10 v_{sa}(222) + 0.20 v_{sa}(-84.2)$$

$$= 0.10 \times 0.5818 + 0.25 \times 0.9962 + 0.05 \times 0.9881 + 0.30 \times 0.3178 + 0.10 \times 0.2525 + 0.20 \times 0.0992$$

$$= 0.4971$$

In the same way we can calculate the value function over the other seven inventory families:

$v\left(\vec{\Delta}^{MOPSEA}_{maneuvering}\right)$=*v*(75.6,-56.4,-9.41,29.1,59.3,-7.90)=…=0.6480

$v\left(\vec{\Delta}^{NERI}_{maneuvering}\right)$=*v*(69.5,1.63,-7.08,-34.2,109,36.1)=…=0.7072

$v\left(\vec{\Delta}^{US\ EPA}_{maneuvering}\right)$=*v*(57.4,0.907,4.86,-42.4,151,-67.9)=…=0.5814

$v\left(\vec{\Delta}^{SMED}_{maneuvering}\right)$=*v*(18.2,-28.1,-0.670,-59.2,149,52.5)=…=0.5534

$v\left(\vec{\Delta}^{IMO}_{maneuvering}\right)$=*v*(45.2,-66.4,-16.1,-78.9,138,-20.8)=…=0.4083

$v\left(\vec{\Delta}^{Tier\ III}_{maneuvering}\right)$=*v*(21.7,-9.26,153,-39.1,653,40.8)=…=0.6390

$v\left(\vec{\Delta}^{ENTEC}_{maneuvering}\right)$= *v*(4.33,-15.8,-0.607,143,653,40.8)=…=0.6173

Following step 6 of the Algorithm the recommended inventory family when maneuvering would be MEET, because it has the highest value of the value function (0.7072). The second-best inventory family would be MOPSEA with value function of 0.6468. The selection of the MEET inventory family is a slight improvement compared to the one achieved with the minimal MAD criterion in section 3.2, where the MOPSEA was selected.

Let us assume that the DM wants to use the same attribute value function for all six attributes in the form $v_{quick}(\Delta_i)$ =1-$|\Delta_i|$/100. This function is shown with dashed line on Figure 6, where it can be seen it somehow resembles the "precise and rational" $v_i(\Delta_i)$ given with solid line. Let the same DM be happy to use six equal scaling constants and therefore a_i=1/6 for i=1,2,…,6. The main advantage of using the v_{quick}(.) with equal weight coefficients is that the six attribute value function can be built quickly by skipping the elaborate procedure in Section 4.1 and demonstrated in Example 6. The function $v_{quick}(\Delta_i)$ is not normalized because it takes negative values for deviations greater than 100%. However, the only place where this normalization matters is the skipped procedure for elicitation of the scaling constants using corner vectors. So, the six-attribute value function which models the preference of the discussed DM will take the form:

$$v\left(\vec{\Delta}\right)=v\left(\Delta\mathrm{NO_x},\Delta\mathrm{SO_x},\Delta\mathrm{CO_2},\Delta\mathrm{CO},\Delta\mathrm{HC},\Delta\mathrm{PM}\right)=$$

$$=\tfrac{1}{6}v_{quick}\left(\Delta\mathrm{NO_x}\right)+\tfrac{1}{6}v_{quick}\left(\Delta\mathrm{SO_x}\right)+\tfrac{1}{6}v_{quick}\left(\Delta\mathrm{CO_2}\right)+\tfrac{1}{6}v_{quick}\left(\Delta\mathrm{CO}\right)+\tfrac{1}{6}v_{quick}\left(\Delta\mathrm{HC}\right)+\tfrac{1}{6}v_{quick}\left(\Delta\mathrm{PM}\right)=$$

$$=\frac{1-\left|\Delta\mathrm{NO_x}\right|/100}{6}+\frac{1-\left|\Delta\mathrm{SO_x}\right|/100}{6}+\frac{1-\left|\Delta\mathrm{CO_2}\right|/100}{6}+\frac{1-\left|\Delta\mathrm{CO}\right|/100}{6}+\frac{1-\left|\Delta\mathrm{NC}\right|/100}{6}+\frac{1-\left|\Delta\mathrm{PM}\right|/100}{6}=$$

$$=1-\tfrac{1}{100}\frac{\left|\Delta\mathrm{NO_x}\right|+\left|\Delta\mathrm{SO_x}\right|+\left|\Delta\mathrm{CO_2}\right|+\left|\Delta\mathrm{CO}\right|+\left|\Delta\mathrm{HC}\right|+\left|\Delta\mathrm{PM}\right|}{6}=1-\tfrac{1}{100}w\left(\vec{\Delta}\right)$$

It is obvious that under the discussed circumstances the value function v(.) is a negative affine transformation of the MAD criterion w(.). So according to the value function uniqueness theorem (French, 1993) the maximization of the six-attribute value function v(.) will produce the same result as the application of the minimal MAD criterion. The later happens to be a special case of the six-attribute value function v(.), where the scaling constants are equal, and the six attribute functions are in the form $v_{quick}(\Delta_i)$ =1-$|\Delta_i|$/100. That is why the ranking of inventory families with the minimal MAD criterion is "quick and dirty" approach, which often produce satisfactory results as in Example 6. However, using the more elaborate 6-atrribute value function approach will guarantee that the selected inventory family will fully correspond to the DM preferences as is the case presented in Example 6.

4.3. Policy Implications of the Case Study

We can formulate some implications from the case study given in sections 2 and 3 and improved in Sections 4.1 and 4.2. It is very likely that for any standard ship in a specific mode of operation there is an inventory method that will produce emission predictions with high precision. If on-board measurement experiments are available, we have a chance of identifying which is the most suitable method and from what we demonstrated in the paper, this is a comparatively easy task. The best inventory method will most likely give small deviations from the measured emissions. However, if we try to choose blindly one inventory family for some mode of operation (without backing this up by any real time measurements) there is a high chance that we will choose a method that produces unacceptably high errors. The case study demonstrated that some methods deviate substantially in their predictions (by well over 100%). In that sense, one of the important contributions of this paper is to demonstrate the importance of experimental data to identify suitable inventory family for each of vessel's modes of operation.

This case study demonstrated an efficient way forward for emission estimation of a ship during technical exploitation in a quick and precise manner. It is possible that on-board measurements of the ship emission can be conducted at the time the ship is put in exploitation as well as at times of regular ship repairs. Using those measurements, the inventory method, which predicts the emissions with minimal error can be identified for each mode of operation of the vessel. The identified inventory methods can be used by various regulatory authorities during exploitation of the ship to calculate emissions during regular exploitation. The discussed inventory methods are beneficial first of all for the policy makers, who need to assess the pollution caused by shipping in order to implement reasonable boundaries to that pollution. Ship owners, on the other hand, can use the identified inventories to get precise prediction on the actual pollution their vessels cause to the environment during various modes of operation so that they can take adequate measures to minimize the penalties imposed by regulatory bodies.

There are four obvious alternatives to the above-formulated policy:

a) To use inventory methods selected by the policy makers without the benefit of verifying them with real measurement for each ship. As it was demonstrated by our case study, this method will almost surely produce shipping emission estimate with low precision. Therefore, the policy changes will most likely be inadequate. In fact, that is the situation now.

b) To regulate that every vessel should acquire and maintain its own measurement devices. They may even design their own family of inventories and justify their applicability for the ships they operate. That alternative would be unreasonably expensive for the ship owners, and very impractical because of the many problems that may arise when the machine crew starts interacting with the emission measurement system. As a result, even if the latter works in a given moment of time, the measurement results will be highly unreliable. Furthermore, the maritime and environmental authorities will use their own measurement systems rather than utilizing those on the ship (due to their necessity to comply with strict international regulations).

c) To require that every vessel should develop ship-specific inventories based on an on-board measurement campaign. This problem is almost impossible mathematically, because the data to create the inventory models will never be enough. On top, the policy makers would have a hard time dealing with so many different unknown models instead of using several known inventories. As a result, the assessed shipping emissions will be with even greater error than they are today.

d) To use only empirical data from on-board measurements. The main disadvantage of that strategy is that the best inventories, for a specific ship and type of operation contain prior knowledge, which will not be utilized. Additionally, the problems with the policy makers will be the same as in the previous alternative.

It seems that neither one of the discussed alternatives is satisfactory.

Based on the arguments given in the current section we propose the following policy for estimating the shipping emissions for future implementation:

Regulate that on-board emission measurements of nitrogen oxides, sulphur oxides, carbon dioxide, carbon monoxide, hydrocarbon, and particulate matter should be conducted for each vessel when put in exploitation and during every regular repair. For each possible inventory method, the deviations of its predicted emissions from the

measured emissions for the different modes of operations should be calculated. Those results should be kept within the official vessel's documents and should be available to the regulating authorities.

Using the available deviations, any authority can identify the best inventory family for each of the three modes of operations, depending on their preferences encoded in the six-attribute value function. Those vessel-specific inventory families will ensure cheap and relatively precise estimation of the primary emissions from shipping both locally and globally.

5. Conclusion

In the paper, a case study was presented about measurement and prediction of the emission from a 27000 GRT bulk carrier, with slow speed diesel main engine and with medium speed diesel auxiliary engines.

During an on-board experimental campaign, the following measurements were taken:

a) NO_x, SO_x, CO_2, CO, HC, and PM emission rates from the main engines when the vessel is at-berth, during maneuvering, and during cruising.

b) NO_x, SO_x, CO_2, and CO emission rates from the auxiliary engines when the vessel is at-berth

c) The instantaneous engine power, the shaft speed, the specific oil consumption, the air consumption, and the exhaust mass flow rate for each of the four experiments described a) and b).

The measured emission rates were converted to instantaneous emission factors and eventually to total emission amounts. The latter were predicted with 13 families of emission inventories (Tier I–III, ENTEC, MEET, STEAM, MOPSEA, IMO, SMED, EMS, US EPA, NERI and Corbett) and prediction deviations have been calculated. A procedure was advised for estimating the prediction inventory deviations of the combined hourly emission amounts from the main engine plus the auxiliary engines. The best inventory families were identified using the minimal mean absolute deviation criterion. The best inventory method at berth happened to be MOPSEA (32.2% mean absolute deviation), for maneuvering the best inventory family was MOPSEA (with 39.6% mean absolute deviation), and for cruising the best inventory family is MEET (with 59.2% mean absolute deviation). However, some of the other inventories produce unacceptably great deviation, well above 100%.

A more rational procedure for inventory ranking was considered, where each inventory family has been formalized as a six-dimensional vector of prediction deviations for a given mode of operation, which treats the missing value problem and constructs a six-attribute value function. We proposed an algorithm to impute missing values in the vectors (in case some of the emission deviations were not calculated), and to construct a six-attribute value function. The calculation of the value function at the six-dimensional vectors of prediction deviations was in position more rationally to identify the best inventory family when the vessel is at-berth, during maneuvering, and during cruising. The relation between the minimal mean absolute deviation criterion ranking and the maximal value function criterion was investigated. It was demonstrated that the former is a "quick and dirty" special case of the latter.

The implications of the case study were used to advise novel future policy for cost-effective and reliable emission estimation caused by the shipping.

Acknowledgments

The authors would like to express special thanks to the National Centre for Maritime Engineering and Hydrodynamic of the Australian Maritime College (University of Tasmania), as well as to our colleagues from the Queensland University of Technology – Thuy Chu Van, Richard Brown and Zoran Ristovski – for the strong support of this study. We also acknowledge and express gratitude to the Port of Brisbane Corporation for their generous cooperation, as well as to Maritime Safety Queensland and to stevedore operators AAT, Patricks and DP World for their contribution to this study.

Funding

The authors received no direct funding for this research.

Citation information

Jahangiri, S., Nikolova, N., & Tenekedjiev, K. (2018). Empirical testing of inventories applying on-board measurements of exhaust emissions at port and at sea. *Journal of Sustainable Development of Transport and Logistics, 3*(2), 6-33. doi:10.14254/jsdtl.2018.3-2.1.

References

Acock, A.C. (2005). Working with Missing Values. *Journal of Marriage and Family, 67*(4), 1012-1016.

Agrawal, H., Malloy, Q. G. J., Welch, W. A., Miller, J. W., & Cocker, D. R. (2008). In-use gaseous and particulate matter emissions from a modern ocean going container vessel. *Atmospheric Environment, 42*(21), 5504–5510.

Browning, L., & Bailey, K. (2006). Current Methodologies and Best Practices for Preparing Port Emission Inventories, 15th International Emission Inventory Conference "Reinventing Inventories – New Ideas in New Orleans", New Orleans, May 15 – 18, 1-20.

Cappa, C. D., Williams, E. J., Lack, D. A., Buffaloe, G. M., Coffman, D., Hayden, K. L., et al. (2014). A case study into the measurement of ship emissions from plume intercepts of the NOAA ship *Miller Freeman*. *Atmospheric Chemistry and Physics, 14*(3), 1337–1352.

Chen, G., Huey, L. G., Trainer, M., Nicks, D., Corbett, J. J., Ryerson, et al. (2005). An investigation of the chemistry of ship emission plumes during ITCT 2002. *Journal of Geophysical Research-Atmospheres, 110*(D10), D10S90, doi: 10.1029/2004JD005236.

Cohen, J., Cohen, P., West, S., & Aiken, L. (2003). *Applied multiple regression/correction analysis for the behavioral sciences*, Third Edition, Mahwah, NJ: Erlbaum.

Cooper, D. A. (2001). Exhaust emissions from high speed passenger ferries. *Atmospheric Environment, 35*(24), 4189–4200.

Cooper, D. A. (2003). Exhaust emissions from ships at berth. *Atmospheric Environment, 37*(27), 3817–3830.

Cooper, D. A., & Andreasson, K. (1999). Predictive NOx emission monitoring on board a passenger ferry. *Atmospheric Environment, 33*(28), 4637–4650.

Cooper, D. A., Peterson, K., & Simpson, D. (1996). Hydrocarbon, PAH and PCB emissions from ferries: A case study in the Skagerak-Kattegatt-Oresund region. *Atmospheric Environment, 30*(14), 2463–2473.

Cooper, D., & Gustafsson, T. (2004). *SCB: Methodology for calculating emissions from ships: 1. Update of emission factors.* SMHI Swedish Meteorological and Hydrological Institute (publisher), Report series SMED and SMED&SLU, No. 4.

Corbett, J. J., & Fischbeck, P. (1997). Emissions from ships. *Science*, *278*(5339), 823–824.

Corbett, J. J., & Koehler, H. W. (2003). Updated emissions from ocean shipping. *Journal of Geophysical Research-Atmospheres, 108*(D20), 4650–4666.

Corbett, J. J., Winebrake, J. J., Green, E. H., Kasibhatla, P., Eyring, V., & Lauer, A. (2007). Mortality from ship emissions: A global assessment. *Environmental Science & Technology, 41*(24), 8512–8518.

Dalsoren, S. B., Eide, M. S., Endresen, O., Mjelde, A., Gravir, G., & Isaksen, I. S. A. (2009). Update on emissions and environmental impacts from the international fleet of ships: The contribution from major ship types and ports. *Atmospheric Chemistry and Physics, 9*(6), 2171–2194.

Deniz, C., & Kilic, A. (2010). Estimation and assessment of shipping emissions in the region of Ambarli Port, Turkey. *Environmental Progress & Sustainable Energy, 29*(1), 107–115.

Du, Y. Q., Chen, Q. S., Quan, X. W., Long, L., & Fung, R. Y. K. (2011). Berth allocation considering fuel consumption and vessel emissions. *Transportation Research Part E–Logistics and Transportation Review, 47*(6), 1021–1037.

Endresen, O., Sorgard, E., Behrens, H. L., Brett, P. O., & Isaksen, I. S. A. (2007). A historical reconstruction of ships' fuel consumption and emissions. *Journal of Geophysical Research-Atmospheres, 112*(D12), D12301, doi:10.1029/2006JD007630.

Endresen, O., Sorgard, E., Sundet, J. K., Dalsoren, S. B., Isaksen, I. S. A., Berglen, T. F., & Gravir, G. (2003). Emission from international sea transportation and environmental impact. *Journal of Geophysical Research-Atmospheres, 108*(D17), 4560, doi: 10.1029/2002JD002898

ENTEC. (2007). Ship emissions inventory – Mediterranean Sea. *Concawe Review, 16*(1), 8-10.

EPA. (2010). *Control of emissions from new marine compression-ignition engines at or above 30 liters per cylinder*. A Proposed Rule by the Environmental Protection Agency on 08/28/2009, 44441-44595

Eyring, V., Kohler, H. W., Van Aardenne, J., & Lauer, A. (2005). Emissions from international shipping: 1. The last 50 years. *Journal of Geophysical Research-Atmospheres, 110*(D17305), doi: 10.1029/2004JD00561

French, S. (1993). *Decision theory: an introduction to the mathematics of rationality*. UK: Ellis Horwood.

French, S. & Insua, D.R. (2010). *Statistical Decision Theory*, Kendall's Library of Statistics 9, Wiley.

Fu, M. L., Ding, Y., Ge, Y. S., Yu, L. X., Yin, H., Ye, W. T., & Liang, B. (2013). Real-world emissions of inland ships on the Grand Canal, China. *Atmospheric Environment, 81*, 222–229.

Goldsworthy, L., & Galbally, I. E. (2011). Ship engine exhaust emissions in waters around Australia: An overview. *Air Quality and Climate Change, 45*(4), 24.

Goldsworthy, L., & Goldsworthy, B. (2015). Modelling of ship engine exhaust emissions in ports and extensive coastal waters based on terrestrial AIS data: An Australian case study. *Environmental Modelling & Software, 63*, 45–60.

Gommers, A., Verbeeck, L., Cleemput, E. V., Schrooten, L., & De Vlieger, I. (2007). *Monitoring programme on air pollution from sea-going vessels EV/43 (MOPSEA) Part 2: Global change, ecosystems and biodiversity*, Scientific support plan for a sustainable development policy (SPSD II), Belgian Science Policy.

Hallquist, A. M., Fridell, E., Westerlund, J., & Hallquist, M. (2013). On-board measurements of nanoparticles from a SCR-equipped marine diesel engine. *Environmental Science & Technology, 47*(2), 773–780.

Hickman, J., Hassel, D., Joumard, R., Samaraz, Z. &Sorenson, S. (1999) *Methodology for calculating transport emissions and energy consumption (MEET)*, Transport Research Board, The National Academies of Sciences, Engineering, and Medicine, USA.

Hockstad, L. & Hanel, L. (2018) Inventory of U.S. Greenhouse Gas Emissions and Sinks. United States: N. p., 2018. Web. doi:10.15485/1464240.

IMO. (2010). *Report of the marine environment protection committee on its sixty-first session, MEPC 61/24/Corr.3*

IMO. (2014). *Reduction of GHG emissions from ships, third IMO GHG study, final report*.

Jalkanen, J. P., Brink, A., Kalli, J., Pettersson, H., Kukkonen, J., & Stipa, T. (2009). A modelling system for the exhaust emissions of marine traffic and its application in the Baltic Sea area. *Atmospheric Chemistry and Physics, 9*(23), 9209–9223.

Jalkanen, J. P., Johansson, L., Kukkonen, J., Brink, A., Kalli, J., & Stipa, T. (2012). Extension of an assessment model of ship traffic exhaust emissions for particulate matter and carbon moNOxide. *Atmospheric Chemistry and Physics, 12*(5), 2641–2659.

Kasper, A., Aufdenblatten, S., Forss, A., Mohr, M., & Burtscher, H. (2007). Particulate emissions from a low-speed marine diesel engine. *Aerosol Science and Technology, 41*(1), 24–32.

Keeney, R. L. & Raiffa, H. (1993). Decisions with multiple objectives: preference and value tradeoffs. Cambridge University Press.

Kilic, A., & Deniz, C. (2010). Inventory of shipping emissions in Izmit Gulf, Turkey. *Environmental Progress & Sustainable Energy, 29*(2), 221-232.

Kim, S., Hwang, J. W., & Lee, C. S. (2010). Experiments and modeling on droplet motion and atomization of diesel and bio-diesel fuels in a cross-flowed air stream. *International Journal of Heat and Fluid Flow, 31*(4), 667-679.

Kristensen, H. O. (2010). *Energy demand and exhaust gas emissions of marine engines*. Technical University of Denmark.

Lu, G., Brook, J. R., Alfarra, M. R., Anlauf, K., Leaitch, W. R., Sharma, S., & Phinney, L (2006). Identification and characterization of inland ship plumes over Vancouver, BC. *Atmospheric Environment, 40*(15), 2767-2782.

Lyyranen, J., Jokiniemi, J., Kauppinen, E. I., & Joutsensaari, J. (1999). Aerosol characterisation in medium-speed diesel engines operating with heavy fuel oils. *Journal of Aerosol Science, 30*(6), 771-784.

Martínez de Osés, X. & La Castells, M. (2010). *Emission models: A comparison to determine the impact of maritime transport on emissions in SW European short sea shipping*. No 207470, Proc. 51st Annual Transportation Research Forum, Arlington, Virginia, March 11-13, Transportation Research Forum

Merk, O. (2014). Shipping emissions in ports, *International Transport Forum (Paris, France)* Discussion Paper No. 2014-20, OECD/ITF.

Michaelowa, A. (2000). The Kyoto Protocol. *Ecological Economics*, *34*(1), 155-156.

Miola, A., & Ciuffo, B. (2011).Estimating air emissions from ships: Meta-analysis of modelling approaches and available data sources. *Atmospheric Environment, 45*(13), 2242-2251.

Moreno-Gutierrez, J., Calderay, F., Saborido, N., Boile, M., Valero, R. R., & Duran-Grados, V. (2015). Methodologies for estimating shipping emissions and energy consumption: A comparative analysis of current methods. *Energy, 86*, 603-616.

Nikolova, N.D., Hirota, K., Kobashikawa, C., & Tenekedjiev, K. (2006). Elicitation of non-monotonic preferences of a fuzzy rational decision maker. *Information Technologies and Control*, Year IV, Volume 1, 36-50.

Nikolova, N.D., Toneva-Zheynova, D., Naydenov, D., Tenekedjiev, K. (2012). Imputing missing values of environmental multi-dimensional vectors using a modified Roweis algorithm, *Proc. IFAC Workshop on Dynamics and Control in Agriculture and Food Processing*, 3-16 June, Plovdiv, Bulgaria, 199-205.

OECD. (1997). *The OECD report on regulatory reform synthesis.* Organisation for Economic Co-operation and Development, France.

Olesen, H. R., Winther, M., Ellermann, T., Christensen, J., & Plejdrup, M. (2009). *Ship emissions and air pollution in Denmark: Present situation and future scenarios,* National Environmental Research Institute Aarhus University, Environmental Project No. 1307 2009 Miljøprojekt.

Petzold, A., Hasselbach, J., Lauer, P., Baumann, R., Franke, K., Gurk, C. & Weingartner, E (2008). Experimental studies on particle emissions from cruising ship, their characteristic properties, transformation and atmospheric lifetime in the marine boundary layer. *Atmospheric Chemistry and Physics, 8*(9), 2387-2403.

Petzold, L.A., Weinzierl, B., Fiebig, M., Lichtenstern, M., Lauer, P., Gurk, C., Franke, K., & Weingartner, E. (2006). Particle emissions from ship engines: emission properties and transformation in the marine boundary layer, Proceedings of the TAC-Conference, 26-29 June, Oxford, UK, pp. 78-82.

Radischat, C., Sippula, O., Stengel, B., Klingbeil, S., Sklorz, M., Rabe, R. & Zimmermann, R (2015). Real-time analysis of organic compounds in ship engine aerosol emissions using resonance-enhanced multiphoton ionisation and proton transfer mass spectrometry. *Analytical and Bioanalytical Chemistry, 407*(20), 5939-5951.

Sinha, P., Hobbs, P. V., Yokelson, R. J., Bertschi, I. T., Blake, D. R., Simpson, I. J. & Novakov, T (2003). Emissions of trace gases and particles from savanna fires in southern Africa. *Journal of Geophysical Research-Atmospheres, 108*(D13).

Skjølsvik, K.O., Andersen, A. B., Corbett, J. J., & Skjelvik, J. M. (2000). *Study of greenhouse gas emissions from ships* (report to International Maritime Organization on the outcome of the IMO Study on Greenhouse Gas Emissions from Ships), M.S.G.C.M.U. MEPC 45/8. Center for Economic Analysis/Det Norske Veritas, Trondheim, Norway.

Trozzi, C., & De Lauretis, R. (2013). International navigation, national navigation, national fishing, EMEP/EEA emission inventory guidebook.

United Nations conference on trade and development – UNCTAD. (2014). *Review of maritime transport*. UNCTAD/RMT/2014, United Nations Publication Sales no. E.14.II.D.5.

Van der Gon, H.D., & Hulskotte, J. (2010) *Methodologies for estimating shipping emissions in Netherlands*, Netherlands Research Program on Particulate Matter.

Wang, C., Corbett, J. J., & Firestone, J. (2000). Improving spatial representation of global ship emissions inventories. *Environmental Science & Technology, 42*(1), 193-199.

Winnes, H., & Fridell, E. (2009). Particle emissions from ships: Dependence on fuel type. *Journal of the Air & Waste Management Association, 59*(12), 1391-1398.

Wright, A. (1997). Marine diesel engine particulate emissions. *Transactions of the Institute of Marine Engineers, 109*, 345-364.

Paper 3 – *Jahangiri S, Nikolova N and Tenekedjiev K. An improved emission inventory method for estimating engine exhaust emissions from ships. Journal of Sustainable Environment Research. Volume 28, Issue 6. Pages 374-381. Doi: https://doi.org/10.1016/j.serj.2018.08.005. October 2018.*

Sustainable Environment Research 28 (2018) 374–381

Contents lists available at ScienceDirect

Sustainable Environment Research

journal homepage: www.journals.elsevier.com/sustainable-environment-research/

Original Research Article

An improved emission inventory method for estimating engine exhaust emissions from ships

Sanaz Jahangiri*, Natalia Nikolova, Kiril Tenekedjiev

Australian Maritime College, University of Tasmania, Launceston 7250, Australia

ARTICLE INFO

Article history:
Received 28 November 2017
Received in revised form
1 May 2018
Accepted 10 August 2018
Available online 23 October 2018

Keywords:
Shipping emissions
On-board measurement
Improved inventory
Regression analysis

ABSTRACT

The maritime transport industry is recognised as one of the cleanest modes of global transport. It is important to measure engine exhaust emissions to maintain its ecological superiority over road, rail, and other forms of transport.

Emission inventories are needed to estimate emissions. Current inventories need to review the emission factors (EFs) they currently employ, which generally yield over- or under-estimations. There is a need to consider more relevant measurements that will enhance the accuracy of emission prediction models. There is also a need to consider different mathematical approaches, to find better ways to manage the many changeable parameters of fuel consumption and engine specifications used to estimate emissions.

In this study, new sets of EF equations are developed to take into consideration real-time emission measurements during 11-d emission measurements on-board of two ocean-going vessels at berth and during sailing. They were tested on two ocean-going vessels, running on slow speed diesel main engines at berth while manoeuvring and cruising. Both vessels ran on heavy diesel fuel. Regression analysis, along with a consideration of fuel consumption and engine parameters, was used to develop the equations.

The results show a better prediction of emission quantity than current inventories for different engine types, in in-port and at-sea activities, with the sum of primary emissions coming closest to the actual sea emission calculations and also to the smallest standard values. This should be helpful when upgrading environmental policies.

1. Introduction

Maritime transport is recognised as the preferred mode of global transport for goods transfer [1]. It is superior to other modes of transport such as road and rail in the large payload it can carry [2]. The global fleet is expected to triple by 2050 [3], so too will their primary emissions (NO_x, SO_x, CO_2 and CO), and it becomes important to monitor the consequent pollution.

As diesel marine fuels combust, heat energy is given out. Crude oil is the source of many of the hydrocarbon compounds which are produced during this process. Contaminants like sulphur, vanadium, nickel, and ash are present in crude oil, and are retained during the production of marine fuels; heavy fuel oils (HFOs) are used to contain them after intensive refining. Several factors influence the quality of marine fuels: the refinery process, the crude oil quality, what kind of demands are there for the middle distillate and other residual fuels, and so on. Refinery processes often influence properties and characteristics of marine fuels like specific gravity, viscosity, asphaltenes, sediment, water, flash point, and compatibility [4].

In general, low quality fuel oil is used in the shipping industry [2]. HFO is the most common, currently used in many low-to medium-speed engines [5]. The sulphur content of HFO used in ships is typically 2.0–3.5%, with a global average around 2.6% [6].

There is also concern that shipping emissions are associated with adverse effects on human health, including lung cancer and heart attacks: for example, NO_x, CO_2 and CO can result in flu-like symptoms [7], while SO_x can cause breathing issues [7] and particulate matter (PM) may be implicated in premature deaths [8]; some

* Corresponding author.
E-mail address: sanaz.jahangiri@utas.edu.au (S. Jahangiri).
Peer review under responsibility of Chinese Institute of Environmental Engineering.

https://doi.org/10.1016/j.serj.2018.08.005

epidemiological studies have revealed instances of asthma and heart disease [9,10]. Researchers have reported that Ocean Going Vessels account for 14–31% of global emissions of NO_x, 4–9% of SO_x, and 3% of CO_2, worldwide [11]. Many studies [11–13] have reviewed the impact of shipping emissions on ecology, using a variety of methodologies on different scales. Emissions from vessels may also have a major effect on marine boundary layers and marine productivity, as well as on ozone production and ocean acidification [14].

The importance of on-board measurement, a practical approach to measuring emissions, has been the focus of many reviews [15–21]. Most studies collecting data from slow speed diesel and medium speed diesel engines are based either on plume measurements or on engine test rigs [18–21], but they should also take into account on-board measurement of emission factors (EFs), which are more up-to-date and detailed, in terms of types of fuel, the regions to be studied, the characteristics of individual vessels, specifics of the engine, and activities both in-port and at-sea [22]. Moreover, they need to be more precise, and revised in terms of mathematical approaches.

Two ocean-going vessels (Vessel I and Vessel II) had their engine exhaust emissions measured in order to develop models for the emissions produced during different shipping operations. Although on-board measurement may be precise but it is not always practical, as time and human resources may be limited; and it can be difficult to find vessel owners willing to install the necessary instrumentation. However, on-board measurement data were acquired in this study in order to develop new sets of EF equations through non-linear regression analysis, to help improve emission models and inventory calculations for different main engine types for at-sea and in-port operations.

2. Method

2.1. On-board measurement campaign

Vessel I, travelling from Port of Brisbane to Port Gladstone, underwent the first on-board measurement at a distance of 700 km; vessel II, travelling from Port Gladstone to Newcastle, underwent the second 1300 km. The routes of these vessels are presented in Fig. S1.

The ports at Brisbane, Gladstone and Newcastle, like many Australian ports, are close to urban centres, and a large percentage of the emissions from the ships, both in transit and at berth, directly affect nearby residents. As many coastal areas around the world are facing rapid and unplanned population growth, demographic change and development [23], there is a strong likelihood that they, and many Australian ports, will grow to keep up with growth in shipping, and the development of a reliable method to quantify and estimate emissions will become increasingly important.

Procedures ISO 8178-1:2006 [24] and ISO 8178-2:2008 [25] were used to measure on-board engine exhaust. These were also used to calculate the gas-phase species emissions [24,25]. Table 1 contains the engine specifications.

Fuel samples were collected from both vessels and analysed in the laboratory to determine their chemical contents. The main chemical composition and physical properties of the HFO tested are presented in Table 2, which also indicates the percentage of sulphur present.

Table 1
Ships' engines specifications.

Vessel	Main engine
Vessel I	MITSUI B&W 6L80GFCA 12,080 kW × 102 RPM
Vessel II	MAN B&W 6S50MC 6880 kW × 102 RPM

These results help to determine the exhaust gas flow rate, used to calculate the EFs of the vessel at various operating loads. The % mass carbon and sulphur contents are of particular interest, as they are considered the most influential when analysing the combustion process and, more importantly, the emissions generated.

Emission measurements were carried out by collecting samples using different portable instruments. Measured parameters and technical details of the applied devices are presented in Table 3 [26].

Emissions were measured and converted to weight (g). Eq. (1) gives the instantaneous emission for gaseous species, whose measurements are in ppm or percentage of gas [27]. The process used specific fuel consumption (SFOC) and formed CO_2 to provide the exhaust gas flow, calculated from fuel flow and air flow—basically the sum of fuel consumption (kg h^{-1}) + air consumption (kg h^{-1}). The exhaust mass flow was converted into volume flow rate by using air density (at 30 °C air density is ~1.2 kg m^{-3}).

$$\text{Emission}_k = \left(\text{ER}_k \times 10^{-6}\right)\frac{PV}{RT}\,\text{MW}_k t \quad (1)$$

where Emission_k is emissions (g), subscript k refers to emission type (NO_x, SO_x, CO_2 and CO), ER (ppm) measures gaseous species ERs, P is average pressure of 101.3 kPa in standard conditions and a temperature of 273.1 K, V (m^3 h^{-1}) is calculated volumetric flow rate of the exhaust based on the available data, R (J mol^{-1} K^{-1}) is ideal gas constant, T (K) is average temperature of 273.1 K in standard conditions and an average pressure of 101.3 kPa, MW (g mol^{-1}) is molecular weight, and t (h) is recorded operation time of the vessels in different shipping modes.

The dilution ratio (DR) of each load and speed settings was then calculated. To determine the DR, CO_2 was used as a tracer gas. The concentration of CO_2 in the raw exhaust was measured directly by the Portable 5-Gas Analyser (Horiba MEXA 584L) (CO_2 (Raw)) and by the concentration of CO_2 after dilution was measured by Sable CA-10 (CO_2 (Diluted)); then the DR was calculated by applying Eq. (2). These calculations assume that all carbon in the fuel is completely converted to CO_2 [28].

$$\text{DR} = \frac{\text{CO}_2(\text{Raw}) - \text{CO}_2(\text{Background})}{\text{CO}_2(\text{Diluted}) - \text{CO}_2(\text{Background})} \quad (2)$$

2.2. Development of emission equations

Equations were developed applying 70% of measured ERs randomly for at berth, manoeuvring and cruising modes for each primary emission.

The regression models were based on the independent variables, which in this study were data on maximum continuous rate (MCR) (as x_1), shaft speed (SS) (as x_2), and emissions (Y). Applying dependant variables affects the accuracy of the results. In the case

Table 2
Chemical composition and physical properties of HFO.

Parameter	Units	Method	Vessel I	Vessel II
Density at 15 °C	kg m^{-3}	ISO 3675	986.2	986.2
Kinetic viscosity at 50 °C	mm^2 s^{-1}	ISO 3140	283.0	377.0
Carbon	% mass	AR 2816	88.1	88.1
Micro-carbon residue	% mass	ISO 10370	18.0	14.7
Sulphur	% mass	ISO 2719	2.9	2.8
Ash	% mass	ISO 6245	0.02	0.06
Nitrogen	% mass	AR 2816	0.6	0.7

Table 3
Applied instrumentation specifications.

Applied devices	Measured parameters	Range	Accuracy	Flow rate (L min^{-1})
A Portable 5-Gas Analyser (The Horiba MEXA 584L)	HC, CO, CO_2, O_2 and NO_x (as well as monitoring air–fuel equivalence ratio λ)	0–60,000 ppm 0–25%	25–60 ppm 0.03–0.01%	
Sable CA-10	CO_2	0–5% standard 0–10% optional	1%	5–500 ($\times 10^{-3}$)
DMS 500	Particle size and concentration	5 nm–2.5 μm	–	8.0
Testo 350 XL	SO_2, CO, CO_2, O_2, NO and NO_2	0–10,000 ppm 0–25%	5% of mass-volume 0.8% of fixed-voltage 5 ppm	1.2
Dust Trak	PM_1, $PM_{2.5}$, PM_{10}	0.1–10 μm	5%	3.0

of this study, fuel consumption was dependent on engine load, and the base SFOC value was influenced by engine stroke type and power. Primarily, engine-model specific base values of SFOC provided by the engine manufacturers were used.

Instantaneous total fuel consumption is influenced by many independent factors. The fuel consumption of main engines used in propulsion is commonly estimated as a product of the constant SFOC and instantaneous engine power, which gives a linear relationship between fuel consumption and engine power. Ideally, all power systems that require fuel to operate should be modelled separately: the main engines for propulsion, auxiliary engines for power generation, and boilers for heat generation; however, in practice separate modelling is currently not feasible. In any case the methodologies for evaluating power and fuel consumption are fairly simple, and different assumptions were observed to provide biased estimates, especially for auxiliary engines. The SFOC effect, dependent on MCR quantities, was hidden in the developed equations; but as the objective was to analyse the variation effect of independent variables over time on final emissions, the chemical contents of the fuel (carbon, sulphur and nitrogen) were not considered as these are not time-dependant.

Table 4 shows the range of on-board measurement datasets used to develop the equations. The data on engine power, engine revolution, and other parameters including intercooled air temperature, scavenging air pressure and cooling fresh water were recorded every 5 s for the main engine. The only restrictions on the use of the developed EF equations would have been any datasets outside the ranges noted in Table 4 for Emissions, MCR and SS, but the applied dataset roughly covered a good range for all the variables mentioned in practical shipping operations.

Datafit 9 software, using different model groups including three-parameter power, three-to eleven-parameter polynomial, six and ten Taylor series polynomial, was employed to define the models. The actual emission rates (measured instantaneously in variable timings (h) and variable engine powers (kW)) recorded every 5 s as the base for EFs in units of either ppm or %. They were then normalised to standard conditions: a temperature of 273.1 K and pressure of 101.3 kPa. Final emissions in grams were then calculated.

Having applied Datafit software, the maximum quantity of six parameters was used in this study. The equations, developed from non-linear regression analysis, are at a 95% confidence interval. The regression model's curve's alignment with the data points can be predicted by the R_a^2 value (Eq. (3)), where n is the number of points in the data sample and k is the number of independent regressors (the number of variables in the models excluding dependant variables and constants) [29]. The adjusted R^2 is necessary because the value of the percentage of variation can only be explained by those independent variables that affect the dependent variables. Simply put, the adjusted R^2 will increase if a more useful variable is added and decrease if an un-useful (dependant) variable is added. The methodology framework is shown in Fig. 1.

$$R_a^2 = 1 - \left[\frac{(1-R^2)\,(n-1)}{n-k-1}\right] \tag{3}$$

Table 4
Applied dataset range (the minimum and maximum points).

Mode		Emissions (g)	MCR[a] (%)	SS[b] (RPM)
At berth	SO_2	8.7–18.8	2.5–12.8	31.5–47.4
	NO_x[c]	6.0–20.0	1.0–12.6	−46.1 to 49.4[d]
	CO_2	337.6–951.5	1.8–12.6	31–47.2
	CO	0.3–0.9	3.3–12.0	30.3–47.2
Manoeuvring	SO_2	60.1–108.5	37.4–60.0	73.8–89.0
	NO_x	31.1–68.4	29.4–63.7	69.8–80.9
	CO_2	2949–4303	29.4–63.7	69.8–80.9
	CO	7.7–15.3	31.3–63.5	71.1–80.9
Cruising	SO_2	108.7–145.0	59.6–91.6	85.9–90.8
	NO_x	81.2–108.8	59.6–91.6	85.9–90.8
	CO_2	4949.0–5888.0	59.6–90.8	85.9–90.8
	CO	8.9–15.7	59.6–91.6	85.9–90.8

[a] Maximum continuous rate.
[b] Shaft speed.
[c] NO + NO_2.
[d] Negative amounts occur when the shaft churns backward to completely stop the ship at berth.

3. Results and discussion

3.1. On-board measurement campaign

Measurements of main engine at berth were conducted when Vessel I arrived at its destination port but before the main engine were turned off. Both shaft power and SS keep changing while berthing to stop the ship making headway (Fig. 2); and both strongly affect the quantity of emissions, as depicted in Fig. 2: that is, when engine speed and power suddenly undergo either positive or negative change, emissions fluctuate accordingly. Sudden change may be caused by external factors such as wind, waves or currents, or by tugs or anchors. Fig. 2 shows the primary emissions, measured while the vessel was manoeuvring at the destination port. As with at-berth conditions, the levels of emissions change abruptly when SS and shaft power undergo a sudden change, often required to ensure smooth and safe berthing [30], but changes may also be caused by the geometry of the hull, the pivot point, lateral motion, the rudder, the propeller or the thrusters. The geological features of the port and under-keel clearance also affect emissions levels. Normal cruising speed was also visible for emissions (Fig. 2).

3.2. Validation of emission equations

Applying the percent-predicted method, the remaining random 30% of the emission datasets of Vessels I and II were predicted using

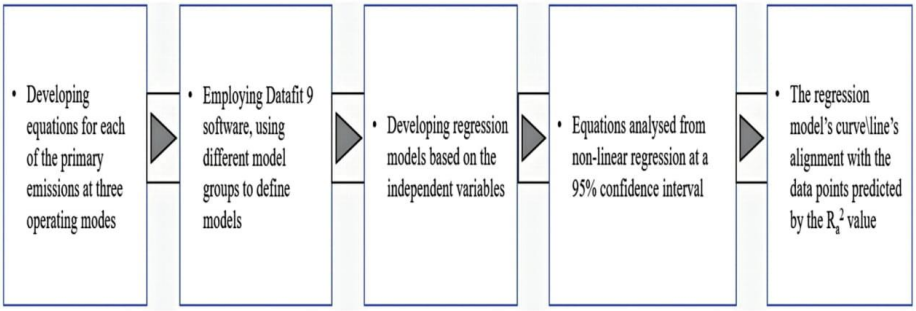

Fig. 1. The methodology framework for developing the equations.

the equations presented in Table S1. By comparing existing inventories with the actual emissions calculated using Eq. (1), it is possible to estimate primary emissions for various engine types. Our predicted inventories are closest to actual on-board estimations, at berth or while manoeuvring or cruising (Table S2).

The standard error of the regression or estimate value (S) (Eq. (4)) demonstrates the mathematical superiority of our predicted emission inventory over other inventories in use. The value is calculated with y' as the instantaneous calculated emission in our and other inventories and N as the total number of datasets for each primary emission of different engine types in different shipping operations. Having the smallest values, our inventories show superiority over other inventories (Table S3).

$$S = \sqrt{\frac{\sum (y - y')^2}{N}} \tag{4}$$

Fig. 3 presents some samples of the trends of instantaneous emissions at different MCRs, and again our predicted inventories show the greatest affinity with on-board measurements (Figs. S2–4). Full samples of the primary emissions in different shipping operations are presented in Figs. S2–4.

Current inventories lack detailed EF datasets for different engine types, shipping modes and emissions. As they also widely ignore national air quality programs, there is a growing need to evaluate their impact on air quality and health.

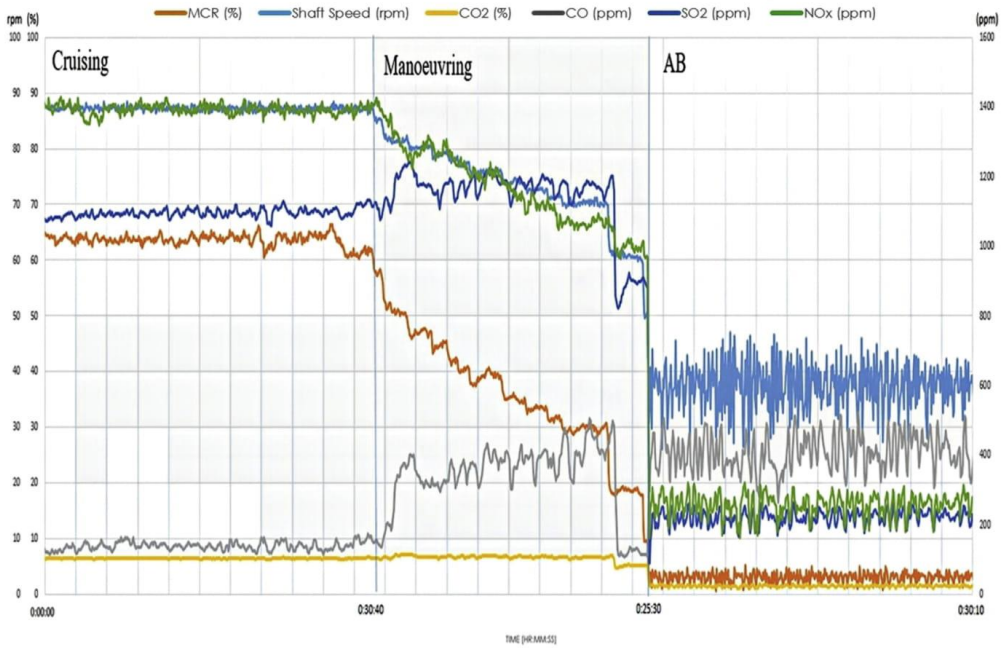

Fig. 2. Main engine emission changes at berth, manoeuvring, and cruising.

The engine ER changes (Fig. 2) are non-linear, indicating a need to simulate emissions more practically in the mathematical model. In our study the effects of changes in engine parameters on emissions are considered for the first time.

Reasons for some non-precise estimations by each of the inventories are provided below:

TIER III [31] datasets do not include CO_2 emissions for main engines; the effects of engine type and shipping activity not taken into account; and only limited averages of the fuel sulphur content and SFOC are considered. The data on fuel consumption are based on national data on sold fuels, not on engine fuel consumption.

Entec [27] assumes the engine EF values in different shipping activities and engine loads; and there is considerable uncertainty in some of the assumptions about engine load use in port. The quantities of fuel sulphur and carbon contents and SFOC are averaged, and when applying the inventory to smaller fleets, the error between the assigned EFs and the fleet value increases. Other factors that may be relevant, such as how cold-started engines or various engine loads affect performance in the course of manoeuvring, are ignored.

Methodology for Emissions and Energy consumption for Transport (MEET) [32] calculates averaged fuel consumption and engine loads for engines rather than addressing specific situations that may affect performance: for instance, the same EF is used for CO engines at berth and manoeuvring; and for the CO engines of slow- and medium-speed diesel engines. It does not consider the effect of using different marine fuels in engine NO_x EFs in different shipping operations.

Ship Traffic Emission Assessment Model [33] datasets do not include CO emissions. As a requirement of the SO_x Emission Control Area regulations of the International Maritime Organisation (IMO), only a sulphur mass-percentage of 1.5 is assumed and modelled for main engines. Different engine specifications or shipping operations are not considered when assigning engine NO_x EFs. Engine loads can often influence EFs: for instance, engines operating under a low load may have higher emissions, particularly during harbour manoeuvring; such variations in EFs as a function of engine load are not taken into account.

Monitoring programme on air pollution from sea-going vessels (MOPSEA)'s [34] activity data are gathered from information systems not designed for inventory emissions, so it takes time and experience to repurpose the data to suit them to the emission model, and the work needs to be simplified and tailored to be fit for inventory purposes. This model too makes various assumptions about fuel use and the percentage of MCR which do not reflect these parameters in practice: for example, averaged engine EFs per

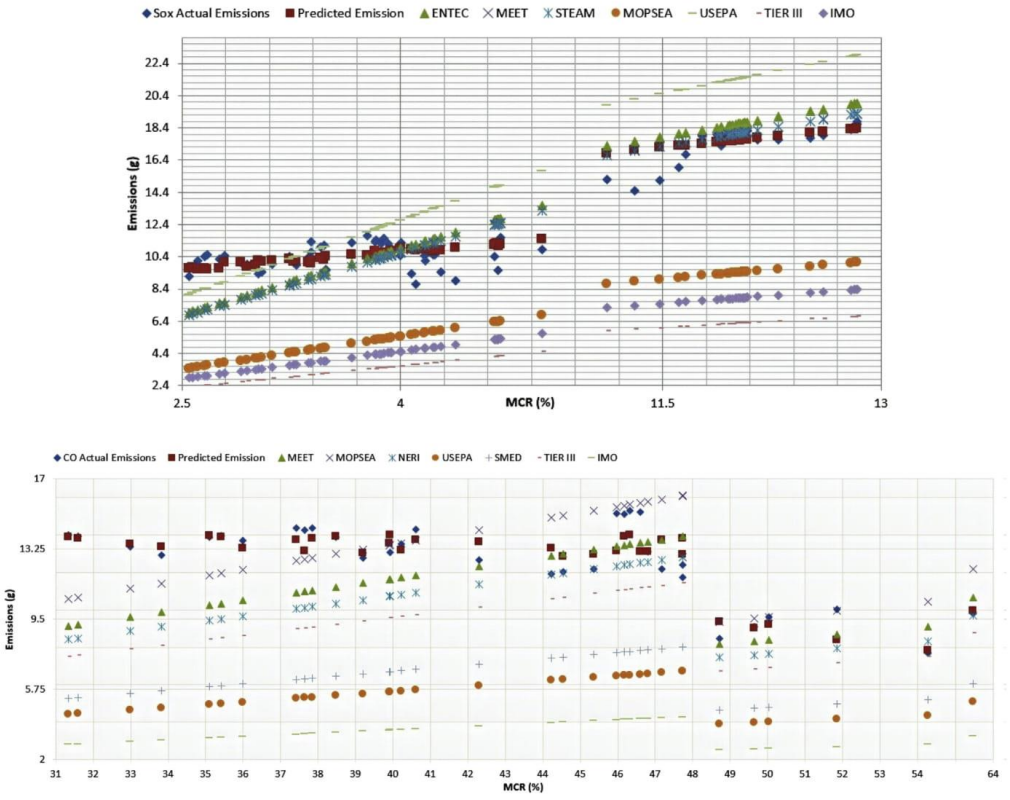

Fig. 3. Sample of some trends of predicted and available inventory ME emissions (g) in different shipping operation.

Fig. 3. (*continued*).

ship type are used instead of specific figures. There is inadequate focus on engine loads during different shipping activities, and no coverage of engine load variations over 85% or under 10% in NO_x and CO EFs. Nor is there adequate direction for dealing with missing data, or for implementing and using Automatic Identification System (AIS) data.

National Environmental Research Institute (NERI) [35] uses the same CO EFs without consideration of engine type or shipping activity; nor are consistent emission data available as a function of the engine age. In addition, country-specific EFs for CO_2 do not consider engine types or shipping activities.

United States Environmental Protection Agency (USEPA)'s [36] basis for its operating data seems to have various assumptions that are not validated by the Energy and Environmental Analysis as their contractor. It categorises engines by individual cylinder displacement, which may not indicate a true relationship with high, medium, and slow speeds. Large inconsistencies appear between the output given at full load and the actual ratings of the engine, pointed out in Lloyd's analysis.

The data analysis is mostly carried out on engines with a rating of less than 8000 kW, and the applicability of the EFs obtained to engines of all sizes is debatable. There is no consistency between

engines' rated power and testing conditions, so EPA categories cannot be determined. There is no agreement on the actual numbers or types of engine, and no reporting of engine markers or displacements. In some instances, the reported maximum power and engine ratings show discrepancies.

The Environment Canada report defines the three modes and engine load factor variations under which its engines were tested, and does not consider the extent of variation that may exist between engines in the same category; 'normal cruise' and 'docking operation' conditions are undefined in the procedures of the BC Ferry Test Program. Engine NO_x and CO have the same EFs, regardless of fuel or engine used or consideration of shipping activity.

Swedish Methodology for Environmental Data [37] inventory likewise Entec [27], mentioned in above paragraphs, suffers from non-precise EFs. Also, there is a great deal of uncertainty about 'manoeuvring' (the assumption is that engines operate at 20% MCR), as well as the need for manoeuvring emissions to take into consideration that emissions from cold state engines, especially CO emissions, which would be significantly different than those from warmer engines. Variability of emissions can also be caused by rapid changes to load during manoeuvring: this study takes none of these into account.

Engine EFs (derived from steady state loads of 70–100%) are multiplied 'at sea' by 0.8 for NO_x and by 2.0 for CO for all engines running on diesel. This means that there is significant uncertainty regarding the results. Emission estimations for engines at berth are not considered. The estimates of the fuel sulphur in various fuels over the years are unspecified, and it is assumed that between 1990 and 2003, fuel-dependent EFs of CO_2 were constant. Considering that EFs are different and there is anticipated uncertainty, specifying exactly how biased emission estimations can be, especially when only at-sea EFs are at play, is difficult.

IMO [38] bases its SO_x base line EFs on a 2.7% sulphur content HMO, although the world average of fuel sulphur is in constant change. The effect of using different fuel types is not considered in applying base SFOC values to engines; the parabolic SFOC dependency on engine load is not considered in HFO; and transient engine load changes are not considered in CO EFs.

There are uncertainties about how many active ships exist, and which are allocated to domestic or international voyages. Currently discrepancies occur between the number of active ships described by the IHSF and those observed on AIS, although this will reduce slightly as the availability of AIS data improves. The bottom-up method is used when location information is available, but AIS coverage is not so consistently high for the voyage-by-voyage details to be identified either. Some uncertainties may also arise if the ship is not visible on AIS and its speed is estimated.

4. Conclusions

The non-linear regression analysis used here to develop new sets of EF equations on each primary emission for engines at berth, manoeuvring, and at sea predicts emissions more accurately than current inventories. The sampling will help in developing emission models and inventory calculations that can be used to outline MCR, SS, and emission datasets more effectively than is currently achieved.

Acknowledgements

Special thanks to National Centre for Maritime Engineering and Hydrodynamic in Australian Maritime College and Queensland University of Technology for their support of this study. The generous cooperation of Port of Brisbane Corporation is acknowledged, as are Maritime Safety Queensland and stevedore operators AAT, Patricks and DP World.

Appendix A. Supplementary data

Supplementary data to this article can be found online at https://doi.org/10.1016/j.serj.2018.08.005.

References

[1] Wang C, Corbett JJ, Firestone J. Improving spatial representation of global ship emissions inventories. Environ Sci Technol 2008;42:193–9.
[2] Deniz C, Kilic A. Estimation and assessment of shipping emissions in the region of Ambarli Port, Turkey. Environ Prog Sustain Energy 2010;29:107–15.
[3] Eyring V, Köhler HW, van Aardenne J, Lauer A. Emissions from international shipping: 1. The last 50 years. J Geophys Res Atmos 2005;110:1–12.
[4] ABS. Notes on Heavy Fuel Oil. Houston, TX: American Bureau of Shipping; 1984.
[5] Goldsworthy L, Galbally IE. Ship engine exhaust emissions in waters around Australia – an overview. Air Qual Clim Change 2011;45:24–32.
[6] IMO. Report of the Marine Environment Protection Committee on its Sixty-first Session. London, UK: International Maritime Organisation; 2010.
[7] Fournier A. Controlling Air Emissions from Marine Vessels: Problems and Opportunities. Santa Barbara, CA: University of California Santa Barbara; 2006.
[8] USEPA. Control of Emissions from New Marine Compression-ignition Engines at or Above 30 Litres Per Cylinder. Washington, DC: US Environmental Protection Agency; 2010.
[9] Kim S, Hwang JW, Lee CS. Experiments and modeling on droplet motion and atomization of diesel and bio-diesel fuels in a cross-flowed air stream. Int J Heat Fluid Flow 2010;31:667–79.
[10] Lu G, Brook JR, Alfarra MR, Anlauf K, Leaitch WR, Sharma S, et al. Identification and characterization of inland ship plumes over Vancouver, BC. Atmos Environ 2006;40:2767–82.
[11] Kilic A, Deniz C. Inventory of shipping emissions in Izmit Gulf, Turkey. Environ Prog Sustain Energy 2010;29:221–32.
[12] Moreno-Gutierrez J, Calderay F, Saborido N, Boile M, Valero RR, Duran-Grados V. Methodologies for estimating shipping emissions and energy consumption: a comparative analysis of current methods. Energy 2015;86:603–16.
[13] Merk O. Shipping Emissions in Ports. Paris, France: Organisation for Economic Co-operation and Development; 2014.
[14] Hassellov IM, Turner DR, Lauer A, Corbett JJ. Shipping contributes to ocean acidification. Geophys Res Lett 2013;40:2731–6.
[15] Cooper DA, Peterson K, Simpson D. Hydrocarbon, PAH and PCB emissions from ferries: a case study in the Skagerrak–Kattegat–Oresund region. Atmos Environ 1996;30:2463–73.
[16] Cooper DA, Andreasson K. Predictive NO_x emission monitoring on board a passenger ferry. Atmos Environ 1999;33:4637–50.
[17] Cooper DA. Exhaust emissions from high speed passenger ferries. Atmos Environ 2001;35:4189–200.
[18] Lyyranen J, Jokiniemi J, Kauppinen EI, Joutsensaari J. Aerosol characterisation in medium-speed diesel engines operating with heavy fuel oils. J Aerosol Sci 1999;30:771–84.
[19] Petzold A, Hasselbach J, Lauer P, Baumann R, Franke K, Gurk C, et al. Experimental studies on particle emissions from cruising ship, their characteristic properties, transformation and atmospheric lifetime in the marine boundary layer. Atmos Chem Phys 2008;8:2387–403.
[20] LRES. Marine Exhaust Emissions Research Programme: Steady State Operation. London, UK: Lloyd's Register Engineering Services; 1990.
[21] Corbett JJ, Koehler HW. Updated emissions from ocean shipping. J Geophys Res Atmos 2003;108:4650.
[22] Jahangiri S, Kam US, Garaniya V, Abbassi R, Enshaei H, Brown RJ, et al. Development of Emission Factors for Ships' Emissions at Berth. Australasian Coasts & Ports. Barton, Australia: Engineers Australia; 2017. p. 646–52.
[23] Satumanatpan S, Chuenpagdee R. Assessing governability of environmental protected areas in Phetchaburi and Prachuap Khiri Khan, Thailand. Marit Stud 2015;14:1–19.
[24] ISO. ISO 8178-1. Reciprocating Internal Combustion Engines – Exhaust Emission Measurement – Part 1: Test-bed Measurement of Gaseous and Particulate Exhaust Emissions. Geneva, Switzerland: International Organization for Standardization; 2006.
[25] ISO. ISO 8178-2. Reciprocating Internal Combustion Engines – Exhaust Emission Measurement – Part 2: Measurement of Gaseous and Particulate Exhaust Emissions under Field Conditions. Geneva, Switzerland: International Organization for Standardization; 2008.
[26] Australian Maritime College. Development of a Methodology to Measure and Assess Ship Emissions. Tokyo, Japan: International Association of Maritime Universities; 2016.
[27] Whall C, Scarbrough T, Stavrakaki A, Green C, Squire J, Noden R. UK Ship Emissions Inventory. London, UK: Entec UK Limited; 2010.
[28] Babaie M. Reduction of Diesel Engine Exhaust Emissions Using Non-thermal Plasma Technology [Ph.D. dissertation]. Brisbane (Australia): Queensland University of Technology; 2015.

[29] Harel O. The estimation of R^2 and adjusted R^2 in incomplete data sets using multiple imputation. J Appl Stat 2009;36:1109–18.
[30] Fu ML, Ding Y, Ge YS, Yu LX, Yin H, Ye WT, et al. Real-world emissions of inland ships on the Grand Canal, China. Atmos Environ 2013;81:222–9.
[31] Trozzi C, De Lauretis R, Rypdal K, Webster A, Fridell E, Reynolds G, et al. International navigation, national navigation, national fishing and military (shipping). In: EMEP/EEA Air Pollutant Emission Inventory Guidebook. Luxembourg: European Environment Agency; 2013.
[32] TRL. Methodology for Calculating Transport Emissions and Energy Consumption. Crowthorne, UK: Transport Research Laboratory; 1999.
[33] Jalkanen JP, Brink A, Kalli J, Pettersson H, Kukkonen J, Stipa T. A modelling system for the exhaust emissions of marine traffic and its application in the Baltic Sea area. Atmos Chem Phys 2009;9:9209–23.
[34] Gommers A, Verbeeck L, Van Cleemput E, Schrooten L, De Vlieger I. Monitoring Programme on Air Pollution from SEA-going Vessels EV/43, Pt 2. Brussels, Belgium: Belgian Science Policy; 2007. http://www.belspo.be/belspo/organisation/publ/pub_ostc/EV/rappEV43_en.pdf.
[35] Olesen HR, Winther M, Ellermann T, Christensen J, Plejdrup M. Ship Emissions and Air Pollution in Denmark. Copenhagen, Denmark: Danish Environmental Protection Agency; 2009.
[36] USEPA. Analysis of Commercial Marine Vessels Emissions and Fuel Consumption Data. Washington, DC: US Environmental Protection Agency; 2000.
[37] Cooper D, Gustafsson T. Methodology for Calculating Emissions from Ships: 1. Update of Emission Factors. Norrköping, Sweden: Swedish Meteorological and Hydrological Institute; 2004.
[38] IMO. Third IMO GHG Study 2014. London, UK: International Maritime Organisation; 2014.

Paper 4 – *Jahangiri S, Kam US, Garaniya V, Abbassi V, Enshaei H, Brown RJ, Van TC, Pourkhesalian AM and Ristovski Z. Development of Emission Factors for Ships' Emissions at Berth. Coasts & Ports 2017 Conference – Cairns. ISBN: 9781922107916. Pages 646-652. June 2017.*

Paper 5 – *Jahangiri S, Nikolova N and Tenekedjiev K. Application of a Developed Dispersion Model to Port of Brisbane. American Journal of Environmental Sciences. Volume 14, Issue 4. Pages 156-169. Doi: 10.3844/ajessp.2018.156.169. October 2018.*

American Journal of Environmental Sciences

Original Research paper

Application of a Developed Dispersion Model to Port of Brisbane

[1]Sanaz Jahangiri, [1,2]Natalia Nikolova and [1,2]Kiril Tenekedjiev

[1]Australian Maritime College, University of Tasmania, Launceston, Tasmania, Australia
[2]Nikola Vaptsarov Naval Academy – Varna, Bulgaria

Article history
Received: 10-07-2018
Revised: 29-08-2018
Accepted: 10-10-2018

Coressponding Author:
Sanaz Jahangiri
Australian Maritime College,
University of Tasmania,
Launceston, Tasmania,
Australia
Email: sanaz.jahangiri@utas.edu.au

Abstract: The emissions from vessels utilising heavy fuel oil include large amounts of nitrogen oxides, sulphur dioxide and particulate matter, presenting significant health risks to people living near ports. To determine the effect of these emissions on human health, complex atmospheric dispersion modelling using CALPUFF assesses ground-level concentrations at receptors surrounding the sources. This paper demonstrates the application of the methodology by applying it to Port of Brisbane for the full 2013 calendar year. Various Health impact assessments as well as carcinogenic and ecological effects are discussed in depth. Results reveal that with the imminent development of many Australian ports, there is a need for continual monitoring of emissions caused by shipping.

Keywords: Shipping, Health Risk, Emission Inventory, Dispersion Modelling

Introduction

It is widely agreed that shipping exhaust emissions are a significant source of air pollution (Corbett *et al*., 1999; Cooper, 2003). The three largest and most worrisome are Nitrogen Oxides (NO_x), Sulphur Oxides (SO_x) and particulate matter (PM). Implementing the amendments to the MARPOL Annex VI regulations is intended to reduce shipping emissions worldwide (Hughes, 2011), but this is not easy because their effects tend to be dispersed and difficult to track to source.

In-port emissions, although a relatively small proportion of total emissions, have significant health impacts on nearby populations (Corbett *et al*., 1999) and are linked to cardiopulmonary- and cancer-related health problems. Winebrake *et al.* (2009), for instance, estimated that in 2012, SO_x emissions from shipping were implicated in approximately 87,000 deaths worldwide. Studies in Australia have considered total emissions both within coastal waters (Goldsworthy and Goldsworthy, 2015) and in a specific port (Goldsworthy and Renilson, 2013), but have not yet quantified their dispersion and deposition across local populations. This paper presents the methodology to obtain emissions concentrations within Australian ports in general and in a case study of Port of Brisbane in particular. It is based on a comprehensive inventory of vessel emissions in Port of Brisbane over a year, using actual vessel movements and applies atmospheric dispersion modelling to this quantified data to predict the ground-level concentrations of gaseous pollutants and the deposition of particulate matter, based on local meteorological and geographical conditions. On the final stage, assessing each resulting emission concentration for its individual health impact, based on a calculated risk values for each concentration has been also identified.

Port Overview

Port of Brisbane is a multi-modal port on the Brisbane River on the east coast of Australia, currently managing 29 operational berths. There are also a number of privately managed berths: Fisherman Islands, at the mouth of the Brisbane River, hosts twelve container berths, a number of bulk product berths and one general purpose berth; and more dry- and wet-bulk terminals are sited up-river towards Hamilton Reach, where a cruise terminal and naval base are located (PB, 2015). The port is unique because of the long distance between the outer port limit and the berths on the river: A channel of 82.9 km to the entrance beacons is located approximately seven kilometres seaward of the outermost berth on Fisherman Islands; a map of this approach appears in Fig. 1. The port boundary extends from the pilot boarding ground at the north to the lowest reaches of the Brisbane River in the south and is defined by Moreton Island to the east and the Australian mainland to the west.

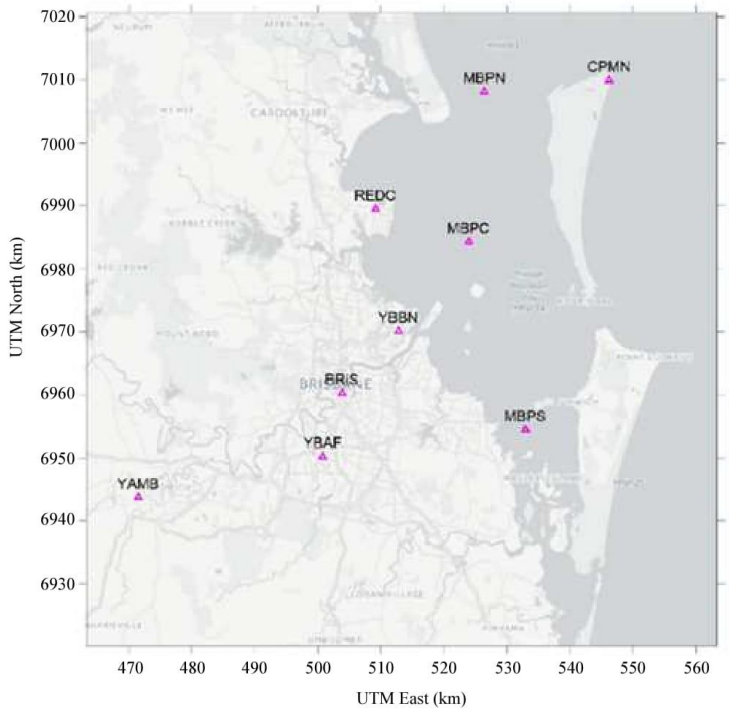

Fig. 1: Port of Brisbane area including the approach from the pilot boarding ground and Surface meteorology stations used in the CALPUFF model

Pilots join the vessels at the pilot boarding ground at the outer port limit, near Caloundra Heads. Vessels then move to the entrance beacon under their own power, typically at a speed close to normal cruising. At the entrance beacons, most are assisted by tugs to their destination berth. During this final leg, vessels travel at a restricted speed dictated by their draft and under-keel clearance. Occasionally vessels may hold fast at the ship-to-ship transfer anchorages near the entrance beacons until a berth becomes available. Once at berth, they load and offload cargo and supplies as required. Some may reposition to another berth during their call at the port, depending on the types of cargo they are handling.

Upon departure, vessels are assisted by tugs to manoeuvre out of the berth and, depending on their length, to move some distance towards the entrance beacons. Some need to wait for suitable tidal movements before proceeding down-river and through the channel. They go under their own power to the pilot boarding ground, where the pilot disembarks and the vessel goes on its way. Departure transits usually take less time than arrivals.

Atmospheric Dispersion Modelling

A number of dispersion models exist, depending on the size and complexity of the domain and the type of pollutant source. The *Good Practice Guide for Atmospheric Dispersion Modelling* compiled by the New Zealand EPA (Bluett *et al*., 2004) provides a solid review of the range of dispersion modelling techniques and their applicability. Similar studies have been undertaken by both the NSW EPA (2005) and the USEPA (Holmes and Morawska, 2006). All agree that atmospheric modelling of coastal regions provides a challenge, given the complex meteorological conditions they present. Modelling is further hampered by the irregular geographical features of many coastlines. Bluett *et al*. (2004) question the ability of simple Gaussian-plume models in these conditions and suggests the need to use more advanced puff or Lagrangian-based models. A number of more advanced dispersion models have been developed to overcome the shortcomings of steady-state Gaussian-plume models (Scire *et al*., 2000a; 2000b). The CALPUFF modelling

system is one of the most commonly used alternatives, modelling the pollutants as 'puffs' of matter emitted from the sources. The nature of puff modelling means it is time dependent and capable of predicting emissions over long ranges (> 50 km). This also means it is capable of dealing with complex terrains and meteorological conditions, making it suitable for coastal regions and areas with widely varying wind conditions. The downside of this is the increased input data required.

Materials and Methods

Vessel Emissions Inventory

To measure the emission rates of the key pollutants, as well as the fuel consumption and greenhouse gas emissions of Ocean Going Vessels (OGVs) within the port, a detailed emissions inventory model was constructed. Being applied to Port of Brisbane for a five-year period, this methodology is then applicable to most ports or wider coastal regions. Harbour craft (including tugs and ferries) were not included in the inventory as studies have shown that compared to OGVs, their emissions are of minor importance (Jalkanen *et al*., 2009; Lucialli *et al*., 2007).

Vessel movement data was obtained from records collected by Port of Brisbane. The five-year dataset, from 2010 to 2014, included identification of individual vessels, their type and the time at which they reached the pilot boarding ground, their destination berths and times of departure (Clarkson, 2015). No information indicated the time at which a vessel passed a key transit mark such as the entrance beacons when entering or departing port. When a vessel was placed at anchor during some part of its call to the port, two separate entries were made: The first listed the anchorage as the destination port and the second listed the actual destination port. Data for vessels repositioning during a call were recorded in the same manner. A large number of anomalies in the data relate to multiple berth visits or those involving anchorage and arrival or departure times are often incomplete or highly erratic. For consistency, such records were discarded: A total of 1268 records (9%) over the five years.

During a visit to the port, vessels undertake a number of movements and each is assigned a single operating mode. Vessels are 'in transit' for most of both the inbound and outbound passages, from the pilot boarding ground to berth and vice-versa. The average speed of the vessel while in transit was calculated from the times recorded in the dataset and the known distance of each transit. While it is known that vessels slowed at the entrance beacons to be assisted by tugs, nothing in the data indicated the time spent in the restricted speed zone. To overcome these limitations, two approaches are taken: First, the restricted speed zone is disregarded and the complete inward and outward voyages are treated as transiting; and second, an approximate time taken to travel from the entrance beacons to the berth is reached by looking at a limited set of automatic identification system data. It was then concluded that in general the times were relatively similar regardless of the vessel type or size and one hour for the inbound voyage and half an hour for the outbound voyage were typical.

A separate operating mode was assigned to a vessel at berth and the time spent at berth was recorded in the original data set. Time taken to dock and un-dock was included as transit time, with arrival and departure times recorded as the time that the first (or last) mooring line was secured (or released). Although the methodology provides for the inclusion both of vessels at anchor and those manoeuvring between berths, these are not included in the case study because most were unreliable entries and were thus excluded.

During the period of interest 2935 unique vessels visited the port, each categorised as one of 32 different types (Clarkson, 2015). For the purpose of the emission inventory, many of these types were similar or the same in terms of operating and engine characteristics and are re-categorised into eleven standard categories, shown in Table 1.

Only one vessel was classed as 'miscellaneous' in the supplied data. This was an auto carrier and it is denoted as such in the redefined categories. One vessel was described as a passenger/general cargo ship, but was in fact a passenger cruise ship. In the data supplied, many self-discharging bulk carriers were incorrectly labelled as bulk/oil carriers. It has been suggested by Star crest (SCG, 2005) that self-discharging bulk carriers have higher berthed emissions, caused by their auxiliary unloading equipment; in this study, all bulk carriers are assigned to one category.

In addition to the OGVs, 30 yachts, 16 dredgers and a number of barges and tugs (fewer than 100) were captured in the dataset. These are deemed irrelevant as they are not OGVs and are consequently are omitted from the emissions inventory. The dredge and tug data were sporadic and did not represent the entire dredge and tug activities within the port and are also omitted.

For each vessel type, default engine powers (both main and auxiliary) are assigned as well as average service speeds, sourced from the USEPA (2009) and based on surveys conducted in nine US ports. The problem with using such values is that they do not consider the size of individual vessels, so the average size of the vessels visiting the ports surveyed has the greatest bearing on the averaged main engine powers; the averaged service speeds and auxiliary engine powers are also affected (Clarkson, 2015). The default vessel values are shown in Table 2. The power ratios between the auxiliary and main engines exhibit strong correlation with those suggested by other studies (Goldsworthy and Renilson, 2013; SCG, 2005).

Table 1: Classifications of vessels based upon the supplied vessel type

Defined vessel types	Data supplied vessel types	Defined vessel type	Data Supplied vessel types
Auto Carrier	miscellaneous class vehicle	Ro-ro	Landing craft
	Carrier		Passenger/ro-ro cargo ship
			Ro-ro cargo ship
Bulk Carrier	Bulk/oil carrier	Tanker	Chemical/oil products tanker
	Bulk carrier		Chemical tanker
	Cement carrier		Crude oil tanker
	Self-discharging bulk carrier		Lpg tanker
	Woodchip carrier		Oil products tanker
Container Ship	Container ship	Navy vessel	Naval ship
Cruise Ship	Passenger/general cargo ship	Reefer	Refrigerated cargo ship
	Passenger cruise ship		
General Cargo ship	general cargo ship		
	Livestock carrier	Not applicable	Barge
			Barge carrier dredger
Miscellaneous	Fishing vessel		Tug
	Heavy load carrier		Yacht
	Research ship		
	Trawler		

Table 2: Averaged vessel specifics based on vessel type

Defined vessel types	Main engine type	Average service speed(knots)	Average main engine power (kW)	Average aux engine power (kW)	Average boiler power (kW) RSZ	Hotel
Auto Carrier	SSD	18.8	11,155	2,967	371	371
Bulk Carrier	SSD	14.5	8,350	2,854	109	109
Container Ship	SSD	21.9	26,122	5,747	506	506
Cruise Ship	MSD	21.1	27,357	7,605	750	750
General Cargo Ship	SSD	15.3	6,709	1,738	106	106
Miscellaneous	MSD	12.7	9,564	2,573	0	0
Navy Vessel	MSD	21.1	27,357	7,605	750	750
Reefer	SSD	19.7	10,060	4,084	464	464
RO-RO	MSD	16.0	11,687	3,027	109	109
Tanker	SSD	14.7	9,667	2,040	371	371

The calculation of the main and auxiliary engines is done separately. As such, during each mode, the main engine load factor is usually based on the propeller relationship law, which according to Browning and Bailey (2006), is Equation one. However, a correction of 0.83 is added to compensate the assumptions that vessels do not function at 100 percent MCR service speed (USEPA, 2009); USEPA suggests that its supplied cruise speeds are approximately 0.94 of the service or maximum speed.

As no information was available on the fuel used by individual vessels, it is assumed that heavy fuel oil was being used in all cases; likewise, all auxiliary engines are assumed to be medium-speed diesel engines. No account was available of vessels operating on gas turbines or unconventional diesel–electric arrangements. For Port of Brisbane, which primarily handles containerised and bulk cargo, any such difference is assumed to be negligible (Clarkson, 2015)-an assumption that might not hold true if this study were adapted for a predominantly cruise or naval port:

$$LF = 0.83 \times \left(\frac{AS}{SS}\right)^3 \quad (1)$$

In the above formula, LF reperesents the load factor, SS depicts the service speed of the vessel, while AS shows the actual speed the vessel operates at. In reference to Clarkson (2015), for auxilarry enginess, the load factors are dependent on the default figure collected from previous studies (SCG, 2005). The information is comprehensively summarised in Table 3. In order to be able to culculate the engine emmisions, particular factors associated with emissions are needed for each pollutant that is being investigated. This utilises the values recomemded by Clarkson (2015), Goldsworthy and Renilson (2013), due to the fact that they are the most relevant ones in regard to Australian conditions. This is well demonstated in Table 4. As such, Equation 2 proposed by (Corbett et al., 1999) is used to calculate the emissions for auxiliary and main engines:

$$E = \frac{P \times LF \times A \times EF}{1000} \quad (2)$$

In this case, P represents the power that is installed in the auxilarty and main engine, E represents the emissions in terms of kilograms, while A is time operation period in that mode. EF further represents the emission factor in $g/(kWh^{-1})$.

Table 3: Auxiliary load factors used in the emission inventory

Defined vessel types	Transit aux LF	RSZ aux LF	Berth aux LF
Auto Carrier	0.15	0.45	0.26
Bulk Carrier	0.17	0.45	0.22
Container Ship	0.13	0.45	0.18
Cruise Ship	0.32	0.32	0.32
General Cargo Ship	0.17	0.45	0.22
Miscellaneous	0.17	0.45	0.22
Navy Vessel	0.32	0.32	0.32
Reefer	0.15	0.45	0.32
RO-RO	0.15	0.45	0.30
Tanker	0.24	0.33	0.26

Table 4: Emission factors expressed in g/kWh

Engine type	BSFC	NO_x	SO_x	CO	CO_2	$PM_{10.0}$	$PM_{2.5}$	VOC	HC	N_2O	CH_4
Main (SSD)	195	18.1	10.30	0.5	622	1.42	1.31	0.3	0.69	0.031	0.006
Main (MSD)	205	13.2	2.00	1.1	654	0.31	0.29	0.2	0.65	0.031	0.004
Aux (MSD)	217	13.9	2.12	1.1	692	0.32	0.29	0.4	0.52	0.031	0.004
Boiler	305	2.1	16.10	0.2	973	1.47	1.35	0.1	0.10	0.08	0.002

Table 5: Surface meteorology stations used in the CALPUFF model

Station name (full)	Station name	Station ID	UTM X (km)	UTM Y (km)	Time zone	Anemometer height (m)
AMBERLEY AMO	YAMB	40004	471.498	6943.783	UTC+1000	10
CAPE MORETON LIGHTHOUSE	CPMN	40043	546.232	7010.001	UTC+1000	10
ARCHERFIELD AIRPORT	YBAF	40211	500.770	6950.241	UTC+1000	10
BRISBANE AERO	YBBN	40842	512.774	6970.173	UTC+1000	10
BRISBANE	BRIS	40913	503.843	6960.309	UTC+1000	10
BANANA BANK NORTH BEACON	MBPS	40925	532.911	6954.517	UTC+1000	10
INNER RECIPROCAL MARKER	MBPC	40926	523.924	6984.334	UTC+1000	10
SPITFIRE CHANNEL BEACON	MBPN	40927	526.420	7008.209	UTC+1000	10
REDCLIFFE	REDC	40958	509.130	6989.537	UTC+1000	10

CALPUFF Modelling: Modelling Domain and Time Period

The modelling domain chosen for the model is a 100×100 km grid with 1 km grid spacing. The domain is centred at the Bureau of Meteorology (BoM), Brisbane Aero monitoring station considering the coordinates for the domain corners. Note that CALPUFF requires all coordinates to be input in universal transverse Mercator format. The modelling period is the full 2013 calendar year from 1 January 2013 00:00 to 1 January 2014 00:00.

Applying a contour plot of land-use categories over the modelling domain, land-use data for Australia is from NOAA (2017). This data set covers all of Australia and can be used for setting up models at other sites in Australia. Elevation data for the modelling domain is from the Shuttle Radar Topography Mission (USGS, 2017). This also includes a contour plot of terrain elevation over the modelling domain. Coastline data for Australia is from the Global Self-consistent Hierarchical High-resolution Geography Database (NOAA, 2017). Surface meteorological data, from the BoM monitoring stations, as well as Precipitation and Upper air data are listed in Table 5 and shown in Fig. 1.

The missing soundings have been repaired by manually substituting upper air data modelled using the fifth-generation Penn State/NCAR Mesoscale Model (2017). For modelling sites in Australia, local upper air data must be purchased and repaired if necessary. If no suitable data are available, then 3D gridded prognostic data can be purchased instead. Overwater meteorological parameters have instead been modelled using CALMET with the Initial Guess overwater meteorology initialised based on the available upper air data. 3D gridded prognostic wind data is not included in the model because suitable observational upper air data (comprehensive data) is available from the Brisbane Aero meteorological monitoring station. For other locations in Australia, it may be necessary to include 3D gridded prognostic data if upper air data is unavailable.

Ten sources were modelled in the CALPUFF model, as summarised in Table 6 and shown in Fig. 2. Three-point sources were positioned at the centre of the berths at Luggage Point, QLC Wharf and Viva Energy Wharf, corresponding to emissions from vessels in port (at berth). A second set of four-point sources extended from the berths to Fisherman Islands, Caltex Tanker Wharf, Pinkenba Bulk Terminal and Hamilton

Wharves, corresponding to emissions while entering the port, manoeuvring. The last three-point sources match the navigation of ships while in transit near the pilot boarding ground, in Moreton Bay and near Dunwich. A stack height of 20m and diameter of 0.8m is assumed for all vessels; and an exit velocity of 25m/s at 539.6K is modelled.

A sample wind rose plot at 517.499 UTM X (km), 6972.094 UTM Y (km) where the Fisherman Islands source is located, is shown in Fig. 3. During the one-year period analysed, winds typically blew along different axes, including SSW to NNE (%10) and S to N (%10) in total. The winds were stronger and more prevalent in the SSW direction. Wind speeds varied from 1.8 to 10 ms^{-1}.

Table 6: Sources used in the CALPUFF model (Emission rates in g/s)

Source numbers	Source name	UTM X (km)	UTM Y (km)	SO_2	NO_2	CO	$PM_{10.0}$	$PM_{2.5}$
1	Pilot Boarding Ground	520.475	7001.062	33.43	53.80	4.30	4.70	4.57
2	Moreton Bay	525.721	6987.281	33.43	53.80	4.30	4.70	4.57
3	Dunwich	533.788	6954.203	33.43	53.80	4.30	4.70	4.57
4	Fisherman Islands	517.499	6972.094	32.44	40.63	3.21	3.78	3.67
5	Caltex Tanker Wharf	515.651	6967.705	32.44	40.63	3.21	3.78	3.67
6	Luggage Point	514.814	6969.871	31.46	27.46	2.12	2.85	2.76
7	QLC Wharf	513.449	6967.051	31.46	27.46	2.12	2.85	2.76
8	Viva Energy Wharf	508.618	6964.238	31.46	27.46	2.12	2.85	2.76
9	Pinkenba Bulk Terminal	507.133	6964.062	32.44	40.63	3.21	3.78	3.67
10	Hamilton Wharves	504.879	6964.804	32.44	40.63	3.21	3.78	3.67

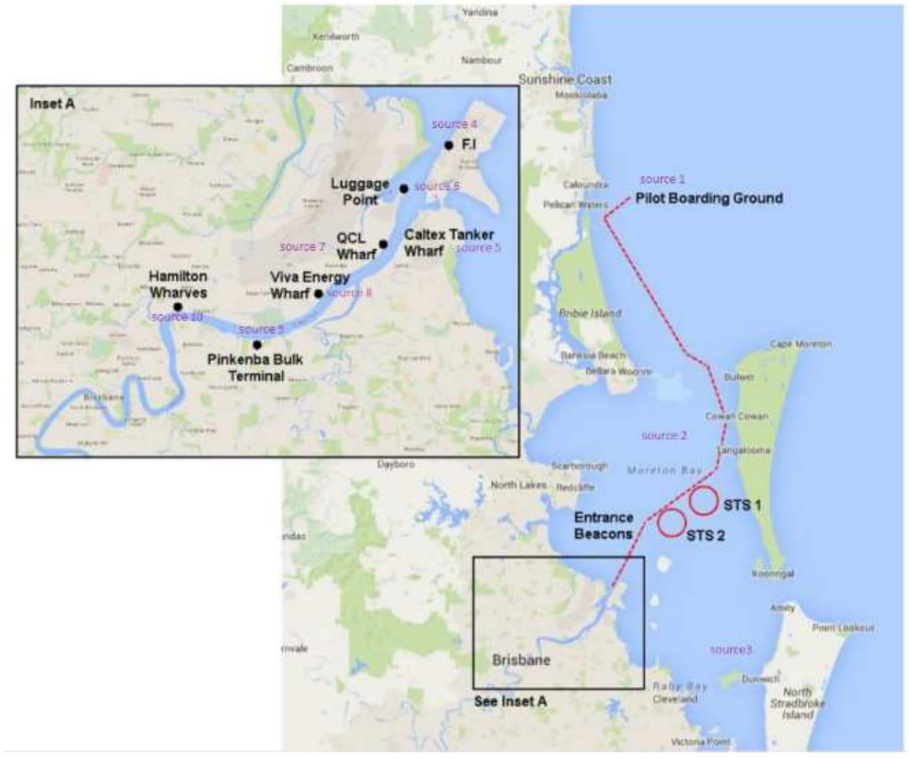

Fig. 2: Sources used in the CALPUFF model

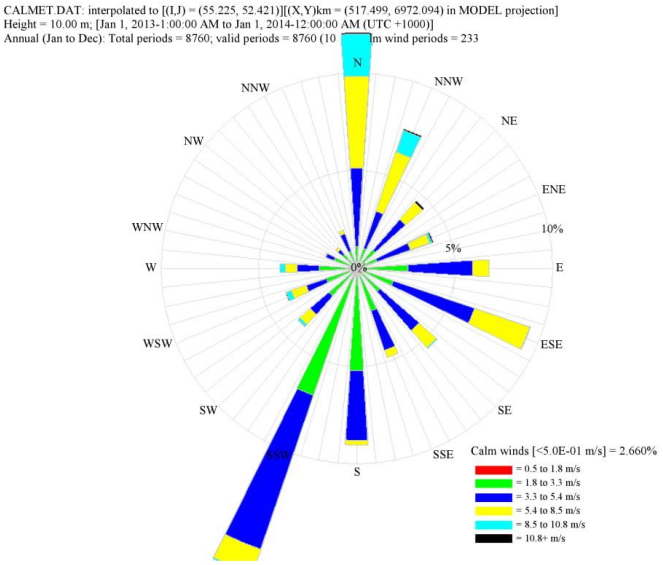

Fig. 3: Wind rose plots at Fisherman Islands location (517.499 UTM X (km), 6972.094 UTM Y (km)

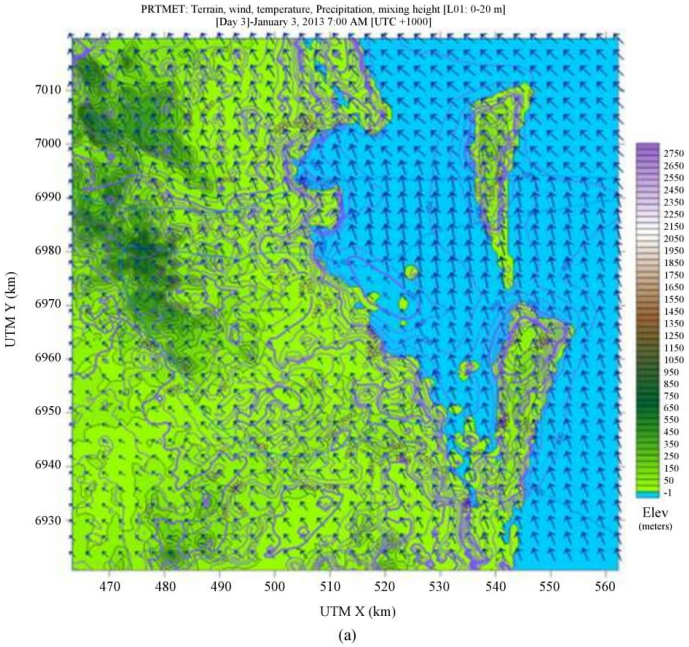

(a)

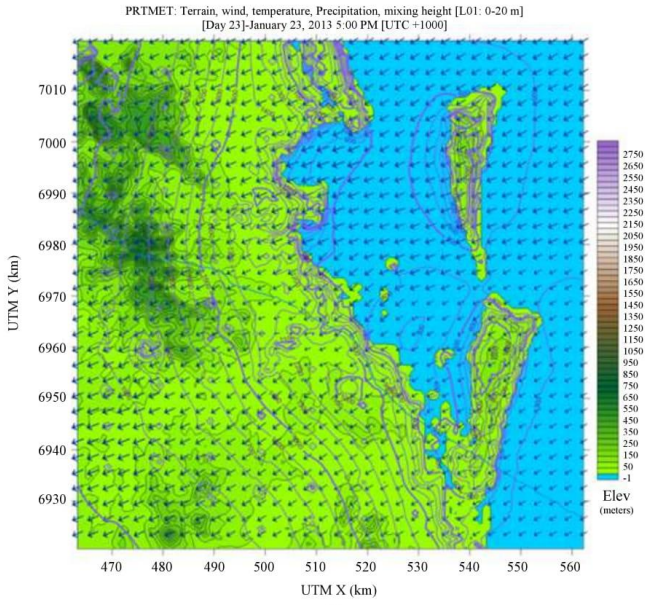
PRTMET: Terrain, wind, temperature, Precipitation, mixing height [L01: 0-20 m]
[Day 23]-January 23, 2013 5:00 PM [UTC +1000]
UTM Y (km)
7010
7000
6990
6980
6970
6960
6950
6940
6930
470
480
490
500
510
520
530
540
550
560
UTM X (km)
2750
2650
2550
2450
2350
2250
2150
2050
1950
1850
1750
1650
1550
1450
1350
1250
1150
1050
950
850
750
650
550
450
350
250
150
50
-1
Elev
(meters)

(b)

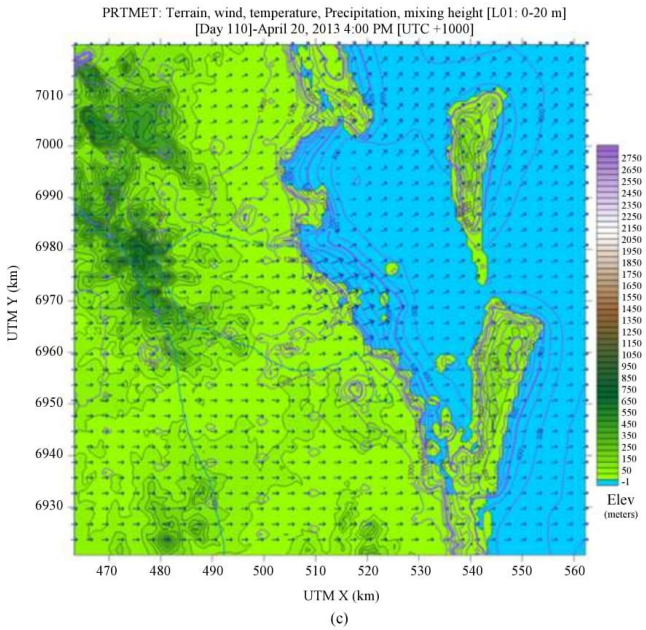
PRTMET: Terrain, wind, temperature, Precipitation, mixing height [L01: 0-20 m]
[Day 110]-April 20, 2013 4:00 PM [UTC +1000]
UTM Y (km)
7010
7000
6990
6980
6970
6960
6950
6940
6930
470
480
490
500
510
520
530
540
550
560
UTM X (km)
2750
2650
2550
2450
2350
2250
2150
2050
1950
1850
1750
1650
1550
1450
1350
1250
1150
1050
950
850
750
650
550
450
350
250
150
50
-1
Elev
(meters)

(c)

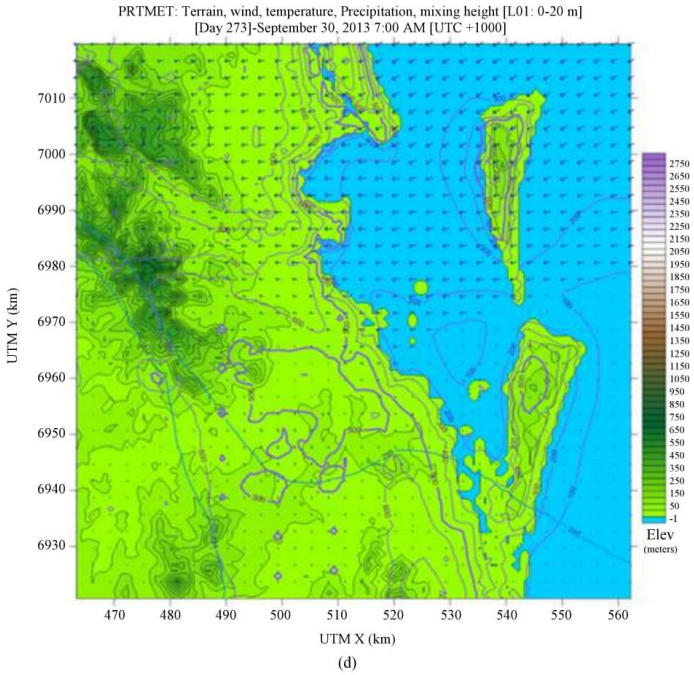

(d)

Fig. 4: Sample wind fields, precipitation and mixing heights across the domain from 0000 January 1 2013 to 0000 January 1 2014; (a) Variances in Day 3 (b) Variances in Day 23 (c) Variances in Day 110 (d) Variances in Day 273

Figure 4 also shows the variances in the flow around the entire model and in particular close to the chosen sources at some arbitrary chosen times. Over the year modelled, the effect of the coast on the meteorology is quite distinct. The diurnal temperature changes and corresponding shifts in wind direction, precipitation and mixing height can be seen to cause confused flow around source points. These flows confirm the need for the more advanced modelling capabilities of CALPUFF. In addition they demonstrate representative domain conditions using observational data, while sufficient data on surface stations are also available.

Results and Discussion

The averaged ground level concentrations of SO_2, NO_x, CO and $PM_{2.5}$ over a year were calculated using CALPUFF. Concentrations across the whole domain were calculated at the 1km spaced gridded receptors. Sample averaged concentration plots of dispersion contour plot are shown below in Fig. 5.

Due to the wide varying wind conditions across the modelling period, dispersion of all pollutants (and deposition of $PM_{2.5}$ and $PM_{10.0}$) showed different trends. The concentrations represented in the figure are based on the emission rates adapted from the Port of Brisbane emissions inventory. The case study coverage, given the availability of full data, is rigorous enough to draw solid conclusions suggesting there is the potential for further investigation into actual risk estimations on Australian ports and the need to calculate hazard values.

Health Impact Assessment

Health Impact Assessment includes calculating average concentrations (Fig. 5) across the air shed for the appropriate averaging times and applying the Concentration-Response Function (CRF) provided from a review of the literature (Williams, 2012; Erbas *et al*., 2005; Jalaludin *et al*., 2008). This study uses demographic data from the Australian Bureau of Statistics. The levels of contaminants were measured twice: Once with and once without background concentrations. This was to reveal the contribution from ships, which it would be useful to compare with impacts from all sources. Addressing particular health points defined by the CRFs, like mortality due to respiratory failure, is a useful aim (Table 7).

Considerably, Health Impact Assessment is an internationally recognised policy tool that evaluates and monitors the potential risks and hazards to certain exposure in particular communities. For instance, a comparison of the hazards exposure to the people dwelling near Brisbane port illustrated the importance of Health Impact Assessment. The study further illustrates the vital components needed to effectively identify when and where the health of the public is likely to be affected negatively, and also recommends the interventions which can be applied to reduce such hazards and risks. Furthermore, the research asserts that shipping activities are likely to affect the health of port residents. When the rate of emissions from shipping activites is high, an immediate response is supposed to be initiated to minimise the exposure to those living near ports.

Arguably, this study is just tip of the iceberge regarding what should be done in terms of occupational exposure, exposure scenarios, and relevant pathways in order to foster better comprehension of the impact that primary emissions have on the public health. As such, with a comprehensive Health Impact Assessment, it is quite easy to identify when and where the health of public can be affected. The assessment also assists in developing strategies which can be used to reduce the threshold of the impacts. Irrefutably, the study conducted in the port of Brisbane regarding the significant health risks faced by those living near the port reveals that further study is needed.

Short-term and Long-term Guideline Validation Assessment

The potential impact on the entire air shed, with pollutant concentrations (Fig. 5) assessed via CALPUFF, are analysed in this section. Averaging times are used as required. Receptors in this case will be:

- The single worst-affected location, not on water, anywhere in the air shed. At this location a comparison against the guidelines for threshold risks and an assessment of carcinogenic risk from diesel particulates, is made.
- Other sensitive receptors of interest, such as schools, kindergartens, hospitals and retirement homes. Data from CALPUFF for those locations have been extracted. Assessment of risks at these locations follows the worst-case location described above.

Table 7: Health endpoints and their reference concentrations

	SO_x Concentration-response function (95 %CI)						
Health outcomes	Australian	UK	Europe	US EPA	WHO	Recommended	This study
Long-term outcomes (annual average concentration)							
Mortality							
Change in forced expiratory volume	No effect in single pollutant model.	n/a	n/a	n/a	n/a	CRF: -6.62 mls (-12.3 to -0.96 mls) per 0.74 PPb in 2pollutant model with NO2 (Williams, 2012).	-12.7mls
Change in forced vital capacity	No effect in single pollutant model.					CRF: -8.92 mls (-16.0 to -1.84 mls) per 0.74 PPb in 2pollutant model with NO_2 (Williams, 2012).	-17.1mls
Emergency department visits							
Asthma	Not assessed. (Erbas *et al.*, 2005)	n/a	n/a	n/a	n/a	CRF: 1.6% (0.72.4%) per 0.8 PPb (Jalaludin *et al.*, 2008).	7.53%
Incidence of myocardial infarction (heart attacks)							
Bronchodilator use	1-hour maximum Night use: 1.0247 (1.0021-1.0478) per 1 PPb (Williams, 2012)- Adelaide, Brisbane,	n/a	n/a	n/a	n/a	CRF for night bronchodilator use: 1.0247 (1.0021-1.0478) per1 PPb from Williams (2012).	3.86

Table 8: Maximum Concentrations ($\mu g/m^3$) versus available guidelines

Pollutants	Averaging time	Concentrations	NEPM	WHO
CO	10 min	1.87	n/a	100000 ug/m^3
CO	30 min	5.83	n/a	60000 ug/m^3
CO	1 h	48.60	n/a	30000 ug/m^3
CO	8h	22.30	9 PPm	10000 ug/m^3
SO_2	10 min	15.70	n/a	500 ug/m^3
SO_2	1 h	93.80	0.2 PPm	n/a
SO_2	24 h	36.20	0.08 PPm	20 ug/m^3
SO_2	1 year	9.98	0.02 PPm	n/a
NO_2	1 h	25.30	0.12 PPm	200 ug/m^3
NO_2	1 year	10.40	0.03 PPm	40 ug/m^3
$PM_{10.0}$	24 h	64.20	50 ug/m^3	50 ug/m^3
$PM_{10.0}$	1 year	8.30	25 ug/m^3	20 ug/m^3
$PM_{2.5}$	24 h	40.30	25 ug/m^3	25 ug/m^3
$PM_{2.5}$	1 year	8.50	8 ug/m^3	10 ug/m^3

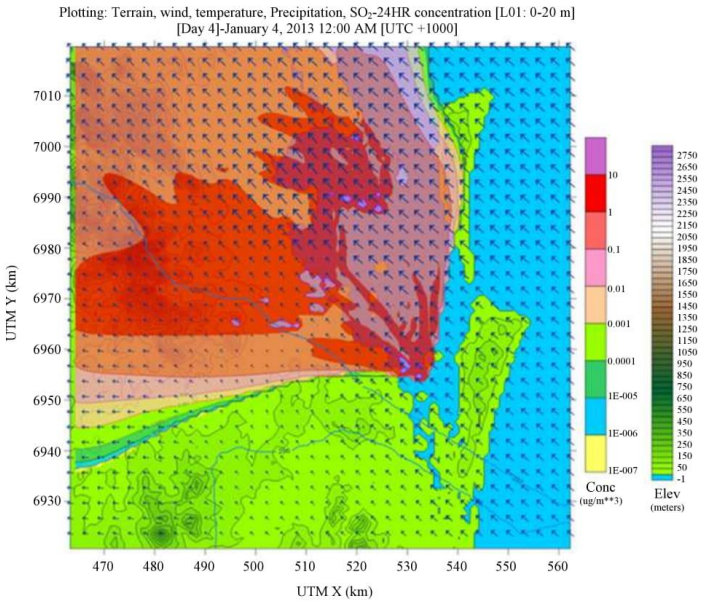
Plotting: Terrain, wind, temperature, Precipitation, SO2-24HR concentration [L01: 0-20 m]
[Day 4]-January 4, 2013 12:00 AM [UTC +1000]
UTM Y (km)
UTM X (km)
Conc (ug/m**3)
Elev (meters)

(a)

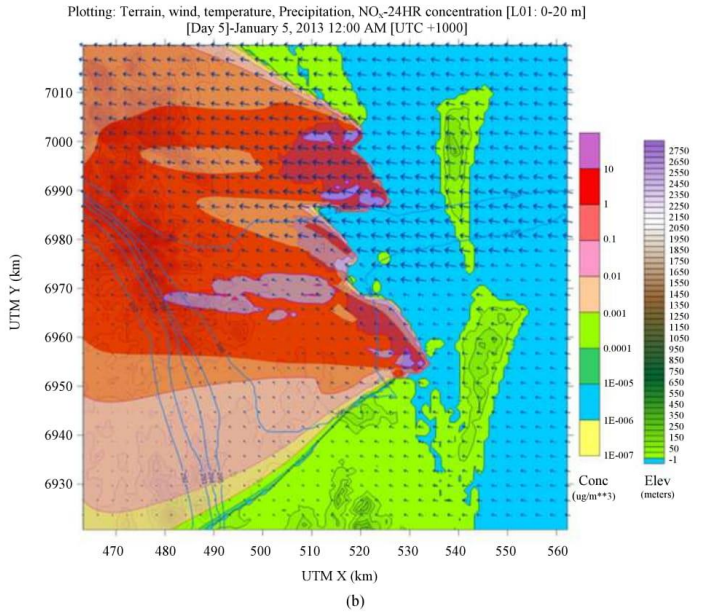
Plotting: Terrain, wind, temperature, Precipitation, NOx-24HR concentration [L01: 0-20 m]
[Day 5]-January 5, 2013 12:00 AM [UTC +1000]
UTM Y (km)
UTM X (km)
Conc (ug/m**3)
Elev (meters)

(b)

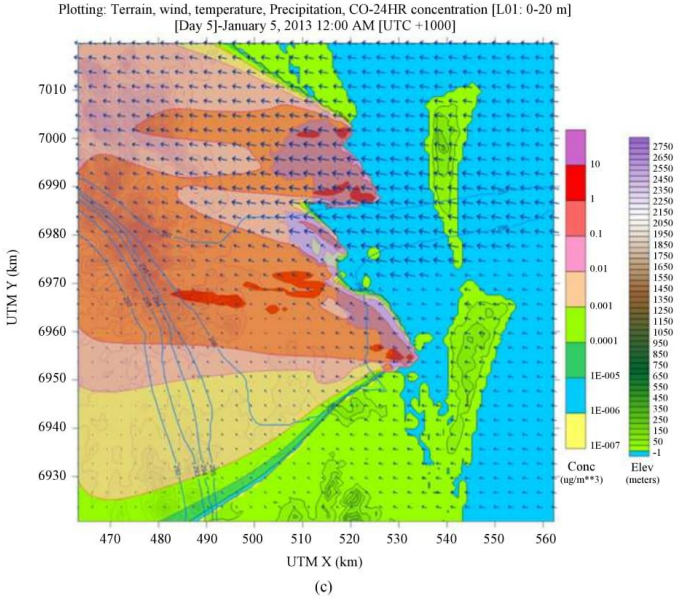

(c)

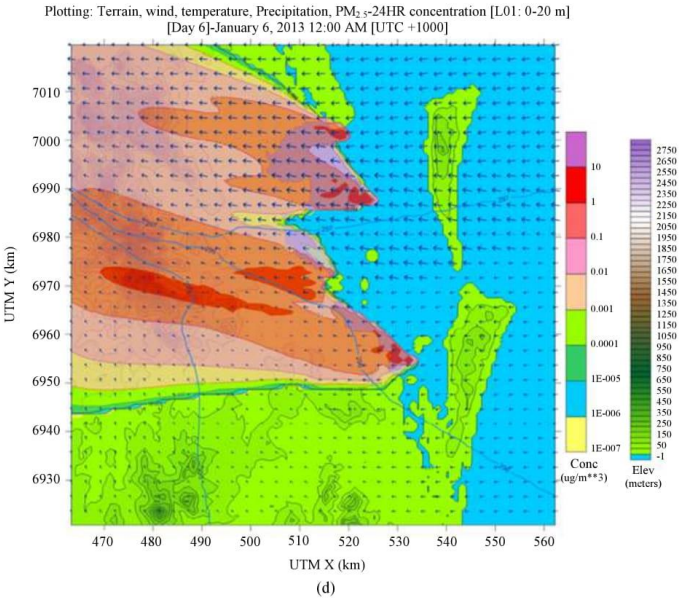

(d)

Fig. 5: Sample averaged concentration plot of SO_2, NO_x, CO and $PM_{2.5}$; (a) Concentration plot of SO_2; (b) Concentration plot of NO_x; (c) Concentration plot of CO; (d) Concentration plot of $PM_{2.5}$

Table 9: Average Concentrations (µg/m^3) versus available guidelines

Pollutant	Averaging time	Concentrations	NEPM	WHO
CO	10 min	0.96	n/a	100000 ug/m^3
CO	30 min	3.25	n/a	60000 ug/m^3
CO	1 h	28.10	n/a	30000 ug/m^3
CO	8 h	17.50	9 PPm	10000 ug/m^3
SO_2	10 min	13.10	n/a	500 ug/m^3
SO_2	1 h	75.80	0.2 PPm	n/a
SO_2	24 h	19.80	0.08 PPm	20 ug/m^3
SO_2	1 year	7.50	0.02 PPm	n/a
NO_2	1 h	19.63	0.12 PPm	200 ug/m^3
NO_2	1 year	9.84	0.03 PPm	40 ug/m^3
$PM_{10.0}$	24 h	49.70	50 ug/m^3	50 ug/m^3
$PM_{10.0}$	1 year	6.12	25 ug/m^3	20 ug/m^3
$PM_{2.5}$	24 h	23.74	25 ug/m^3	25 ug/m^3
$PM_{2.5}$	1 year	6.87	8 ug/m^3	10 ug/m

Available guidelines from Australia - NEMP (most relevant locally) (WHO, 2000) and from the World Health Organisation (most applicable on a global scale) WHO (2012) were applied to validate the results against (Table 8 and 9).

In this advanced dispersion modelling, chemically inert emissions have been considered to be transported by advection and diffusion and are deposited on both land and sea. Sea breezes and air flows influenced by landforms, along with other elements relevant to local levels of air contamination, are predicted in our model, set against the 2013 meteorology. It is of paramout importance to have local meteorology as the model predicts. Plume Rise Module (PRM), quality of air utilised in the simulations, and Lagrangian Particle Model (LPM) represents near-source dispersion which is accurate. The worst case approach discusssed, managed to assess the exposure to toxic compounds through inhalation which is caused by the primary emissions.

The model value usually depends on the quality of data to be processed and this is the truth behind integrated emission models and advanced dispersion. If there is inadequacy of available data, excellent results can be acquired using geo statistical models or land use regression, just as the approach used in this study.

Conclusion

This paper offered a methodology utilising a robust emissions inventory to quantify the emissions of Ocean Going Vessels and incorporating CALPUFF for dispersion modelling. To demonstrate the effectiveness of methodology, it has been applied to Port of Brisbane and returns representative emissions results.

This study highlights the need for any assessment of the dispersion of in-port ship emissions to consider all emissions within port boundaries. This is particularly so in ports like Brisbane where long transit passages take place near densely populated suburbs.

This study demonstrates that applying emission inventory results to detailed dispersion modelling of Port of Brisbane and completing an associated risk assessment provides a convincing demonstration of the need to combat the widespread effects of ship emissions.

With further studies, the existing uncertainities in the present assessment can be reduced regarding the exposure to air emissiions. Moreover, the studies can contribute immensly to directing efforts to curtail the exposure and also effectively address the dispersion modelling limitations. As such, the study may model long-term and short-term esposures and collect relevant data in terms of personal exposure, area and residence with great emphasis on the peak short-term emissions.

Examination of the toxicity of hydrocarbons such as alkanes, and effects of air pollutants on health attributed to primary emissiions is also needed. When this data is combined with local topography and meteorological conditions, a guideleine will be enacted pertaining the mimimum distance between emissions sources, businesees, schools, and homes that is needed to protect the health of humans. Continued evaluation of these results from the ports for a longer period is also prudent. Evaluating long-term developments in the data with regard to both shipping and meteorological traffic fluctuations will also add more insight to the baseline results.

Acknowledgment

Special thanks to National Centre for Maritime Engineering and Hydrodynamic in Australian Maritime College for their support of this study. The generous cooperation of Port of Brisbane Corporation is as well acknowledged.

Author's Contributions

Sanaz Jahangiri: She conducted the design of the technique and analysis.

Natalia Nikolova and Kiril Tenekedjiev: Involved in the model development and data analysis.

Ethics

The authors declare no conflicts of interest and confirm that the manuscript has been submitted solely to this journal and is not published, in press, or submitted elsewhere.

References

Bluett, J., N. Gimson, G. Fisher, C. Heydenrych and T. Freeman *et al*., 2004. Good practice guide for atmospheric dispersion modelling. New Zealand Ministry for the Environment

Browning, L. and K. Bailey, 2006. Current methodologies and best practices for preparing port emission inventories [Internet]. ICF Consulting report to Environmental Protection Agency.

Clarkson, D., 2015. Development of a risk-based methodology to assess the impact of vessel emissions within Australian ports. Australian Maritime College.

Cooper, D.A., 2003. Exhaust emissions from ships at berth. Atmos. Environ., 37: 3817-3830. DOI: 10.1016/S1352-2310(03)00446-1

Corbett, J.J., P.S Fischbeck and S.N Pandis, 1999. Global nitrogen and sulfur inventories for oceangoing ships. J. Geophysical Res., 104: 3457-3470. DOI 10.1029/1998JD100040

Environment, D.O.T. 2016. National environment protection (Ambient Air Quality) Measure.

Erbas, B., A.M. Kelly, B. Physick, C. Code and M. Edwards, 2005. Air pollution and childhood asthma emergency hospital admissions: Estimating intra-city regional variations. Int. J. Environ. Health Res., 15: 11-20. DOI: 10.1080/09603120400018717

Goldsworthy, L. and B. Goldsworthy, 2015. Modelling of ship engine exhaust emissions in ports and extensive coastal waters based on terrestrial AIS data–an Australian case study. Environ. Model Software 63: 45-60. DOI: 10.1016/j.envsoft.2014.09.009

Goldsworthy, L. and M. Renilson, 2013. Ship engine exhaust emission estimates for Port of Brisbane. Air Qual. Climate Change, 47: 26-36.

Holmes, N.S and L. Morawska, 2006. The dispersion of particles: An overview of different dispersion models available. Atmos. Environ., 40: 5902-5928. DOI: 10.1016/j.atmosenv.2006.06.003

Hughes, E., 2011. MARPOL annex VI-prevention of air pollution from ships [Internet]. International Marine Organisation.

Jalaludin, B., B. Khalaj, V. Sheppeard and G. Morgan, 2008. Air pollution and ED visits for asthma in Australian children: a case-crossover analysis. Int. Arch. Occup Environ. Health, 81: 967-974. DOI: 10.1007/s00420-007-0290-0

Jalkanen, J.P., A. Brink, J. Kalli, H. Pettersson and J. Kukkonen *et al*., 2009. A modelling system for the exhaust emissions of marine traffic and its application in the Baltic Sea area. Atmos. Chem. Phys., 9: 9209-9223. DOI: 10.5194/acpd-9-15339-2009

Lucialli, P., P. Ugolini and E. Pollini, 2007. Harbour of Ravenna: the contribution of harbour traffic to air quality. Atmos. Environ., 41: 6421-6431. DOI: 10.1016/j.atmosenv.2007.05.003

NOAA, 2017. GSHH—a global self-consistent, hierarchical, high-resolution geography database. NOAA National Centers for Environmental Information.

NSW EPA, 2005. Approved methods for the modelling and assessment of air pollutants in New South Wales. NSW EPA.

PB, 2015. Port of Brisbane. Shipping Handbook.

SCG, 2005. Port of Long Beach inventory of air emissions inventory. SCG.

Scire, J., D. Strimaitis and R. Yamartino, 2000a. A user's guide for the CALPUFF dispersion model [Internet].

Scire, J.S., F. Robe, M. Fernau and R. Yamartino, 2000b. A user's guide for the CALMET meteorological model.

USEPA, 2009. Regulatory impact analysis: Control of emissions of air pollution from category 3 marine diesel engines. USEPA.

USGS, 2017. Shuttle radar topography mission (SRTM) 1 Arc-second global. USGS.

WHO, 2000. Air quality guidelines. WHO.

WHO, 2012. Diesel engine exhaust carcinogenic. WHO.

Williams, G.E.A., 2012. Australian Child Health and Air Pollution Study (ACHAPS) final report. University of Queensland: National Environment Protection Council.

Winebrake, J.J., J.J Corbett, E.H Green, A. Lauer and V. Eyring, 2009. Mitigating the health impacts of pollution from oceangoing shipping: An assessment of low-sulfur fuel mandates. Environ. Sci. Technol., 43: 4776-4782. DOI: 10.1021/es803224q

Paper 6 – *Jahangiri S, Nikolova N and Tenekedjiev K. Health Risk Assessment of engine exhaust emissions within Australian Ports: A case study of Port of Brisbane. Journal of Environmental Practice. Volume 21, Issue 1. Pages 20-35. Doi:https://doi.org/10.1080/14660466.2019.1564427. March 2019.*

Appendix C: Other Publications

Candidate's other relevant publications as co-author during the candidacy are as follow:

Paper 1 - *T. Van, Z. Ristovski, A. Pourkhesalian, Th. Rainey, V. Garaniya, R.Abbassi,* ***S. Jahangiri****, H. Enshaei , U. Kam, R. Kimball, L.Yang, A. Zare, H.Bartlett, R.Brown. On-board measurements of particle and gaseous emissions from a large cargo vessel at different operating conditions. Journal of Environmental Pollution. Volume 237. Pages 832-841. Doi: https://doi.org/10.1016/j.envpol.2017.11.008 . November 2017.*

Environmental Pollution 237 (2018) 832–841

Contents lists available at ScienceDirect

Environmental Pollution

journal homepage: www.elsevier.com/locate/envpol

On-board measurements of particle and gaseous emissions from a large cargo vessel at different operating conditions

Thuy Chu-Van [a, b, c], Zoran Ristovski [a, b], Ali Mohammad Pourkhesalian [a, b], Thomas Rainey [a, b], Vikram Garaniya [d], Rouzbeh Abbassi [d], Sanaz Jahangiri [d], Hossein Enshaei [d], U-Shen Kam [d], Richard Kimball [e], Liping Yang [a, f], Ali Zare [a, b], Harry Bartlett [g], Richard J. Brown [a, b, *]

[a] Biofuel Engine Research Facility, Queensland University of Technology (QUT), QLD, 4000, Australia
[b] International Laboratory for Air Quality and Health, Queensland University of Technology (QUT), QLD, 4000, Australia
[c] Vietnam Maritime University (VMU), Haiphong, 180000, Vietnam
[d] Australian Maritime College (AMC), TAS, 7250, Australia
[e] Maine Maritime Academy (MMA), ME, 04420, USA
[f] Institute of Power and Energy Engineering, Harbin Engineering University, Harbin, 150001, China
[g] School of Mathematical Sciences, Queensland University of Technology (QUT), QLD, 4000, Australia

ARTICLE INFO

Article history:
Received 11 July 2017
Received in revised form
2 November 2017
Accepted 2 November 2017
Available online 13 November 2017

Keywords:
Ship emissions
At-berth
Manoeuvring
Ocean-going
Particle number sized distributions

ABSTRACT

This study investigated particle and gaseous emission factors from a large cargo vessel for her whole voyage including at berth, manoeuvring and cruising. Quantification of these factors assists in minimising the uncertainty in the current methods of exhaust gas emission factor estimation. Engine performance and emissions from the main marine engine were measured on-board while the ship was manoeuvring and cruising at sea. Emissions of an auxiliary engine working at 55% of maximum continuous rating (MCR) were measured when the ship was at actual harbour stopovers. Gaseous and particle emission factors in this study are presented in g kWh^{-1} or # kWh^{-1}, and compared with previous studies. Results showed that the SO_2 emission factor is higher than that of previous studies due to the high sulphur content of the fuel used. The particle number size distributions showed only one mode for different operating conditions of the ship, with a peak at around 40–50 nm, which was dominated by ultrafine particles. Emission factors of CO, HC, PM and PN observed during ship manoeuvring were much higher than that of those recorded at cruising condition. These findings highlight the importance of quantification and monitoring ship emissions in close proximity to port areas, as they can have the highest impact on population exposure.

1. Introduction

Exhaust emissions from ships have negative effects on both the environment and public health (Anderson et al., 2015; Blasco et al., 2014; Chu Van et al., 2016; Corbett et al., 2007; Reda et al., 2015; Ristovski et al., 2012). Based on sufficient evidence in 2012, the International Agency for Research on Cancer (IARC), which is part of the World Health Organization (WHO), classified diesel engine exhaust as carcinogenic substance to human health (Group 1, same as asbestos). According to Viana et al. (2014) shipping-related emissions are one of the major contributors to global air pollution, especially in coastal areas. An assessment published in 2010 found that over 70% of ship emissions have been detected up to 400 km inland, and significantly contribute to air pollution in the vicinity of harbours (Eyring et al., 2010). Ship emissions also caused an increase in the concentrations of both particulate matter and gaseous pollutants, and the formation of new particles in densely-populated regions (González et al., 2011; Viana et al., 2014).

Fine particle ($PM_{2.5}$) emissions have been related to increased mortality associated with cardiopulmonary and lung problems (Abramesko and Tartakovsky, 2017; Corbett et al., 2007; Pope Iii

* Corresponding author. Biofuel Engine Research Facility, Queensland University of Technology (QUT), QLD, 4000, Australia
E-mail addresses: thuy.chuvan@qut.edu.au, thuy.chuvan@hdr.qut.edu.au, chuthuy.vimaru@gmail.com (T. Chu-Van), z.ristovski@qut.edu.au (Z. Ristovski), richard.brown@qut.edu.au (R.J. Brown).

https://doi.org/10.1016/j.envpol.2017.11.008
0269-7491/

Paper 2 - *T. Van, Z. Ristovski, A. Pourkhesalian, Th. Rainey, V. Garaniya, R.Abbassi,* ***S. Jahangiri,*** *H. Enshaei , U. Kam, R. Kimball, L.Yang, A. Zare, H.Bartlett, R.Brown. On-Board Measurements of Particle Emissions from Two Large Cargo Vessels Operating in the East Coast of Australia during Manoeuvring Conditions. Journal of Atmospheric Environment (Under Review).*

On-Board Measurements of Particle Emissions from Two Large Cargo Vessels Operating in the East Coast of Australia during Manoeuvring Conditions

Thuy Chu-Van [a, b, c], Zoran Ristovski [a, b], Ali Mohammad Pourkhesalian [a, b], Thomas Rainey [a, b], Vikram Garaniya [d], Rouzbeh Abbassi [d], Sanaz Jahangiri [d], Richard Kimball [e], Nho Luong Cong [c], Nicholas Surawski [f], Richard J. Brown [a, b, *]

[a] Biofuel Engine Research Facility (BERF),

[b] International Laboratory for Air Quality and Health (ILAQH),

Queensland University of Technology (QUT), QLD 4000, Australia

[c] Vietnam Maritime University (VMU), Haiphong 180000, Vietnam

[d] Australian Maritime College (AMC), TAS 7250, Australia

[e] Maine Maritime Academy (MMA), ME 04420, USA

[f] University of Technology Sydney (UTS), Ultimo NSW 2007, Australia

[*]Corresponding Author

Richard J. Brown, Biofuel Engine Research Facility, Queensland University of Technology (QUT), QLD 4000, Australia;

Email: richard.brown@qut.edu.au (Richard J. Brown); z.ristovski@qut.edu.au (Zoran Ristovski); thuy.chuvan@qut.edu.au, chuthuy.vimaru@gmail.com (Thuy Chu Van);

Tel: +61 7 3138 5157; +61 7 3138 1129;

Fax: +61 7 3138 1516

HIGHLIGHTS

- Measurements done on two commercial vessels using HFO with different sulphur contents during manoeuvring conditions.
- The difference in PN and PM observed properly due to the difference in sampling location, engine age and fuel sulphur content.
- Different sampling points associated with the difference in particle number size distributions between the two vessels.
- Results from ship campaigns were compared to investigate the impact of fuel sulphur content on particle mass and number.

Paper 3 - *T. Van, H. Lan, N. Cong, V. Garaniya,* ***S. Jahangiri****, R. Abbassi, R. Situ, M. Ferraris, R. Kimbal, Z.Ristovski, Th. Rainey, Ali. Pourkhesalian, R. Brown. Numerical Simulation of Performance and Exhaust Emissions of a Marine Main Engine Using Heavy Fuel Oil during the whole Voyage. International Conference on Sustainable Energy, Vietnam. Pages 29-35. 2017.*

The 3rd ASEAN Smart Grid Congress
The 5th International Conference on Sustainable Energy

Numerical Simulation of Performance and Exhaust Emissions of a Marine Main Engine Using Heavy Fuel Oil during the whole Voyage

Thuy Chu Van[1, 2], Huong Nguyen Lan[2], Nho Luong Cong[2], Vikram Garaniya[3], Sanaz Jahangiri[3], Rouzbeh Abbassi[3], Rong Situ[4], Michael D. Ferraris[4], Richard Kimball[5], Zoran Ristovski[1], Thomas Rainey[1], Ali Mohammad Pourkhesalian[1], Richard J. Brown[1]

[1]Queensland University of Technology
2 George St, Brisbane City, Queensland, 4000, Australia
[2]Vietnam Maritime University
484 Lach Tray street, district Le Chan, Hai Phong, Vietnam.
[3]Australian Maritime College
100 Newnham Dr, Newnham, Tasmania, 7248, Australia
[4]James Cook University
1 James Cook Dr, Townsville City, Queensland, 4811, Australia
[5]Maine Maritime Academy
1 Pleasant St, Castine, Maine, 04420, USA

Abstract

In this study, the performance and exhaust emissions of the marine main engine (ME) of a large cargo vessel operating on the east coast of Australia by numerical thermodynamic simulation were investigated. The simulation were validated using on-board measurements of the ME conducted in October and November 2015 on a large cargo ship cruising between Ports of Brisbane, Gladstone and Newcastle. The commercial engine modelling/design software, AVL Boost, was used with special adaptation to marine engines and Heavy Fuel Oil (HFO). All measurements here carried out on the ME at different engine speeds and loads when the ship experienced different working conditions such as manoeuvring near port areas and cruising at sea. Specific engine parameters including in-cylinder mean and peak pressure, power, exhaust temperature and turbocharger boost were investigated. A good agreement between experimental and numerical results was observed for engine emissions of NO_x and soot at higher engine speed conditions. The capacity of AVL Boost for marine engine simulation is evaluated, including prediction on the engine performance and emissions under different engine working conditions where they cannot be measured in the experiment.

Keywords: *Exhaust emissions, AVL Boost, Heavy Fuel Oil, performance*

1. INTRODUCTION

Shipping is considered one of the most fuel efficient means of transportation [1], it accounts for over 90% of world trade by some 90,000 marine vessels [2]. However, exhaust emissions from ships have a negative impact on environment and consequently on human health [3]-[10] and have become of global concern over the last decade [11]. To make the matters worse, these ships also burn low quality Heavy Fuel Oil (HFO) owing to its economic benefit [5]. HFO is the main fuel for around 95% of 2-stroke low-speed large-power marine main engine and approximately 70% of 4-stroke medium-speed engines [1]. HFO combustion results in different